Functions of the Yeast GTPase-Activating Proteins Age1 and Gcs1 for Post-Golgi Vesicular Transport

by

Jeremy J. R. Benjamin

Submitted in partial fulfilment of the requirements
for the degree of Doctor of Philosophy

at

Dalhousie University
Halifax, Nova Scotia
August 2011

DALHOUSIE UNIVERSITY

DEPARTMENT OF MICROBIOLOGY & IMMUNOLOGY

The undersigned hereby certify that they have read and recommend to the Faculty of Graduate Studies for acceptance a thesis entitled "Functions of the Yeast GTPase-Activating Proteins Age1 and Gcs1 for Post-Golgi Vesicular Transport" by Jeremy J. R. Benjamin in partial fulfilment of the requirements for the degree of Doctor of Philosophy.

Dated: August 22, 2011

External Examiner: _____

Research Supervisor: _____

Examining Committee: _____

_____

_____

Departmental Representative: _____

DALHOUSIE UNIVERSITY

DATE: August 22, 2011

AUTHOR: Jeremy J. R. Benjamin

TITLE: Functions of the Yeast GTPase-Activating Proteins Age1 and Gcs1 for Post-Golgi Vesicular Transport

DEPARTMENT OR SCHOOL: Department of Microbiology & Immunology

DEGREE: PhD CONVOCATION: October YEAR: 2011

_____

Signature of Author

TABLE OF CONTENTS

LIST OF TABLES

LIST OF FIGURES

ABSTRACT

Organelles within the endomembrane system of all eukaryotic cells exchange membrane lipids and proteins using membrane-bound transport vesicles. This highly conserved vesicular transport process is essential for life and is highly regulated. Much of this regulation is provided by small monomeric GTP-binding proteins such as Arf and Arl that act as molecular switches, cycling between inactive GDP-bound and active GTP-bound states. This cycle of GTP binding and hydrolysis is controlled by guanine-nucleotide exchange factors (GEFs) and GTPase activating proteins (GAPs), respectively. I have investigated regulatory interactions involving two ArfGAPs, Age1 and Gcs1, involved in post-Golgi vesicular transport in the budding yeast *Saccharomyces cerevisiae*.

In yeast, the Age2 + Gcs1 ArfGAP pair is essential and facilitates post-Golgi transport. I found that overexpression of either the poorly characterized ArfGAP Age1 or the Sfh2 phosphatidylinositol-transfer protein can bypass the requirement for Age2 and Gcs1. Indeed, endogenous Age1 is required for efficient Sfh2-bypass. Moreover, the yeast phospholipase D protein, Spo14, which is activated by Sfh2 and regulates membrane lipid composition, is required for Age1 to effectively alleviate the deleterious effects of defective Age2 + Gcs1 function. My findings suggest that Age1 is regulated by membrane lipid composition and can provide ArfGAP function for post-Golgi transport.

Gcs1 is involved in multiple vesicular transport stages, is a dual-specificity GAP for both Arf and Arl1 proteins and, as shown here, also has functions independent of its GAP activity. The absence of Gcs1 causes cold sensitivity for growth and endocytic transport. The cold sensitivity of cells lacking Gcs1 is alleviated by the elimination of either the Arl1 or Ypt6 vesicle-tethering pathway at the *trans*-Golgi, or by overexpression of Imh1, an effector of the Arl1 pathway. I found elimination of the Ypt6 pathway also prevents Arl1 activation and membrane localization, that Arl1 binding by Imh1 is necessary and sufficient for alleviation, and that the Gcs1 function required for growth and transport in the cold is independent of any GAP activity. My findings suggest that in the absence of this GAP-independent function of Gcs1 the resulting dysregulated Arl1 causes the *gcs1*Δ defects through the sequestration of a yet-to-be-determined cellular factor.

LIST OF ABBREVIATIONS AND SYMBOLS USED

ALPS	amphipathic lipid packing sensor
Arf	ADP ribosylation factor
Arl	Arf like
bp	base pair
BSA	bovine serum albumin
C	carboxyl
COG	conserved oligomeric Golgi
COPI	coat protein complex I
COPII	coat protein complex II
CORVET	class C core vacuole/endosome tethering
DAG	diacylglycerol
ER	endoplasmic reticulum
GAP	GTPase activating protein
GARP	Golgi-associated retrograde protein
GDP	guanosine diphosphate
GEF	guanine nucleotide-exchange factor
GFP	green fluorescent protein
GST	glutathione S-transferase
GTP	guanosine triphosphate
GTPase	GTP binding protein
HOPS	homotypic fusion and vacuole protein sorting
kbp	kilo base pairs
N	amino
ORF	open reading frame
PA	phosphatidic acid
PC	phosphatidylcholine
PCR	polymerase chain reaction
PEG	polyethylene glycol
PI	phosphatidylinositol

PI(4)P	phosphatidylinositol 4-phosphate
$PI(4,5)P_2$	phosphatidylinositol 4,5-bisphosphate
PITP	phosphatidylinositol transfer protein
RFP	red fluorescent protein
SDS	sodium dodecyl sulfate
SFH	Sec14 homologue
SNARE	soluble N-ethylmaleimide-sensitive factor attachment protein receptor
TRAPP	transport protein particle
YEPD	enriched medium – yeast extract, peptone, and dextrose
YNB	yeast nitrogen base

Yeast Nomenclature

YFG1	wild-type gene
yfg1-1	recessive mutant allele
YFG1-1	dominant mutant allele
*yfg1*Δ	gene deletion mutation
[*YFG1*]	plasmid borne gene
Yfg1	wild-type protein
Yfg1-1	mutant protein

ACKNOWLEDGEMENTS

I would like to thank my supervisor Dr. Gerald C. Johnston and my co-supervisor Dr. Richard A. Singer for having me as a graduate student in their lab, for thorough reading and constructive editing of this thesis, and for their scientific mentorship throughout the course of my studies.

I would also like to acknowledge my unofficial co-supervisor Dr. Pak Phi Poon with whom I conversed daily about the specifics of my research and his, as well as science in general (amongst many other things). We collaborated well together and my projects would not have been as successful without Pak's input, guidance and contributions.

No research exists solely on its own. I would like to acknowledge the groundwork that was laid by previous graduate students in this lab including Dr. Stephen M. Lewis, Dr. Andréanne Auger, Dr. Tania Wong, Dr. John Drysdale, and Dr. Xiangmin Wang. Their findings formed the foundation of my research and contributed to my success.

I have had many influential mentors in my life. I would like to acknowledge my grade 12 biology teacher M. Lewis who was willing to accept that a trouble maker from his junior high science class could be an A student in his high school biology class. After completing my undergraduate degree, I had no idea what graduate school was, and was certainly not considering doing a PhD. My introduction to research and grad school came when Dr. Melanie Dobson, and Dr. Lois Murray (kind of – its ok no hard feelings) hired me as a laboratory technician. Thank-you for giving a kid in a Canadian Tire shirt with no lab experience a chance, and for introducing me to research and academia.

My training has been enriched by my committee members most of whom were mentioned above, (thanks Dr. Roy Duncan for joining my committee when I switched over to the PhD program), by the members of the Dalhousie Yeast Research group, the members of the molecular biology (no pizza week) journal club, the members of the Cancer Research Training Program and the former students of the Singer/Johnston lab.

I thank David Carruthers and Kendra Walker for technical assistance in the lab; Steve Whitefield and the Dalhousie University Cellular Microscopy and Digital Imaging facility for technical assistance with microscopy; Christopher Burd, Sean Munro, Joel Moss, Vytas Bankaitis, Scott Emr, Joanne Engebrecht, Dan Cassel, Elizabeth Conibear, and Anne Rosenwald for plasmids; and Amy Curwin for yeast strain FRY107.

I was financially supported by a trainee award from the Beatrice Hunter Cancer Research Institute with funds provided by The Terry Fox Foundation Strategic Health Research Training Program in Cancer Research at CIHR, and a Dalhousie Graduate Studentship funded by a grant from the Canadian Institutes of Health Research (CIHR) held jointly by Dr. Gerald C. Johnston and Dr. Richard A. Singer.

Finally, of course, I thank my family. My beautiful wife Tawnya, who has picked up the slack allowing me to work long hours on this thesis while simultaneously moving to a new house; my lovely two year old daughter Calla, who doesn't hold my recent absence against me; and my unborn son Aven, I promise you will get more attention now that this is wrapping up, thank-you for holding off on your grand entrance and please remember not the 22nd of August, thanks buddy.

CHAPTER 1. INTRODUCTION

1.1 Overview of Vesicular Transport

A defining feature of eukaryotic cells is a complex endomembrane system partitioning the cell into various functional and structural compartments. These specialized membrane-bound compartments are termed organelles and carry out diverse processes required for cell function and viability. The creation of these membrane-bound organelles allows processes to be carried out in a concerted manner and avoids interference among the many functions that a cell must perform. The eukaryotic endomembrane system includes the endoplasmic reticulum (ER), Golgi apparatus, vacuole/lysosome, endosomes, and the plasma membrane. An example of the advantage that membrane-bound organelles impart to eukaryotic cells is the yeast vacuole (metazoan lysosome). This organelle contains hydrolytic enzymes that function for intracellular digestion, degrading cellular constituents and/or extracellular molecules that have been internalized by the cell. The vacuole provides the low-pH environment required for these hydrolases to function and segregates these potentially damaging processes from cellular components that need to be maintained. In the absence of membrane-bound organelles, it is hard to imagine how a cell could perform the processes that take place in the vacuole without damaging the integrity of the cell itself.

Although the various organelles in the endomembrane system are distinct compartments, the membranes that make up the different compartments are inter-related through the exchange of membrane components and proteins. Small membrane-bound vesicles are formed from the membranes of organelles and transported *via* the process of vesicular transport between organelles. In this way, proteins within the lumens and membranes of these organelles, as well as the lipids that make up the membranes themselves, are transported throughout the cell. The process of vesicular transport (reviewed in Bonifacino and Glick, 2004) is essential for cell viability, highly regulated, and highly conserved. In general, vesicular transport consists of the formation of a transport vesicle from a so-called donor membrane (or donor compartment), directed transport of the vesicle through the cytoplasm to its intended destination, and fusion of the transport vesicle with the so-called target membrane (or target compartment),

resulting in the transfer of proteins (generally termed 'cargo') and lipids from the donor compartment to the target compartment.

There are many defined routes, termed transport pathways, that transport vesicles follow within the cell. The secretory transport pathway is involved in the 'forward' (anterograde) movement of proteins from the ER to the Golgi, through the Golgi, and from the *trans*-Golgi to the plasma membrane or to endocytic compartments (Novick *et al.*, 1980; Harsay and Bretscher, 1995). The protein machinery that is involved in anterograde transport as well as resident proteins that are inadvertently packaged into the nascent vesicle are recycled back to the donor compartment by 'backward' (retrograde) transport, for example from the Golgi back to the ER (Letourneur *et al.*, 1994; Poon *et al.*, 1999). The endocytic transport pathway removes proteins, such as receptors, from the plasma membrane surface and delivers them to early endosomes, where they are sorted and may next be delivered to late endosomes *en route* to the vacuole/lysosome for degradation, or may be returned back to the plasma membrane either directly or *via* the *trans*-Golgi membrane (Conibear, 2010). From the *trans*-Golgi membrane, proteins can also be transported to late endosomes *en route* to the vacuole/lysosome *via* the CPY (carboxypeptidase Y) pathway (Marcusson *et al.*, 1994), or directly to the vacuole/lysosome *via* the ALP (alkaline phosphatase) pathway (Cowles *et al.*, 1997; Piper *et al.*, 1997). Different subsets of proteins are involved in carrying out and regulating the fundamental processes of vesicular transport that comprise each of the different transport pathways.

Vesicle budding (the formation of a nascent vesicle) is mediated by coat proteins on the donor membrane and involves cargo selection processes which ensure the appropriate cargo proteins are incorporated into the forming vesicle, while resident proteins are excluded from the vesicle and retained within the donor compartment. Vesicle budding and cargo selection are discussed further in the next section. Once formed, vesicles are transported through the cytoplasm either by diffusion or by molecular motor proteins that carry vesicles along microtubules or actin cables to their destination (Cai *et al.*, 2007). Upon arrival at the target compartment, two levels of interaction facilitate target-compartment recognition, binding, and ultimately vesicle fusion resulting in delivery of the vesicle's cargo to the compartment (Cai *et al.*, 2007).

The first interaction is termed vesicle tethering, and involves the selective binding of transport vesicles by proteins or multisubunit protein complexes on the target membrane. SNARE (soluble N-ethylmaleimide-sensitive factor attachment protein receptor) proteins that are present on both the vesicle and target membranes carry out the second level of recognition and binding, and are thought to provide the mechanical energy required to induce membrane fusion. Vesicle tethering and SNARE protein interactions are discussed further below. The effective transport of cargo between organelles is vital to maintain organelle integrity and composition, and thus the processes involved in vesicular transport are tightly regulated.

1.2 Transport-Vesicle Budding and Cargo Selection

Protein coats mediate vesicle budding and cargo selection. There are three well-studied protein coat complexes that function in distinct transport pathways and are conserved between yeast and metazoan cells. These complexes are: the coat protein complex II (COPII), which functions in the secretory pathway from the ER to the Golgi (Barlowe, 1998); the coat protein complex I (COPI), also referred to as coatomer, which functions in intra-Golgi and Golgi-to-ER retrograde transport (Cosson and Letourneur, 1997); and the clathrin coat and adaptor complexes which function in post-Golgi transport stages including transport from the *trans*-Golgi membrane, the plasma membrane, and endosomes (Schmid, 1997). These coat complexes are recruited to donor membranes by activated monomeric GTP-binding proteins (G proteins) that are members of the Arf (ADP ribosylation factor) subfamily within the Ras superfamily of GTPases. In general, small monomeric G proteins function as molecular switches that 'toggle' between an inactive GDP-bound form and an active GTP-bound form. When activated these G proteins interact with specific effector molecules that mediate a variety of cellular functions (Chavrier and Menetrey, 2010). How this cycle of GDP/GTP binding is regulated is described below for the Arf GTPases, but similar regulatory mechanisms are involved in the regulation of all small monomeric G proteins.

The Arf family includes three closely related groups of proteins: Arf, Arl (Arf-like), and Sar proteins. In the budding yeast *Saccharomyces cerevisiae,* the Arf family contains 6 members: 3 Arf proteins (Arf1, Arf2, and Arf3); 2 Arl proteins (Arl1 and

Arl3); and 1 Sar protein (Sar1) (Pasqualato *et al.*, 2002). These G proteins cycle between inactive GDP-bound and active GTP-bound forms, and two other protein families regulate this GDP/GTP cycle. Guanine-nucleotide exchange factors (GEFs) catalyze the exchange of GDP for GTP, activating the G proteins, and GTPase-activating proteins (GAPs) stimulate GTP hydrolysis, inactivating the GTPases. Upon activation, GTP-bound Arf proteins undergo a conformational change exposing an N-terminal amphipathic helix that is myristoylated in Arf1-3 and Arl1 but not Arl3 or Sar1 (Pasqualato *et al.*, 2002). The exposed hydrophobic face of the N-terminal amphipathic helix interacts with membranes, thus coupling the activation of Arf-family proteins with their recruitment to membranes.

Vesicle budding is initiated by these activated membrane-bound GTPases. Activated Sar1 is localized to the ER and recruits the COPII coat complex (Barlowe, 1998). Activated Arf1/Arf2 (Arf1 and Arf2 are 96% identical and functionally interchangeable [Stearns *et al.*, 1990]) localized to the *cis*-Golgi membrane recruits the COPI coat complex (Cosson and Letourneur, 1997), whereas activated Arf1/Arf2 localized to the *trans*-Golgi and post-Golgi membranes recruits the clathrin coat and adaptor complexes (Bonifacino, 2004). Recruited coat subunits bind to the activated G protein on the donor membrane and also bind the cytoplasmic tail of transmembrane cargo proteins, cargo receptor proteins, and v-SNARE proteins. Indeed, additional interactions with membrane proteins that are unique to the donor membrane may provide the specificity for COPI and clathrin coat recruitment to the distinct transport stages in which they function, despite binding the same activated Arf1/Arf2 proteins (Springer *et al.*, 1999). These interactions involving an activated GTPase, a coat subunit, and a membrane protein have been suggested to constitute the formation of a priming complex (Springer *et al.*, 1999). The accumulation of priming complexes on the donor membrane results in polymerization of the coat subunits, forming a lattice that deforms the donor membrane into the curved membrane of the nascent vesicle which eventually buds from the donor membrane, forming a coated transport vesicle carrying cargo proteins as well as v-SNARE proteins that are required for target-compartment recognition (Springer *et al.*, 1999).

1.3 Transport-Vesicle Docking and Fusion

Fully formed transport vesicles must recognize and fuse with the appropriate target compartment to deliver cargo. As noted above, two levels of interaction facilitate target-compartment recognition. The initial interaction between the vesicle and the target membrane is carried out at a distance from the membrane and is termed vesicle tethering, which is then followed by SNARE-complex formation (reviewed in Jahn and Scheller, 2006). There are 25 members of the SNARE protein family in yeast (36 members in humans), characterized by the highly conserved heptad-repeat SNARE motif of 60-70 amino acids, which facilitates SNARE-complex formation between a monomeric v-SNARE on the vesicle membrane and an oligomeric t-SNARE, generally composed of three separate proteins, on the target membrane. These interacting SNAREs form a *trans*-SNARE complex (composed of a four-helix bundle), bringing the two membranes into close proximity and providing the free energy required to drive membrane fusion. Fusion results in a *cis*-SNARE complex in the fused membrane and cargo delivery. A protein complex containing an ATPase then disassembles the *cis*-SNARE complex in an ATP-dependent process, allowing the SNARE proteins to be recycled for further rounds of vesicle transport.

SNARE interactions were once thought to provide the specificity of target membrane recognition (Sollner *et al.*, 1993). The SNARE hypothesis proposed that each distinct type of transport vesicle carries a specific v-SNARE that recognizes and binds a cognate t-SNARE on the target membrane, providing specificity (Rothman, 1994). Several lines of evidence, however, indicate that SNARE proteins do not act alone in this regard. First, the ubiquitous distribution of t-SNAREs across some membranes does not account for the localization of vesicle-fusion sites to sub-domains on those membranes. For example, the t-SNARE proteins Sso1 and Sso2 are distributed across the surface of the plasma membrane in yeast, yet vesicle fusion takes place at specific sub-domains of the plasma membrane during polarized cell growth (Brennwald *et al.*, 1994). Second, because v-SNAREs are recycled by retrograde transport, the same v-SNARE can reside on vesicles being transported in the anterograde and retrograde directions. Thus, the presence of a v-SNARE cannot be the sole determinant of compartment recognition. Third, SNAREs are promiscuous: both v-SNAREs and t-SNAREs can bind multiple

partners within the same cell (von Mollard *et al.*, 1997; Tsui and Banfield, 2000), a feature not ideally suited to specificity in target-compartment recognition. Fourthly, disruption of SNARE-complex formation blocks membrane fusion but does not block vesicle tethering, and leads to an increase in tethered vesicles at the membrane (Hunt *et al.*, 1994; Broadie *et al.*, 1995), strongly indicating that while SNARE interactions are required for vesicle membrane fusion, they are not required for vesicle docking. Finally, the rate of vesicle fusion driven by SNARE proteins alone in a reconstituted *in vitro* assay is slower than the rate of vesicle fusion *in vivo*, suggesting that additional factors in the cell (possibly tethering factors) increase the efficiency and rate of vesicle docking and fusion (Fasshauer *et al.*, 2002).

1.4 Vesicle-Tethering Factors

Vesicle-tethering factors are proposed to initiate the first contact between membranes and incoming transport vesicles, and are thought to provide both docking and specificity functions prior to the formation of a *trans*-SNARE complex. There are two general classes of vesicle-tethering factors, long coiled-coil proteins (reviewed in Gillingham and Munro, 2003), and multisubunit complexes (reviewed in Whyte and Munro, 2002). In yeast there are five long coiled-coil proteins proposed to mediate vesicular transport: Coy1, Imh1, Uso1, Sgm1, and Rud3; they are all localized to the Golgi and have human homologues: CASP, Golgin-245, p115, TMF1, and GMAP-210, respectively (Gillingham and Munro, 2003). (There are several additional long coiled-coil proteins in human cells, termed Golgins, that are localized to the Golgi and endosomes and that do not have homologues in yeast.) Proteins of the coiled-coil class of vesicle tethers have the potential to form homodimeric coiled coils that when anchored to a membrane at one end can extend a long distance into the cytoplasm. Indeed, the yeast Uso1 protein and its mammalian homologue p115 have been observed by electron microscopy to form long coiled-coil structures (Yamakawa *et al.*, 1996). This characteristic structure, combined with the localization of many of these proteins to Golgi and endosomal membranes, lends itself to the proposed mechanism that these proteins are anchored to the target membrane at one end while the other end of the protein extends into the cytoplasm where it is ideally located to form specific contacts with incoming transport vesicles. There are

varied mechanisms by which these long coiled-coil proteins interact with membranes; some have C-terminal transmembrane domains, while others interact with peripheral membrane proteins. Many of the long coiled-coil and multisubunit tethering complexes (discussed below) interact with Rab/Ypt GTPases, allowing membrane localization to be regulated by the Rab GTPase cycle (Gillingham and Munro, 2003). Additionally, Imh1 and four human Golgins have C-terminal GRIP domains (named after four proteins in which it is contained: golgin-97, RanBP2α, Imh1, and p230/golgin-245) that facilitate binding to the *trans*-Golgi GTPase Arl1 (Lu and Hong, 2003; Panic *et al.*, 2003a). Likewise, Rud3 and its human homologue GMAP-210 are recruited to the *cis*-Golgi by binding the GTPase Arf1 *via* a similar C-terminal domain, termed the GRIP-related Arf-binding (GRAB) domain (Gillingham *et al.*, 2004).

For many of the long coiled-coil proteins a mechanism of vesicle binding at the cytoplasmic N terminus of the protein has not been determined; however, p115 binds v-SNAREs and promotes *trans*-SNARE complex formation (Gillingham and Munro, 2003; Cai *et al.*, 2007), and other Golgins (including the four human GRIP-domain Golgins) have been shown to have binding sites for multiple Rab GTPases along their length, suggesting a mechanism for vesicle recognition (Sinka *et al.*, 2008; Hayes *et al.*, 2009). In the case of the human Golgin GMAP-210 the mechanisms of vesicle and membrane binding have both been determined. As described above, GMAP-210 is recruited to the *cis*-Golgi through binding of activated Arf1 by a C-terminal GRAB domain (Gillingham *et al.*, 2004). At the N terminus of GMAP-210 an amphipathic lipid packing sensor (ALPS) motif mediates vesicle membrane binding by forming an amphipathic helix on the highly curved membrane of the transport vesicle (Drin *et al.*, 2008). Thus, the long coiled-coil tethering factors have many diverse mechanisms for membrane recognition and binding.

There are eight large multisubunit complexes that are proposed to function in vesicle tethering at multiple transport stages; all were initially identified and characterized in yeast and have mammalian homologues (Whyte and Munro, 2002; Cai *et al.*, 2007). These complexes are the exocyst complex, which functions in the fusion of Golgi-derived vesicles at the plasma membrane, specifically at sites of polarized growth (Guo *et al.*, 1999; Brymora *et al.*, 2001); the conserved oligomeric Golgi (COG)

complex, which functions at the *cis*-Golgi to tether vesicles arriving from within the Golgi and from endosomes (Whyte and Munro, 2001); the Golgi-associated retrograde protein (GARP) complex, which functions in retrograde transport from endosomes to the *trans*-Golgi (Conboy and Cyert, 2000; Conibear and Stevens, 2000); the transport protein particle (TRAPP) complex, which shares subunits between two related complexes, the TRAPP I complex (seven subunits), which appears to be involved in COPII vesicle ER-to-Golgi transport, and the TRAPP II complex (three additional subunits), which appears to be involved in COPI-vesicle intra-Golgi retrograde transport (Sacher *et al.*, 2001); the Class C Vps complex, also known as the homotypic fusion and vacuole protein sorting (HOPS) complex, which functions in fusion of endosomal transport vesicles with the vacuole (Rieder and Emr, 1997); the class C core vacuole/endosome tethering (CORVET) complex, which shares subunits of the HOPS complex and functions in *trans*-Golgi to endosome transport; and the Dsl1 complex, which functions in Golgi-to-ER retrograde transport (Ren *et al.*, 2009).

All of these tethering complexes, except the TRAPP complexes, function downstream of Rab GTPases; that is, they are Rab effectors. The TRAPP complexes along with the HOPS complex have been shown to have Rab GEF activity for various Rab proteins, and therefore function upstream of these Rab GTPases (Cai *et al.*, 2007). Several of these complexes (COG, TRAPP I, TRAPP II, and Dsl1) have been shown to interact with coat protein subunits or coat complexes, suggesting the mechanism by which these complexes function in vesicle tethering. Furthermore, many tethering factors (of the coiled-coil and multisubunit types) physically interact with SNAREs or proteins that regulate SNARE-complex formation. There are two mechanisms suggested for these interactions. SNARE interactions could recruit tethering factors to membranes, and/or tethering factors could stimulate *trans*-SNARE complex formation. Both of these models have been shown to be valid for different tethering factors (Cai *et al.*, 2007).

The structural mechanism of how the Dsl1 complex in yeast mediates the tethering and fusion of Golgi-derived COPI-coated vesicles at the ER is well described and does indeed utilize these general themes of Rab, coat, and SNARE binding (Ren *et al.*, 2009). The Dsl1 complex (made up of three subunits: Dsl1, Sec39, and Tip20) is anchored to the ER membrane through interactions between two of its subunits and two

ER SNARE proteins, while the third subunit, at the opposite end of the complex, interacts with COPI-coat subunits on incoming Golgi-derived vesicles (Schmitt and Jahn, 2009). The Dsl1 complex is suggested to trigger vesicle uncoating exposing the v-SNARE protein on the vesicle membrane, and to facilitate *trans*-SNARE complex formation (Schmitt and Jahn, 2009). The involvement of the vesicle coat in the tethering and fusion of transport vesicles has changed previously held views of vesicle uncoating, which was thought to happen almost immediately following vesicle budding; vesicle coats are now thought to remain at least partially intact until the initiation of vesicle tethering. The timing and regulation of the vesicle uncoating process has thus been questioned, and remains to be answered (Trahey and Hay, 2010).

1.5 The Arl1 and Ypt6 Vesicle-Tethering Pathways

Two vesicle-tethering pathways in yeast are regulated by the Arl1 and Ypt6 G proteins. These pathways involve a sequence of protein interactions that result in recruitment of activated Arl1 or activated Ypt6 to the *trans*-Golgi membrane, where these G proteins then recruit and bind their effectors, the long coiled-coil tethering factor Imh1 and the multisubunit tethering complex GARP, respectively (Figure 1.1).

The Arl1 pathway was described in two pairs of papers with complementary findings published simultaneously from two labs (Panic *et al.*, 2003b; Setty *et al.*, 2003; Behnia *et al.*, 2004; Setty *et al.*, 2004). The cascade of molecular interactions required to recruit activated GTP-bound Arl1 to the *trans*-Golgi membrane begins with N-terminal acetylation of the small GTPase Arl3 by the NatC N-terminal acetyltransferase complex, composed of Mak3, Mak10, and a third subunit, Mak31, which itself is not required for the acetylation of Arl3 (Polevoda and Sherman, 2001; Setty *et al.*, 2004). Acetylated Arl3 is then recruited to the *trans*-Golgi membrane through direct binding to the *trans*-Golgi localized integral membrane protein Sys1, which acts as a receptor for acetylated Arl3. The binding of acetylated Arl3 by Sys1 is independent of the nucleotide status of Arl3 (Setty *et al.*, 2004). The human homologues of Sys1 (hSys1) and Arl3 (ARFRP1) are also localized to the Golgi and, like the yeast proteins, hSys1 forms a complex with acetylated ARFRP1 and controls its cellular localization, indicating that the mechanisms in yeast are

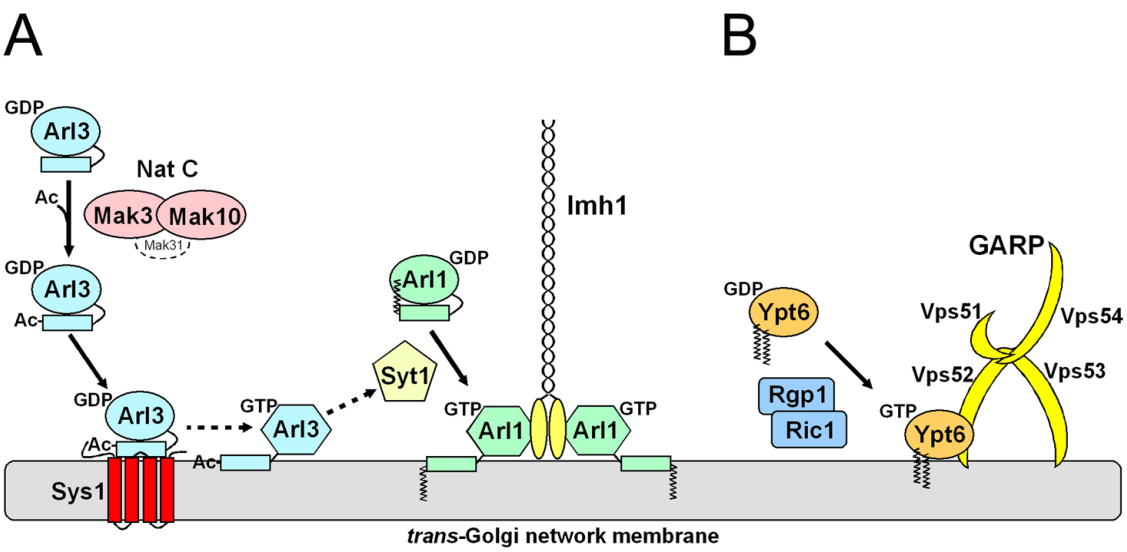

Figure 1.1 The Arl1 and Ypt6 vesicle-tethering pathways. (A) The Arl1 pathway is a cascade of protein interactions that results in the recruitment and activation of Arl1 at the *trans*-Golgi membrane. Activated Arl1 then binds its effector Imh1; see text for details. The interactions comprising the Arl1 pathway are as follows: NatC N-terminally acetylates Arl3; Sys1 acts as a receptor for acetylated Arl3 on the membrane; Arl3 becomes activated, which is required for the activation of Arl1, although exact mechanisms here are not known; Syt1 acts as a GEF, activating Arl1; Arl1 activation results in membrane binding and one activated Arl1 molecule then binds to each GRIP domain of a homodimeric Imh1 molecule. Adapted from (Munro, 2005). (B) The Ypt6 pathway results in the recruitment and activation of Ypt6 at the *trans*-Golgi membrane. Activated Ypt6 then binds its effector GARP; see text for details. The heterodimeric Ric1 – Rgp1 GEF complex activates Ypt6, resulting in its membrane localization. Activated Ypt6 recruits GARP to the membrane through interaction with the Vps52 subunit. Adapted from (Graham, 2004).

likely conserved (Behnia *et al.*, 2004). (A question that remains unresolved is what determines the localization of Sys1 itself to the *trans*-Golgi membrane.) Arl3 is then activated through mechanisms that are not understood but likely involve an Arl3GEF, which remains unidentified. Activated, membrane-bound Arl3 then recruits activated Arl1 to the membrane. Again, the exact mechanism involved is not clear. Nonetheless, activated membrane-bound Arl1 then recruits its effector Imh1 to the *trans*-Golgi membrane. The details of this interaction have been determined and involve two GTP-bound Arl1 proteins that bind the C-terminal GRIP domains of two homodimerized Imh1 proteins (Panic *et al.*, 2003a).

Recently, a protein with GEF activity towards Arl1 was reported. Syt1 has Arl1GEF activity and promotes Arl1 activation and recruitment of Imh1 to the Golgi (Chen *et al.*, 2010). Furthermore, the authors of this Syt1 study suggest that Syt1 is not the only protein in yeast with Arl1GEF activity, and that multiple Arl1GEFs (that are yet to be determined) allow Arl1 to exert distinct biological activities. One possibility for how Arl3 promotes Arl1 activation and membrane localization is that Arl3 (either directly or indirectly) recruits an Arl1GEF to the membrane, where it activates Arl1. This possible mechanism, however, does not appear to be the case for Syt1, because Arl3 does not directly bind Syt1 and the localization of Syt1 to the Golgi does not require Arl3 (Chen *et al.*, 2010). Other possibilities are that Arl3 recruits Arl1 to the membrane either by interacting with Arl1 directly, or indirectly through an effector of Arl3 that interacts with Arl1 (Jackson, 2003). The Arl1 pathway is thought to function in retrograde vesicular transport from endosomes to the *trans*-Golgi (Burd *et al.*, 2004).

Ypt6, the yeast homologue of mammalian Rab6, is a small GTPase in the Rab subfamily of Ras GTPases. Like the Arf proteins described above, Rab proteins cycle between an inactive cytosolic GDP-bound form and an active membrane-localized GTP-bound form, and are regulated by GEF and GAP proteins. The Ypt6 pathway is straightforward compared to the Arl1 pathway, involving the activation and recruitment of Ypt6 to the *trans*-Golgi membrane by its Golgi-localized heterodimeric GEF composed of Ric1 and Rgp1 (Siniossoglou *et al.*, 2000). Activated Ypt6 then recruits its effector, the GARP tethering complex (composed of Vps51, Vps52, Vps53, and Vps54) to the *trans*-Golgi membrane through direct interaction with the Vps52 subunit

(Siniossoglou and Pelham, 2001; Siniossoglou and Pelham, 2002). GARP also binds the N-terminal domain of the yeast t-SNARE Tlg1, which is involved in the fusion of endosome-derived vesicles with the *trans*-Golgi membrane, through direct interaction with the Vps51 subunit (Siniossoglou and Pelham, 2001). Mammalian Vps53 and Vps54 have additionally been shown to bind the SNARE motifs of other SNAREs involved in endosome-to-Golgi transport; moreover, mammalian GARP also binds SNARE complexes, and depletion of GARP decreases the formation of *trans*-Golgi SNARE complexes (Bonifacino and Hierro, 2011). Although the C terminus of the yeast Vps54 subunit of GARP binds endosomes (Quenneville *et al.*, 2006), the receptor(s) for GARP on endosomes and transport vesicles derived from endosomes have not been identified (Bonifacino and Hierro, 2011). Thus, like the Arl1 pathway, Ypt6 and GARP are suggested to function in the retrograde transport pathway from endosomes to the *trans*-Golgi membrane (Conibear and Stevens, 2000; Bensen *et al.*, 2001).

The Arl1 and Ypt6 pathways are each dispensable for viability in yeast; however, elimination of both pathways is lethal, suggesting that the Arl1 and Ypt6 pathways provide redundant function in tethering endosome-derived retrograde-transport vesicles at the *trans*-Golgi membrane (Graham, 2004). Furthermore, there is potential for cross-talk between these two pathways, as activated Arl1 also binds GARP through direct interaction with the Vps53 subunit (Panic *et al.*, 2003b). The biological significance of this finding, however, is not clear. Ypt6 appears to be the primary determinant of GARP localization to the Golgi, because elimination of Ypt6 perturbs GARP localization (Siniossoglou and Pelham, 2001), whereas elimination of Arl1 does not (Panic *et al.*, 2003b). It is possible that GARP is an effector of both Ypt6 and Arl1, or that Ypt6 and Arl1 cooperate in the localization of GARP at the *trans*-Golgi membrane (with Ypt6 playing the dominant role).

1.6 The *gcs1*Δ Reentry Defect

One area of research in our lab has resulted in the identification and characterization of members of the ArfGAP family of proteins in yeast (discussed in the next section). This research on ArfGAPs was initiated because of a mutation that causes an interesting defect in cell proliferation that specifically affects the developmental transition from the

quiescent state (in yeast termed stationary phase) to active cell proliferation (Drebot *et al.*, 1987). The mutant gene responsible for this phenotype was named *GCS1* for growth cold sensitive (Drebot *et al.*, 1987), and further work showed that deletion of the *GCS1* gene results in the same phenotype (Ireland *et al.*, 1994). Stationary-phase *gcs1*Δ cells are impaired for reentry into the proliferative cell cycle at 14°C when stimulated by the addition of fresh medium; in contrast, actively proliferating *gcs1*Δ cells shifted to 14°C continue to proliferate as long as nutrients are available. We have termed this cold-sensitivity phenotype the *gcs1*Δ 'reentry' defect, but also refer to the reentry defect simply as *gcs1*Δ cold sensitivity.

Stationary phase in yeast has been equated to G_0 or quiescence, a non-proliferative resting state that all eukaryotic cells are able to enter during times of suboptimal growth conditions or when triggered to do so by the absence of growth factors (reviewed in Gray *et al.*, 2004). Indeed, most eukaryotic cells spend the majority of their lives in a quiescent state, and exhibit biochemical and physiological differences compared to actively proliferating cells. In the lab, stationary-phase (quiescent) yeast cells are obtained by allowing cells in liquid culture to grow to saturation. As nutrients are depleted from the culture, cells become starved for carbon and respond to this starvation by entering quiescence. These quiescent cells exhibit several characteristic features including a specific transcriptional profile, a decreased rate of protein synthesis, increased autophagy, increased thermotolerance and osmotolerance, an accumulation of storage carbohydrates, a reorganization of the actin cytoskeleton (Sagot *et al.*, 2006), and a thickened cell wall (to name a few). Importantly, quiescence is reversible; upon sensing the return of favourable nutrient conditions quiescent cells are triggered to exit quiescence and reenter the proliferative cell cycle. This transition is accompanied by loss of the characteristic features of quiescent cells. Moreover, resumption of cell proliferation is accomplished when cells complete a process termed 'START' which heralds the onset of S phase of the mitotic cell cycle. Upon completing START the cell is committed to one round of the proliferative cell cycle, which results in duplication of the cell producing a mother and daughter cell, both in the G_1 phase of the cell cycle. Depending on nutrient availability after each round of the mitotic cell cycle, the cell will either divide once again or enter quiescence.

Deletion of the *GCS1* gene creates a cold-sensitive block in resumption of cell proliferation from stationary phase that is manifested before a cell completes 'START' and begins S phase (Drebot *et al.*, 1987). The absence of Gcs1 does not inhibit the ability of stationary-phase cells to sense the resupply of nutrients that trigger the cell to exit quiescence and attempt to reenter the mitotic cell cycle; stationary-phase *gcs1*Δ cells under restrictive conditions are able to sense the resupply of nutrients and mutant cells begin to respond appropriately to this signal. However, *gcs1*Δ cells (under restrictive conditions) become blocked, do not complete START, and do not resume cell proliferation (Drebot *et al.*, 1987; Drebot *et al.*, 1990; Ireland *et al.*, 1994). Since the requirement for Gcs1 is unique to the process of cell-cycle reentry and is not imposed upon cells that are actively dividing, the processes carried out by stationary-phase cells reentering the mitotic cell cycle from quiescence must somehow be different from those carried out by actively dividing cells in preparation for another round of mitotic cell division.

The characterization of the *gcs1*Δ reentry defect caused our lab to appreciate that Gcs1 belongs to the class of proteins termed ArfGAPs that play a regulatory role for vesicular transport. The *GCS1* gene encodes the yeast orthologue of mammalian ArfGAP1 (Poon *et al.*, 1996), and we showed that Gcs1 has ArfGAP activity *in vitro* (Poon *et al.*, 1996). More recently Gcs1 was shown by others to also have Arl1GAP activity *in vitro* (Liu *et al.*, 2005). Furthermore, in addition to the *gcs1*Δ reentry defect, the *gcs1*Δ mutation also results in defective endocytosis in stationary-phase cells at 14°C (Wang *et al.*, 1996). Thus, the Gcs1 protein is required for proliferation from stationary phase (cell-cycle reentry) and for endocytic transport in the cold. The endocytic transport defect of *gcs1*Δ cells is consistent with the function of Gcs1 as a regulator (GAP) for the small GTPases Arf1 and Arl1, which themselves regulate various aspects of vesicular transport, as discussed above (Poon *et al.*, 1996; Liu *et al.*, 2005). This suggests that vesicular-transport processes involving Gcs1 and Arf1 and/or Arl1 may be required for the transition from quiescence to active cell proliferation. Further support for the importance of vesicular transport in cell-cycle reentry came from a screen for yeast genes that, when overexpressed, alleviate the *gcs1*Δ reentry defect (Wang, 1996; Wang *et al.*, 1996). This screen identified overexpression of *IMH1*, encoding a putative vesicle-

tethering factor (Tsukada *et al.*, 1999); *YPT31* and *YPT32*, encoding small GTPases that belong to the Ypt/Rab family and are involved in vesicular transport (Jedd *et al.*, 1997; Chen *et al.*, 2005); *YCK1, YCK2,* and *YCK3*, encoding three membrane-associated casein kinase I isoforms and are involved in vesicular transport (Robinson et al., 1999; Anand et al., 2009); and *CDC55*, encoding a regulatory subunit of protein phosphatase 2A (Wang and Burke, 1997). Furthermore, overexpression of *YCK2* also alleviates the *gcs1*Δ endocytosis defect (Wang *et al.*, 1996), suggesting that these two defects of *gcs1*Δ cells may be linked.

To gain more insight into the nature of the *gcs1*Δ reentry defect, our lab carried out another screen, this time to identify gene deletions in yeast that alleviate the defect (Drysdale, 2006). This screen identified 171 gene deletions that appeared to alleviate *gcs1*Δ cold sensitivity. In my study (chapter 4) I have reassessed these alleviating deletions and confirmed that 92 of the deletions do indeed alleviate *gcs1*Δ cold sensitivity. A number of these deletions were found to disrupt the Golgi localization of Imh1, including deletions of members of the Arl1 and Ypt6 vesicle-tethering pathways, which are thought to provide overlapping function. Because of the identification of multiple alleviating deletions that may provide overlapping function for vesicle tethering at the *trans*-Golgi membrane and the finding that Gcs1 has Arl1GAP activity *in vitro* (Liu *et al.*, 2005), I focused on these alleviating deletions, along with the previously identified alleviation of *gcs1*Δ cold sensitivity by overexpression of *IMH1*. My results suggest that the *gcs1*Δ reentry defect is caused by sequestration of a cellular factor by dysregulated Arl1 due to the absence of a GAP-independent function of Gcs1.

Further objectives of my study and the background for them are presented in the next sections.

1.7 ArfGAP Proteins in Vesicular Transport

The Arf family of small GTPases, which are involved in various vesicular-transport stages (discussed above), require ArfGAPs (Arf GTPase activating proteins) to stimulate and control the hydrolysis of bound GTP. Activated, GTP-bound Arf associates with membranes and with effector proteins responsible for Arf signalling. Hydrolysis of GTP

on Arf inactivates Arf through a conformational change that results in dissociation of Arf from the membrane and termination of Arf signalling by disrupting effector binding. By regulating the inactivation of Arf GTPases, ArfGAPs are themselves involved in the process of vesicular transport. ArfGAPs are characterized by a conserved ArfGAP domain that is ~130 amino acids in length and contains a cysteine-rich zinc-finger motif and a conserved arginine residue with characteristic spacing ($CxxCx_{16}CxxCx_4R$ – where C is cysteine, R is arginine and x is any amino acid) that are required for ArfGAP activity (Goldberg, 1999). There are 31 putative human ArfGAP proteins that each contain the conserved ArfGAP domain based on sequence homology (Kahn *et al.*, 2008; East and Kahn, 2011). The human ArfGAPs are modular proteins that contain an array of domains in addition to the ArfGAP domain, and have been classified into 10 subfamilies based on sequence similarities within the ArfGAP domain and on their overall domain architecture outside of the ArfGAP domain (Kahn *et al.*, 2008; East and Kahn, 2011). The auxiliary domains of the human ArfGAPs facilitate protein-protein and protein-lipid interactions that impart specific localization and function to the various ArfGAP proteins. The human ArfGAPs vary in size from relatively small proteins that resemble the ArfGAPs in yeast (discussed below) to large multi-domain proteins proposed to function as scaffolds for cell signalling or as G-protein regulatory hubs that coordinate the activation of multiple classes of G proteins (Kahn *et al.*, 2008; East and Kahn, 2011).

ArfGAPs display various degrees of specificity for individual Arf substrates in both *in vitro* and *in vivo* assays. In nine of the ten ArfGAP subfamilies, at least one member has ArfGAP activity toward one or more of the human Arf proteins (Arf1-6) (Kahn *et al.*, 2008; East and Kahn, 2011). For the most part ArfGAP proteins discriminate between the Arf, Arl, and Sar G proteins as substrates; however, there are exceptions to this. As mentioned above, the yeast ArfGAP Gcs1 functions as a GAP for yeast Arf1 and Arl1 (Liu *et al.*, 2005), and a human Arl2GAP also functions as a GAP for Arf proteins, despite lacking a canonical ArfGAP domain (Bowzard *et al.*, 2007), suggesting there could be additional proteins that function as GAPs for Arf in addition to those displaying a conserved ArfGAP domain. (No conserved ArlGAP domain has been identified.) Additionally, members of one human ArfGAP subfamily have no detectable ArfGAP activity, and cellular functions of other ArfGAPs have been identified that do

not require ArfGAP activity, indicating that ArfGAPs are not restricted to functioning solely as negative regulators of Arf, but can also have GAP-independent functions (Spang *et al.*, 2010).

The best-studied ArfGAPs are members of the ArfGAP1 and ArfGAP2/3 subfamilies. Functions determined for these ArfGAP proteins have directed models of ArfGAP function in general, but caution should be taken in extrapolating these models to the functions of other ArfGAP proteins, especially the larger multi-domain proteins (East and Kahn, 2011). The classic function proposed for ArfGAPs in vesicular transport is in vesicle uncoating. ArfGAP function is proposed to trigger vesicle uncoating by inactivating Arf1 on Arf1-dependent coated vesicles, causing Arf1–membrane dissociation and resulting in destabilization of the coat to produce an uncoated vesicle. This model was suggested based on the presumed need to remove the vesicle coat to expose v-SNAREs on the membrane for target-compartment recognition and vesicle fusion (Serafini *et al.*, 1991), and was supported by the finding that GTP hydrolysis on Arf is required for dissociation of the COPI coat from vesicles (Tanigawa *et al.*, 1993). Further studies have refined this model; ArfGAP activity and the removal of Arf from the membrane is still thought to be a prerequisite for vesicle uncoating, but due to the experimentally determined timing of Arf1 and COPI membrane dynamics, and several studies that failed to detect Arf1 as a protein component on Arf1-dependent coated vesicles, ArfGAP activity is not likely the trigger for vesicle uncoating. Instead, ArfGAP activity has been suggested to function in vesicle biogenesis, causing the release of Arf1 from the membrane of the nascent vesicle before the vesicle itself is fully detached from the donor membrane (East and Kahn, 2011). Several additional functions of ArfGAPs have been demonstrated, including termination of Arf signalling, functions as effectors of Arf, and even functions independent of Arf and ArfGAP activity (reviewed in East and Kahn, 2011). Functions relevant to vesicular transport include cargo selection, coat recruitment, and SNARE incorporation into vesicles.

1.8 The ArfGAP Family in Yeast

The ArfGAP family in yeast consists of 6 proteins that each contain the conserved ArfGAP domain. These proteins are Gcs1, Glo3, Age1, Age2, Sps18, and Gts1. Four of

these potential ArfGAP proteins (Gcs1, Glo3, Age1, and Age2) have been shown to have ArfGAP activity *in vitro* and are most relevant to the present study (Poon *et al.*, 1996; Poon *et al.*, 1999; Poon *et al.*, 2001; Zhang *et al.*, 2003). Although Gts1 has not been shown biochemically to have ArfGAP activity, it has been proposed to function in endocytosis as a GAP for Arf3 (Smaczynska-de *et al.*, 2008). In contrast, there is no indication that Sps18 has ArfGAP activity or functions in vesicular-transport processes. Sps18 is expressed only during sporulation and may function in the process of spore wall formation (Coe *et al.*, 1994).

Like the human ArfGAP subfamilies, there is little sequence similarity among these proteins outside of the conserved ArfGAP domain, and these differences are thought to enable the various ArfGAP proteins to provide specific functions (Ireland *et al.*, 1994; Zhang *et al.*, 2003). The two best-characterized ArfGAPs in yeast are Gcs1 and Glo3, and these proteins share the modular domain architecture that is found in their human homologues. Gcs1, the yeast homologue of ArfGAP1, has an ALPS motif that localizes Gcs1 to membranes of high curvature such as those of transport vesicles (Bigay *et al.*, 2005), while Glo3, the yeast homologue of ArfGAP2/3, has both a BoCCS (binding of coatomer cargo and SNAREs) motif that binds coatomer, cargo, and SNAREs, and a C-terminal regulatory motif that senses and communicates this binding with the ArfGAP domain (Kliouchnikov *et al.*, 2009; Schindler *et al.*, 2009).

Although Arf activity (provided by the functionally homologous Arf1 and Arf2 pair) is essential in yeast (Stearns *et al.*, 1990), none of the ArfGAPs is individually essential, suggesting a level of redundancy in the functions provided by the ArfGAP proteins. Indeed, there are two essential pairs of ArfGAPs that provide overlapping functions. The Glo3 + Gcs1 pair functions in Golgi-to-ER retrograde transport (Poon *et al.*, 1999), while the Age2 + Gcs1 pair functions in post-Golgi transport (Poon *et al.*, 2001). To facilitate the study of these two transport pathways, our lab has developed a collection of temperature-sensitive *gcs1* mutant alleles that encode mutant forms of Gcs1 with compromised function at 37°C. The *gcs1-3* allele encodes a mutant protein that is unstable at 37°C and is thus impaired for both Glo3-related retrograde transport and Age2-related post-Golgi transport functions; *glo3*Δ *gcs1-3* and *age2*Δ *gcs1-3* cells are impaired for growth at 37°C (Poon *et al.*, 2001). In contrast, the *gcs1-4* allele encodes a

mutant protein that is specifically defective for Age2-related post-Golgi function; *age2*Δ *gcs1-4* cells are impaired for growth at 37°C whereas *glo3*Δ *gcs1-4* cells are not (Wong *et al.*, 2005). Conversely, the *gcs1-28* allele encodes a mutant protein that is specifically defective for Glo3-related retrograde transport; *glo3*Δ *gcs1-28* cells are impaired for growth at 37°C whereas *age2*Δ *gcs1-28* cells are not (Poon *et al.*, 1999; Wong *et al.*, 2005). These temperature-sensitive alleles of *GCS1* have permitted us to investigate the functions of ArfGAPs in these two transport pathways.

Genetic screens have been performed in our lab to identify genes that, when overexpressed, can alleviate the temperature sensitivity caused by defective ArfGAP function in the Glo3-related Golgi-to-ER retrograde transport pathway and the Age2-related post-Golgi transport pathway (Auger, 2000; Lewis, 2004; Wong, 2005; Wong *et al.*, 2005). These screens showed that increased abundance of the Age1 ArfGAP can alleviate temperature sensitivity caused by deficient ArfGAP activity and restore effective vesicular transport in both of these transport pathways (Auger, 2000; Lewis, 2004). Further analysis of the ability of increased Age1 abundance to provide Glo3-related function found that removal of the N terminus of Age1 allows the truncated Age1ΔN protein to function more efficiently (Lewis, 2004), suggesting that the N-terminal sequences of Age1 restrict Age1 function with respect to the Golgi-to-ER retrograde transport pathway. These screens also showed that increased abundance of the phosphatidylinositol transfer protein (PITP) Sfh2 can alleviate temperature sensitivity caused by deficient ArfGAP activity and restore effective vesicular transport in the Age2-related post-Golgi transport pathway, but not the Glo3-related Golgi-to-ER retrograde transport pathway (Wong *et al.*, 2005). Sfh2 is one of the six-member Sec14 family of PITPs in yeast. These proteins facilitate the transfer of phosphatidylinositol from donor membranes to acceptor membranes *in vitro*, and maintain the appropriate levels of phosphatidylinositol 4-phosphate (PI[4]P) for secretory pathway function (Griac, 2007). Overexpression of Sfh2 stimulates phosphatidylinositol 4,5-bisphosphate (PI[4,5]P) synthesis and results in the activation of the yeast phospholipase D, Spo14, which modulates the membrane lipid composition in a manner that is favourable to ArfGAP activity (Griac, 2007). Nonetheless, the mechanism by which increased abundance of Sfh2 restores post-Golgi transport in these cells is not known.

In my study (chapter 3), I have further examined the ability of overexpressed *AGE1* and *SFH2* to alleviate situations of deficient ArfGAP activity. I found that overexpression of these genes can completely bypass the requirement for the essential Age2 + Gcs1 ArfGAP pair. Further analysis of the Sfh2-bypass situation showed that endogenous Age1 is required for efficient growth. Moreover, Spo14 was shown to be required for Age1 to effectively alleviate the deleterious effects of defective Age2 + Gcs1 function. My results suggest that Sfh2-mediated changes in lipid metabolism, produced through the activation of Spo14, allow endogenous Age1 to provide the ArfGAP activity required for post-Golgi transport in the absence of Age2 and Gcs1.

1.9 Overview of My Results

I have examined regulatory interactions involving two ArfGAP family members in yeast, Age1 and Gcs1. My findings show that endogenous Age1 can provide the ArfGAP activity required for post-Golgi transport in the absence of the Age2 + Gcs1 ArfGAP pair, and suggest that Age1 function is regulated by phospholipase-D-mediated changes in membrane lipid composition. Furthermore, my findings have advanced our understanding of Gcs1 function to show that additional activities of Gcs1, independent of its GAP activity, regulate Arl1. Specifically, in the absence of a GAP-independent regulation by Gcs1, the resulting dysregulated Arl1 negatively affects endosomal transport and cell-cycle reentry.

CHAPTER 2. MATERIALS AND METHODS

2.1 Yeast Strains and Plasmids

Yeast strains used in this study are isogenic to either the wild-type diploid strain W303 and its haploid derivatives W303-1A (*MAT***a**) and W303-1B (*MAT*α) (Archambault *et al.*, 1992), or the haploid strains BY4741 (*MAT***a**) and BY4742 (*MAT*α) (Brachmann *et al.*, 1998), and are described in Table 2.1. The plasmids used in this study are listed in Table 2.2.

2.2 Chemicals and Enzymes

The chemicals and reagents used in this study were obtained from Invitrogen (Mississauga, ON) unless otherwise specified. Difco yeast extract, Bacto-yeast nitrogen base, and peptone were obtained from Fisher Scientific (Ottawa, ON).

2.3 Media, Growth Conditions, and Long-Term Storage of Strains

2.3.1 Yeast Growth

For routine growth, yeast cells were propagated in enriched liquid medium (YM-1: 1% succinic acid, 0.6% sodium hydroxide, 0.5% yeast extract, 1% peptone, 0.67% yeast nitrogen base without amino acids with ammonium sulfate, 0.002% adenine, 0.002% uracil, 2% dextrose), or on enriched solid medium (YEPD: 1% yeast extract, 2% peptone, 2% dextrose, and 2% agar) (Hartwell, 1967). To maintain plasmid selection during growth in liquid medium, yeast cells were propagated in synthetic complete medium lacking the amino acid(s) and/or nucleoside base(s) for which marker genes on plasmids rendered the strain prototrophic; all other auxotrophic requirements were satisfied. [Synthetic complete medium: 1% succinic acid, 0.6% sodium hydroxide, 2% dextrose, 0.17% yeast nitrogen base without amino acids or ammonium sulfate, 0.5% ammonium sulfate, supplemented as required with 40 µg/ml of each of the amino acids arginine, aspartate, histidine, isoleucine, leucine, lysine, methionine, phenylalanine, serine, threonine, tryptophan, tyrosine, and valine and 20 µg/ml of each of the nucleoside bases adenine and uracil (Johnston *et al.*, 1977)]. To maintain plasmid selection during growth on solid medium, yeast cells were propagated on solid synthetic complete medium

Table 2.1 Yeast strains used in this study

Strain	Genotype	Source or reference
W303	homozygous diploid *ade2-1 can1-100 his3-11,15 leu2-3,112 trp1-1 ura3-1*	(Archambault *et al.,* 1992)
BY4741	*MAT***a** *his3Δ1 leu2Δ0 ura3Δ0 met15Δ0*	(Brachmann *et al.,* 1998)
BY4742	*MATα his3Δ1 leu2Δ0 ura3Δ0 lys2Δ0 mfa1Δ::MFA1pr-HIS3 can1Δ*	(Brachmann *et al.,* 1998)
JBY122	W303 *MAT*? *age2Δ::HIS3 gcs1Δ::URA3* [pMG4-4]	This study
SL112	W303 *MAT*? *glo3Δ::HIS3 gcs1Δ::URA3* [pSL314.28]	(Lewis, 2004)
AAY10	W303 *age2Δ::HIS3/AGE2 gcs1Δ::URA3/GCS1*	(Benjamin *et al.,* 2011b)
AAY20	W303 *age2Δ::HIS3/AGE2 gcs1Δ::LEU2/GCS1*	(Benjamin *et al.,* 2011b)
JBY26	W303 *glo3Δ::HIS3/GLO3 gcs1Δ::URA3/GCS1*	This study
JBY10	W303 *age2Δ::HIS3/AGE2 gcs1Δ::LEU2/GCS1 age1Δ::nat/AGE1*	This study
JBY12	W303 *age2Δ::HIS3/AGE2 gcs1Δ::URA3/GCS1 sfh2Δ::kan/SFH2*	This study
JBY64	W303 *MAT*? *age2Δ::HIS3 gcs1Δ::LEU2 spo14Δ::kan* [pMG4-4]	This study
JBY65	W303 *MAT*? *age2Δ::HIS3 gcs1Δ::LEU2* [pMG4-4]	This study
JBY33	W303 *MAT*? *age2Δ::HIS3 gcs1Δ::LEU2 spo14Δ::kan* [pMG4-4, pJJ14]	This study
PPY203G-Chc1-28B	W303 *MAT*? *age2Δ::HIS3 gcs1Δ::LEU2 ADE2 CHC1-mRFP::kan* [pMG4-4]	(Benjamin *et al.,* 2011b)
PPY203G-Snf7-5C	W303 *MAT*? *age2Δ::HIS3 gcs1Δ::LEU2 ADE2 SNF7-mRFP::kan* [pMG4-4]	(Benjamin *et al.,* 2011b)
PPY203G-Chc1-11A	W303 *MAT*? *ADE2 CHC1-mRFP::kan*	(Benjamin *et al.,* 2011b)
PPY203G-Snf7-4A	W303 *MAT*? *ADE2 SNF7-mRFP::kan*	(Benjamin *et al.,* 2011b)
PPY169-4	BY4742 *gcs1*Δ::*nat* (query strain)	(Benjamin *et al.,* 2011a)
*arl1*Δ	BY4741 *arl1*Δ*::kan*	(Giaever *et al.,* 2002)
*arl1*Δ *gcs1*Δ	BY4741 *arl1*Δ*::kan gcs1*Δ*::nat*[a]	This study
*arl3*Δ	BY4741 *arl3*Δ*::kan*	(Giaever *et al.,* 2002)
*arl3*Δ *gcs1*Δ	BY4741 *arl3*Δ*::kan gcs1*Δ*::nat*[a]	This study
*sys1*Δ	BY4741 *sys1*Δ*::kan*	(Giaever *et al.,* 2002)
*sys1*Δ *gcs1*Δ	BY4741 *sys1*Δ*::kan gcs1*Δ*::nat*[a]	This study
*mak3*Δ	BY4741 *mak3*Δ*::kan*	(Giaever *et al.,* 2002)
*mak3*Δ *gcs1*Δ	BY4741 *mak3*Δ*::kan gcs1*Δ*::nat*[a]	This study
*mak10*Δ	BY4741 *mak10*Δ*::kan*	(Giaever *et al.,* 2002)
*mak10*Δ *gcs1*Δ	BY4741 *mak10*Δ*::kan gcs1*Δ*::nat*[a]	This study
*mak31*Δ	BY4741 *mak31*Δ*::kan*	(Giaever *et al.,* 2002)
*mak31*Δ *gcs1*Δ	BY4741 *mak31*Δ*::kan gcs1*Δ*::nat*[a]	This study
*syt1*Δ	BY4741 *syt1*Δ*::kan*	(Giaever *et al.,* 2002)
*syt1*Δ *gcs1*Δ	BY4741 *syt1*Δ*::kan gcs1*Δ*::nat*[a]	This study
*ypt6*Δ	BY4741 *ypt6*Δ*::kan*	(Giaever *et al.,* 2002)
*ypt6*Δ *gcs1*Δ	BY4741 *ypt6*Δ*::kan gcs1*Δ*::nat*[a]	This study
*ric1*Δ	BY4741 *ric1*Δ*::kan*	(Giaever *et al.,* 2002)

Strain	Genotype	Source or reference
*ric1*Δ *gcs1*Δ	BY4741 *ric1*Δ*::kan gcs1*Δ*::nat*[a]	This study
*rgp1*Δ	BY4741 *rgp1*Δ*::kan*	(Giaever *et al.,* 2002)
*rgp1*Δ *gcs1*Δ	BY4741 *rgp1*Δ*::kan gcs1*Δ*::nat*[a]	This study
*ypr050C*Δ	BY4741 *ypr050C*Δ*::kan*	(Giaever *et al.,* 2002)
*ylr261c*Δ	BY4741 *ylr261c*Δ*::kan*	(Giaever *et al.,* 2002)
*ydr136c*Δ	BY4741 *ydr136c*Δ*::kan*	(Giaever *et al.,* 2002)
*mnn9*Δ	BY4741 *mnn9*Δ*::kan*	(Giaever *et al.,* 2002)
*rpe1*Δ	BY4741 *rpe1*Δ*::kan*	(Giaever *et al.,* 2002)
*rpl43a*Δ	BY4741 *rpl43a*Δ*::kan*	(Giaever *et al.,* 2002)
JBY72-21B	W303 *MAT*? *ADE2*	This study
JBY72-12B	W303 *MAT*? *ADE2 gcs1*Δ*::nat*	This study
JBY72-26C	W303 *MAT*? *ADE2 gcs1*Δ*::nat*	This study
JBY72-13C	W303 *MAT*? *ADE2 arl1*Δ*::kan*	This study
JBY72-14B	W303 *MAT*? *ADE2 arl1*Δ*::kan*	This study
JBY72-3A	W303 *MAT*? *ADE2 gcs1*Δ*::nat arl1*Δ*::kan*	This study
JBY72-44D	W303 *MAT*? *ADE2 gcs1*Δ*::nat arl1*Δ*::kan*	This study
JBY72-11D	W303 *MAT*? *ADE2 gcs1*Δ*::nat imh1*Δ*::HIS3*	This study
JBY72-10C	W303 *MAT*? *ADE2 arl1*Δ*::kan imh1*Δ*::HIS3*	This study
JBY72-4C	W303 *MAT*? *ADE2 gcs1*Δ*::nat arl1*Δ*::kan imh1*Δ*::HIS3*	This study
JBY72-24C	W303 *MAT*? *ADE2 imh1*Δ*::HIS3*	This study
JBY120-1C	W303 *MAT*? *ADE2*	This study
JBY120-2B	W303 *MAT*? *ADE2*	This study
JBY120-2A	W303 *MAT*? *ADE2 ypt6*Δ*::kan*	This study
JBY120-5C	W303 *MAT*? *ADE2 ypt6*Δ*::kan*	This study
JBY120-5A	W303 *MAT*? *ADE2 gcs1*Δ::*nat*	This study
JBY120-6C	W303 *MAT*? *ADE2 gcs1*Δ::*nat*	This study
JBY120-1B	W303 *MAT*? *ADE2 gcs1*Δ::*nat ypt6*Δ*::kan*	This study
JBY120-2C	W303 *MAT*? *ADE2 gcs1*Δ::*nat ypt6*Δ*::kan*	This study
JBY113	W303 *imh1*Δ*::HIS3/IMH1 ypt6*Δ*::kan/YPT6*	This study
JBY3	W303 *MAT*? *gcs1*Δ::*nat*	This study
JBY29	W303 *MAT*? *gcs1*Δ*::LEU2 age2*Δ*::HIS3* [pMG4-4]	This study
JBY31	W303 *MAT*? *gcs1*Δ*::LEU2 age2*Δ*::HIS3* [pLAA314-3]	This study
JBY70	W303 *MAT*? *gcs1*Δ*::LEU2 age2*Δ*::HIS3* [pTW12]	This study
PPY147.28.2a	W303 *MAT*? *gcs1*Δ*::URA3 glo3*Δ*::HIS3* [pPP805.28]	(Poon *et al.,* 1999)
JBY18	W303 *MAT*? *glo3*Δ*::HIS3*	This study
*vps51*Δ	BY4741 *vps51*Δ*::kan*	(Giaever *et al.,* 2002)

Strain	Genotype	Source or reference
*vps52*Δ	BY4741 *vps52*Δ*::kan*	(Giaever *et al.,* 2002)
FRY107	BY4741 vps53Δ*::kan*	(Reggiori *et al.,* 2003)
*vps54*Δ	BY4741 *vps54*Δ*::kan*	(Giaever *et al.,* 2002)
JBY103	W303 *gcs1*Δ::*nat/GCS1 vps51*Δ*::kan/VPS51*	This study
JBY104	W303 *gcs1*Δ::*nat/GCS1 vps52*Δ*::kan/VPS52*	This study
JBY105	W303 *gcs1*Δ::*nat/GCS1* vps53Δ*::kan/VPS53*	This study
JBY106	W303 *gcs1*Δ::*nat/GCS1 vps54*Δ*::kan/VPS54*	This study
JBY85	W303 *gcs1*Δ::*na/GCS1t arl1*Δ*::URA3/ARL1 vps51*Δ*::kan/VPS51*	This study
JBY86	W303 *gcs1*Δ::*nat/GCS1 arl1*Δ*::URA3/ARL1 vps52*Δ*::kan/VPS52*	This study
JBY87	W303 *gcs1*Δ::*nat/GCS1 arl1*Δ*::URA3/ARL1* vps53Δ*::kan/VPS53*	This study
JBY88	W303 *gcs1*Δ::*nat/GCS1 arl1*Δ*::URA3/ARL1 vps54*Δ*::kan/VPS54*	This study
JBY114	W303 *arl1*Δ*::URA3/ARL1 ypt6*Δ*::kan/YPT6*	This study
JBY1670:1	W303 *ypt6*Δ*::URA3/YPT6 vps51*Δ*::kan/VPS51*	This study
JBY1670:3	W303 *ypt6*Δ*::URA3/YPT6 vps52*Δ*::kan/VPS52*	This study
JBY1670:5	W303 *ypt6*Δ*::URA3/YPT6* vps53Δ*::kan/VPS53*	This study
JBY1670:8	W303 *ypt6*Δ*::URA3/YPT6 vps54*Δ*::kan/VPS54*	This study

[a]Haploid segregant from BY4741 *orf*Δ::*kan* x PPY169-4 cross; status of alleles other than those marked by *kan* and *nat* were not determined.

Table 2.2 Plasmids used in this study

Plasmid	Descritption	Reference
pJB1711	2μ[a] *HIS3* *GFP-IMH1*	This study
pEP1	2μ *LEU2* *GCS1*	(Benjamin *et al.,* 2011b)
pRS425	2μ *LEU2* vector	(Christianson *et al.,* 1992)
pSL377	2μ *LEU2* *AGE1*	(Benjamin *et al.,* 2011b)
pSL489	2μ *LEU2* *AGE1ΔN* (167-482)[c]	(Benjamin *et al.,* 2011b)
pSL494	*CEN*[b] *LEU2* *AGE1ΔN* (167-482)	(Benjamin *et al.,* 2011b)
pSL340	*CEN* *LEU2* *AGE1*	(Benjamin *et al.,* 2011b)
pSL485	2μ *LEU2* *AGE1*promoter	(Benjamin *et al.,* 2011b)
pRS315	*CEN* *LEU2* vector	(Sikorski and Hieter, 1989)
pJB315-AGE1-61	*CEN* *LEU2* *AGE1* (61-482)	This study
pJB315-AGE1-71	*CEN* *LEU2* *AGE1* (71-482)	This study
pJB315-AGE1-81	*CEN* *LEU2* *AGE1* (81-482)	This study
pJB315-AGE1-91	*CEN* *LEU2* *AGE1* (91-482)	This study
pJB315-AGE1-101	*CEN* *LEU2* *AGE1* (101-482)	This study
pJB315-AGE1-111	*CEN* *LEU2* *AGE1* (111-482)	This study
pJB315-AGE1-121	*CEN* *LEU2* *AGE1* (121-482)	This study
pJB315-AGE1-131	*CEN* *LEU2* *AGE1* (131-482)	This study
pJB315-AGE1-141	*CEN* *LEU2* *AGE1* (141-482)	This study
pJB315-AGE1-161	*CEN* *LEU2* *AGE1* (161-482)	This study
pJB351-AGE1-61	2μ *LEU2* *AGE1* (61-482)	This study
pJB351-AGE1-71	2μ *LEU2* *AGE1* (71-482)	This study
pJB351-AGE1-81	2μ *LEU2* *AGE1* (81-482)	This study
pJB351-AGE1-91	2μ *LEU2* *AGE1* (91-482)	This study
pJB351-AGE1-101	2μ *LEU2* *AGE1* (101-482)	This study
pJB351-AGE1-111	2μ *LEU2* *AGE1* (111-482)	This study
pJB351-AGE1-121	2μ *LEU2* *AGE1* (121-482)	This study
pJB351-AGE1-131	2μ *LEU2* *AGE1* (131-482)	This study
pJB351-AGE1-141	2μ *LEU2* *AGE1* (141-482)	This study
pJB351-AGE1-161	2μ *LEU2* *AGE1* (161-482)	This study
pPPL38	2μ *LEU2* *GLO3*	Dr. Pak Phi Poon
pPP805.28	*CEN* *LEU2* *gcs1-28*	(Poon *et al.,* 1999)
pKO	*CEN* *LEU2* *GFP-SEC7* from *TPI1* promoter	(Panic *et al.,* 2003b)
pVPS54-GFP	*CEN* *LEU2* *VPS54-GFP* from *VPS54* promoter	(Panic *et al.,* 2003b)
pR54A315	*CEN* *LEU2* *gcs1-R54A*	This study
pR54K315	*CEN* *LEU2* *gcs1-R54K*	This study

Plasmid	Descritption	Reference
pR54Q315	*CEN LEU2 gcs1-R54Q*	This study
pR54A425	2µ *LEU2 gcs1-R54A*	This study
pR54K425	2µ *LEU2 gcs1-R54K*	This study
pR54Q425	2µ *LEU2 gcs1-R54Q*	This study
pSH4	*CEN LEU2 GCS1*	(Robinson *et al.,* 2006)
pXW110	*CEN LEU2 IMH1*	(Benjamin *et al.,* 2011a)
pSL344	2µ *LEU2 AGE2*	(Lewis, 2004)
pJBVPS53-425	2µ *LEU2 VPS53*	This study
pLC998	2µ *LEU2 VPS54*	(Quenneville *et al.,* 2006)
pJB1598-9	2µ *LEU2 GFP-IMH1*	This study
pGCS1-314	*CEN TRP1 GCS1*	This study
pRS314	*CEN TRP1* vector	(Sikorski and Hieter, 1989)
pLAA314-3	*CEN TRP1 gcs1-3*	(Wong *et al.,* 2005)
pMG4-4	*CEN TRP1 gcs1-4*	(Wong *et al.,* 2005)
pSL314.28	*CEN TRP1 gcs1-28*	(Lewis, 2004)
pGCS1 1-162	*CEN TRP1 GCS1* (1-162)	Dr. Dan Cassel
pGCS1 1-189	*CEN TRP1 GCS1* (1-189)	Dr. Dan Cassel
pGCS1 1-200	*CEN TRP1 GCS1* (1-200)	Dr. Dan Cassel
pGCS1 1-211	*CEN TRP1 GCS1* (1-211)	Dr. Dan Cassel
pGCS1 1-292	*CEN TRP1 GCS1* (1-292)	Dr. Dan Cassel
pGCS1 1-314	*CEN TRP1 GCS1* (1-314)	Dr. Dan Cassel
pGCS1 L246A	*CEN TRP1 GCS1-L246A*	Dr. Dan Cassel
pGCS1 1-L246D	*CEN TRP1 GCS1-L246D*	Dr. Dan Cassel
pGCS1 1-F296D	*CEN TRP1 GCS1-F296D*	Dr. Dan Cassel
pGCS1 1-VI268/9AA	*CEN TRP1 GCS1-VI268,269AA*	Dr. Dan Cassel
pLK	*CEN TRP1 GFP-IMH1* from *TPI1* promoter	(Panic *et al.,* 2003b)
pLL	*CEN TRP1 GFP-IMH1-Y870A* from *TPI1* promoter	(Panic *et al.,* 2003b)
pGRIP-177	*CEN TRP1 GFP-IMH1*(734-911) from *TPI1* promoter	This study
pRS426	2µ *URA3* vector	(Christianson *et al.,* 1992)
pGCS1-316	*CEN URA3 GCS1*	This study
pRS316	*CEN URA3* vector	(Sikorski and Hieter, 1989)
pJB1736	*CEN URA3 AGE1ΔN* (167-482)	This study
pJB1737	2µ *URA3 AGE1ΔN* (167-482)	This study
pSL473	2µ *URA3 AGE1*	(Benjamin *et al.,* 2011b)
pPP421	2µ *URA3 GCS1*	(Benjamin *et al.,* 2011b)
pRS426	2µ *URA3* vector	(Christianson *et al.,* 1992)

Plasmid	Descritption			Reference
pCTY201	2µ	*URA3*	*SFH2*	(Li *et al.,* 2000)
pRS426-SPO14	2µ	*URA3*	*SPO14*	This study
pRS426-MSS4	2µ	*URA3*	*MSS4*	Dr. Scott Emr
pRS426-PIK1	2µ	*URA3*	*PIK1*	Dr. Scott Emr
pRS426-STT4	2µ	*URA3*	*STT4*	Dr. Scott Emr
pJB-Age1-GFP	*CEN*	*URA3*	$GAL1_{prom}$ *-AGE1-GFP*	This study
pPPL149	*CEN*	*URA3*	$GAL1_{prom}$*-AGE1ΔN-GFP*	(Benjamin *et al.,* 2011b)
pTW12	*CEN*	*URA3*	*gcs1-4*	(Wong, 2005)
pSR15	2µ	*URA3*	*GFP-IMH1*	(Setty *et al.,* 2003)
p2T	*CEN*	*URA3*	*ARL1-GFP* from *PHO5* promoter	(Panic *et al.,* 2003b)
p6J	*CEN*	*URA3*	*SYS1-GFP* from *SYS1* promoter	(Behnia *et al.,* 2003b)
pR54A316	*CEN*	*URA3*	*gcs1-R54A*	This study
pR54K316	*CEN*	*URA3*	*gcs1-R54K*	This study
pR54Q316	*CEN*	*URA3*	*gcs1-R54Q*	This study
pR54A426	2µ	*URA3*	*gcs1-R54A*	This study
pR54K426	2µ	*URA3*	*gcs1-R54K*	This study
pR54Q426	2µ	*URA3*	*gcs1-R54Q*	This study
pJBARL1-316	*CEN*	*URA3*	*ARL1*	This study
pARY1-3	2µ	*URA3*	*ARL1*	(Rosenwald *et al.,* 2002)
pSR39	*CEN*	*URA3*	*ARL1-Q72L*	Dr. Christopher Burd
pJBARL1Q-426	2µ	*URA3*	*ARL1-Q72L*	This study
pSR44	*CEN*	*URA3*	*ARL1-T32N*	Dr. Christopher Burd
pJBARL1T-426	2µ	*URA3*	*ARL1-T32N*	This study
pPPL103	2µ	*nat*	vector	Dr. Pak Phi Poon
pJJ14	2µ	*nat*	*SPO14*	This study
pPPL21	*E. coli* expression Gcs1			(Poon *et al.,* 1996)
pSL396	*E. coli* expression Age1ΔN			(Benjamin *et al.,* 2011b)
pPPL21	*E. coli* expression His6-Gcs1			(Poon *et al.,* 1996)
pPP14:142	*E. coli* expression His6-Gcs1-R54K			(Benjamin *et al.,* 2011a)
pET-Arf1	*E. coli* expression Arf1-His6			(Poon *et al.,* 1996)
pRA8	*E. coli* expression Arl1-His6			(Benjamin *et al.,* 2011a)
pACY177/ET3d/yNMT	*E. coli* expression Nmt1 (N-myristoyl transferase)			(Haun et al., 1993)

[a]high-copy, [b]low-copy, [c]bracketed numbers indicate encoded amino acids

(1% succinic acid, 0.6% sodium hydroxide, 2% dextrose, 0.17% yeast nitrogen base without amino acids or ammonium sulfate, 0.5% ammonium sulfate, and 2% agar) lacking the amino acid(s) and/or nucleoside base(s) for which marker genes on plasmids rendered the strain prototrophic. All other nutritional requirements were provided as follows: 0.5% arginine, 0.8% aspartate, 0.2% histidine, 0.5% isoleucine, 1% leucine, 0.5% lysine, 0.2% methionine, 0.5% phenylalanine, 0.2% serine, 1% threonine, 0.5% tryptophan, 0.5% tyrosine, 1.4% valine, 0.1% adenine, and 0.2% uracil. The inhibitory drugs nourseothricin and G418 were used for plasmid selection, for strain construction, and to track the genetic marker genes *nat* and *kan*, respectively. These drugs were added to the yeast media described above at 100mg/L (nourseothricin) or 200 mg/L (G418). Selective medium containing these drugs was made with 0.1% monosodium glutamic acid as the nitrogen source in place of ammonium sulfate because ammonium sulfate impedes the function of these drugs (Tong *et al.*, 2001).

Growth temperatures varied depending on the experiment. For standard growth, yeast cells were incubated at either 23°C or 30°C. Prior to being used in any experiments, temperature-sensitive yeast cells were grown at the permissive temperature of 23°C rather than 30°C to minimize stress and avoid accumulation of suppressor mutations. Temperature-sensitivity experiments were carried out at the restrictive temperature of 37°C, with permissive-temperature controls incubated at either 23°C or 30°C. Prior to being used in any experiments, cold-sensitive yeast cells were grown at the permissive temperature of 30°C rather than 23°C to minimize stress and avoid accumulation of suppressor mutations. Cold-sensitivity experiments were carried out at the restrictive temperature of 14°C, with permissive-temperature controls incubated at either 23°C or 30°C. Cold-sensitive yeast cells were never stored at 4°C to avoid the potential accumulation of suppressor mutations.

2.3.2 *Escherichia coli* Growth

Escherichia coli (*E. coli*) cells were propagated at 37°C in 2xYT medium (1% yeast extract, 1.6% tryptone, and 0.5% NaCl) or on solid 2xYT medium containing 2% agar (Messing, 1983). Ampicillin was added to 2xYT medium at a concentration of 50 µg/ml to select for *E. coli* cells containing plasmids carrying the β-lactamase gene that confers resistance to the antibiotic ampicillin. 2xYT medium containing ampicillin was stored at

4°C to minimize degradation of the drug. The *E. coli* strain TOP 10 was used for plasmid propagation and long-term plasmid storage.

2.3.3 Long-Term Storage Conditions

Yeast strains (Table 2.1) and *E. coli* cells carrying plasmids (Table 2.2) generated in this study were frozen at –80°C in 25% glycerol for long-term storage.

2.4 Routine Molecular Biology Techniques

2.4.1 Isolation of Plasmid DNA From *E. coli* Cells

Plasmid DNA was isolated from *E. coli* cells using either the Invitrogen Quick Plasmid Miniprep Kit (Invitrogen, Mississauga, ON) according to the manufacturer's instructions, or an alkaline lysis protocol essentially as described by Birnboim (1983). The alkaline lysis procedure was used when highly pure DNA was not required, such as when plasmid DNA was isolated from multiple *E. coli* transformants for diagnostic purposes to confirm cloning success. For alkaline lysis, *E. coli* cells inoculated from a single colony were grown overnight in 2xYT medium containing ampicillin at 37°C. Cells from a 1.5-ml sample were harvested by centrifugation at 15,000 rpm for 1 minute in a microcentrifuge. The cell pellet was then thoroughly suspended in 100 µl GTE solution (50 mM glucose, 25 mM Tris-Cl pH 8, 10 mM EDTA) and incubated at room temperature for 5 minutes. 200 µl of alkaline solution (0.2 M NaOH and 1% [w/v] sodium dodecyl sulfate [SDS]) was added, the tube was inverted to mix and then incubated at room temperature for 5 minutes to allow cell lysis to occur. To neutralize the solution, 150 µl of 3 M potassium acetate pH 4.8 was added and the solution was vortexed to mix. The cell debris was then removed by centrifugation at 15,000 rpm for 15 minutes, and the supernatant was transferred to a new tube. Ice-cold 95% ethanol was added to a final concentration of 70%, and the solution was incubated at room temperature for 2 minutes to precipitate plasmid DNA from the supernatant. The DNA was pelleted by centrifugation at 15,000 rpm for 1 minute, and the pellet was washed with 70% ethanol to remove excess salt. After drying to remove the ethanol, DNA pellets were suspended in ~20 µl ddH_2O or TE buffer (10 mM Tris-Cl pH 8, 1 mM EDTA).

2.4.2 Isolation of Plasmid DNA From Yeast Cells

Plasmid DNA was isolated from yeast cells using a glass-bead disruption protocol essentially as described by Hoffman (1997). Yeast cells inoculated from a single colony were grown overnight in selective medium at 30°C; cells from a 1.5-ml sample of culture were harvested by centrifugation at 15,000 rpm in a microcentrifuge for 10 seconds. The supernatant was removed and the cell pellet was disrupted by vortexing. The cells were then suspended in 200 µl breaking buffer (2% Triton X-100, 1% SDS, 100 mM NaCl, 10 mM Tris-Cl pH 8, 1 mM EDTA) to which 0.3 g of acid-washed glass beads (~200 µl volume) and 200 µl of phenol/chloroform/isoamyl alcohol (25/24/1) were added. This mixture was vortexed for ~2 minutes at high speed, followed by centrifugation at 15,000 rpm for 5 minutes. The resulting aqueous layer was transferred to a new tube and treated differently depending on the downstream application. For transformation into *E. coli* cells, 1-5 µl was used for electroporation into competent cells, whereas 15 µl was used for transformation of yeast cells. For PCR use, ice-cold 95% ethanol was added to a final concentration of 70%, and after inverting to mix, the solution was incubated at –20°C for 10 minutes to precipitate the plasmid DNA. The DNA was pelleted by centrifugation at 15,000 rpm for 15 minutes at 4°C, and the pellet was washed with 70% ethanol to remove excess salt. After drying to remove the ethanol, DNA pellets were suspended in 50 µl ddH_2O and 1 µl was used as template in a 20-µl PCR reaction.

2.4.3 Isolation of Chromosomal DNA From Yeast Cells

Chromosomal DNA was isolated from yeast cells using a scaled-up version of the protocol used to isolate plasmid DNA from yeast cells (Hoffman, 1997). Yeast cells inoculated from a cell colony were grown overnight in 5 ml of YM-1 medium at 30°C and then pelleted by centrifugation and washed once in 500 µl ddH_2O. The cells were then suspended in 200 µl breaking buffer (2% Triton X-100, 1% SDS, 100 mM NaCl, 10 mM Tris-Cl pH 8, 1 mM EDTA) to which 0.3 g of acid-washed glass beads (~200 µl volume) and 200 µl of phenol/chloroform/isoamyl alcohol (25/24/1) were added. This mixture was then vortexed for ~3 minutes at high speed and 200 µl TE buffer was added before centrifugation at 15,000 rpm for 5 minutes. The resulting aqueous layer was transferred to a new tube. Ice-cold 95% ethanol was added to a final concentration of

70% to precipitate the nucleic acids, which were then pelleted by centrifugation at 15,000 rpm for 3 minutes, dried to remove the ethanol, and suspended in 400 µl of TE buffer. RNA was degraded by adding 30 µl of 1 mg/ml DNase-free RNase A and incubating at 37°C for 5 minutes. The DNA was then precipitated by first adding 10 µl of 4 M ammonium acetate and then ice-cold 95% ethanol to a final concentration of 70%. The DNA was pelleted by centrifugation at 15,000 rpm for 3 minutes, dried to remove the ethanol, and suspended in 100 µl TE buffer. For PCR, 1 µl was used as template in a 20-µl PCR reaction.

2.4.4 Restriction Digestion of DNA

Restriction digests were used to produce DNA fragments with compatible ends for cloning, and for diagnostic purposes. DNA was digested using restriction enzymes (Invitrogen, Mississauga, ON) with the supplied buffers according to the manufacturer's recommendations.

2.4.5 Purification of DNA Fragments

DNA fragments for cloning were isolated from enzymes and/or undesired DNA fragments in two ways. To purify a DNA fragment from large (>300 bp) undesired DNA fragments and enzymes, the DNA fragments were separated by agarose gel electrophoresis and the band made up of the desired fragment was purified using the Invitrogen Quick Gel Extraction Kit (Invitrogen, Mississauga, ON) according to the manufacturer's instructions. To purify a DNA fragment from small (<300 bp) undesired DNA fragments and/or enzymes, the Invitrogen PCR purification Kit (Invitrogen, Mississauga, ON) was used according to the manufacturer's instructions.

2.4.6 DNA Ligations

Ligation of DNA fragments was carried out using T4 DNA ligase (Invitrogen, Mississauga, ON) according to the manufacturer's instructions. When cloning an insert into a vector backbone, a vector-only ligation reaction was set up as a control to assess the background levels of undigested or re-circularized vector in the ligation. 2 µl of ligation reactions were used directly for electroporation of 80 µl of competent *E. coli* cells.

2.4.7 PCR Amplification

DNA fragments were amplified by PCR for cloning, yeast transformation by homologous recombination, and diagnostic purposes. Depending on the application, different DNA polymerases were used; each was obtained from Invitrogen (Mississauga, ON) and was used according to the manufacturer's instructions. For diagnostic amplifications, when fidelity was not required, either *Taq* DNA polymerase or Platinum® *Taq* DNA polymerase was used. In contrast, Platinum® *Taq* DNA polymerase high fidelity or Platinum® *Pfx* DNA polymerase where used when high fidelity was required, because these enzymes possess a proofreading 3'-to-5' exonuclease activity.

Templates for PCR amplifications varied; plasmid DNA and yeast chromosomal DNA were used. Yeast colonies and *E. coli* colonies were also used in place of DNA template. For *E. coli* colony PCR, DNA template was omitted from the PCR reaction mix and bacterial cells from a single colony were transferred to the bottom of the PCR tube prior to adding the PCR reaction mix to the tube. Yeast colony PCR was carried out in a similar fashion to *E. coli* colony PCR except that after being transferred to the PCR tube the yeast cells were microwaved at high power for 2 minutes, and after adding the reaction mix to the tube, the tube was gently flicked to suspend the cells. When high fidelity was required with yeast colony PCR, Platinum® *Taq* DNA polymerase high fidelity was used because Platinum® *Pfx* DNA polymerase did not perform well under these conditions. All PCR reactions were assembled in 0.2-ml thin-walled microcentrifuge tubes and were cycled in a heated-top thermocycler (MJ Research, Waltham, MA).

Oligonucleotides used as 'primers' in PCR reactions were purchased from Invitrogen (Mississauga, ON). Primers were designed to be 17-28 bp in length, and to terminate (3') with a G, C, CG, or GC whenever possible to prevent 'breathing' at the 3' end and increase priming efficiency. Runs of three or more Gs or Cs in a row were avoided at the 3' end of primers to decrease mispriming at G- or C-rich sequences. The melting temperatures (Tm) of primers were designed to be between 55-80°C and were estimated by allotting 2°C for every A or T and 4°C for every G or C in the sequence. Melting temperatures for primer pairs were matched. When the amplified fragment was to be cloned, restriction enzyme sites were added to the 5' ends of the primers and were

preceded at their 5' end by 6 Cs. This was done to maximize the efficiency of restriction enzyme digestion.

2.4.8 DNA Sequencing

Fluorescent-dye terminator DNA sequencing was performed by the DNA sequencing facility at Robarts Research Institute (London, ON). The sequencing data generated by Robarts was analyzed using ChromasPro software (Technelysium Pty Ltd, Brisbane, Australia). Standard primers were used for sequencing plasmid inserts and were provided by Robarts. When custom primers were required they were designed as outlined above for PCR primer design and were obtained from Invitrogen (Mississauga, ON).

2.5 Plasmid Construction

The plasmids generated in this study were constructed as follows:

pGCS1-314 (*GCS1 – CEN – TRP1*): A ~1850-bp *Eco*RI/*Bam*HI fragment containing the *GCS1* ORF along with ~340 bp of upstream flanking sequence and ~450 bp of downstream flanking sequence was subcloned from pPP421 into the pRS314 backbone.

pGCS1-316 (*GCS1 – CEN – URA3*): A ~1850-bp *Eco*RI/*Bam*HI fragment containing the *GCS1* ORF along with ~340 bp of upstream flanking sequence and ~450 bp of downstream flanking sequence was subcloned from pPP421 into the pRS316 backbone.

pJB1736 (*AGE1*Δ*N – CEN – URA3*): A ~1.9-kbp *Bam*HI/*Sal*I fragment containing the *AGE1*Δ*N* allele under the control of the *AGE1* promoter along with ~300 bp of downstream flanking sequence was subcloned from pSL494 into the pRS316 backbone.

pJB1737 (*AGE1*Δ*N – 2*μ *– URA3*): A ~1.9-kbp *Bam*HI/*Sal*I fragment containing the *AGE1*Δ*N* allele under the control of the *AGE1* promoter along with ~300 bp of downstream flanking sequence was subcloned from pSL494 into the pRS426 backbone.

pJB-Age1-GFP (*GAL1*$_{\mathbf{prom}}$*-AGE1-GFP – CEN – URA3*): The *AGE1* ORF was amplified by PCR from pSL340 and cloned into the pGREG600 vector by *in vivo* ligation (homologous recombination) in yeast (Jansen *et al.*, 2005).

pRS426-SPO14 (*SPO14 – 2*μ *– URA3*): A ~6-kbp *Xho*I/*Sst*II fragment containing the *SPO14* ORF along with ~560 bp of upstream flanking sequence and ~320 bp of downstream flanking sequence was subcloned from pKR325 (Rose *et al.*, 1995) into the pRS426 backbone. Sequencing confirmed that the insert contains the proper sequence.

pJJ14 (*SPO14* – 2μ – *nat*): A ~6-kbp *Not*I/*Xho*I fragment containing the *SPO14* ORF along with ~560 bp of upstream flanking sequence and ~320 bp of downstream flanking sequence was subcloned from pKR325 into the pPPL103 backbone.

pJB1711 (*GFP-IMH1* – 2μ – *HIS3*): A ~4-kbp *Bam*HI/*Sal*I fragment containing *GFP-IMH1* coding sequence was subcloned from pSR15 into the pRS423 backbone.

pJB1598-9 (*GFP-IMH1* – *CEN* – *TRP1*): A ~4-kbp *Bam*HI/*Sal*I fragment containing *GFP-IMH1* coding sequence was subcloned from pSR15 into the pRS425 backbone.

pGRIP-177: An *Eco*RI digest was used to remove all *IMH1* coding sequence from pLK. A ~700-bp region of *IMH1* including the 534 bp of the *IMH1* ORF (encoding the C-terminal 177 residues of Imh1) and ~180 bp of downstream flanking sequence was amplified by PCR from pLK and cloned back into the *EcoRI*-digested pLK backbone. Sequencing confirmed that this plasmid encodes an N-terminally tagged GFP-Imh1 GRIP-domain fusion protein encompassing the C-terminal 177 amino acids of Imh1, which is expressed from the *TPI1* promoter.

pJBARL1-316 (*ARL1* – *CEN* – *URA3*): A ~1.5-kbp *Eco*RI/*Hind*III fragment containing the *ARL1* ORF along with ~500 bp of upstream flanking sequence and ~500 bp of downstream flanking sequence was subcloned from pARY1-3 into the pRS316 backbone.

pJBARL1Q-426 (*ARL1-Q72L* – 2μ – *URA3*): A ~1.2-kbp *Not*I/*Bam*HI fragment containing the *ARL1-Q72L* allele along with ~370 bp of upstream flanking sequence and ~180 bp of downstream flanking sequence was subcloned from pSR39 into the pRS426 backbone. Sequencing confirmed that the desired point mutation is the only change in the *ARL1* ORF.

pJBARL1T-426 (*ARL1-T32N* – 2μ – *URA3*): A ~1.2-kbp *Not*I/*Bam*HI fragment containing the *ARL1-T32N* allele along with ~370 bp of upstream flanking sequence and ~180 bp of downstream flanking sequence was subcloned from pSR44 into the pRS426 backbone. Sequencing confirmed that the desired point mutation is the only change in the *ARL1* ORF.

pJBVPS53-425 (*VPS53* – 2μ – *LEU2*): A ~2.7-kbp fragment containing the *VPS53* ORF along with 118 bp of upstream flanking sequence and 95 bp of downstream flanking sequence was amplified by PCR from yeast chromosomal DNA and cloned into the *Sst*I and *Hind*III sites in the pRS425 backbone.

Plasmids encoding Age1 N-terminal truncations: The *AGE1* sequences encoding the various truncations plus ~300 bp of downstream sequence were amplified by PCR and cloned into the *Xba*I and *Bam*HI sites downstream of the *AGE1* promoter in the pSL485 backbone to yield the various high-copy plasmids expressing the *AGE1* truncations. To create the low-copy plasmids expressing the *AGE1* truncations, the *AGE1* sequences from the high-copy plasmids (including the *AGE1* promoter) were subcloned into the *Pst*I and *Bam*HI sites in the pRS315 backbone.

Plasmids encoding GAP-dead Gcs1-R54 mutants: ~1.8-kbp fragments containing the *gcs1-R54A*, *gcs1-R54K,* and *gcs1-R54Q* alleles plus ~300 bp upstream and ~500 bp downstream flanking sequence from pCTY922, pCTY924, and pCTY925 (Yanagisawa *et al.*, 2002) were subcloned into the *Xho*I and *Sst*I sites of the pRS315, pRS425, pRS316 and pRS426 backbones.

2.6 Yeast Cell Transformation

Plasmid DNA was transformed into yeast cells essentially as described by Gietz *et al.* (1995). Yeast cells were grown in YM-1 medium at 30°C to a concentration of between 7 x 10^6 - 1.5 x 10^7 cells/ml, harvested by centrifugation, washed once with ddH_2O and once with a TE / lithium acetate solution (10 mM Tris-Cl pH 8, 1 mM EDTA pH 8, 0.1 M lithium acetate) and then resuspended in 250 µl TE / lithium acetate for every 50 ml of original culture and incubated at 30°C for 15 minutes. Transformations were set up in 1.5-ml tubes and each contained 5 µl boiled salmon sperm DNA (10 mg/ml), 1 µl plasmid DNA, 50 µl yeast cell suspension, and 300 µl polyethylene glycol (PEG) solution (40% PEG, 10 mM Tris-Cl pH8, 1 mM EDTA pH 8, 0.1 M lithium acetate). Transformation solutions were mixed by vortex and then incubated at 30°C for 30 minutes followed by a heat shock at 42°C for 20 minutes. Cells were pelleted by centrifugation, washed with ddH_2O, and resuspended in 150 µl ddH_2O before being spread on solid selective medium appropriate to select for transformants and incubated at 30°C. Colony growth was usually noted in 2-3 days.

A modified yeast transformation protocol was adopted when seeking to introduce linear DNA fragments into cells, allowing homologous recombination to direct insertion of the fragment at the appropriate chromosomal locus. Transformations of this sort were

employed for gene replacement in which a DNA fragment was targeted to a locus in yeast, replacing the endogenous gene with a marker gene such as the *nat* gene. These transformation reactions contained 10 µl boiled salmon sperm DNA (10 mg/ml), 40 µl of linear DNA directly from a PCR reaction, 100 µl yeast cell suspension, and 600 µl PEG solution. Transformation solutions were mixed by vortex, and then heat shocked at 42°C for 60 minutes. After removing the PEG solution and washing the cells with ddH_2O, cells were suspended in 3 ml warm YM-1 and incubated at 30°C overnight. The cells were then concentrated by centrifugation and spread on solid selective medium to select for transformants and incubated at 30°C. Colony growth was usually obvious in 2-3 days.

2.7 *E. coli* Cell Electroporation

Electroporation was used to introduce plasmid DNA into *E. coli* cells (Seidman *et al.*, 2001). First, electro-competent *E. coli* cells were prepared. *E. coli* cells were grown in 500 ml 2xYT at 37°C to A_{600} of 0.5 to 0.7. The cells were then chilled on ice for 60 minutes and all subsequent steps were carried out on ice or at 4°C. Cells were harvested by centrifugation at 4500 rpm in JA14 rotor for 15 minutes, washed twice in 500 ml ddH_2O, washed once in 40 ml 10% glycerol, and finally suspended in 10% glycerol to a final volume of 6 ml. Cells were stored at –80°C as 80-µl samples in 1.5-ml tubes.

For electroporation of plasmid DNA directly from a ligation reaction, each transformation tube contained 80 µl of competent cells thawed on ice. To this tube 2 µl of the ligation reaction was added and incubated on ice for 1 minute. The cells were then transferred to a chilled 0.2-cm electroporation cuvette (Invitrogen, Mississauga, ON), and tapped to the bottom of the cuvette. A Gene Pulser (Bio-Rad laboratories, Mississauga, ON) was used to deliver a 2.5-kV pulse (200 ohms) to the cells, and was followed immediately by the addition of 1 ml 2xYT medium. The cells were incubated at 37°C for 30-60 minutes, then concentrated by centrifugation and plated onto solid 2xYT medium containing ampicillin and incubated overnight at 37°C to select for transformants.

2.8 Yeast Genetic Techniques

2.8.1 Obtaining Diploid Cells

Diploid strains were created by routine mating of two haploid strains of opposite mating type, *MAT***a** and *MAT*α. This procedure involves a small amount of each haploid population of cells mixed together on solid enriched growth medium and incubated at 30°C overnight. The easiest way to obtain diploid cells from a mated population is by selection. If the haploid parent strains have two different mutations causing auxotrophic phenotypes (for example one is *ura3* and the other is *his3*), both auxotrophies are complemented in the diploid cell by the presence of at least one wild-type gene provided by the haploid parents. For this example, the mated cells are streaked for single colonies on solid selective medium lacking both uracil and histidine, which prevents the growth of both haploid parent strains while allowing diploid cells to grow, thus selecting for the diploid cells. If two different mutations (or drug-resistance marker genes) are not provided by the parental haploid strains, diploid cells can be obtained manually. Zygotes are identified under light microscopy based on their characteristic dumbbell shape and a micromanipulator (Singer Instruments Co., Watchet, England) is used to isolate these zygotes from the population. Isolated, putative zygotes are incubated on solid enriched medium at 30°C. Once a colony forms from a putative zygote, those cells are sporulated to confirm that they are indeed diploid cells.

2.8.2 Sporulation of Diploid Cells

When starved for nitrogen in the presence of a non-fermentable carbon source, diploid yeast cells undergo sporulation (meiosis) to produce four haploid meiotic segregants (spores). These spores are retained within the ascus formed from the cell wall of the parental cell. To induce sporulation, diploid cells are grown in 3 ml of either enriched or selective medium at 30°C overnight to mid or late log phase, then 200 µl of these cells are diluted in 3 ml of pre-sporulation medium (YEPA; 1% yeast extract, 2% potassium acetate, 2% peptone) and incubated at 30°C for ~8 hours. Cells are then washed with ddH_2O and suspended in 1 ml sporulation medium (1% potassium acetate, 0.05% dextrose, 0.1% yeast extract) and incubated at 23°C for 3-5 days.

2.8.3 Tetrad Dissection

Tetrad dissection separates the 4 haploid spores derived from one meiotic event on solid medium and subsequent incubation allows the spores to germinate and form colonies that can then be analysed. For this study, tetrad dissection was used for strain construction and to investigate gene interactions. To dissect tetrads, I diluted 100 µl of sporulated cells in 900 µl phosphate-buffered saline pH 7.4, and added 2 µl Zymolyase (5 mg/ml) to digest the ascus surrounding the spores. This mixture was vortexed to mix and incubated at room temperature for 10 minutes. The digested mixture was then spread on a slab of solid synthetic complete medium. Cells were visualized by light microscopy and sporulated cells (tetrads) were identified by their characteristic cruciform structure. Using a micromanipulator (Singer Instruments Co.) a tetrad was separated from the population of digested cells, the ascus was disrupted manually with the micromanipulator needle to release the 4 spores contained within, and the spores were then distributed in a row on the surface of the agar slab at 4-mm intervals. Additional tetrads were dissected in the same way; rows of spores from individual tetrads were separated by 5 mm on the agar slab. The agar slab was then transferred to either solid enriched or solid selective medium and incubated at 23° or 30°C; colonies generally formed within 3-5 days. The genotypes of individual colonies were determined by assessing growth under various selective conditions to indicate the presence of genetic markers inherited from the parental diploid cell.

2.8.4 Determination of Mating Type

Haploid yeast cells are one of two mating types, either *MAT***a** or *MAT*α. To determine mating type, the strain in question is crossed to haploid strains of known mating type (tester strains) and assessed for the ability to form diploids (see section 2.8.1 above). The strain in question is the opposite mating type from the tester strain with which it produces diploid cells.

2.8.5 Measuring Yeast Cell Concentrations

The concentration of yeast cells in liquid culture was determined either by counting cells under light microscopy using a haemocytometer (Hausser Scientific, Horsham, PA) or by counting with a Coulter electronic particle counter, model ZM (Coulter Electronics, Mississauga, ON). For the latter, 800 µl of yeast cell culture was diluted with 7.2 ml of a

fixing solution (3:7 formalin:isoton dilution; BDH, Toronto, ON) and then sonicated for 10 seconds at 30% power using a Sonifier cell disrupter, model W140 (Heat Systems Ultrasonics Inc., Long Island, NY) to disrupt cell clumps. The fixed cells were then further diluted 10-fold in an isotonic saline solution before being counted using the Coulter counter.

2.9 Cell-Growth Assays

Growth assays were used to compare yeast strains with different genotypes to determine any impact the genetic differences had on cell growth and colony formation. Two types of growth assay were used, termed patch tests and serial-dilution assays. Patch tests were used as a preliminary experiment to assess growth differences. For all experiments, a minimum of four independent isogenic isolates (individual meiotic segregants or individual yeast transformants) were assessed for each genotype being tested. This was done to account for unintended genetic mutations affecting growth efficiency that may arise in any individual isolate. As long as consistent growth was displayed by three of the four independent isolates for any genotype, that growth efficiency was considered to be representative of the genotype. If the genotypes being tested displayed dramatic growth differences, then patch-test analysis was sufficient to reveal these differences. However, if the growth differences between the genotypes being tested were subtle, then serial-dilution assays were used to provide a more quantitative comparison. Serial-dilution assays used genetic isolates that had already been determined to be representative in a patch test. Where subtle differences were being analysed, multiple representative independent isogenic isolates were used to show consistent behaviour.

For assessing temperature-sensitivity phenotypes using patch tests, cells from single yeast colonies were streaked in small rectangular patches on solid medium using the blunt end of a sterile wooden toothpick. The patched cells were then incubated at 23°C for 2 days to allow growth and colony formation, which resulted in a thick patch of cells where streaks had been made. The cell patches were observed to ensure relatively equal growth in all patches before being replica plated to fresh solid growth medium. Replicate plates were then incubated at either 23° or 30°C, and at 37°C. Plates were observed daily and digital photographs were taken to record growth using either a Gel

Doc 1000 (Bio-Rad laboratories, Mississauga, ON) and Molecular Analyst software v2.1.2 or a Versa Doc Imaging System (Bio-Rad laboratories, Mississauga, ON) and Quantity One software v4.6.7. Patch tests to assess the reentry phenotype were carried out as described for assessing temperature-sensitivity phenotypes with the following changes. The initial growth of patched cells was carried out at 30°C for 5 days to allow cells to enter stationary phase, and replicate plates were incubated at either 23° or 30°C, and at 14°C.

To assess temperature-sensitivity phenotypes using a serial-dilution assay, cells from single yeast colonies were first grown in liquid cultures incubated at 23°C for several days to allow the cell concentrations to equilibrate as the cultures reached stationary phase. Cells from each culture were then 'balanced' at an A_{600} of 0.5, and 5 µl of 5-fold serial dilutions were spotted onto solid medium as described for each experiment and incubated at 23° and 37°C. Plates were observed daily and digital photographs were taken to record growth as described above.

To assess the reentry phenotype using a serial-dilution assay, yeast cells from single yeast colonies were first grown in liquid cultures incubated at 30°C for 5 to 7 days to ensure all cells entered stationary phase. Stationary-phase cells from each culture were then concentrated to $1x10^8$ or $1x10^9$ cells/ml and 5 µl of 10-fold serial dilutions were spotted onto solid medium and incubated at either 23° or 30°C, and at 14°C. Due to the long incubation times required at 14°C, these plates were wrapped in perforated plastic bags during incubation to slow the drying out of the agar medium. Plates were observed daily and digital photographs were taken to record growth as described above.

2.10 Refining the List of Gene Deletions that Alleviate *gcs1*Δ Cold Sensitivity

To reassess the gene deletions identified as putatively alleviating *gcs1*Δ cold sensitivity (Drysdale, 2006), the *gcs1*Δ query strain (PPY169-4) was crossed to the 169 gene deletion strains of interest from the deletion collection (Giaever *et al.*, 2002) and double-mutant cells were obtained as described by Tong *et al.* (2001). Cell manipulations were carried out by Kendra Gillis Walker in our lab, using a VersArray colony arrayer (Bio-Rad laboratories, Mississauga, ON) housed in a VersArray environmental control chamber (Bio-Rad laboratories, Mississauga, ON). The 169 deletion strains of interest

(each harbouring a deletion mutation marked with the *kan* gene, which confers resistance to G418) were inoculated in an array on solid YEPD medium; this array was then crossed to the *gcs1*Δ::*nat* query strain (PPY169-4), and diploid cells were selected on YEPD +G418 +nourseothricin. Diploid cells were sporulated on sporulation medium (2% agar, 1% potassium acetate, 0.1% yeast extract, 0.05% dextrose, supplemented with uracil, histidine, and leucine) by incubation at 23°C for 5 days. To remove unsporulated diploid cells, *MAT***a** segregants were selected on haploid selection medium (synthetic complete medium lacking histidine and arginine but containing 50 mg/ml canavanine) incubated at 30°C for 2 days, then transferred to the same medium and incubated at 30°C for 1 day. *MAT***a** segregants are able to grow if they contain the *can1*Δ mutation and the *MFA1*promoter-*HIS3* 'magic-marker' gene construct, which is only expressed in *MAT***a** cells, and is not expressed in *MAT*α cells or diploid cells. *MAT***a** haploids containing the gene deletion from the collection were then selected on haploid selection medium containing G418 and grown for 1 day at 30°C. Finally, double-mutant haploid cells were selected on haploid selection medium containing G418 and nourseothricin by incubation at 30°C for 2 days.

I streaked these haploid double-mutant cell populations for single colonies on haploid selection medium containing G418 and nourseothricin and incubated them at 30°C to allow colonies to grow. For each of the 169 double-mutant strains, 10 single colonies were patched on synthetic complete medium, with 4 strains to be assessed per plate, and each plate also contained 4 positive-control patches of wild-type cells (strain Y150) and 4 negative-control patches of *gcs1*Δ cells (strain PPY169-4). These patched plates were incubated at 30°C for 6 days to allow cells to enter stationary phase and were then replica plated to solid enriched medium and solid synthetic complete medium and incubated at 14°C for 5 days, and growth was recorded. This procedure was repeated twice and the results were tabulated (see Table 4.2).

2.11 FM 4-64 Endocytosis Assay

A 20 mM FM 4-64 stock solution was prepared in DMSO and stored at 4°C wrapped in foil. The FM 4-64 assays were carried out essentially as described by Wang *et al.* (1996). Cells were grown in 3 ml liquid cultures at 30°C for 5 days; if the cells carried a plasmid,

selection for the plasmid was maintained. Stationary-phase cells were harvested, washed once in water, once in cold enriched medium, and then suspended in 1 ml cold enriched medium and incubated on ice for 15 minutes. Cells were stained with 40 µM FM 4-64 on ice for 1 hour, and were vortexed every 10 minutes. Staining was always carried out in enriched medium regardless of the original growth conditions because FM 4-64 does not stain efficiently in selective medium. After staining, cells were harvested and suspended in 30 ml of dye-free pre-chilled enriched medium. The zero-time sample was taken: 1.5 ml of cells was transferred to a 1.5-ml tube with 10 mM NaN_3. The remaining stained cells were transferred to two 50-ml flasks, with one incubated at 30°C and the other at 14°C. samples were taken at later times as described above for the zero-time sample. All samples were stored in the dark at 4°C until the end of the experiment. The cells from each sample were then harvested and suspended in 500 µl YNB (0.6% sodium hydroxide, 1% succinic acid, 0.17% yeast nitrogen base without amino acids or ammonium sulfate) + 10 mM NaN_3. Prior to visualization by fluorescence microscopy the cells were pelleted and resuspended in residual medium to concentrate them. The cells were suspended in YNB for visualization because YNB exhibits less autofluorescence than enriched medium does. Cells were visualized using a Zeiss Axiovert 200 inverted microscope (Thornwood, NY). FM 4-64 fluorescence (filter set No. 15, BP 546/12, LP 590), and DIC images were captured with a Hamamatsu (Solna, Sweden) ORCA-R2 digital monochromatic camera and Axiovision 4.8 software, and contrast was enhanced using Adobe Photoshop software.

2.12 Methylene-Blue Viability Assay

Viability assays were carried out essentially as described (Gurr, 1965). Samples were concentrated by centrifugation and mixed on a cover slip with an equal volume of a 0.02% methylene blue solution in PBS pH 7.4. Prepared cells were visualized by light microscopy; dead cells stained blue while living cells remained unstained. For each sample at least 500 cells were counted. The numbers of blue (dead) and white (viable) cells were used to determine percent viability of the culture.

2.13 Localization of GFP Fusion Proteins

Cells expressing GFP-tagged proteins were grown overnight in medium that maintained plasmid selection. Live log-phase cells were concentrated by centrifugation immediately prior to mounting for visualization as described above for the FM 4-64 assay except that GFP fluorescence (filter set No. 10, BP 450-490, BP 515-565) and, for co-localization studies, RFP fluorescence (filter set No. 20, BP 546/12, BP 575-640) images were captured. Images were false coloured using Axiovision 4.8 software, and contrast was enhanced using Adobe Photoshop software. For each situation at least three individual transformants were assessed and found to display the same GFP staining pattern.

2.14 GTPase-Activating Protein Assays

The *in vitro* GAP assays presented in Figures 3.11 and 4.11 were performed by Dr. Pak Phi Poon in our lab. The procedures followed in carrying out these assays are described in Benjamin *et al.* (2011b) and Benjamin *et al.* (2011a), respectively.

CHAPTER 3. RESULTS – The Yeast ArfGAP Age1 is Regulated by Phospholipase D for Post-Golgi Vesicular Transport

Note: The majority of the research described in this chapter was originally published in the Journal of Biological Chemistry as: Benjamin JJ, Poon PP, Lewis SM, Auger A, Wong TA, Singer RA, Johnston GC. The yeast Arf GTPase-activating protein Age1 is regulated by phospholipase D for post-Golgi vesicular transport**.** *J. Biol. Chem*. 2011; 286(7):5187-5196. © the American Society for Biochemistry and Molecular Biology. Figures appearing in this chapter that are wholly or partially reproduced from figures appearing in that paper include Figures: 3.1, 3.2, 3.3, 3.5, 3.7, 3.9, 3.10, and 3.11. For Figures 3.2, 3.3, 3.5, and 3.9 additional unpublished results have been added. Figures 3.6 and 3.8 display published results that were cited as 'data not shown' in that paper.

3.1 N-Terminal Sequences of the Age1 Protein Restrict Age1 Function in the Post-Golgi Transport Pathway

As described in the Introduction, increased abundance of the Age1 ArfGAP can alleviate temperature sensitivity and restore effective vesicular transport at multiple vesicular-transport stages in cells with ArfGAP deficiencies that cause these defects. Specifically, increased *AGE1* gene dosage alleviates temperature sensitivity and restores effective Golgi-to-ER retrograde transport in *glo3*Δ *gcs1-28* cells (Lewis, 2004), and also alleviates temperature sensitivity and restores effective post-Golgi transport in *age2*Δ *gcs1-3* cells and *age2*Δ *gcs1-4* cells (Auger, 2000; Wong *et al.*, 2005; Benjamin *et al.*, 2011b). Further analysis of Age1 found that removal of the N-terminal residues 3-166, creating an Age1 protein termed Age1ΔN, provides more efficient alleviation of *glo3*Δ *gcs1-28* temperature sensitivity than does full length Age1 (Lewis, 2004), suggesting that these N-terminal sequences of Age1 restrict Age1 function in the Golgi-to-ER retrograde transport pathway.

To test whether the N-terminal sequences of Age1 also restrict Age1 function in the post-Golgi transport pathway, I overexpressed the *AGE1* and *AGE1ΔN* genes from high-copy and low-copy plasmids in *age2*Δ *gcs1-4* cells and assessed growth at 37°C. As previously reported by Wong *et al.* (2005), increased *AGE1* gene dosage from a high-

copy plasmid alleviated the temperature sensitivity of *age2*Δ *gcs1-4* cells (Figure 3.1). Furthermore, removal of the N-terminal sequences of Age1 improved the ability of Age1 to alleviate the temperature sensitivity of *age2*Δ *gcs1-4* cells. Temperature-sensitive *age2*Δ *gcs1-4* cells carrying a high-copy *AGE1*ΔN plasmid grew better than cells carrying the intact *AGE1* gene on a high-copy plasmid (Figure 3.1). This difference was even more pronounced when these *AGE1* alleles were on low-copy plasmids: cells carrying low-copy *AGE1*ΔN grew well at 37°C, whereas cells carrying low-copy intact *AGE1* did not (Figure 3.1). Thus, increased *AGE1* gene dosage can indeed alleviate the temperature sensitivity of *age2*Δ *gcs1-4* cells and removal of the N-terminal residues of Age1 (amino acids 3-166) has the same enhancing effect on Age1 function for Age2-related post-Golgi transport as it does on Age1 function for Glo3-related Golgi-to-ER retrograde transport. This result suggests that the N-terminal sequences of Age1 inhibit Age1 function in these two distinct transport stages.

3.2 Amino Acids 81-90 in the N Terminus of Age1 Are Necessary to Inhibit Age1 Function

To better define the N-terminal residues of Age1 that inhibit Age1 function in the transport pathways at issue here, I assessed various *AGE1* N-terminal truncation alleles for alleviation of the growth defects of *glo3*Δ *gcs1-28* and *age2*Δ *gcs1-4* mutant cells. I constructed the truncation alleles in a manner similar to *AGE1*Δ*N*, with the deletion of sequences from codon 3 to downstream codons ranging from codon 60 to 160. Like *AGE1*Δ*N*, each truncation allele was expressed from the endogenous *AGE1* promoter on low-copy and high-copy plasmids. When growth at 37°C was assessed, the *AGE1* truncation alleles behaved the same in both temperature-sensitive strains (Figure 3.2). When expressed from low-copy plasmids, the truncated proteins lacking up to the first 80 residues of Age1 behaved like full-length Age1 and failed to alleviate temperature sensitivity. Also like full-length Age1, these truncations did alleviate temperature sensitivity when expressed from high-copy plasmids, (with the exception of the truncation that removed the first 70 residues of Age1, which failed to alleviate temperature sensitivity even when expressed at high-copy). In contrast, the truncated

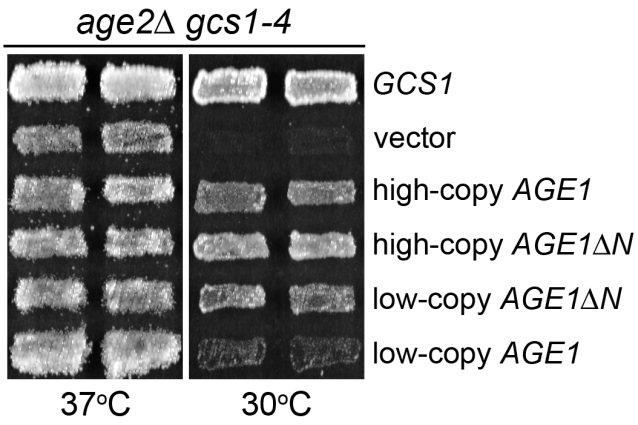

Figure 3.1 Increased *AGE1* gene dosage alleviates *age2*Δ *gcs1-4* temperature sensitivity. Patches of temperature-sensitive *age2*Δ *gcs1-4* cells (strain JBY122; W303 genetic background) harbouring plasmids (pEP1, pRS425, pSL377, pSL489, pSL494, pSL340) expressing the indicated genes were grown on solid selective medium at 23°C for 2 days before being replica-plated to solid enriched medium and incubated at 30°C for 2 days, or 37°C for 1 day. Four individual transformants were assessed for each plasmid and in each case showed consistent behaviour; two transformants are shown for each. (Originally published in Benjamin *et al.*, 2011b.)

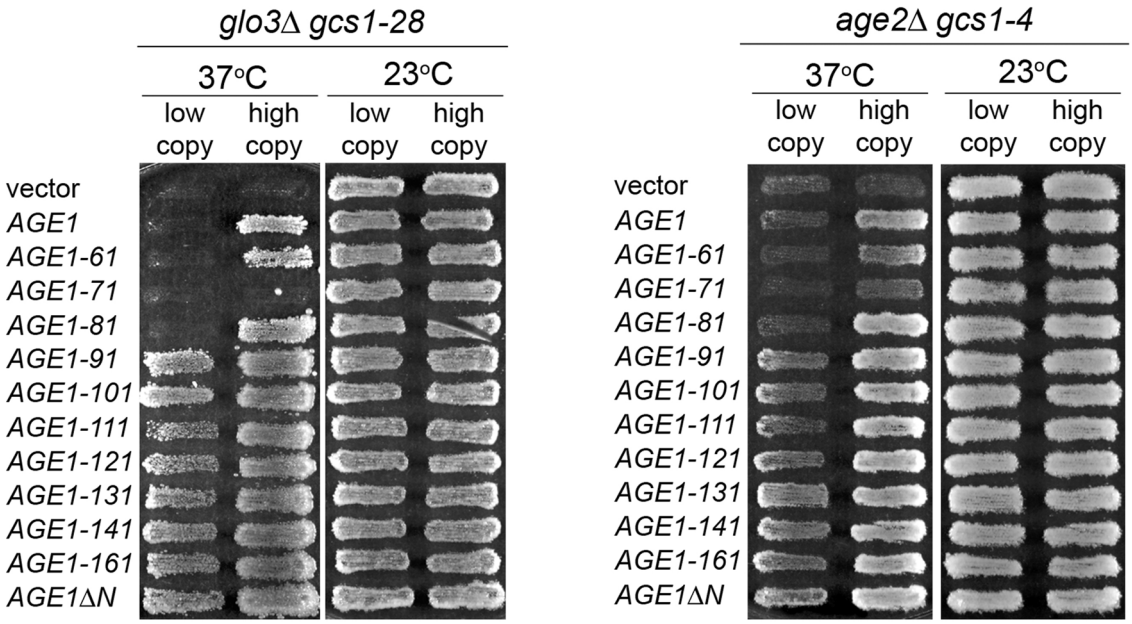

Figure 3.2 The N terminus of Age1 inhibits the ability of Age1 to alleviate *glo3*Δ *gcs1-28* and *age2*Δ *gcs1-4* temperature sensitivity. Patches of temperature-sensitive *glo3*Δ *gcs1-28* cells (strain SL112; W303 genetic background) or *age2*Δ *gcs1-4* cells (strain JBY122; W303 genetic background) harbouring the indicated plasmid-borne N-terminal truncations of Age1 were grown on solid selective medium at 23°C for 2 days before being replica-plated to fresh medium and incubated at 23°C for 2 days, or 37°C for 3 days (*glo3*Δ *gcs1-28*) or 1 day (*age2*Δ *gcs1-4*). Four individual transformants were assessed for each plasmid and in each case showed consistent behaviour; one transformant is shown for each. (*age2*Δ *gcs1-4* results were originally published in Benjamin *et al.*, 2011b.)

proteins lacking the first 90 residues or more of Age1 behaved like the AgeΔN protein and alleviated temperature sensitivity even when expressed from low-copy plasmids.

This Age1 truncation analysis showed that some truncations function like full-length Age1, and therefore still contain inhibitory N-terminal Age1 sequences, while other truncations function like Age1ΔN, and therefore have had inhibitory N-terminal Age1 sequences removed. This difference in function distinguishes the Age1 truncations lacking the first 80 residues from those lacking the first 90 residues of Age1, suggesting that the minimal region of Age1 that is required to inhibit Age1 function is contained between residues 80 and 90 within the N terminus of Age1. The presence of these 10 residues (plus downstream sequences) inhibits Age1 function to the same extent as the full Age1 N terminus does and, indeed, the first 80 residues of the Age1 N terminus are not required for this inhibition. Further N-terminal truncations of Age1 spanning these 10 residues would likely identify one amino acid whose presence and absence corresponds to inhibited and un-inhibited Age1 function. This residue would therefore represent the N-terminal most residue that is required for inhibition of Age1 function. The complete region of Age1 that is necessary and sufficient to inhibit Age1 function cannot be identified by testing N-terminal truncations of Age1, and is likely much larger than one residue.

3.3 Increased Age1 or Age1ΔN Abundance Can 'Bypass' the Need for Otherwise Essential ArfGAP Pairs

Alleviation of temperature sensitivity by increased Age1 abundance in *glo3*Δ *gcs1-28*, *age2*Δ *gcs1-4*, and *age2*Δ *gcs1-3* mutant cells may reflect the ability of Age1 to enhance the activity of the mutant Gcs1-28, Gcs1-4, and Gcs1-3 proteins, respectively, enabling the mutant Gcs1 proteins to provide the functions required for transport and cell growth in each situation. Alternatively, increased abundance of the Age1 ArfGAP protein may bypass the requirement for the Age2 + Gcs1 or Glo3 + Gcs1 ArfGAP protein pair, and provide the essential functions that are normally provided by these essential ArfGAP pairs, even in their complete absence.

To distinguish between these two alternatives, I determined whether increased Age1 abundance could compensate for (bypass) the complete absence of the Age2 +

Gcs1 or Glo3 + Gcs1 pairs. Diploid cells heterozygous for *age2*Δ and *gcs1*Δ deletion mutations or for *glo3*Δ and *gcs1*Δ deletion mutations were first transformed with a high-copy *AGE1* or *AGE1*Δ*N* plasmid, or with empty vector. These cells were then sporulated (allowed to undergo meiosis), and the resulting haploid meiotic segregants were analyzed for the ability to form colonies on solid selective medium. The genotype of each colony was then determined by assessing the effects of marker genes that replace the chromosomal copies of the deleted ArfGAP genes and that allow plasmid selection. As expected, when the heterozygous diploid parent cells contained empty vector, all haploid segregants predicted to be *age2*Δ *gcs1*Δ double mutants (based on the genotypes of the living segregants) failed to form colonies (Figure 3.3), confirming that deletion of *AGE2* is lethal in combination with deletion of *GCS1*. In contrast, *age2*Δ *gcs1*Δ double-mutant segregants were able to form colonies if the *AGE1* or *AGE1*Δ*N* plasmid was present (Figure 3.3). These results indicate that increased abundance of Age1 or Age1ΔN bypasses the requirement for any Age2 and Gcs1 protein, and suggest that increased abundance of Age1 or Age1ΔN can provide the functions required for post-Golgi transport that are normally provided by the Age2 + Gcs1 ArfGAP pair.

In the Glo3 + Gcs1 situation, *glo3*Δ *gcs1*Δ double-mutant cells were only able to form colonies if the high-copy *AGE1*Δ*N* plasmid was present; viable double-mutant segregants carrying high-copy *AGE1* were not found (Figure 3.4). These results indicate that increased abundance of Age1ΔN can bypass the requirement for any Glo3 and Gcs1 protein, and suggest that increased abundance of Age1ΔN can provide the functions required for Golgi-to-ER retrograde transport that are normally provided by the Glo3 + Gcs1 ArfGAP pair.

3.4 Increased Abundance of the Glo3 ArfGAP Protein Bypasses the Need for the Otherwise Essential Age2 + Gcs1 ArfGAP Pair

As described in the Introduction, four yeast proteins have been shown to have ArfGAP activity *in vitro*: Gcs1, Glo3, Age2, and Age1 (Poon *et al.*, 1996; Poon *et al.*, 1999; Poon *et al.*, 2001; Zhang *et al.*, 2003; Benjamin *et al.*, 2011b), and two ArfGAP pairs provide essential ArfGAP activity for two separate transport pathways: Age2 + Gcs1 for post-

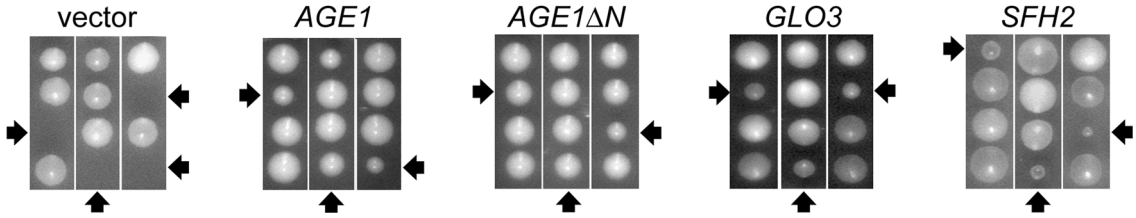

Figure 3.3 Increased abundance of Age1, Age1ΔN, Glo3, or Sfh2 bypasses the requirement for the essential Age2 + Gcs1 ArfGAP pair. Diploid cells heterozygous for *age2*Δ and *gcs1*Δ deletion mutations (strains AAY20 or AAY10; W303 genetic background) and harbouring vector (pRS426) or high-copy plasmids carrying *AGE1* (pSL377), *AGE1*Δ*N* (pSL489), *GLO3* (pPPL38), or *SFH2* (pCTY210) were sporulated and the resulting haploid segregants were incubated on solid selective medium at 30°C for 5 days. In each column of colonies the four meiotic segregants from a single sporulated diploid cell (tetrad) are displayed. Arrows indicate *age2*Δ *gcs1*Δ double-mutant segregants that are either non-viable (vector) or are kept alive by the plasmid-borne gene. (Vector, *AGE1*, *AGE1*Δ*N*, and *SFH2* results were originally published in Benjamin *et al.*, 2011b.)

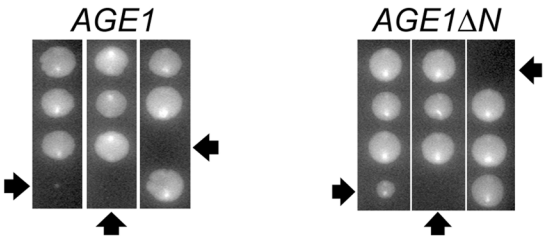

Figure 3.4 Increased abundance of Age1ΔN, but not Age1, bypasses the requirement for the essential Glo3 + Gcs1 ArfGAP pair. Diploid cells heterozygous for *glo3*Δ and *gcs1*Δ deletion mutations (strain JBY26-1; W303 genetic background) and harbouring high-copy plasmids carrying *AGE1* (pSL377) or *AGE1*Δ*N* (pSL489) were sporulated and the resulting haploid segregants were incubated on solid selective medium at 30°C for 5 days. In each column of colonies the four meiotic segregants from a single sporulated diploid cell (tetrad) are displayed. Arrows indicate *glo3*Δ *gcs1*Δ double-mutant segregants that are either non-viable or kept alive by plasmid-borne *AGE1*Δ*N*.

Golgi transport (Poon *et al.*, 2001), and Glo3 + Gcs1 for Golgi-to-ER retrograde transport (Poon *et al.*, 1999). The previous section showed that increased abundance of Age1 can functionally replace each essential ArfGAP pair, something that normal levels of Age1 is unable to do. Can increasing the abundance of any ArfGAP protein allow it to function in transport pathways where that particular ArfGAP does not normally function?

Not every ArfGAP can function anywhere. Previous results show that increased abundance of the Age2 ArfGAP protein does not alleviate *glo3*Δ *gcs1-28* temperature sensitivity (Lewis, 2004). Since Age2 cannot provide sufficient ArfGAP activity for retrograde transport in this less demanding genetic test, increased Age2 was not assessed for the ability to bypass Gcs1 + Glo3. In contrast, our lab previously showed that increased abundance of the Glo3 ArfGAP protein alleviates *age2*Δ *gcs1-3* and *age2*Δ *gcs1-4* temperature sensitivity (Auger, 2000; Wong *et al.*, 2005), and Glo3 has been reported by others to bypass deletion of the Age2 + Gcs1 ArfGAP pair (Zhang *et al.*, 2003). To confirm this finding, diploid cells heterozygous for *age2*Δ and *gcs1*Δ deletion mutations were first transformed with a high-copy *GLO3* plasmid. These cells were then sporulated, and the resulting haploid meiotic segregants were analyzed for the ability to form colonies on solid selective medium. The genotype of each colony was then determined by assessing marker genes. The *age2*Δ *gcs1*Δ double-mutant segregants harbouring the high-copy *GLO3* plasmid were indeed able to form colonies (Figure 3.3). This result confirms that increased abundance of Glo3 can bypass the requirement for any Age2 and Gcs1 protein at all, and suggests that increased abundance of Glo3 can provide the functions required for effective post-Golgi transport in the complete absence of the Age2 + Gcs1 ArfGAP pair.

3.5 Increased Abundance of the Sfh2 Phosphatidylinositol Transfer Protein Bypasses the Need for the Otherwise Essential Age2 + Gcs1 ArfGAP Pair

As described in the Introduction, *gcs1-4* provides temperature-sensitive ArfGAP function specifically for post-Golgi transport in the absence of the *AGE2* + *GCS1* genes. In a previous copy-suppressor approach using *age2*Δ *gcs1-4* temperature-sensitive mutant cells, increased abundance of the *SFH2* gene was found to alleviate the *age2*Δ *gcs1-4* temperature-sensitive defect and restore effective post-Golgi transport at 37°C (Wong *et*

al., 2005). This effect is specific, because increased *SFH2* gene dosage fails to alleviate the temperature sensitivity of *glo3*Δ *gcs1-28* double-mutant cells (Wong *et al.*, 2005). Sfh2 is one of the six-member Sec14 family of phosphatidylinositol transfer proteins (PITP) in yeast. The mechanism by which increased abundance of Sfh2 restores post-Golgi transport in *age2*Δ *gcs1-4* cells at 37°C is unknown. However, one proposed mechanism is that an increased abundance of Sfh2, through membrane remodelling, lowers the threshold of ArfGAP activity required for post-Golgi transport so that at 37°C the enfeebled ArfGAP activity of the Gcs1-4 mutant protein is sufficient (Wong *et al.*, 2005). An alternative possibility is that increased abundance of Sfh2 restores post-Golgi transport in a Gcs1-4 independent manner (i.e., Sfh2 bypasses the need for the Age2 + Gcs1 pair).

To assess this latter possibility directly, I first transformed diploid cells heterozygous for *age2*Δ and *gcs1*Δ deletion mutations with a high-copy *SFH2* plasmid. These cells were then sporulated and the resulting haploid meiotic segregants were analyzed for their ability to form colonies on solid selective medium. The genotype of each colony was then determined by assessing the effects of marker genes that replace the chromosomal copies of the deleted ArfGAP genes and that allow plasmid selection. Colonies formed by *age2*Δ *gcs1*Δ double-mutant segregants harbouring the high-copy *SFH2* plasmid were readily recovered (Figure 3.3). Thus, increased abundance of Sfh2 bypasses the requirement for any Age2 and Gcs1 protein. Bypass of Age2 + Gcs1 by increased Sfh2 abundance does not, however, restore wild-type growth. The colonies formed by *age2*Δ *gcs1*Δ double-mutant segregants with high-copy *SFH2* were significantly smaller than the colonies formed by the single-mutant and wild-type segregants, indicating impaired growth.

3.6 Age1 is Required for Effective Sfh2 Bypass of the Age2 + Gcs1 ArfGAP Pair

The finding that increased Sfh2 abundance bypasses the need for the Age2 + Gcs1 ArfGAP pair may reflect an altered lipid environment that permits vesicular transport in the absence of ArfGAP activity, or that allows another ArfGAP to substitute for the absent Age2 + Gcs1 pair. Of the four yeast proteins known to have ArfGAP activity *in vitro* only Age1 and Glo3 are present in the *age2*Δ *gcs1*Δ cells being kept alive by high-

copy *SFH2* (herein referred to as *age2*Δ *gcs1*Δ [*SFH2*] cells, with the square brackets indicating the presence of the gene on a plasmid). My results above show that increased abundance of either Age1 or Glo3 can supply the necessary functions for post-Golgi transport in the complete absence of Age2 and Gcs1. Although wild-type levels of Age1 and Glo3 are not sufficient to maintain viability when Age2 and Gcs1 are eliminated, perhaps increased abundance of the Sfh2 protein enhances the ArfGAP activity of Age1 and/or Glo3 to a level sufficient for effective post-Golgi transport. If this were the case, then additional deletion of the *AGE1* or *GLO3* gene in *age2*Δ *gcs1*Δ [*SFH2*] cells should compromise Sfh2-mediated bypass, and result either in decreased growth efficiency or a complete loss of cell viability.

The effect of deleting the *GLO3* gene in *age2*Δ *gcs1*Δ [*SFH2*] cells was not tested because *glo3*Δ *gcs1*Δ is itself a lethal genetic combination (Poon *et al.*, 1999); therefore, the additional deletion of the *GLO3* gene in these cells would likely result in lethality. In contrast, deletion of the *AGE1* gene in combination with deletion of either the *GCS1* or *AGE2* gene has no negative effect on cell growth (Zhang *et al.*, 2003), and therefore the effect of additionally deleting the *AGE1* gene in *age2*Δ *gcs1*Δ [*SFH2*] cells can be assessed directly. To do so, diploid cells heterozygous for *gcs1*Δ, *age2*Δ, and *age1*Δ deletion mutations were first transformed with a high-copy *SFH2* plasmid. These cells were then sporulated and the resulting haploid meiotic segregants were analyzed for their ability to form colonies on solid selective medium. The genotype of each colony was then determined by assessing marker genes. Colonies formed by *age2*Δ *gcs1*Δ [*SFH2*] double-mutant segregants were readily recovered, as were colonies formed by the sought-after *age2*Δ *gcs1*Δ *age1*Δ triple-mutant segregants harbouring the high-copy *SFH2* plasmid (herein referred to as *age2*Δ *gcs1*Δ *age1*Δ [*SFH2*] cells or segregants). There was no difference in the size of colony formed by the triple-mutant (*age2*Δ *gcs1*Δ *age1*Δ [*SFH2*]) and double-mutant (*age2*Δ *gcs1*Δ [*SFH2*]) segregants; however, as seen before for the double-mutant segregants, the colonies formed by these double and triple-mutant segregants were significantly smaller than the colonies formed by the various single-mutant and wild-type segregants (Figure 3.5A). Thus, the additional deletion of the *AGE1* gene in *age2*Δ *gcs1*Δ [*SFH2*] cells had no effect on the ability of these cells to form colonies on solid selective medium, or on the size of the colony formed.

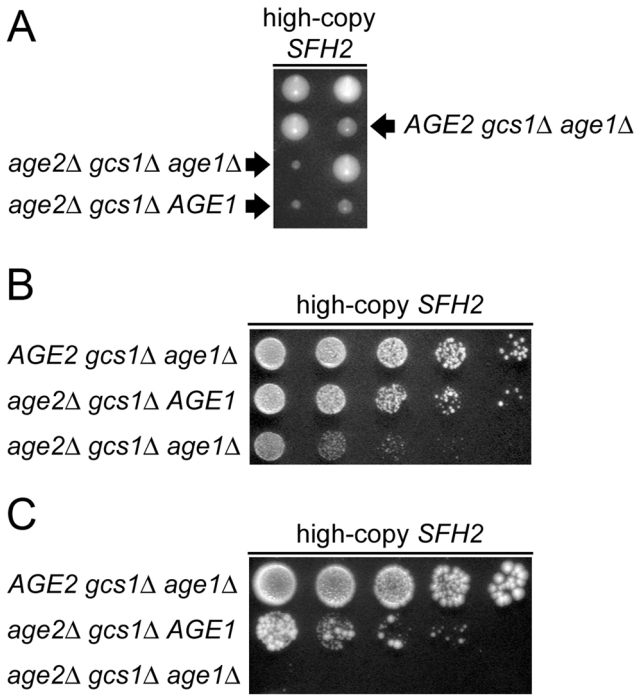

Figure 3.5 Effective *SFH2* bypass of the essential Age2 + Gcs1 ArfGAP pair requires Age1. (A) Diploid cells heterozygous for *age2*Δ, *gcs1*Δ, and *age1*Δ deletion mutations (strain JBY10; W303 genetic background) and carrying a high-copy *SFH2* plasmid (pCTY201) were sporulated and the resulting haploid segregants were incubated on solid selective medium at 30°C for 5 days. In each column of colonies the four meiotic segregants from a single sporulated diploid cell (tetrad) are displayed. (B and C) Equal numbers of cells from the colonies indicated in panel A were serially diluted (5-fold serial dilutions), and then spotted onto solid selective medium (panel B) or solid enriched medium (panel C) and incubated at 30°C for 5 days. (Results in panels A and C were originally published in Benjamin *et al.*, 2011b.)

To further investigate any effect of additionally deleting the *AGE1* gene in *age2*Δ *gcs1*Δ [*SFH2*] cells, I compared the growth of *age2*Δ *gcs1*Δ [*SFH2*] and *age2*Δ *gcs1*Δ *age1*Δ [*SFH2*] cells in a serial-dilution assay on solid selective and solid enriched media (Figure 3.5B and C). Serial-dilution assays of this sort are more sensitive to growth differences between strains than simply comparing colony size following tetrad analysis. Cells with wild-type *AGE2* (*AGE2 gcs1*Δ *age1*Δ [*SFH2*]) served as a control for growth of a strain that does not have a lethal genetic combination of deleted ArfGAP genes. As expected, this control population grew well on both selective and enriched media (Figure 3.5B and C). On selective medium the *age2*Δ *gcs1*Δ [*SFH2*] cells grew almost as well as the *AGE2 gcs1*Δ *age1*Δ [*SFH2*] control cells, whereas the *age2*Δ *gcs1*Δ *age1*Δ [*SFH2*] cells exhibited markedly decreased growth efficiency (Figure 3.5B). The decreased growth of the *age2*Δ *gcs1*Δ *age1*Δ [*SFH2*] cells was further exaggerated on enriched medium, where the growth of *age2*Δ *gcs1*Δ [*SFH2*] cells was severely impaired compared to the growth of the control cells, and the ability of the *age2*Δ *gcs1*Δ *age1*Δ [*SFH2*] cells to grow was completely abolished (Figure 3.5C). In total I assessed 11 individual *age2*Δ *gcs1*Δ [*SFH2*] double-mutant segregants and 6 individual *age2*Δ *gcs1*Δ *age1*Δ [*SFH2*] triple-mutant segregants, and all exhibited consistent behaviours: double-mutant cells harbouring the high-copy *SFH2* plasmid grew better than triple-mutant cells (lacking the *AGE1* gene) harbouring the *SFH2* plasmid. Thus Age1 is indeed involved in Sfh2-mediated bypass of Age2 + Gcs1. The elimination of Age1 greatly decreases the efficacy of Sfh2-mediated bypass of Age2 + Gcs1, suggesting that Sfh2 bypass acts in part through Age1. As such, Age1 function may be regulated by membrane phospholipid composition, which in turn is modulated by Sfh2. This regulation of Age1 could function by affecting Age1 localization, Age1 activity, or both.

3.7 Sfh2 is Not Required for Age1 (or Age1ΔN) Bypass of the Age2 + Gcs1 ArfGAP Pair

As shown earlier in this chapter, increased abundance of either the Age1 ArfGAP protein or the Sfh2 PITP can bypass the otherwise essential Age2 + Gcs1 ArfGAP pair. Thus, both proteins can function in the post-Golgi vesicular-transport pathway. Sfh2 and Age1 were further shown to function together to restore effective post-Golgi transport, the

Age1 protein being important for effective Sfh2-mediated bypass of Age2 + Gcs1. Presumably the increased abundance of Sfh2 results in increased PITP activity that alters the membrane lipid environment, allowing Age1 protein at wild-type levels to functionally replace Age2 + Gcs1. Since increased Sfh2 activity enables normal levels of Age1 to provide the necessary functions for post-Golgi transport, perhaps wild-type levels of Sfh2 are similarly required for the increased abundance of Age1 (or Age1ΔN) to provide the necessary functions for post-Golgi transport in the absence of Age2 + Gcs1. To test this idea directly, diploid cells heterozygous for *gcs1*Δ, *age2*Δ and *sfh2*Δ deletion mutations were first transformed with a high-copy *AGE1* or *AGE1*Δ*N* plasmid. These cells were then sporulated and the resulting haploid meiotic segregants were analyzed for their ability to form colonies on solid selective medium. The genotype of each colony was then determined by assessing marker genes. Colonies formed by *age2*Δ *gcs1*Δ *sfh2*Δ triple-mutant segregants harbouring either the *AGE1* or *AGE1*Δ*N* plasmid were readily recovered (data not shown), and there was no significant difference in the size of colony formed by *age2*Δ *gcs1*Δ *sfh2*Δ triple-mutant segregants or *age2*Δ *gcs1*Δ double-mutant segregants harbouring the *AGE1* or *AGE1*Δ*N* plasmids. The colonies formed by these bypassed segregants were only slightly smaller than the colonies formed by the various other segregants (data not shown; see Figure 3.3 for representative colony sizes of *age2*Δ *gcs1*Δ double-mutant segregants that are kept alive by *AGE1* and *AGE1*Δ*N* bypass of Age2 + Gcs1).

To more accurately assess any growth differences that result from additionally deleting the *SFH2* gene in *age2*Δ *gcs1*Δ [*AGE1*] cells, and *age2*Δ *gcs1*Δ [*AGE1*Δ*N*] cells, I compared the growth of *age2*Δ *gcs1*Δ double-mutant cells with that of *age2*Δ *gcs1*Δ *sfh2*Δ triple-mutant cells, each harbouring the *AGE1* plasmids, in serial-dilution assays on solid enriched and solid selective media. Figure 3.6 shows the growth of representative segregants on solid enriched medium; identical results were also seen on selective medium (data not shown). In total I assessed 6 individual *age2*Δ *gcs1*Δ *SFH2* [*age1*Δ*N*] segregants, 6 *age2*Δ *gcs1*Δ *sfh2*Δ [*age1*Δ*N*] segregants, 4 *age2*Δ *gcs1*Δ *SFH2* [*AGE1*] segregants and 3 *age2*Δ *gcs1*Δ *sfh2*Δ [*AGE1*] segregants, and all exhibited consistent behaviour. For both high-copy *AGE1* plasmids, the growth of *age2*Δ *gcs1*Δ double-

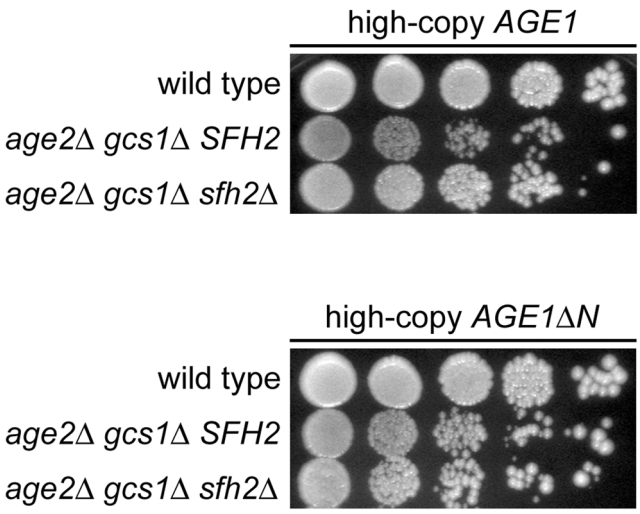

Figure 3.6 *AGE1* bypass of the essential Age2 + Gcs1 ArfGAP pair does not require Sfh2. Isogenic strains (W303 genetic background) deleted for the indicated genes and carrying either a high-copy *AGE1* plasmid (pSL377), or a high-copy *AGE1*Δ*N* plasmid (pSL489), were grown in selective medium at 30°C for 3 days. Equal numbers of cells from these strains were then serially diluted (5-fold serial dilutions), and spotted onto solid enriched medium and incubated at 30°C for 3 days. (Originally published in Benjamin *et al.*, 2011b and cited as 'data not shown'.)

mutant cells and *age2*Δ *gcs1*Δ *sfh2*Δ triple-mutant cells was similar, and in both cases was slightly impaired compared to the growth of wild-type control cells.

These results show that even though the Age1 protein is required for efficient Sfh2-mediated bypass of Age2 + Gcs1, the opposite is not true; the Sfh2 protein is not required for efficient Age1-mediated bypass of Age2 + Gcs1. This finding suggests that Sfh2 function is required upstream of Age1 function in a pathway that leads to bypass of Age2 + Gcs1. It is possible that Age1 in increased abundance does not require any PITP activity to functionally replace Age2 + Gcs1 for post-Golgi transport. However, it is also possible that the remaining Sec14-family proteins, which are known to have overlapping function with Sfh2 (Routt *et al.*, 2005), are able to provide the PITP activity that Age1 requires. Consistent with this possibility, increased *SFH3, SFH4,* or *SFH5* gene dosage also alleviates the temperature sensitivity of *gcs1-4 age2*Δ cells, albeit poorly in comparison to increased *SFH2* (Wong *et al.*, 2005).

3.8 Phospholipase D Mediates Effective *AGE1* Alleviation of *age2*Δ *gcs1-4* Temperature Sensitivity

The *SPO14* gene encodes the sole phospholipase D enzyme in yeast, which catalyzes the hydrolysis of phosphatidylcholine (PC), releasing choline and phosphatidic acid (PA); PA is then further hydrolyzed to produce diacylglycerol (DAG). The substrate of Spo14, PC, inhibits Gcs1 ArfGAP activity, whereas the products of Spo14 activity, PA and DAG, stimulate Gcs1 and Age2 ArfGAP activity (Antonny *et al.*, 1997; Yanagisawa *et al.*, 2002). Members of the yeast PITP family regulate Spo14 activity, with Sec14 acting as a negative regulator (Sreenivas *et al.*, 1998; Li *et al.*, 2000), while increased abundance of Sfh2 highly upregulates Spo14 activity (Schnabl *et al.*, 2003). The phospholipase D activity of Spo14 is activated by phosphoinositides, and Sfh2 activation of Spo14 has been suggested to function through Sfh2 delivery of phosphatidylinositol (PI) to lipid kinases such as Stt4 and Mss4 that in turn provide the phosphoinositides required for the stimulation of Spo14 (Routt *et al.*, 2005). This regulation raises the possibility that increased abundance of Sfh2 can activate ArfGAP activity by activating Spo14 phospholipase D activity, which in turn results in decreased levels of the ArfGAP-inhibiting phospholipid PC, and increased levels of the ArfGAP-stimulating lipids PA

and DAG. Indeed, increased Sfh2 abundance requires Spo14 for alleviation of *age2*Δ *gcs1-4* temperature sensitivity (Wong *et al.*, 2005), which combined with my finding that effective Sfh2 bypass of Age2 + Gcs1 requires Age1, suggests that Age1 may be activated by Spo14 phospholipase D activity. If this were the case, then elimination of Spo14 would be expected to compromise the ability of Age1 to alleviate *age2*Δ *gcs1-4* temperature sensitivity. To test this directly I assessed the ability of high-copy *AGE1* and *AGE1*Δ*N* to alleviate the temperature sensitivity of *age2*Δ *gcs1-4* cells that either had the *SPO14* gene intact or had a *spo14*Δ deletion mutation. In both cases (*AGE1* and *AGE1*Δ*N*), alleviation of *age2*Δ *gcs1-4* temperature sensitivity was compromised by the elimination of Spo14 (Figure 3.7). Thus Spo14, a downstream target of Sfh2 activity, is required for optimal Age1 function in place of Age2 + Gcs1 in post-Golgi transport, despite the fact that Sfh2 is not required for Age1 bypass of Age2 + Gcs1. As mentioned above, Sfh2 may be dispensable due to redundant functions provided by the remaining PITPs (Sfh3-Sfh5). Indeed, Sfh2 is not the only PITP that activates Spo14 (Schnabl *et al.*, 2003), and for this reason deletion of Sfh2 may have little or no effect on the activation of Spo14.

3.9 Increased Phosphatidylinositol Kinase Gene Dosage Fails to Alleviate *age2*Δ *gcs1-4* Temperature Sensitivity

A model for how increased Sfh2 abundance bypasses Age2 + Gcs1 is as follows. Increased Sfh2 abundance results in increased delivery of PI as a substrate to lipid kinases which produce increased amounts of $PI(4,5)P_2$ required for Spo14 activation. This delivery leads to increased Spo14 activity, which results in less PC, and more PA and DAG in the membrane, producing a lipid environment that is favourable to ArfGAP activity. This favourable lipid environment alters Age1 function in a way that allows the Age1 present at wild-type levels in *age2*Δ *gcs1*Δ cells to functionally replace Age2 + Gcs1 for post-Golgi transport. In agreement with this model, Age1 does indeed have the ability to function in place of Age2 + Gcs1 for post-Golgi transport, Age1 is required for efficient Sfh2 bypass of Age2 + Gcs1, and the elimination of Spo14 compromises the ability of Age1 to functionally replace Age2 + Gcs1 for post-Golgi transport, suggesting that overexpression of other potential downstream effectors of Sfh2 activity may also

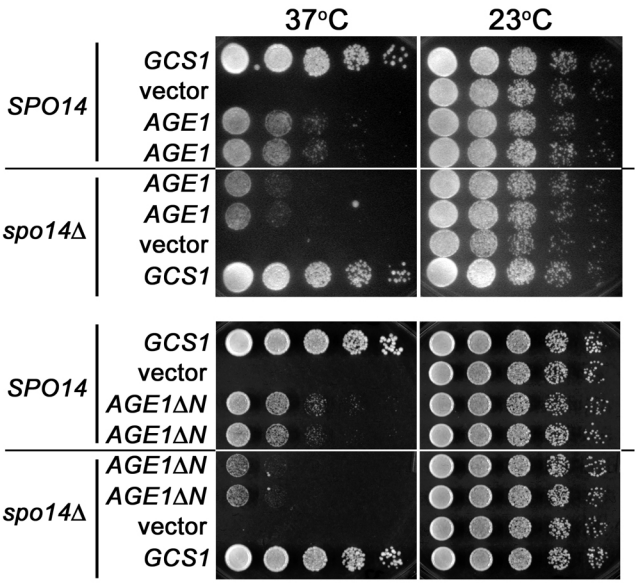

Figure 3.7 Effective alleviation of *age2*Δ *gcs1-4* temperature sensitivity requires Spo14. Temperature sensitive *age2*Δ *gcs1-4* cells (W303 genetic background) with the wild type *SPO14* gene (strain JBY65) or a *spo14*Δ deletion mutation (strain JBY64) and carrying either vector (pRS316), *GCS1* (pGCS1-316), high-copy *AGE1* (pSL473), or low-copy *AGE1*ΔN (pJB1736) plasmids were grown in selective medium at 23°C. Equal numbers of cells were then serially diluted (5-fold serial dilutions), and spotted onto solid enriched medium and incubated at 37°C or 23°C for 2 days. Two independent transformants are shown for cells carrying the *AGE1* or *AGE1*Δ*N* plasmid. (Originally published in Benjamin *et al.*, 2011b.)

have the ability to alleviate the *age2*Δ *gcs1-4* temperature-sensitive growth defect. To directly test this possibility I assessed the growth at 37°C of *age2*Δ *gcs1-4* cells carrying high-copy plasmids expressing the lipid kinase genes *STT4, PIK1,* and *MSS4*. Stt4 and Pik1 are PI 4-kinases that phosphorylate PI to produce phosphatidylinositol 4-phosphate (PI[4]P), and account for the majority of the PI 4-kinase activity in yeast cells (Flanagan *et al.*, 1993; Yoshida *et al.*, 1994; Audhya *et al.*, 2000). Mss4 is a PI(4)P 5-kinase that phosphorylates PI(4)P to produce phosphatidylinositol 4,5-bisphosphate (PI[4,5]P_2) (Boronenkov and Anderson, 1995). As positive controls for alleviation and growth at 37°C I also assessed *age2*Δ *gcs1-4* cells carrying high-copy plasmids expressing the *GCS1, AGE1, SFH2,* or *SPO14* gene. As expected, cells overexpressing *GCS1, AGE1,* or *SFH2* were able to grow at 37°C (Figure 3.8). Much like the negative-control cells carrying an empty vector, cells overexpressing the lipid kinase genes *STT4, PIK1,* or *MSS4* failed to grow at 37°C (Figure 3.8). Surprisingly, and contrary to our previously published result (Wong *et al.*, 2005), cells overexpressing the *SPO14* gene also failed to grow at 37°C (Figure 3.8). Thus, unlike increased *SFH2* gene dosage, increased dosage of genes whose functions may be affected by Sfh2 activity does not alleviate the temperature sensitivity of *age2*Δ *gcs1-4* cells.

The model described above suggests that increased expression of the proteins downstream of Sfh2 in an Sfh2-mediated phosphoinositide metabolic pathway that activates Spo14, including increased expression of Spo14 itself, might alleviate *age2*Δ *gcs1-4* temperature sensitivity through increased activation of Age1. The finding that this is not the case does not, however, disqualify the proposed model. It is possible that alleviation of *age2*Δ *gcs1-4* temperature sensitivity requires increased flux through the Sfh2-mediated phosphoinositide metabolic pathway that leads to Spo14 activation and membrane remodelling to allow Age1 to function in place of Age2 + Gcs1, and that increased flux through the pathway is uniquely provided by increased Sfh2 and is not provided by increasing the abundance of the other pathway components downstream of Sfh2. Although overexpression of *MSS4* does result in increased cellular levels of PI(4,5)P_2 (Desrivieres *et al.*, 1998), which should translate to increased Spo14 activity, it is possible that these levels are less than those achieved by increased flux through the pathway caused by increased abundance of Sfh2 itself, and are insufficient to activate

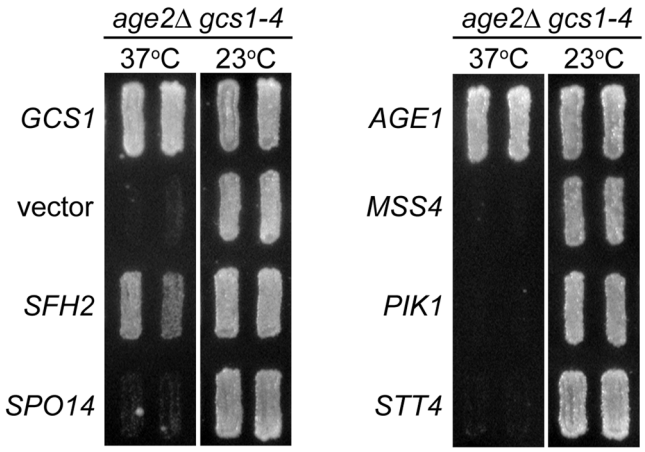

Figure 3.8 Increased gene dosages for phosphatidylinositol kinases fails to alleviate *age2Δ gcs1-4* temperature sensitivity. Patches of temperature-sensitive *age2*Δ *gcs1-4* cells (strain JBY33; W303 genetic background) harbouring plasmids (pPP421, pRS426, pCTY201, pRS426-SPO14, pSL473, pRS426-MSS4, pRS426-PIK1, pRS426-STT4) expressing the indicated genes were grown on solid selective medium at 23°C for 2 days before being replica-plated to solid enriched medium and incubated at 23°C and 37°C for 2 days. Eight individual transformants were assessed for each plasmid and in each case showed consistent behaviour; two transformants are shown for each. (Originally published in Benjamin *et al.*, 2011b and cited as 'data not shown'.)

Age1 to the level required for effective post-Golgi transport in the absence of Age2 + Gcs1. It is also possible that the increase in $PI(4,5)P_2$ levels that I am proposing may result from increased flux through the Sfh2 pathway are specifically localized to membrane domains where they are required for Age1 activation, and that the increased levels of $PI(4,5)P_2$ that result from overexpression of *MSS4* lack this localization. As such, increased flux through the Sfh2 pathway may result in local membrane lipid modifications that activate Age1 activity for post-Golgi transport precisely where it is required, whereas increased abundance of downstream components of the Sfh2 pathway may result in cellular lipid modifications that are more dispersed, and insufficient to activate Age1 at the membranes where Age1 activity is required for post-Golgi transport.

3.10 Age1-GFP and Age1ΔN-GFP Colocalize With Golgi and Endosomal Markers

The observation that increased abundance of Age1 can functionally replace Age2 + Gcs1 for post-Golgi function suggests that Age1 might be localized to Golgi and/or endosomal compartments. Age1-GFP and Age1ΔN-GFP fusion proteins, expressed under control of the inducible *GAL1* promoter, were therefore used to assess the localization of Age1 and Age1ΔN. To ensure that fusion of GFP to the C terminus of these Age1 proteins did not interfere with the ability to provide post-Golgi function, I assessed the ability of these GFP fusion proteins to alleviate *age2*Δ *gcs1-4* temperature sensitivity. When expression of the GFP fusion proteins was induced on galactose-containing medium both Age1-GFP and Age1ΔN-GFP alleviated the temperature sensitivity of *age2*Δ *gcs1-4* cells (data not shown), demonstrating that these fusion proteins retain the ability to provide post-Golgi function.

I assessed the localization of these GFP-fusion proteins in wild-type cells and *age2*Δ *gcs1-4* cells growing at 37°C. In both cell types, Age1-GFP and Age1ΔN-GFP were predominantly localized to large punctate dots that were typically present once or twice per cell, and were often localized near the vacuole (Figure 3.9). As a negative control I visualized the localization of GFP alone expressed from the inducible *GAL1* promoter in wild-type cells under the same growth conditions and temperatures; these control cells did not exhibit punctate staining (data not shown).

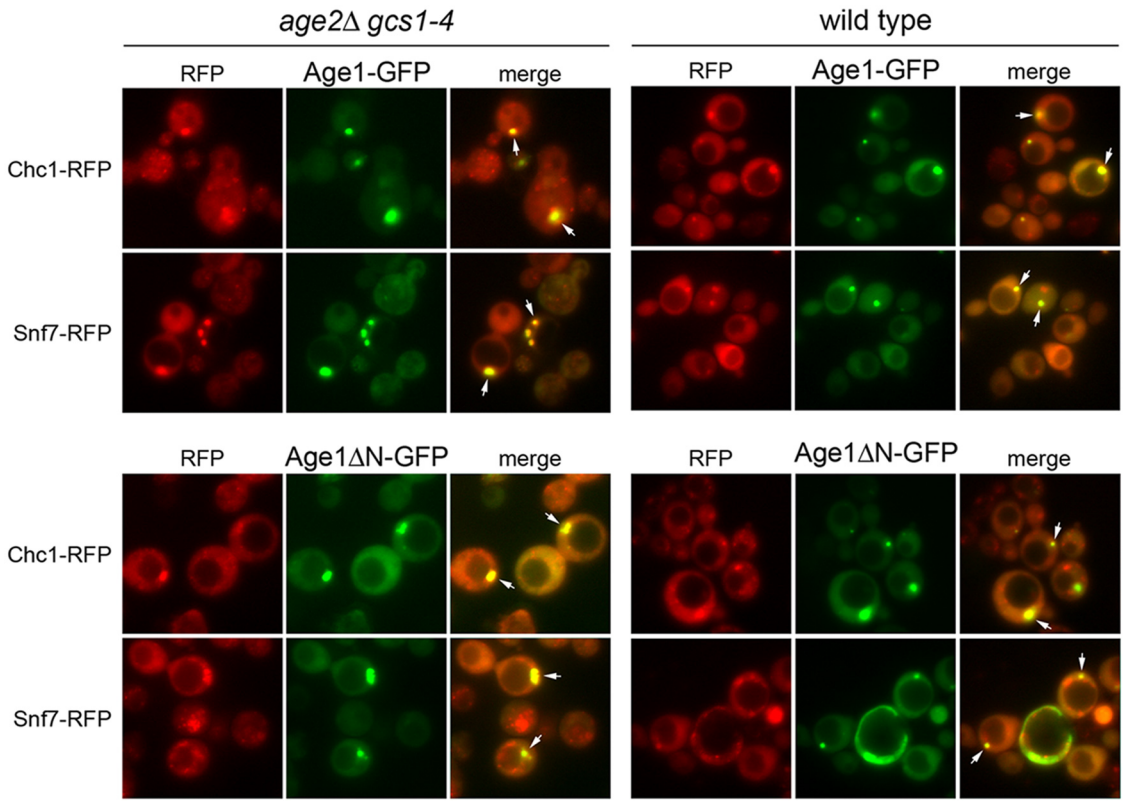

Figure 3.9 Age1-GFP and Age1ΔN-GFP colocalize with *trans*-Golgi and endosomal markers. Fluorescence micrographs are shown for logarithmically growing wild-type and *age2*Δ *gcs1-4* yeast cells (W303 genetic background) expressing RFP-tagged organelle marker proteins Chc1-RFP (*trans*-Golgi) or Snf7-RFP (endosomes) and harbouring plasmids expressing Age1-GFP (pJBAge1-GFP) or Age1ΔN-GFP (pPPL149-11) under control of the inducible *GAL1* promoter. Cells were grown to late log-phase in selective medium at 23°C with galactose as the sole carbon source before being diluted in fresh medium and incubated at 37°C for 16-18 hours. Logarithmically growing cells were concentrated in growth medium by centrifugation immediately prior to analysis by fluorescence microscopy. Arrows in the merged panels indicate representative colocalization. The wild type strains used were PPY203-G-Chc1-11A and PPY203-G-Snf7-4A; the *age2*Δ *gcs1-4* strains used were PPY203-G-Chc1-28B and PPY203-G-Snf7-5C. (*age2*Δ *gcs1-4* results were originally published in Benjamin *et al.*, 2011b.)

To determine whether the punctate localization of Age1-GFP and Age1ΔN-GFP corresponded to Golgi or endosomal compartments, I assessed the colocalization of Age1-GFP and Age1ΔN-GFP with organelle-specific proteins fused to red fluorescent protein (RFP) (Huh *et al.*, 2003). The Age1-GFP and Age1ΔN-GFP fusion proteins both colocalized with the Chc1-RFP and Snf7-RFP organelle-markers, which are localized to the *trans*-Golgi and endosomal compartments, respectively (Figure 3.9). The localization of Age1-GFP and Age1ΔN-GFP to Golgi and endosomal compartments is consistent with the ability of these Age1 proteins to functionally replace the Age2 + Gcs1 ArfGAP pair for post-Golgi transport.

3.11 Phospholipase D is Not Required for Age1-GFP Localization

The membrane lipid modifications produced by increased Spo14 activity (increased DAG and PA levels) stimulate the ArfGAP activities of Gcs1 and Age2 (Antonny *et al.*, 1997; Yanagisawa *et al.*, 2002). For Gcs1, this lipid stimulation of ArfGAP activity is caused, at least in part, by increased recruitment of Gcs1 to membranes enriched in these lipids (Antonny *et al.*, 1997). The requirement for Spo14 in Age1-mediated alleviation of *age2*Δ *gcs1-4* temperature sensitivity raised the possibility that Age1 localization to Golgi and endosomal compartments may be affected by Spo14 activity. To address the possibility that Spo14 is required for Age1 localization to Golgi and endosomal compartments, I assessed the localization of Age1-GFP and Age1ΔN-GFP fusion proteins in *age2*Δ *gcs1-4* cells with and without a *spo14*Δ deletion mutation. The elimination of Spo14 did not affect the localization of either of these GFP fusion proteins. Both Age1-GFP and Age1ΔN-GFP remained localized to one or two punctate dots in *spo14*Δ cells (Figure 3.10), indicating that Spo14 is not required for the localization of Age1 or Age1ΔN to Golgi and endosomal compartments. Since Spo14 is required for increased Age1 to functionally replace Age2 + Gcs1 for post-Golgi transport, but Spo14 is dispensable for the localization of Age1 to Golgi and endosomal compartments, it is likely that Spo14 functions to activate Age1 activity for post-Golgi transport in a manner that does not involve Age1 localization. Perhaps Spo14 exerts this effect through activation of the ArfGAP activity of Age1.

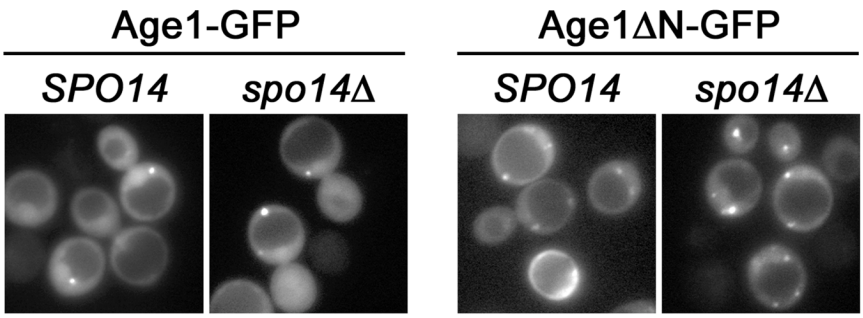

Figure 3.10 Deletion of Spo14 does not alter the localization of Age1-GFP or Age1ΔN-GFP. Fluorescence micrographs are shown for logarithmically growing *age2*Δ *gcs1-4* cells (W303 genetic background) with the wild type *SPO14* gene (strain JBY65) or a *spo14*Δ deletion mutation (strain JBY64) and harbouring plasmids expressing Age1-GFP (pJBAge1-GFP) or Age1ΔN-GFP (pPPL149-11) under control of the *GAL1* promoter. Cells were grown to late log-phase in selective medium at 23°C with galactose as the sole carbon source before being diluted in fresh medium and incubated at 37°C for 16 hours. Logarithmically growing cells were concentrated in growth medium by centrifugation immediately prior to analysis by fluorescence microscopy. (Originally published in Benjamin *et al.*, 2011b.)

3.12 DAG Enhances the *in vitro* ArfGAP Activity of Age1

As described above, Spo14 influences Age1 function to alleviate the temperature-sensitive growth of *age2*Δ *gcs1-4* cells, but is not required for Age1 localization to Golgi and endosomal compartments. These findings suggest that Spo14 may activate the ArfGAP activity of Age1. Indeed, the ArfGAP activity of Gcs1 and Age2 is activated by increased abundance of the lipids DAG and PA, the products of the phospholipase D activity of Spo14 (Antonny *et al.*, 1997; Yanagisawa *et al.*, 2002). To address whether DAG or PA similarly stimulate the ArfGAP activity of Age1, Dr. Pak Phi Poon in our lab employed an *in vitro* assay to assess the stimulation of Arf1-bound GTP hydrolysis by Age1ΔN-His_6 in the presence and absence of DAG or PA. In this assay, GTP-loaded Arf1 was bound to unilamellar lipid vesicles of uniform size. Substituting 15% of the lipid content with DAG resulted in increased stimulation of GTP hydrolysis, which was greater than that observed when the lipid content was substituted with 15% phosphatidic acid (Figure 3.11). At 1 nM Age1ΔN-His_6, the presence of DAG enhanced GTP hydrolysis by 50% compared to what was seen in the absence of DAG. This result indicates that, like Gcs1 and Age2, the *in vitro* ArfGAP activity of Age1 is stimulated by DAG. Therefore, the *in vivo* requirement for Spo14 to mediate effective Age1 alleviation of *age2*Δ *gcs1-4* temperature sensitivity is likely due to Spo14-mediated increases in the level of DAG in the membrane. Increased DAG levels then serve to activate Age1 ArfGAP activity allowing Age1 to functionally replace Age2 + Gcs1 for post-Golgi transport.

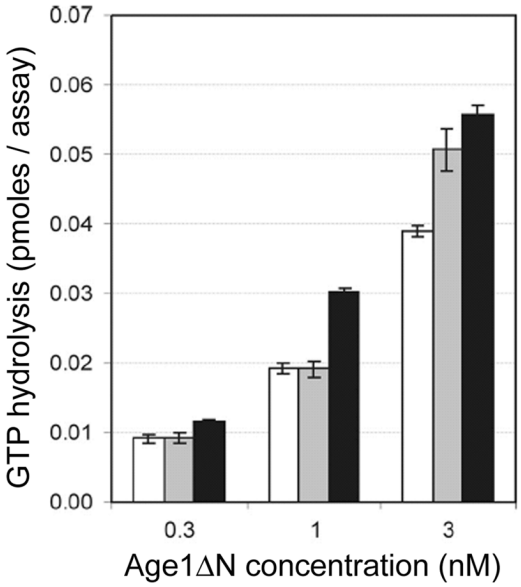

Figure 3.11 DAG stimulates *in vitro* ArfGAP activity of Age1ΔN. Activation of hydrolysis of GTP-loaded myristoylated-Arf1 by Age1ΔN-His_6 was assessed in assays in which the lipid content was either 100% dimyristoylphosphatidylcholine (white bar); 85% dimyristoylphosphatidylcholine, 15% phosphatidic acid (grey bar); or 85% dimyristoylphosphatidylcholine, 15% dioleoylglycerol (black bar). The low level of background radioactivity observed in the absence of Age1 protein was subtracted from all data values. Standard deviations were calculated from triplicate samples. (Originally published in Benjamin *et al.*, 2011b. Figure courtesy of Dr. Pak Phi Poon.)

CHAPTER 4. RESULTS – Dysregulated Arl1 Inhibits Endosomal Transport and Cell Proliferation

Note: The majority of the research described in this chapter was originally published in Molecular Biology of the Cell as: Benjamin JJ, Poon PP, Drysdale JD, Wang X, Singer RA, Johnston GC. Dysregulated Arl1, a regulator of post-Golgi vesicle tethering, can inhibit endosomal transport and cell proliferation in yeast**.** *Mol. Biol. Cell*. 2011; 22:2337-2347. © the American Society for Cell Biology.
Figures appearing in this chapter that are wholly reproduced from figures appearing in that paper include Figures: 4.1, 4.3, 4.5, 4.8, 4.9, 4.11, 4.12, 4.13, and 4.18. Figures 4.2, 4.10, 4.21, 4.23, and 4.28A display published results that were cited as 'unpublished results' in that paper.

4.1 Identifying Gene Deletions that Alleviate *gcs1*Δ Cold Sensitivity

Inadequate Gcs1 function blocks cell-cycle reentry from stationary phase at 14°C causing stationary-phase *gcs1*Δ cells to be cold sensitive and unable to proliferate. This cold sensitivity is conditional so that only cells in the developmental state of stationary phase are defective for cell proliferation. Actively proliferating *gcs1*Δ cells are not cold sensitive when transferred to 14°C and can continue to proliferate at this low temperature (Drebot *et al.*, 1987; Ireland *et al.*, 1994). It is important to note that *gcs1*Δ cold sensitivity, also referred to as the '*gcs1*Δ reentry defect,' is distinct from the typical cold sensitivity that is exhibited regardless of the developmental state of mutant cells upon transfer to the cold. For example, cells lacking the related *GLO3* gene (Poon *et al.*, 1999), are cold sensitive whether transferred to the cold from stationary phase or from active cell proliferation.

A former graduate student in our lab, John Drysdale, carried out a genetic screen to identify yeast proteins that affect the reentry defect imposed by the absence of Gcs1. To do so, he assessed whether *gcs1*Δ cold sensitivity could be alleviated by the additional deletion of other protein-coding genes. A *gcs1*Δ 'query strain' (PPY169-4) was crossed to each strain in the yeast deletion collection (approximately 4700 different non-essential gene-deletion strains) (Giaever *et al.*, 2002), and double-mutant haploid derivatives were

generated following the well-described SGA procedure (Tong *et al.*, 2001), each deleted for the *GCS1* gene plus one other non-essential gene. Deletion mutations that alleviated *gcs1*Δ cold sensitivity were identified by the ability of stationary-phase, double-mutant cells to form colonies at 14°C. Drysdale repeated this screen four times and identified 171 gene deletions that appeared to alleviate *gcs1*Δ cold sensitivity, with 35 of the gene deletions identified in two or more of the repeated screens (Table 4.1) (Drysdale, 2006).

4.2 Refining the List of Gene Deletions that Alleviate *gcs1*Δ Cold Sensitivity

The putative alleviating gene deletions identified by Drysdale were the foundation for this component of my thesis research. To follow up on these genetic screens, I first reassessed the putative alleviating deletions to eliminate any false positives (deletions that actually do not alleviate *gcs1*Δ cold sensitivity). Also, I chose to directly assess three additional gene deletions (*sbh2*Δ*, ssh1*Δ*,* and *alp1*Δ) that were not identified in the screen. I chose to assess the *sbh2*Δ deletion because Sbh2 is homologous to Sbh1, which was identified in the screen, and the *ssh1*Δ deletion because Ssh1 forms a complex with Sbh2. Likewise, I assessed the *alp1*Δ deletion because the Alp1 protein has strong similarity to the basic amino acid permeases Can1 and Lyp1, which were identified in the screen.

To reassess the putative alleviating gene deletions, and to directly assess the three additional gene deletions for alleviation of *gcs1*Δ cold sensitivity, I set out to construct diploid strains heterozygous for deletion of the *GCS1* gene and one of the 174 non-essential genes of interest, by crossing the *gcs1*Δ query strain (PPY169-4) to each of the deletion strains. [Note: Five of the deletion strains identified by Drysdale (*COX20, IMD3, RNR4, SUM1* and *YDR230W*) were not pursued because they were not contained in the deletion collection that was being used in the lab at the time I performed my analysis (Table 4.2). The deletion collection is periodically 'pinned' onto growth medium from frozen stocks of each strain. This pinned collection then serves as the working collection from which strains are obtained, until the collection is again freshly pinned from the frozen stocks. The five deletion strains that were missing from the pinned collection are contained in the frozen stocks, and were evidently present in the collection that Drysdale used for the screens (as they were identified as alleviators). Their absence from the

Table 4.1 Gene deletions that putatively alleviate *gcs1*Δ cold sensitivity

Number of screens in which the gene deletion was identified						
one				two	three	four
AAT2	*HAL9*	*RHK1*	*YAL004W*	*AVT6*	*LYP1*	***ARL1*** [a]
ADA2	*HIS7*	*RIM11*	*YAL058C-A*	*CBF1*	***RGP1*** [b]	***ARL3*** [a]
ADE16	*HXT8*	*RNR4*	*YAR043C*	*EGD1*	***RIC1*** [b]	***MAK3*** [a]
ADE2	*IMD3*	*RPL21A*	*YBL083C*	*GAL3*	*RPE1*	*SCS2*
ADE3	*JLP1*	*RPL24A*	*YBR241C*	*MNN9*	*YKL047W*	*SWH1*
AKR1	*KAP120*	*RPS27B*	*YBR250W*	*RPL43A*	***YLR261C*** [b]	***SYS1*** [a]
ARF3	*KAR4*	*RSM24*	*YBR266C*	*SBH1*	*YML079W* [c]	*YML078W* [c]
ARR2	*KEX2*	*SAM1*	*YDR065W*	*YBR238C*	*YML081W* [c]	*YML080W* [c]
ATP2	*LST7*	*SBE2*	*YDR161W*	***YDR136C*** [b]	*YML082W* [c]	*YML086C* [c]
BEM2	*LTP1*	*SDH2*	*YDR230W*	*YMR315W*	*YML083C* [c]	*YML088W* [c]
CAN1	***MAK10*** [a]	*SKN7*	*YDR249C*	***YPR050C*** [a]	*YML084W* [c]	
CAX4	*MAL13*	*SLI1*	*YDR539W*		*YML087C* [c]	
CDC10	*MDY2*	*SNT309*	*YEL008W*		*YML089C* [c]	
CHD1	*MET17*	*SPO12*	*YEL033W*		***YPT6*** [b]	
CHL1	*MET32*	*SPT3*	*YEL041W*			
CKI1	*MRPL13*	*SPT7*	*YGL230C*			
COX15	*MRPS8*	*SRY1*	*YGR201C*			
COX18	*MSD1*	*SSA1*	*YHR162W*			
COX20	*MTC5*	*STD1*	*YIL096C*			
CPA1	*MUS81*	*STO1*	*YJL007C*			
CSF1	*NAT1*	*SUM1*	*YJL215C*			
CTK2	*NPL6*	*SWA2*	*YJR088C*			
DAL4	*OAF1*	*TPM2*	*YKE2*			
ECM40	*ODC1*	*TRK1*	*YKL222C*			
ECM8	*PDX3*	*UMP1*	*YLL023C*			
ENT2	*PER1*	*UPS1*	*YML096W*			
ERG3	*PET18*	*URA5*	*YOR214C*			
EST1	*POP2*	*UTH1*	*YOR277C*			
FAA3	*POS5*	*VMA8*	*YOR309C*			
FPR1	*PPH21*	*VPS25*	*YPL109C*			
FUN19	*PSR1*	*VPS35*	*YPL144W*			
FYV7	*PTC1*	*VPS41*	*YPR092W*			
GAD1	*RAD4*	*WSC4*	*YPS1*			
GAT3	*RGT2*	*XYL2*	*ZUO1*			

[a]Component of the Arl1 pathway; [b]Component of the Ypt6 pathway; [c]Neighbouring genes on chromosome XIII (Drysdale, 2006)

Table 4.2 Retesting gene deletions for alleviation of *gcs1*Δ cold sensitivity

Strength of alleviation						
Strong	Medium	Weak	Variable	None		Not tested
AKR1	*AVT6*	*FAA3*	*AAT2*	*ADA2*	*RIM11*	*COX20*
ARL1 [a]	*NPL6*	*LTP1*	*CAN1*	*ADE16*	*RPL21A*	*IMD3*
ARL3 [a]	*STD1*	*POS5*	*CHD1*	*ADE2*	*RSM24*	*RNR4*
BEM2	*UMP1*	***RIC1*** [b]	*CHL1*	*ALP1*	*SDH2*	*SUM1*
CAX4	*YBL083C*	*VPS25*	*CKI1*	*ARF3*	*SNT309*	*YDR230W*
CBF1	***YDR136C*** [b]		*EGD1*	*ARR2*	*SPT3*	
LST7	*YGL230C*		*EST1*	*ATP2*	*SRY1*	*ADE3*
MAK3 [a]	***YLR261C*** [b]		*GAT3*	*COX15*	*SSA1*	*CDC10*
MNN9	***YPR050C*** [a]		*HXT8*	*COX18*	*TRK1*	*CPA1*
MTC5	***YPT6*** [b]		*LYP1*	*CSF1*	*URA5*	*ERG3*
POP2			*MDY2*	*CTK2*	*UTH1*	*HIS7*
PPH21			*MET32*	*DAL4*	*WSC4*	*SWA2*
SBH1			*MUS81*	*ECM40*	*XYL2*	*VMA8*
SBH2			*NAT1*	*ECM8*	*YAL004W*	
SSH1			*OAF1*	*ENT2*	*YAL058C-A*	
STO1			*PDX3*	*FPR1*	*YBR241C*	
SWH1			*PER1*	*FUN19*	*YBR250W*	
SYS1 [a]			*PET18*	*FYV7*	*YBR266C*	
VPS35			*PTC1*	*GAD1*	*YDR065W*	
VPS41			***RGP1*** [b]	*GAL3*	*YDR539W*	
YAR043C			*RPE1*	*HAL9*	*YEL033W*	
YGR201C			*RPL24A*	*JLP1*	*YEL041W*	
YKL047W			*RPL43A*	*KAP120*	*YIL096C*	
YML078W [c]			*RPS27B*	*KAR4*	*YJL007C*	
YML079W [c]			*SAM1*	*KEX2*	*YJL215C*	
YML080W [c]			*SBE2*	***MAK10*** [a]	*YJR088C*	
YML081W [c]			*SCS2*	*MAL13*	*YKE2*	
YML082W [c]			*SKN7*	*MET17*	*YKL222C*	
YML083C [c]			*SLI1*	*MRPL13*	*YLL023C*	
YML084W [c]			*SPO12*	*MRPS8*	*YML096W*	
YML086C [c]			*SPT7*	*MSD1*	*YMR315W*	
YML087C [c]			*TPM2*	*ODC1*	*YOR309C*	
YML088W [c]			*UPS1*	*PSR1*	*YPL109C*	
YML089C [c]			*YBR238C*	*RAD4*	*YPL144W*	
YPR092W			*YDR161W*	*RGT2*	*ZUO1*	
			YDR249C	*RHK1*		
			YEL008W			
			YHR162W			
			YOR214C			
			YOR277C			
			YPS1			

[a]Component of the Arl1 pathway; [b]Component of the Ypt6 pathway; [c]Neighbouring genes on chromosome XIII

pinned collection from which I obtained the deletion strains may have been the result of technical issues during pinning from the frozen stocks that resulted in these deletion strains being missed.] In total, 169 diploid strains were generated; these were then sporulated following the SGA procedure (Tong *et al.*, 2001). These sporulated diploid cells were then subjected to a random-spore selection procedure to obtain double-mutant haploid segregants by selection on medium that only allowed these cells to grow and which counter-selected growth of diploid cells and wild-type or single-mutant haploid cells. Seven of the diploids did not yield viable double-mutant haploid segregants through the random-spore procedure. This outcome was unexpected, because double-mutant cells with the same deletion mutations (*gcs1*Δ and either *ade3*Δ, *cdc10*Δ, *cpa1*Δ, *erg3*Δ, *his7*Δ, *swa2*Δ, or *vma8*Δ) had been identified in our screens as being alleviated for *gcs1*Δ cold sensitivity. It may be worth noting that each of these gene deletions was only identified in one of the four replicates of the screen. Why these double-mutant cells were previously able to grow (during the screens) but failed to grow here was not pursued, and these gene deletions were not assessed further (Table 4.2). For the remaining alleviating deletions, multiple double-mutant haploid segregants from each diploid were assessed for growth from stationary phase at 14°C. This procedure showed that 71 of the gene deletions actually do not alleviate the *gcs1*Δ-mediated cold sensitivity; these were not pursued further (with the notable exception of *mak10*Δ - see below). However, 91 gene deletions did indeed alleviate *gcs1*Δ cold sensitivity. I have divided the gene deletions that did alleviate cold sensitivity into 4 broad categories (Table 4.2). The strong, medium and weak alleviation categories contain gene deletions for which all double-mutant segregants examined behaved consistently, and allowed either strong, medium, or weak growth, respectively. In many cases growth was inconsistent between the multiple segregants assessed for a given deletion (*i.e.* some but not all of the double-mutant segregants were alleviated for *gcs1*Δ cold sensitivity); these deletions are listed in the variable alleviation category (Table 4.2). Wild-type and *gcs1*Δ cells were used as positive and negative controls, respectively, for growth throughout this process. This reassessment was useful, especially in identifying the strong and medium alleviators. Nevertheless, determining growth was at times difficult and subjective. The 91 gene deletions of interest are listed in Table 4.3, along with brief descriptions of what is known about their functions. It should

Table 4.3 Gene deletions that alleviate *gcs1*Δ cold sensitivity

Gene name	Description/Function [d]	Gene name	Description/Function
ARL1 [a]	G-protein; regulates membrane traffic	*RPL43A*	Large (60S) ribosomal subunit
ARL3 [a]	G-protein; regulates membrane traffic	*RPS27B*	Small (40S) ribosomal subunit
SYS1 [a]	Integral membrane protein; targets Arl3 to Golgi	*SAM1*	S-adenosylmethionine synthetase
MAK3 [a]	NatC N-terminal acetyltransferase subunit	*SBE2*	Golgi to PM transport of cell wall components
YPR050C [a]	Dubious ORF; partially overlaps *MAK3*	*SBH1*	ER translocation complex subunit
MAK10 [a]	NatC N-terminal acetyltransferase subunit	*SBH2*	ER translocation complex subunit
YPT6 [b]	G-protein; endosome to Golgi vesicle fusion	*SCS2*	Regulates phospholipid metabolism at ER
YLR261C [b]	Dubious ORF; overlaps *YPT6*	*SKN7*	Transcription factor; oxidative stress response
RGP1 [b]	Ypt6 GEF subunit	*SLI1*	N-acetyltransferase
YDR136C [b]	Dubious ORF; overlaps *RGP1*	*SPO12*	Nuclear regulator of mitotic exit
RIC1 [b]	Ypt6 GEF subunit	*SPT7*	Subunit of SAGA transcriptional regulator
AAT2	Cytosolic aspartate aminotransferase	*SSH1*	Translocon subunit; protein translocation into ER
AKR1	Protein palmitoyl transferase	*STD1*	Controls glucose-regulated gene expression
AVT6	Vacuolar aspartate/glutamate exporter	*STO1*	Nuclear mRNA cap-binding complex subunit
BEM2	RhoGAP; control of cytoskeleton organization	*SWH1*	Golgi-localized oxysterol-binding protein
CAN1	Plasma membrane arginine permease	*TPM2*	Stabilizes actin cables/filaments
CAX4	ER. Dolichyl pyrophosphate phosphatase	*UMP1*	Chaperone for 20S proteasome maturation
CBF1	Transcription factor	*UPS1*	regulates mitochondrial cardiolipin levels
CHD1	Nucleosome remodeling factor; transcription	*VPS25*	ESCRT-II subunit; sorts proteins into MVB
CHL1	Nuclear protein; sister-chromatid pairing	*VPS35*	Retromer subunit; endosome to TGN transport
CKI1	Choline kinase; phosphatidylcholine synthesis	*VPS41*	HOPS subunit; docking/fusion post Golgi
EGD1	Subunit of NAC for protein targeting	*YPS1*	Aspartic protease; cell wall growth/maintenance
EST1	Involved in telomere length regulation	*YAR043C*	Deleted ORF, no protein encoded; overlaps *SWH1*
FAA3	Long chain fatty acyl-CoA synthetase	*YBL083C*	Dubious ORF; overlaps *ALG3*
GAT3	Protein containing GATA family zinc finger motifs	*YBR238C*	Mitochondrial membrane protein
HXT8	Unknown function; similarity to hexose transporter	*YDR161W*	Unknown function
LST7	Possibly involved in a post-Golgi secretory pathway	*YDR249C*	Unknown function
LTP1	Protein phosphotyrosine phosphatase	*YEL008W*	Dubious ORF; predicted role in metabolism
LYP1	Lysine permease	*YGL230C*	Unknown function
MDY2	Inserts tail-anchored proteins into ER membrane	*YGR201C*	Unknown function
MET32	Transcription factor; Met biosynthetic genes	*YHR162W*	Unknown function; localizes to mitochondria
MNN9	Subunit of Golgi mannosyltransferase complex	*YKL047W*	Unknown function; localizes to cytoplasm
MTC5	Unknown function	*YOR214C*	Unknown function
MUS81	endonuclease subunit; cleaves branched DNA	*YOR277C*	Dubious ORF; overlaps *CAF20*
NAT1	NatA N-terminal acetyltransferase subunit	*YPR092W*	Dubious ORF
NPL6	RSC chromatin remodeling complex subunit	*YML078W* [c]	Mitochondrial peptidyl-prolyl cis-trans isomerase
OAF1	Oleate-activated transcription factor	*YML079W* [c]	Unknown function; localizes to nucleus/cytoplasm
PDX3	Pyridoxine (pyridoxamine) phosphate oxidase	*YML080W* [c]	Dihydrouridine synthase; modifies pre-tRNA(Phe)
PER1	ER protein; remodels GPI anchors	*YML081W* [c]	Unknown function; localizes to nucleus
PET18	Weak similarity to thiamin metabolism proteins	*YML082W* [c]	Unknown function; localizes to nucleus/cytoplasm
POP2	RNase subunit of mRNA deadenylation complex	*YML083C* [c]	Unknown function
POS5	Mitochondrial NADH kinase	*YML084W* [c]	Dubious ORF
PPH21	Catalytic subunit of protein phosphatase 2A (PP2A)	*YML086C* [c]	Mitochondrial D-Arabinono-1,4-lactone oxidase
PTC1	Type 2C protein phosphatase (PP2C)	*YML087C* [c]	Unknown function
RPE1	Functions in pentose-phosphate pathway	*YML088W* [c]	E3 ubiquitin ligase subunit
RPL24A	Large (60S) ribosomal subunit	*YML089C* [c]	Dubious ORF

[a] Component of the Arl1 pathway; [b] Component of the Ypt6 pathway; [c] Neighbouring genes on chromosome XIII

[d] SGD project. "Saccharomyces Genome Database" http://www.yeastgenome.org/ (Accessed September 6, 2010)

be noted that the *mak10*Δ strain, which showed no alleviation during this assessment, was later more thoroughly assessed and showed robust alleviation (Figure 4.1).

Remarkably, 11 of the deletions that were strong alleviators of *gcs1*Δ cold sensitivity eliminate neighbouring genes (on chromosome XIII). I believe that these 11 gene deletions represent a linkage group, and are not *bone fide* alleviators of *gcs1*Δ cold sensitivity. Such a linkage group would be identified in the screen if the parental strain used to create these particular deletion mutations contained an unmarked mutation that alleviates *gcs1*Δ cold sensitivity. Indeed, these deletion strains were created in the same lab and are therefore likely to have been developed from a common parental strain (http://www-sequence.stanford.edu/group/yeast_deletion_project/strainsbylab.txt). The position of the linkage group indicates the location of this unmarked alleviating mutation. It is therefore likely that one of the genes in the middle of this linkage group is a *bona fide* alleviator of *gcs1*Δ cold sensitivity when deleted or mutated; its identification requires further analysis.

4.3 Elimination of Vesicle-Tethering Pathways at the *trans*-Golgi Membrane Alleviates *gcs1*Δ Cold Sensitivity

A striking observation made by Drysdale was that eight of the alleviating gene deletions eliminate members of two related and well-conserved vesicular-transport pathways involved in transport-vesicle tethering: five eliminate members of the Arl1 pathway (*arl1*Δ, *arl3*Δ, *sys1*Δ, *mak3*Δ, and *mak10*Δ), and three eliminate members of the Ypt6 pathway (*ypt6*Δ, *ric1*Δ, and *rgp1*Δ). Both of these vesicle-tethering pathways function at the *trans*-Golgi membrane (Figure 1.1) (Siniossoglou *et al.*, 2000; Panic *et al.*, 2003b; Setty *et al.*, 2003; Behnia *et al.*, 2004; Setty *et al.*, 2004). The remainder of this thesis chapter focuses on these vesicle-tethering pathways and the roles they play in *gcs1*Δ cold sensitivity.

I performed tetrad analyses on the eight gene deletions noted above (*arl1*Δ, *arl3*Δ, *sys1*Δ, *mak3*Δ, *mak10*Δ, *ypt6*Δ, *ric1*Δ, and *rgp1*Δ) that alleviate *gcs1*Δ cold sensitivity. To do so, diploid strains were first constructed by mating the *gcs1*Δ query strain (PPY169-4) with the eight gene-deletion strains from the deletion collection. These heterozygous

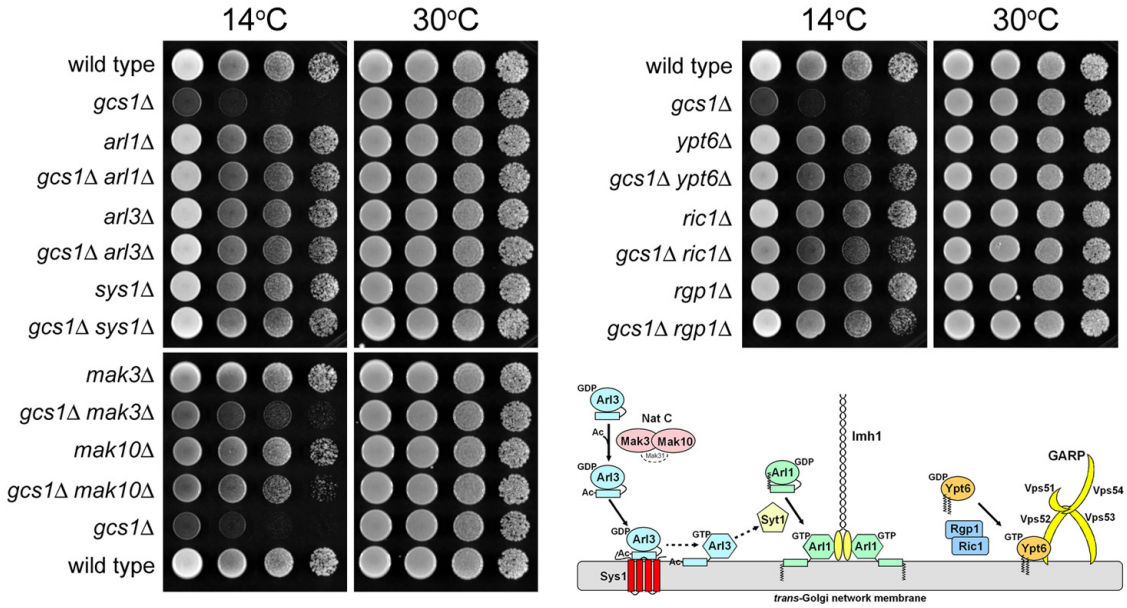

Figure 4.1 Deletion of genes in the Arl1 and Ypt6 pathways alleviates *gcs1Δ* cold sensitivity. Isogenic strains deleted for the indicated genes (S288C genetic background) were grown in enriched medium to stationary phase by incubation at 30°C for 5 days; ten-fold serial dilutions were then spotted onto solid enriched medium and incubated at 14°C for 12 days or 30°C for 2 days. (Originally published in Benjamin *et al.*, 2011a.) The diagram of the Arl1 and Ypt6 vesicle tethering pathways from Figure 1.1 has been added here as a reminder of where these proteins function. For details please refer to Figure 1.1.

diploids were then sporulated and the resulting tetrads were dissected to obtain haploid meiotic segregants. For each deletion, four single-mutant segregants deleted for the gene in question (*e.g. arl1*Δ) and four double-mutant segregants deleted for the *GCS1* gene and the gene in question (*e.g. gcs1*Δ *arl1*Δ) were assessed for growth from stationary phase at 14°C. The four single- and double-mutant segregants tested for each gene deletion behaved consistently; the eight different gene deletions were all confirmed to alleviate *gcs1*Δ cold sensitivity. Shown in Figure 4.1 is the growth of representative single- and double-mutant segregants in a serial-dilution assay. Wild-type and *gcs1*Δ cells served as controls.

To assess if the deletion of *ARL1* and *YPT6* could alleviate *gcs1*Δ cold sensitivity in other yeast strains, I first reconstructed the *gcs1*Δ, *arl1*Δ, and *ypt6*Δ deletions in the widely used W303 genetic background. These deletions were confirmed by PCR using primers outside of the *ARL1* and *YPT6* regions subjected to homologous recombination when the deletion strains were created. From these W303 deletion strains, I then constructed diploid strains that were heterozygous for the *gcs1*Δ deletion and either the *arl1*Δ (JBY72) or *ypt6*Δ (JBY120) deletion. These heterozygous deletion strains were then sporulated and the resulting tetrads were dissected to obtain haploid meiotic segregants. Multiple segregants were then assessed for growth from stationary phase at 14°C. As with strain S288C, the *arl1*Δ and *ypt6*Δ deletion mutations also alleviated *gcs1*Δ cold sensitivity in the W303 context; shown in Figure 4.2 is the growth of two representative single- and double-mutant segregants for each deletion in a serial-dilution assay, with wild-type and *gcs1*Δ cells serving as controls. Thus, the alleviation of *gcs1*Δ cold sensitivity by the *arl1*Δ and *ypt6*Δ deletion mutations is not strain specific, but rather seems to be a general feature of these gene deletions. Importantly, this finding has allowed both genetic backgrounds (W303 and S288C) to be used in further investigations.

These results reveal that impairment of two vesicle-tethering pathways at the *trans*-Golgi membrane relieves the reentry defect caused by the absence of Gcs1. Both of these vesicle-tethering pathways operate through the activation and recruitment, by GTP

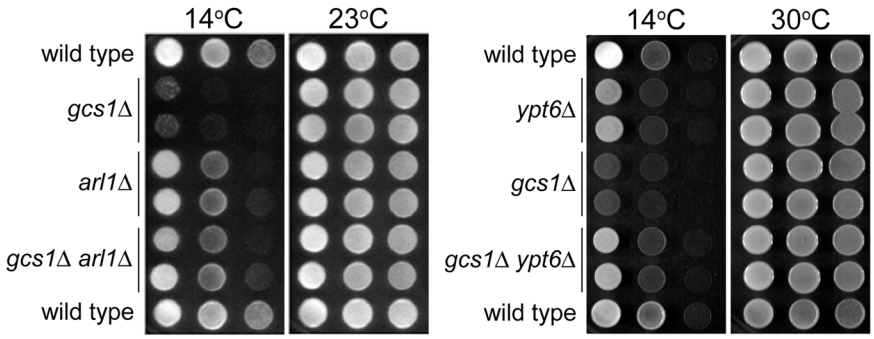

Figure 4.2 Alleviation of *gcs1*Δ cold sensitivity by *ARL1* and *YPT6* gene deletions is not strain specific. Isogenic strains deleted for the indicated genes (W303 genetic background) were grown in enriched medium to stationary phase by incubation at 30°C for 3 days (*arl1*Δ strains) or 7 days (*ypt6*Δ strains); ten-fold serial dilutions were then spotted onto solid enriched medium and incubated at 14°C for 8 days (*arl1*Δ strains) or 5 days (*ypt6*Δ strains), 23°C for 2 days, or 30°C for 1 day. (Originally published in Benjamin *et al.*, 2011a and cited as 'data not shown'.)

binding, of small G-proteins: in one case Arl1, and in the other, Ypt6. Therefore, the activated, GTP-bound forms of Arl1 and Ypt6 are implicated in the *gcs1*Δ reentry defect.

4.4 The NatC Subunit Mak31 is Not Involved in the Cold Sensitivity Imposed by the Arl1 Pathway

N-terminal acetylation of the Arl3 protein by the NatC complex is required for Golgi targeting of Arl3, which is essential for proper Arl1-pathway function (Behnia *et al.*, 2004; Setty *et al.*, 2004). The NatC complex is comprised of a catalytic subunit, Mak3, and two auxiliary or regulatory subunits, Mak10 and Mak31 (Polevoda and Sherman, 2001). All three subunits of NatC are required for the N-terminal acetylation of several NatC substrates tested *in vitro* (Polevoda and Sherman, 2001); however, Mak31 is not required for the N-terminal acetylation of Arl3 (Setty *et al.*, 2004). As such, Mak31 is not involved in recruiting activated GTP-bound Arl1 to the Golgi. Therefore, based on our results that elimination of components of the Arl1 pathway required for the activation of Arl1 alleviates *gcs1*Δ cold sensitivity, elimination of Mak31 is not expected to alleviate. Indeed, our screen for gene deletions that alleviate *gcs1*Δ cold sensitivity identified multiple members of the Arl1 pathway, including Arl3 and the NatC subunits Mak3 and Mak10, but did not identify the third subunit, Mak31. To directly test if deletion of the *MAK31* gene alleviates *gcs1*Δ cold sensitivity, I first constructed a diploid strain by mating the *gcs1*Δ query strain (PPY169-4) with the *mak31*Δ deletion strain from the collection. This heterozygous strain was then sporulated and the resulting tetrads were dissected to obtain haploid meiotic segregants. Deletion of the *MAK31* gene was confirmed by PCR using primers defining regions outside of the *MAK31* regions that were subjected to homologous recombination to create the deletion strain. Consistent with Mak31 being dispensable for the acetylation of Arl3 (Setty *et al.*, 2004), I found that deletion of *MAK31* did not alleviate *gcs1*Δ cold sensitivity; *gcs1*Δ *mak31*Δ double mutant cells remained cold sensitive (Figure 4.3). This observation, combined with results showing that Arl3 is properly localized to the Golgi in *mak31*Δ cells but not in *mak3*Δ or *mak10*Δ cells (Setty *et al.*, 2004), and that the Arl1 effector Imh1 is properly targeted to the Golgi in *mak31*Δ cells while being completely mislocalized in *mak3*Δ and *mak10*Δ

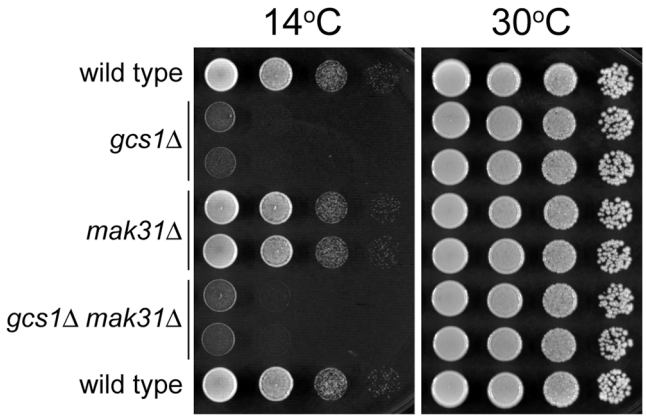

Figure 4.3 Elimination of the NatC subunit Mak31 does not alleviate *gcs1*Δ cold sensitivity. Isogenic strains deleted for the indicated genes (S288C genetic background) were grown in enriched medium to stationary phase by incubation at 30°C for 5 days; ten-fold serial dilutions were then spotted onto solid enriched medium and incubated at 14°C for 7 days or 30°C for 2 days. (Originally published in Benjamin *et al.*, 2011a.)

cells (Behnia *et al.*, 2004), is in agreement with activated Arl1 being implicated in the *gcs1*Δ reentry defect.

4.5 Deletion of the Arl1GEF Syt1 Alleviates *gcs1*Δ Cold Sensitivity

The activation of GDP-bound G-proteins is a controlled process carried out by proteins termed guanine-nucleotide exchange factors (GEFs), which interact with GDP-bound G-proteins to stimulate exchange of the bound GDP for GTP. Although many of the components of the Arl1 pathway have been determined, the identities of the GEF proteins that activate Arl1 or Arl3 have been elusive. Recently, a protein with GEF activity towards Arl1 was reported: Syt1 has Arl1GEF activity and promotes Arl1 activation (Chen *et al.*, 2010). Our genetic results indicate that elimination of many of the components of the Arl1 pathway required for the activation of Arl1 alleviates *gcs1*Δ cold sensitivity. If Syt1 activates Arl1, then deletion of the *SYT1* gene may also alleviate the *gcs1*Δ phenotype, although *syt1*Δ was not identified as an alleviator in our genetic screens. To directly test deletion of the *SYT1* gene for alleviation of *gcs1*Δ cold sensitivity, I first constructed a diploid strain by mating the *gcs1*Δ query strain (PPY169-4) with the *syt1*Δ strain from the collection. This heterozygous strain was then sporulated and the resulting tetrads were dissected to obtain haploid meiotic segregants. Deletion of the *SYT1* gene was not confirmed by PCR; however, the marker genes for the *gcs1*Δ and *syt1*Δ deletions (*nat* and *kan*, respectively) both segregated in a 2:2 fashion, consistent with marker integration solely at the correct chromosomal location. To test if deletion of *SYT1* alleviates *gcs1*Δ cold sensitivity, four *syt1*Δ single-mutant segregants and four *gcs1*Δ *syt1*Δ double-mutant segregants were assessed for growth from stationary phase at 14°C. For both situations the four representative single- and double-mutant segregants behaved consistently: deletion of the *SYT1* gene alleviated *gcs1*Δ cold sensitivity. Shown in Figure 4.4 is the growth of two representative single- and double-mutant segregants in a serial-dilution assay; wild-type and *gcs1*Δ cells serve as controls.

The alleviation provided by the deletion of most of the genes in the Arl1 pathway is robust. With the exception of *mak3*Δ, the double-mutant cells deleted for *GCS1* and an

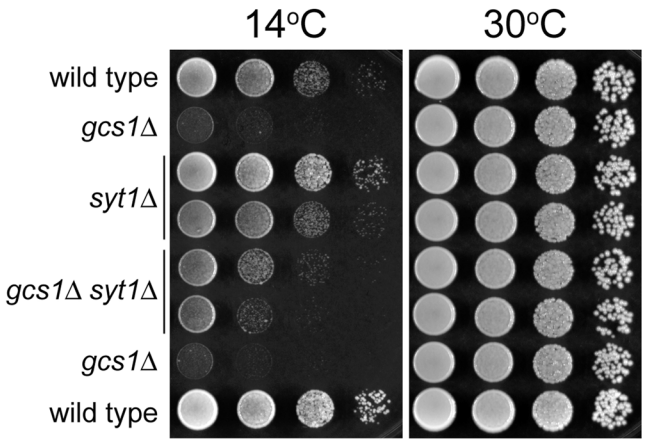

Figure 4.4 Elimination of the Arl1GEF Syt1 alleviates *gcs1*Δ cold sensitivity.
Isogenic strains deleted for the indicated genes (S288C genetic background) were grown in enriched medium to stationary phase by incubation at 30°C for 7 days; ten-fold serial dilutions were then spotted onto solid enriched medium and incubated at 14°C for 10 days or 30°C for 2 days.

Arl1-pathway gene grow as well at 14°C as the single mutant cells deleted only for the Arl1-pathway gene (Figure 4.1). In contrast, the alleviation provided by the deletion of *SYT1* is not particularly obvious, which may account for the absence of this deletion mutation in the list of 'hits' from our initial genetic screens. Although *gcs1*Δ *syt1*Δ double-mutant cells did exhibit growth compared to *gcs1*Δ control cells, these double-mutant cells did not grow as well as *syt1*Δ single-mutant cells. It has been proposed that Syt1 is not the only GEF for Arl1, and that there is at least one other protein (unidentified) that also provides Arl1GEF activity (Chen *et al.*, 2010). The activity of this proposed additional Arl1GEF in the absence of Syt1 might explain the lower level of alleviation seen in the *syt1*Δ situation compared to the robust alleviation caused by deletion of other Arl1-pathway members. Nevertheless, alleviation of *gcs1*Δ cold sensitivity by deletion of the *SYT1* gene is consistent with the proposed GEF activity of Syt1 that would promote Arl1 activation, and with alleviation caused by blocking the activation of Arl1.

4.6 In Addition to Alleviating *gcs1*Δ Cold Sensitivity, the Elimination of Arl1 or Ypt6 Also Restores Effective Endocytic Transport in *gcs1*Δ Cells

Endocytic transport is impaired in *gcs1*Δ cells, and previously identified conditions that alleviate *gcs1*Δ cold sensitivity also relieve the endocytic-transport defect (Wang *et al.*, 1996). To assess whether the absence of Arl1 or Ypt6 relieves the endocytic-transport defect caused by the *gcs1*Δ mutation, I used the lipophilic dye FM 4-64 to monitor endocytic transport in *gcs1*Δ cells also harbouring the *arl1*Δ or *ypt6*Δ mutation. As controls, wild-type and *gcs1*Δ cells as well as *arl1*Δ and *ypt6*Δ single-mutant cells were also assessed. The wild-type and mutant cells used for this assay are haploid meiotic segregants from the heterozygous diploid strains in the W303 genetic background that were described above: JBY72 (*arl1*Δ strains) and JBY120 (*ypt6*Δ strains, wild-type and *gcs1*Δ controls). After FM 4-64 staining of the plasma membrane, cells were incubated in fresh medium and transport of the dye was monitored over time by fluorescence microscopy. If endocytic transport is functional, membrane-bound FM 4-64 is internalized from the plasma membrane, transported through intermediate endocytic

compartments, and accumulated at the vacuolar membrane (Vida and Emr, 1995). Wild-type cells resuming cell proliferation from stationary phase at 14°C transported FM 4-64 to the vacuolar membrane resulting in a characteristic ring-staining pattern (Figure 4.5). As expected, the use of stationary-phase cells and a low incubation temperature led to kinetics of dye transport that were considerably slower than those of actively proliferating cells at 30°C (Vida and Emr, 1995; Wang *et al.*, 1996). In contrast to wild-type cells, *gcs1*Δ cells treated in the same way, while able to internalize the dye from the plasma membrane, were unable to deliver dye to the vacuole. As a result, in *gcs1*Δ mutant cells the dye remained trapped in endocytic compartments (Wang *et al.*, 1996; Figure 4.5). The *arl1*Δ and *ypt6*Δ gene deletions that alleviated *gcs1*Δ cold sensitivity also relieved the endocytic-transport defect in *gcs1*Δ cells and allowed FM 4-64 to be efficiently transported to the vacuole (Figure 4.5). Note that the *arl1*Δ and *ypt6*Δ mutations resulted in moderately fragmented vacuoles, consistent with previously published results with these deletions (Tsukada *et al.*, 1999; Bonangelino *et al.*, 2002), and additional deletion of the *GCS1* gene from *arl1*Δ and *ypt6*Δ mutant cells did not appear to affect this fragmentation. Thus, similar to previously identified conditions that alleviate *gcs1*Δ cold sensitivity, alleviation by the elimination of Arl1 or Ypt6 also restores effective endocytic transport in *gcs1*Δ cells.

4.7 The Ypt6 Pathway is Required for Normal Localization of the Arl1 Effector Imh1

As an effector of activated Arl1, the Imh1 protein is thought to be involved in tethering of transport vesicles at the *trans*-Golgi membrane, facilitating target-compartment recognition and vesicle fusion. Proper functioning of the Arl1 pathway results in recruitment of Imh1 to the *trans*-Golgi membrane through direct interaction of Imh1 with activated Arl1 (Munro and Nichols, 1999; Panic *et al.*, 2003a). Deletion of any of the known components of the Arl1 pathway (Arl1, Arl3, Sys1, Mak3, Mak10) blocks the activation and membrane localization of Arl1, resulting in mislocalization of Imh1. Expression of a version of Imh1 fused to green fluorescent protein (GFP-Imh1) in wild-type cells reveals punctate structures characteristic of proper Golgi localization but only diffuse staining when the Arl1 pathway is defective, indicating that Imh1 does not

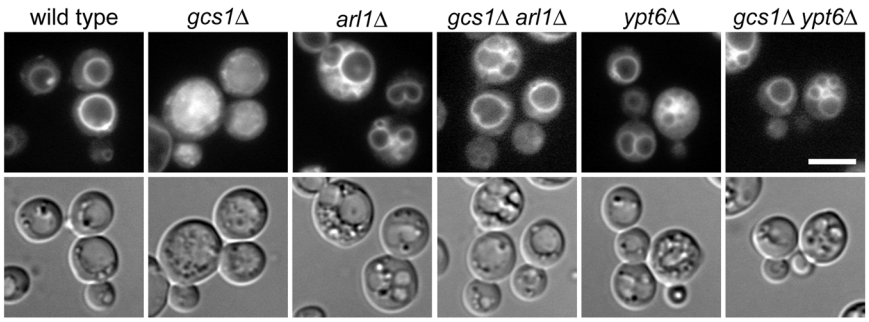

Figure 4.5 Deletion of the *ARL1* or *YPT6* gene restores effective endocytic transport in *gcs1*Δ cells. Stationary-phase cells deleted for the indicated genes (W303 genetic background) were loaded with the lipophilic dye FM 4-64 on ice before being diluted in fresh enriched medium and incubated at 14°C. Membrane transport was assessed by fluorescence microscopy after 0, 5, 10, and 24 hours. Data from the 24-hour time point are shown. Dye-bound membranes were visualized by fluorescence microscopy (top panels) and cells were visualized by differential interference contrast microscopy (bottom panels). The FM 4-64 stain began to accumulate at the vacuole in cells of all strains except *gcs1*Δ by 10 hours, and clear vacuolar ring staining was apparent in the majority of cells by 24 hours. In the *gcs1*Δ control cells the FM 4-64 stain remained trapped in endocytic compartments within the cytoplasm and had not been transported to the vacuolar membrane by 24 hours. Under these assay conditions all strains remained greater than 95% viable for up to 96 hours; cell viability was assessed by methylene blue dye exclusion. Scale bar, 5 µm. (Originally published in Benjamin *et al.*, 2011a.)

localize to the Golgi but remains cytoplasmic (Panic *et al.*, 2003b; Setty *et al.*, 2003; Behnia *et al.*, 2004; Setty *et al.*, 2004).

The screen for gene deletions that alleviate *gcs1*Δ cold sensitivity was effective in identifying components of the Arl1 pathway, having identified all of the known components (Arl1, Arl3, Sys1, Mak3, Mak10) with the exception of the recently identified Arl1GEF protein Syt1 (Chen *et al.*, 2010). Because there may be components of the Arl1 pathway that have yet to be identified (for example the GEF for Arl3 and another GEF for Arl1), I wondered if any of the other alleviating gene deletions identified in the screen also eliminate proteins involved in the activation of Arl1. To address this possibility, I used the localization of a GFP-Imh1 fusion protein as a readout to indicate which gene deletions prevent the activation of Arl1. I transformed a plasmid encoding a GFP-Imh1 fusion protein into cells of the 92 deletion strains from the deletion collection that were found to alleviate *gcs1*Δ cold sensitivity (Table 4.3), and in a blinded experiment assessed the localization of GFP-Imh1 in each deletion strain. GFP-Imh1 was mislocalized and exhibited a diffuse cytoplasmic pattern in several of these deletion strains. As expected, mislocalization of GFP-Imh1 occurred in the five strains with Arl1-pathway deletions (*arl1*Δ, *arl3*Δ, *sys1*Δ, *mak3*Δ, and *mak10*Δ) that have previously been shown to mislocalize GFP-Imh1 (Panic *et al.*, 2003b; Setty *et al.*, 2003; Behnia *et al.*, 2004; Setty *et al.*, 2004) (Figure 4.6). Surprisingly, the three strains with Ypt6-pathway deletions (*ypt6*Δ, *ric1*Δ, and *rgp1*Δ) also mislocalized GFP-Imh1 (Figures 4.6 and 4.8). Three other deletions that mislocalized GFP-Imh1 were *ypr050c*Δ*, ylr261c*Δ*,* and *ydr136c*Δ (Figure 4.6); each of these deletions eliminates a dubious open reading frame that overlaps a gene in the Arl1 or Ypt6 pathway (*MAK3, YPT6,* and *RGP1,* respectively). The most likely interpretation is that each of these deletions impairs the *bona fide* gene with which it overlaps.

These results indicate that my blinded analysis of the deletion strains was effective in identifying known components of the Arl1 pathway required for the proper localization of GFP-Imh1. Remarkably, this approach revealed that the Ypt6 pathway is also required for the proper localization of GFP-Imh1. This finding was unexpected because the Ypt6 and Arl1 pathways have been considered to be parallel pathways (Graham, 2004), although there is some potential 'cross talk' between them

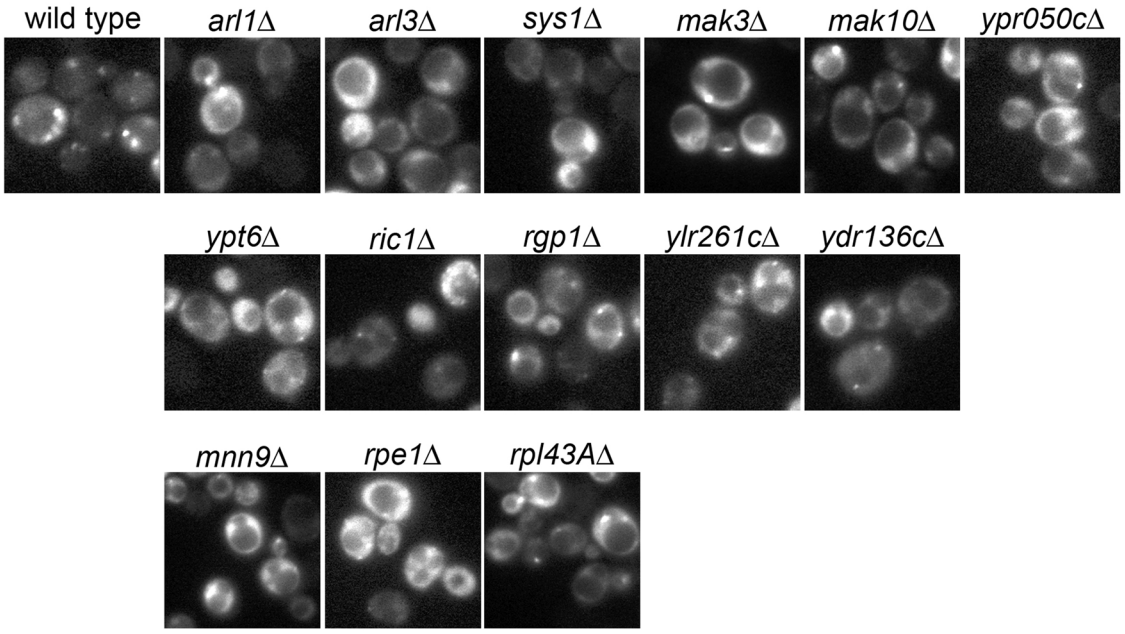

Figure 4.6 A subset of the gene deletions that alleviate *gcs1*Δ cold sensitivity also mislocalize GFP-Imh1. Fluorescence micrographs displaying live yeast cells with the indicated gene deletions (S288C genetic background) and harbouring a plasmid (pSR15) expressing GFP-Imh1. Cells growing logarithmically in selective medium at 30°C were concentrated in growth medium by centrifugation immediately prior to analysis by fluorescence microscopy. The wild type strain used was BY4741; deletion strains were from the deletion collection.

(Panic *et al.*, 2003b). The fact that deletion of the genes encoding the GEF for Ypt6 (Ric1–Rgp1) affects GFP-Imh1 localization in the same way as deletion of *YPT6* itself, indicates that it is the activated, GTP-bound form of Ypt6 that is required for proper GFP-Imh1 localization.

4.8 The Arl1GEF Syt1 is Not Required for Localization of the Arl1 Effector Imh1

The Arl1 pathway functions to recruit activated Arl1 to the *trans*-Golgi membrane, which in turn recruits Imh1. The elimination of any component of the Arl1 pathway blocks activation of Arl1 and results in mislocalization of GFP-Imh1 (Panic *et al.*, 2003b; Setty *et al.*, 2003; Behnia *et al.*, 2004; Setty *et al.*, 2004). Mislocalization of GFP-Imh1 in the absence of Arl1, Arl3, Sys1, Mak3, and Mak10 was confirmed in the blinded analysis of GFP-Imh1 localization in the alleviating deletion strains (Figure 4.6). Consistent with the Arl1GEF activity of Syt1 being required for the activation of Arl1, GFP-Imh1 is reported to be mislocalized in the absence of Syt1 (Chen *et al.*, 2010). The *syt1*Δ deletion strain was not included in the blinded analysis of GFP-Imh1 localization because it was not identified in the screen as an alleviating deletion. After finding that deletion of *SYT1* also alleviates *gcs1*Δ cold sensitivity (Figure 4.4), I did assess GFP-Imh1 localization in *syt1*Δ cells. Unlike elimination of the other Arl1-pathway components, and contrary to the reported localization of GFP-Imh1 in the absence of Syt1, I found that GFP-Imh1 was properly localized in *syt1*Δ cells (Figure 4.7). This was not the first discrepancy between my results and those from the group that reported the mislocalization of GFP-Imh1 in the absence of Syt1 (Chen *et al.*, 2010). These several differences could be attributed to strain differences or perhaps to differences in the expression levels of GFP-Imh1 used. I also recognize that the *syt1*Δ strain used in my experiments is taken directly from the deletion collection, and deletion of the *SYT1* gene was not confirmed by PCR. Nevertheless, the same *syt1*Δ mutation did alleviate *gcs1*Δ cold sensitivity (Figure 4.4), suggesting that the deletion strain from the collection is correct. It is likely that persistence of correctly localized GFP-Imh1 in the absence of the Arl1GFF Syt1 is explained by the presence of another protein with Arl1GEF activity, as has been proposed (Chen *et al.*, 2010).

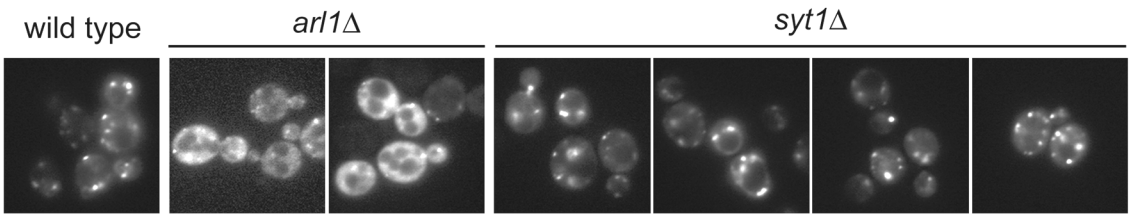

Figure 4.7 The Arl1GEF Syt1 is not required for the proper localization of GFP-Imh1. Fluorescence micrographs displaying live yeast cells with the indicated gene deletions (S288C genetic background) and harbouring a plasmid (pSR15) expressing GFP-Imh1. Cells growing logarithmically in selective medium at 30°C were concentrated in growth medium by centrifugation immediately prior to analysis by fluorescence microscopy. The wild type strain used was BY4741; *arl1*Δ and *syt1*Δ strains were from the deletion collection.

4.9 Three Other Alleviating Gene Deletions are Required for Normal Localization of the Arl1 Effector Imh1

Three additional alleviating gene deletions mislocalized GFP-Imh1 in the blinded analysis described above, causing cytoplasmic localization similar to that seen in the *arl1*Δ control: *mnn9*Δ, *rpe1*Δ, and *rpl43a*Δ (Figure 4.6). For completeness I briefly discuss these genes here, although no further work has been done with these deletions and they are not discussed elsewhere in this thesis.

The *MNN9* gene encodes a subunit of the Golgi mannosyltransferase complex (Jungmann and Munro, 1998). The *MNN9* gene is located immediately downstream (220 bp away) from the *ARL3* gene and runs in the opposite direction. The mislocalization of GFP-Imh1 in the *mnn9*Δ deletion strain and the proximity of the *MNN9* gene to a gene encoding a known component of the Arl1 pathway could be a coincidence, but it is likely that *ARL3* expression is somehow perturbed in the *mnn9*Δ deletion strain. Mislocalization of GFP-Imh1 would then be caused by the impaired expression of Arl3, which is already known to cause GFP-Imh1 mislocalization (Panic *et al.*, 2003b; Setty *et al.*, 2003), rather than the absence of Mnn9 itself.

The *RPE1* gene encodes a D-ribulose-5-phophate 3-epimerase that is a component of the non-oxidative part of the pentose-phosphate pathway (Miosga and Zimmermann, 1996), and the *RPL43A* gene encodes a protein component of the large (60S) ribosomal subunit (Planta and Mager, 1998). It is likely that the pentose-phosphate pathway and mRNA translation respectively, are perturbed in these deletion strains, and that these perturbations somehow result in the mislocalization of GFP-Imh1, although no explanation is immediately apparent. It is also possible that the proteins encoded by these genes have a second, uncharacterized, function that is either directly or indirectly required for the correct localization of GFP-Imh1.

A feature shared by the *rpe1*Δ and *rpl43a*Δ deletions is that they both partially overlap a dubious ORF (*YJL120W* and *YPR044C*, respectively) and deletion of each of these dubious ORFs confers sensitivity to an anti-angiogenesis drug called GSAO (4-(N-(S-glutathionylacetyl)amino) phenylarsenoxide) (Dilda *et al.*, 2005). GSAO inhibits angiogenesis by targeting the mitochondria of actively dividing endothelial cells, which leads to cell cycle arrest and apoptosis (Dilda *et al.*, 2005). In a screen for gene deletions

in yeast that confer sensitivity to GSAO, 88 gene deletions were identified, including the *yjl120w*Δ and *ypr044c*Δ gene deletions (Dilda *et al.*, 2005). The *rpe1*Δ and *rpl43a*Δ deletions each provided variable alleviation of *gcs1*Δ cold sensitivity (Table 4.2), but the *yjl120w*Δ and *ypr044c*Δ gene deletions were not identified in the *gcs1*Δ screen even though both dubious-ORF deletions are contained in the deletion collection. Likewise, the *rpe1*Δ and *rpl43a*Δ deletions were not identified in the GSAO screen. Whether this apparent similarity between the *rpe1*Δ and *rpl43a*Δ deletions has anything to do with the mislocalization of GFP-Imh1 is not clear. Other than the physically overlapping genes discussed above, there was very little functional overlap between the lists of deletions identified in the two screens. Only one gene deletion was common between the *gcs1*Δ and GSAO screens; deletion of the *CBF1* gene was a strong alleviator of *gcs1*Δ cold sensitivity (Table 4.2), and also confers sensitivity to GSAO. Interestingly, although GFP-Imh1 localization was not cytoplasmic in the *cbf1*Δ strain, it was abnormal. The GFP-Imh1 signal was still punctate, but there seemed to be more, smaller, and less-bright dots compared to what is seen for wild–type cells (data not shown). The Cbf1 protein encoded by the *CBF1* gene is a transcription factor, and also a centromere-binding factor involved in mitotic segregation. The effects of the elimination of Cbf1 are therefore likely the result of altered expression of a gene product that is regulated by Cbf1 at the transcriptional level that has impact on Imh1 localization.

Other than the observations discussed above, no further work was done to pursue these particular gene deletions or their involvement in *gcs1*Δ cold sensitivity. Instead, I chose to focus on the Arl1 and Ypt6 pathways, and the newly identified effect the Ypt6 pathway has on GFP-Imh1 localization.

4.10 The Ypt6 Pathway Mediates the Localization of Proteins in the Arl1 Pathway

Each protein in the Arl1 pathway is required for the recruitment of activated Arl1 to the *trans*-Golgi membrane; activated Arl1 then recruits Imh1. Inactivation of any protein in the Arl1 pathway results in mislocalization of both Arl1-GFP and GFP-Imh1 fusion proteins, so that the normal punctate staining patterns become diffuse and cytoplasmic (Panic *et al.*, 2003b; Setty *et al.*, 2003; Behnia *et al.*, 2004; Setty *et al.*, 2004). The simplest explanation for the mislocalization of GFP-Imh1 in the absence of a functional

Ypt6 pathway is that activated Ypt6 is required for the recruitment of activated Arl1 to the *trans*-Golgi membrane. To address this possibility, I assessed the localization of Arl1-GFP and Sys1-GFP fusion proteins in cells missing Ypt6-pathway components. Similar to the mislocalization of GFP-Imh1, the punctate staining patterns of Arl1-GFP and Sys1-GFP were lost when components of the Ypt6 pathway were absent (Figure 4.8). In these cells the distribution of Arl1-GFP was diffuse and cytoplasmic, leading to homogeneous staining of the cytoplasm. Unlike Arl1-GFP, Sys1-GFP was not homogeneously distributed within the cytoplasm, but instead appeared somewhat granular, with many small dots throughout the cytoplasm. Because Sys1 is an integral membrane protein predicted to have four trans-membrane domains (Tsukada and Gallwitz, 1996), the Sys1-GFP fusion protein most likely remains associated with membranous structures, resulting in the small dots and granular staining pattern. The mislocalization of GFP-Imh1, Arl1-GFP, and Sys1-GFP is apparently due to defects in targeting these proteins rather than a general disruption of the Golgi, because the Golgi marker GFP-Sec7 retained its normal punctate distribution in *ypt6*Δ, *ric1*Δ, and *rgp1*Δ deletion strains (Figure 4.8).

These data reveal that the Ypt6 pathway is required for the normal localization of proteins in the Arl1 pathway. The similar effects seen by deleting genes for the Ypt6 GEF (Ric1–Rgp1) and for Ypt6 itself indicate that the GTP-bound (activated) form of Ypt6 mediates the Golgi localization of Sys1. The loss of Golgi-localized Sys1 in the absence of activated Ypt6 results in the mislocalization of proteins downstream of Sys1 in the Arl1 pathway, including Arl1 and Imh1.

4.11 Cytoplasmic Imh1 Does Not Itself Alleviate *gcs1*Δ Cold Sensitivity

The finding that the Ypt6 pathway is required for effective Arl1-pathway function reveals two features shared by the three alleviating deletion mutations affecting the Ypt6 pathway and the five alleviating deletion mutations affecting the Arl1 pathway: all result in the depletion of activated Arl1 at the *trans*-Golgi membrane and, as a result, all cause an abnormal cytoplasmic localization of Imh1. I therefore considered the possibility that increased levels of cytoplasmic Imh1 might be the common condition that allows Ypt6-pathway and Arl1-pathway impairment to alleviate *gcs1*Δ cold sensitivity.

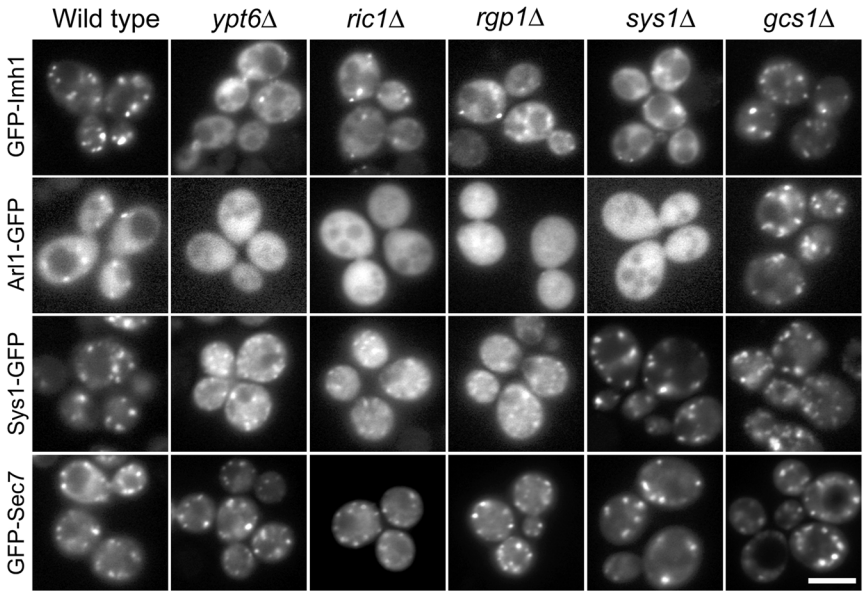

Figure 4.8 The Ypt6 pathway is required for the Golgi localization of proteins in the Arl1 pathway. Fluorescence micrographs of live yeast cells with the indicated gene deletions (S288C genetic background) and harbouring plasmids expressing GFP-Imh1 (pSR15), Arl1-GFP (p2T), Sys1-GFP (p6J), or GFP-Sec7 (pKO) are displayed. Cells growing logarithmically in selective medium at 30°C were concentrated in growth medium by centrifugation immediately prior to analysis by fluorescence microscopy. The wild type strain used was BY4741; the *gcs1*Δ strain was PPY169-4; all other deletion strains were from the deletion collection. Scale bar, 5 μm. (Originally published in Benjamin *et al.*, 2011a.)

If alleviation of *gcs1*Δ cold sensitivity by the *arl1*Δ mutation does indeed function through increased abundance of cytoplasmic Imh1, then deletion of the *IMH1* gene should abolish the beneficial effects of the *arl1*Δ deletion. To determine if Imh1 is required for *arl1*Δ-mediated relief of *gcs1*Δ cold sensitivity I first constructed a diploid strain (JBY72) with the W303 genetic background that is heterozygous for the deletions of *GCS1, ARL1,* and *IMH1*; each deletion was confirmed by PCR. This diploid was then sporulated and the resulting tetrads were dissected to obtain haploid meiotic segregants. In these tetrads the marker genes for each deletion segregated 2:2, confirming that the diploid strain was indeed heterozygous for each deletion, and that the deletion cassettes did not additionally integrate at a second locus during strain construction. Multiple segregants with each genotype were assessed for growth from stationary phase at 14°C; shown in Figure 4.9 is the growth of one representative segregant for each genotype in a serial-dilution assay. Deletion of the *IMH1* gene did not affect the ability of the *arl1*Δ mutation to alleviate *gcs1*Δ cold sensitivity: triple-mutant (*gcs1*Δ *arl1*Δ *imh1*Δ) segregants grew as well as double-mutant (*gcs1*Δ *arl1*Δ) segregants. These results clearly show that Imh1 is not required for the alleviating effects of the *arl1*Δ mutation: the deletion of the *ARL1* gene does not alleviate through release of Imh1.

To conduct a similar genetic analysis to assess whether Imh1 is required for *ypt6*Δ alleviation of *gcs1*Δ cold sensitivity it is necessary to delete both the *IMH1* and *YPT6* genes. Unfortunately, *imh1*Δ *ypt6*Δ double-mutant cells are reported to be dead (Tsukada *et al.*, 1999; Siniossoglou *et al.*, 2000; Setty *et al.*, 2003; Tong *et al.*, 2004). To reassess this deleterious genetic interaction, I first constructed a diploid strain (JBY113) with the W303 genetic background that is heterozygous for *IMH1* and *YPT6* gene deletions; each deletion was confirmed by PCR. This diploid strain was then sporulated and the resulting tetrads were dissected to assess the viability of the haploid meiotic segregants. The genetic segregation of the marker genes in these tetrads confirmed that the diploid strain was indeed heterozygous for each deletion, and that the deletion cassettes did not additionally integrate at a second locus during strain construction. Although wild-type and single-mutant segregants were viable as indicated by colony formation, none of the double-mutant *imh1*Δ *ypt6*Δ segregants formed a colony (Figure 4.10), indicating that

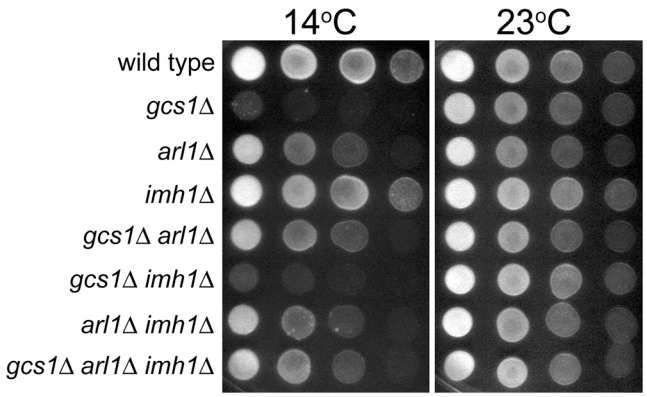

Figure 4.9 Imh1 is not required for *arl1*Δ alleviation of *gcs1*Δ cold sensitivity. Isogenic strains deleted for the indicated genes (W303 genetic background) were grown in enriched medium to stationary phase by incubation at 30°C for 5 days; ten-fold serial dilutions were then spotted onto solid enriched medium and incubated at 14°C for 8 days or 23°C for 1 day. (Originally published in Benjamin *et al.*, 2011a.)

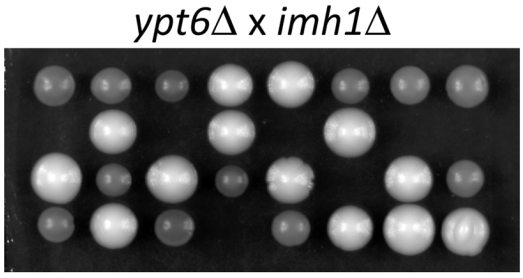

Figure 4.10 Deletion of *YPT6* is lethal in combination with the deletion of *IMH1*. Meiotic tetrads produced by sporulation of a diploid strain (JBY113; W303 genetic background) heterozygous for *ypt6*Δ::*kan* and *imh1*Δ::*HIS3* deletions were dissected on synthetic complete medium and the resulting meiotic segregants were incubated at 30°C. In each column of colonies the four meiotic segregants from a single sporulated diploid cell (tetrad) are displayed. The genotypes of viable segregants were determined by assessing histidine prototrophy (to detect *HIS3*) and G418 drug resistance (to detect *kan*). All spores predicted to be *ypt6*Δ *imh1*Δ double mutants (based on the genotypes of the living spores) failed to form colonies. The diploid strain is also heterozygous for the *ade2-1* mutation, causing 2:2 segregation of red vs. white colony colour. (Originally published in Benjamin *et al.*, 2011a and cited as 'our unpublished results'.)

*imh1*Δ *ypt6*Δ double-mutant cells are indeed not viable and confirming the reported lethal interaction. Thus, I was precluded from using such a genetic analysis to determine if Imh1 is required for *ypt6*Δ alleviation of *gcs1*Δ cold sensitivity.

Another noteworthy result from this analysis is that deletion of *IMH1* did not alleviate *gcs1*Δ cold sensitivity, because *gcs1*Δ *imh1*Δ double-mutant cells remained cold sensitive (Figure 4.9). Therefore, unlike the deletion of genes in the Arl1 pathway upstream of Arl1 activation, deletion of the Arl1 pathway effector Imh1, which functions downstream of Arl1 activation, does not alleviate *gcs1*Δ cold sensitivity. These results suggest that active Arl1 may have deleterious consequences in the absence of Gcs1 and impairing the activation and membrane localization of Arl1 may be the common condition that allows Ypt6-pathway and Arl1-pathway inactivation to alleviate *gcs1*Δ cold sensitivity.

4.12 Gcs1 GAP Activity is Dispensable for Low-Temperature Growth and Effective Endocytosis

The Gcs1 protein is well characterized as a GAP for the small G-proteins Arf1 and Arf2 (Poon *et al.*, 1996), and also has GAP activity for the related GTPase Arl1 (Liu *et al.*, 2005). This latter observation, coupled with the findings that active Arl1 may have deleterious consequences in the absence of Gcs1, raised the possibility that the Arl1GAP activity of Gcs1 is critical for growth and endosomal transport at 14°C.

To assess the involvement of the Arl1GAP activity of Gcs1 in the Gcs1-dependent processes at issue here, I wished to test a mutant version of Gcs1 lacking Arl1GAP activity. ArfGAP-deficient mutant versions of Gcs1 exist in which arginine 54 is substituted with alanine (R54A), lysine (R54K), or glutamine (R54Q). These changes dramatically impair the *in vitro* ArfGAP activity of each mutant protein (Yanagisawa *et al.*, 2002). To assess if these substitutions also impair the Arl1GAP activity of Gcs1, Dr. Pak Phi Poon in our lab employed an *in vitro* assay to test the mutant protein with the most conservative of the Gcs1-R54 substitutions (R54K) for Arl1GAP activity. Poon measured the stimulation of GTP hydrolysis on GTP-bound Arl1 and GTP-bound Arf1 in the presence of Gcs1-R54K over a wide range of protein concentrations; wild-type Gcs1 protein and bovine serum albumin (BSA) protein were used as positive and negative

controls, respectively (Figure 4.11). Increasing amounts of BSA had no stimulatory effect on Arl1- or Arf1-bound GTP hydrolysis, indicating that any stimulation of GTP hydrolysis in the presence of wild-type or mutant Gcs1 is specific. Increasing amounts of wild-type Gcs1 protein resulted in a dose-dependent increase in Arl1- and Arf1-bound GTP hydrolysis, consistent with Gcs1 acting as a GAP for these two GTPases (Poon *et al.*, 1996; Liu *et al.*, 2005). The mutant Gcs1-R54K protein displayed only weak GAP activity *in vitro* not only for Arf1, but also for Arl1 (Figure 4.11), indicating that the R54K substitution disrupts the Arl1GAP activity of Gcs1. Although not tested, it is likely that the R54A and R54Q substitutions have the same effect.

To determine whether the Arl1GAP (and ArfGAP) activity of Gcs1 is required for growth in the cold, I tested the ability of the GAP-deficient R54 mutant versions of Gcs1 to provide function for growth at 14°C. Each of these GAP-deficient Gcs1 mutant proteins, expressed from genes on low-copy plasmids present at only one or two copies per cell, relieved the cold sensitivity of *gcs1*Δ cells (Figure 4.12A), indicating that these mutant forms of Gcs1 provide function for growth from stationary phase at 14°C. I also assessed the requirement of Gcs1 GAP activity for effective endocytosis. Fluorescence microscopy revealed that *gcs1*Δ cells expressing GAP-deficient Gcs1-R54K were able to efficiently transport the lipophilic dye FM 4-64 to the vacuole, whereas in *gcs1*Δ control cells carrying an empty vector the dye remained trapped in endocytic compartments (Figure 4.13). Thus, like *gcs1*Δ cold sensitivity, defective endocytic transport in *gcs1*Δ mutant cells is remedied by a GAP-deficient version of Gcs1.

In light of the low levels of GAP activity measured *in vitro*, I wished to assess if the Gcs1-R54 mutants could provide Gcs1 GAP activity *in vivo.* I therefore determined whether expression of each R54 mutant protein could provide Gcs1 ArfGAP activity known to be required in the absence of another ArfGAP, Age2 (Poon *et al.*, 2001). The GAP-deficient Gcs1 mutants failed to provide ArfGAP activity in two temperature-sensitive double-mutant situations, *gcs1-4 age2*Δ (Wong *et al.*, 2005) and *gcs1-3 age2*Δ (Poon *et al.*, 2001), even when overexpressed from high-copy plasmids (Figure 4.12B and data not shown). Thus, the R54A, R54K, and R54Q mutant forms of Gcs1 that lack ArfGAP and Arl1GAP activity *in vitro* also fail to provide Gcs1 ArfGAP activity *in vivo*,

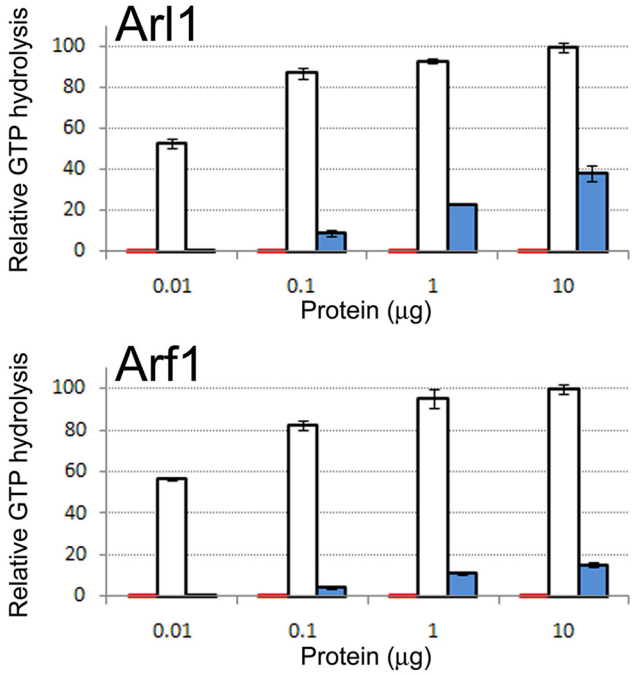

Figure 4.11 The ArfGAP-deficient Gcs1-R54K mutant form of Gcs1 has significantly decreased Arl1GAP activity *in vitro*. Activation of GTP hydrolysis by GTP-loaded myristoylated Arl1 (top) and myristoylated Arf1 (bottom) was assessed in the presence of BSA (red bar), wild-type Gcs1 (white bar), and mutant Gcs1-R54K (blue bar), over a range of protein concentrations. The Gcs1 and Gcs1-R54K proteins were bacterially expressed and affinity purified. The assays were carried out in triplicate; one standard deviation is displayed. The data presented are from one of two repeated experiments, which gave similar results. (Originally published in Benjamin *et al.*, 2011a. Figure courtesy of Dr. Pak Phi Poon.)

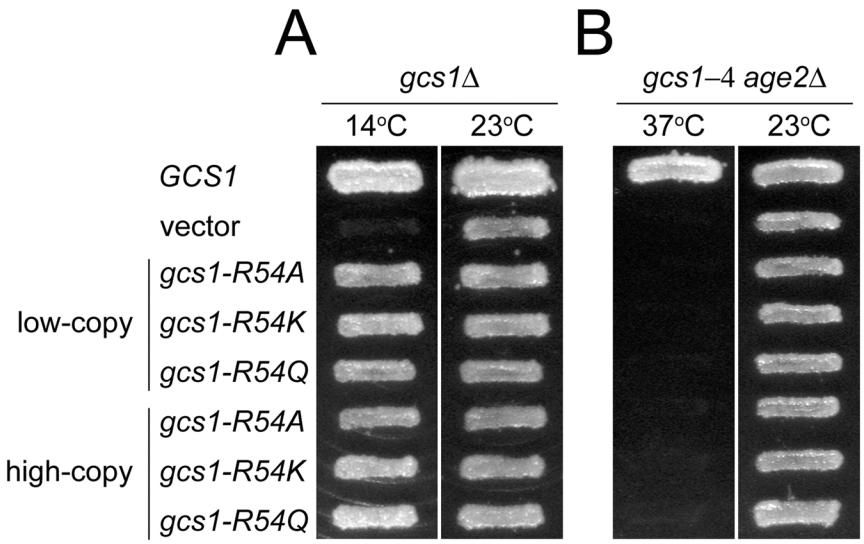

Figure 4.12 ArfGAP-deficient Gcs1-R54K alleviates *gcs1*Δ cold sensitivity. (A) Cold-sensitive *gcs1*Δ cells (strain JBY3; W303 genetic background) harbouring plasmids (pEP1, pRS425, pR54A315, pR54K315, pR54Q315, pR54A425, pR54K425, and pR54Q425) expressing the indicated genes were grown to stationary phase on solid selective medium by incubation at 30°C for 5 days before being replica-plated to solid enriched medium and incubated at 14°C for 8 days or 23°C for 3 days. Four individual transformants were assessed for each plasmid and in each case showed consistent behaviour; only one transformant is shown for each. (B) Temperature-sensitive *gcs1-4 age2*Δ cells (strain JBY29; W303 genetic background) harbouring plasmids (pPP421, pRS426, pR54A316, pR54K316, pR54Q316, pR54A426, pR54K426, and pR54Q426) expressing the same genes as in panel A were grown on solid selective medium by incubation at 23°C for 2 days and then replica-plated to solid enriched medium for further incubation at 37°C or 23°C for 2 days. Four individual transformants were assessed for each plasmid and in each case showed consistent behaviour; only one transformant is shown for each. (Originally published in Benjamin *et al.*, 2011a.)

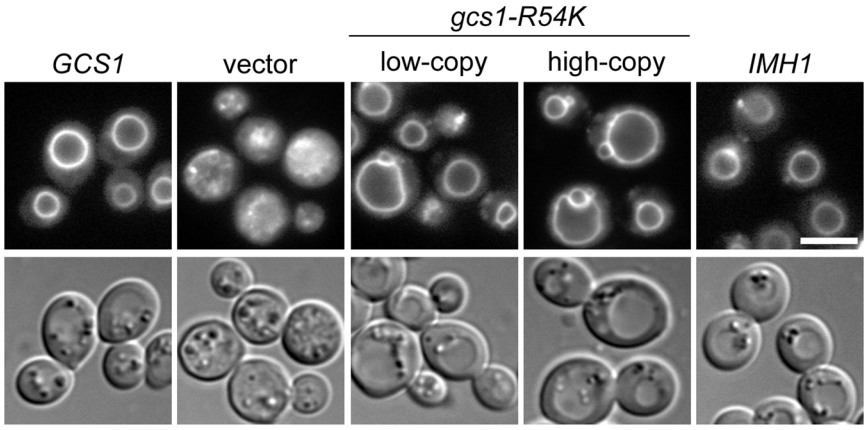

Figure 4.13 Effective endocytic transport in *gcs1*Δ cells is restored by ArfGAP-deficient Gcs1-R54K and by increased abundance of Imh1. Stationary-phase *gcs1*Δ cells (strain JBY72-12B; W303 genetic background) harbouring plasmids expressing the indicated genes were loaded with the lipophilic dye FM 4-64 on ice before being diluted in fresh enriched medium and incubated at 14°C. Membrane transport was assessed by fluorescence microscopy after 0, 5, 13, 23, 29, 36, 46, and 53 hours. Data from the 53-hour time point are shown. Dye-bound membranes were visualized by fluorescence microscopy (top panels) and cells were visualized by differential interference contrast microscopy (bottom panels). Cells expressing *GCS1* from a low-copy plasmid (pSH4) displayed clear vacuolar ring staining by 23 hours. The FM 4-64 stain began to accumulate at the vacuolar membrane in cells expressing *gcs1-R54K* from low-copy or high-copy plasmids (pR54K315 and pR54K425) and *IMH1* from a high-copy plasmid (pXW110) by 29 hours, and clear vacuolar ring staining was apparent in these cells by 46 hours. In the *gcs1*Δ vector (pRS315) control cells the FM 4-64 stain remained trapped in endocytic compartments within the cytoplasm and had not been transported to the vacuolar membrane by 53 hours. Under these assay conditions all strains remained greater than 95% viable for up to 96 hours; cell viability was assessed by methylene blue dye exclusion. Scale bar, 5 µm. (Originally published in Benjamin *et al.*, 2011a.)

but do provide the Gcs1 activity required to alleviate defective *gcs1*Δ growth and endocytic transport in the cold.

These data provide little support for the notion that the Arl1-related activity of Gcs1 that is critical for growth and endocytic transport in the cold is its Arl1GAP (or ArfGAP) activity, and suggest that the GAP activity of Gcs1 is dispensable for these processes. I therefore propose that another Arl1-related activity of Gcs1, independent of GAP activity, is important for preventing the deleterious effects of activated Arl1. The absence of this GAP-independent Gcs1 function results in dysregulated active Arl1, cold sensitivity, and defective endocytic transport.

4.13 Increased Abundance of the Other Yeast ArfGAPs Does Not Robustly Alleviate *gcs1*Δ Cold Sensitivity

The ArfGAP protein family in yeast consists of six proteins based on conserved sequence homology (Gcs1, Glo3, Age2, Age1, Sps18 and Gts1). Of these six potential ArfGAP proteins, four have been shown to have ArfGAP activity *in vitro*: Gcs1, Glo3, Age2 and Age1 (Poon *et al.*, 1996; Poon *et al.*, 1999; Poon *et al.*, 2001; Zhang *et al.*, 2003; Benjamin *et al.*, 2011b). The sequence conservation among these ArfGAP proteins is for the most part restricted to the ArfGAP domain comprised of approximately 120 residues (8-129 in Gcs1) at the N terminus of most of these proteins, which promotes GTP hydrolysis in Arf (Goldberg, 1999; Robinson *et al.*, 2006). Other than the conserved ArfGAP domain there is little sequence similarity among these proteins, and these differences are thought to provide protein-specific functions (Ireland *et al.*, 1994; Zhang *et al.*, 2003), allowing the various ArfGAP proteins in yeast to function in different stages of vesicular transport (Poon *et al.*, 1999; Poon *et al.*, 2001; Zhang *et al.*, 2003). None of the ArfGAPs is individually essential, but certain pairs share overlapping essential functions (Poon *et al.*, 1999; Poon *et al.*, 2001), and in some cases the increased expression of a third ArfGAP protein has the ability to compensate for the absence of these essential pairs, presumably by providing ArfGAP activity that is required in their absence (Wong *et al.*, 2005; Benjamin *et al.*, 2011b; and see Chapter 3 above). To determine if increased gene copy number of the other yeast ArfGAPs could compensate for the loss of Gcs1 and alleviate *gcs1*Δ cold sensitivity, I assessed growth at 14°C of

stationary-phase *gcs1*Δ cells overexpressing various yeast ArfGAP genes (*GLO3, AGE2, AGE1,* and *AGE1*Δ*N*) from high-copy plasmids. Increasing the gene copy number of these ArfGAPs failed to alleviate *gcs1*Δ cold sensitivity. None of the cells overexpressing these ArfGAP genes grew as well as cells expressing *GCS1*. However, after prolonged incubation the overexpression of the *AGE2* gene consistently allowed some growth that was not provided by the overexpression of the other ArfGAP genes, or by empty vector (Figure 4.14). This result suggests that the other yeast ArfGAP proteins do not efficiently provide the GAP-independent function of Gcs1 that is required for reentry in the cold. It is possible that Age2 can provide this function, albeit poorly compared to Gcs1. Alternatively the increased abundance of Age2 may alleviate *gcs1*Δ cold sensitivity in some other way.

Another consideration is whether overexpression of the ArfGAP genes results in increased ArfGAP protein abundance under the conditions tested here. I did not do Westerns to assess if overexpression of the ArfGAP genes resulted in increased ArfGAP protein abundance. Overexpression of some of the ArfGAP genes has biological effects under certain conditions, and therefore under those conditions, overexpression of the ArfGAP genes appears to result in increased ArfGAP protein abundance (Wong *et al.*, 2005; Benjamin *et al.*, 2011b; and see Chapter 3 above). However, it is possible that the ArfGAP genes are not expressed effectively under the conditions tested here, resumption of cell proliferation at 14°C. The inability of increasing the copy number of the various ArfGAP genes to alleviate *gcs1*Δ cold sensitivity may not be a result of these other ArfGAPs lacking the GAP-independent function of Gcs1 that is required for reentry in the cold, but rather could result from inadequate gene expression, increased degradation of the message, or increased protein turnover of the other ArfGAPs under these conditions.

4.14 Temperature-Sensitive Alleles of *GCS1* Complement *gcs1*Δ Cold Sensitivity

Our lab has developed other mutant versions of Gcs1 that conditionally affect Gcs1 function. Specifically, we have a collection of temperature-sensitive mutant forms of Gcs1 that compromise function at 37°C. Gcs1 itself is not an essential protein, but it does

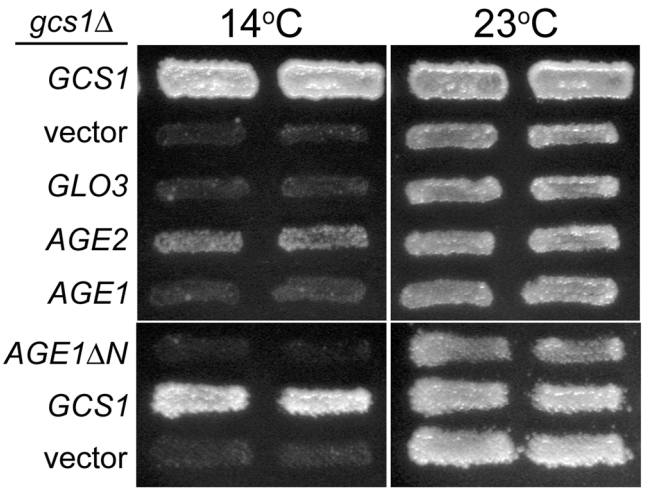

Figure 4.14 Increased abundance of the other yeast ArfGAPs does not robustly alleviate *gcs1*Δ cold sensitivity. Cold-sensitive *gcs1*Δ cells (strain JBY3; W303 genetic background) harbouring high-copy plasmids (pEP1, pRS425, pPPL38, pSL344, pSL377, and pSL489) expressing the indicated genes were grown to stationary phase on solid selective medium by incubation at 30°C for 5 days before being replica-plated to solid enriched medium and incubated at 14°C for 8 days or 23°C for 2 days. Four individual transformants were assessed for each plasmid and in each case showed consistent behaviour; two transformants of each are shown.

share overlapping essential function for post-Golgi transport with the Age2 ArfGAP (Poon *et al.*, 2001), and also shares overlapping essential function for retrograde transport from the Golgi to the ER with the Glo3 ArfGAP (Poon *et al.*, 1999). By eliminating the ArfGAPs with which Gcs1 shares essential functions (Age2 or Glo3) and expressing temperature-sensitive versions of Gcs1 as the only Gcs1 in the cell, the conditional function of these mutants is revealed by loss of proliferative ability at the restrictive temperature. The *gcs1-3* temperature-sensitive allele of *GCS1* encodes a mutant Gcs1 protein that is unstable at 37°C and is therefore impaired for both Age2-related post-Golgi functions and Glo3-related retrograde transport functions (Poon *et al.*, 2001; Wong *et al.*, 2005). The *gcs1-4* temperature-sensitive allele of *GCS1* encodes a mutant Gcs1 protein that is stable at 37°C, and is specifically defective for Age2-related post-Golgi function (Wong *et al.*, 2005); in contrast, the *gcs1-28* temperature sensitive allele of *GCS1*, which encodes a mutant Gcs1 protein that is also stable at 37°C, is specifically defective for Glo3-related retrograde transport (Poon *et al.*, 1999; Wong *et al.*, 2005). The mutant Gcs1 proteins encoded by each of these temperature-sensitive alleles of *GCS1* are stable and provide function at 30°C. It is possible that these mutant alleles of *GCS1* may also compromise Gcs1 function in the cold. Specifically, I was interested to know if any of these mutant versions of Gcs1 is impaired in the GAP-independent Arl1-related function of Gcs1 that is required for reentry at 14°C. I therefore tested if these mutant versions of Gcs1 could complement the absence of endogenous Gcs1 and allow growth from stationary phase at 14°C. To do so, stationary-phase *gcs1*Δ cells expressing the mutant *GCS1* alleles from low-copy plasmids at one or two copies per cell were assessed for the ability to grow at 14°C (Figure 4.15). Each of the mutant alleles of *GCS1* was able to complement the absence of wild-type Gcs1. Cells expressing the mutant alleles of *GCS1* grew as well at 14°C as cells expressing wild-type *GCS1*, whereas cells expressing vector failed to grow (Figure 4.15). Thus, the point mutations causing temperature sensitivity for these mutant alleles do not impair the GAP-independent Arl1-related function of Gcs1 at 14°C.

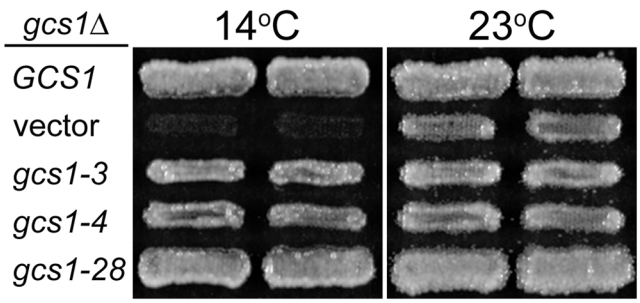

Figure 4.15 Temperature-sensitive alleles of *GCS1* complement *gcs1*Δ cold sensitivity. Cold-sensitive *gcs1*Δ cells (strain JBY72-12B; W303 genetic background) harbouring low-copy plasmids (pGCS1-314, pRS314, pLAA314-3, pMG4-4, and pSL413-28) expressing the indicated *GCS1* alleles were grown to stationary phase on solid selective medium by incubation at 30°C for 5 days before being replica-plated to solid enriched medium and incubated at 14°C for 4 days or 23°C for 2 days. Four individual transformants were assessed for each plasmid and in each case showed consistent behaviour; two transformants are shown for each.

4.15 The ALPS Motif of Gcs1 is Not Required for Growth in the Cold but is Required for Effective Post-Golgi and Retrograde Transport Functions

We received ten mutant *GCS1* alleles from Dr. Dan Cassel (Technion-Israel Institute of Technology, Haifa, Israel), including six alleles with nonsense mutations that encode a series of C-terminal Gcs1 truncations, and four alleles with missense mutations that encode various point mutant forms of Gcs1 (Figure 4.16). These mutant alleles of *GCS1* were constructed by site-directed mutagenesis and each is expressed from the endogenous *GCS1* promoter on a low-copy plasmid. The nonsense mutations introduce stop codons within the *GCS1* open reading frame that result in the truncation of the normally 352-residue Gcs1 protein at residues 162, 189, 200, 211, 292, or 314. The missense mutations encode the following substitutions: L246A, L246D, VI268/269AA, and F296D. These mutant forms of Gcs1 were designed to assess if the amphipathic lipid packing sensor (ALPS) motif of Gcs1 is required for Gcs1 function.

The ALPS motif in Gcs1 is contained within a central region of about 75 amino acids that is conserved between Gcs1 and its homologue in metazoans (ArfGAP1) (Figure 4.16) (Bigay *et al.*, 2005). The ALPS motif is unstructured in solution or in the presence of flat membranes, but forms an amphipathic helix on highly curved membranes through insertion of bulky hydrophobic residues between the loosely packed lipids that are a consequence of membrane curvature (Bigay *et al.*, 2005). As such, the ALPS motif has the ability to sense and bind to highly curved membranes such as those occurring during transport-vesicle formation, and recruit Gcs1 to these regions. The point-mutant forms of Gcs1 described above target conserved hydrophobic residues within or near the ALPS motif. A substitution analogous to the L246A substitution in Gcs1 made in the human Gcs1 homologue, ArfGAP1, drastically impairs the sensitivity of ArfGAP1 to membrane curvature (Bigay *et al.*, 2005).

I assessed each of these mutant forms of Gcs1 for alleviation of *gcs1*Δ cold sensitivity, alleviation of *gcs1-4 age2*Δ temperature sensitivity, and alleviation of *gcs1-28 glo3*Δ temperature sensitivity. Stationary-phase *gcs1*Δ cells expressing the mutant *GCS1* alleles at one or two copies per cell grew as well at 14°C as cells expressing wild-type *GCS1* (Figure 4.17A), indicating that the ALPS motif of Gcs1 is not required for reentry

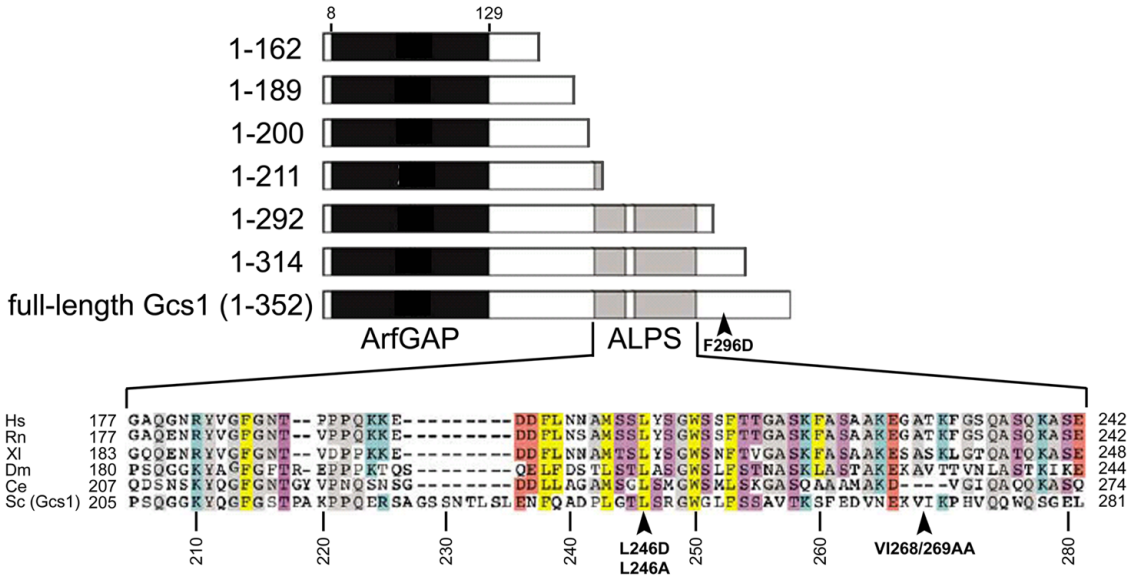

Figure 4.16 C-terminal truncations and amino acid substitutions in Gcs1. Full-length Gcs1 and C-terminal truncations in Gcs1 used in this study are represented by rectangles; numbers at left indicate the Gcs1 residues included in each peptide. The black box represents the ArfGAP domain (between residues 8 and 129), and the grey box represents the region of Gcs1 that contains the ALPS motif (between residues 205 and 281). Black arrows indicate the location of the point mutations used in this study. Also shown is a sequence alignment of the region of Gcs1 that contains the ALPS motif and the analogous regions of several metazoan orthologs of Gcs1 (ArfGAP1). Conserved residues are highlighted using the following colour code: yellow, hydrophobic; purple, serine and threonine; blue, basic; red, acidic; grey, other residues. The abbreviations used are as follows: Hs. *Homo sapiens*, Rn. *Rattus norvegicus*, Xl. *Xenopus laevis*, Dm. *Drosophila melanogaster*, Ce. *Caenorhabditis elegans*, Sc. *Saccharomyces cerevisiae*. (Sequence alignment from Bigay *et al.*, 2005)

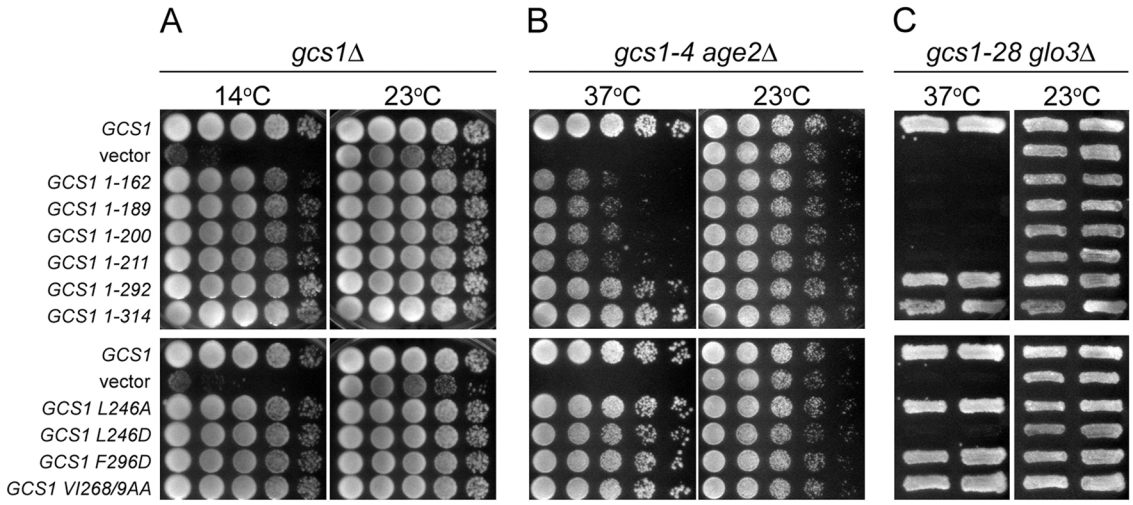

Figure 4.17 The ALPS domain of Gcs1 is not required for growth in the cold but is required for effective post-Golgi and retrograde transport functions. (A) Cold-sensitive *gcs1*Δ cells (strain JBY3; W303 genetic background) harbouring low-copy plasmids (pGCS1-314, pRS314, pGCS1 1-162, pGCS1 1-189, pGCS1 1-200, pGCS1 1-211, pGCS1 1-292, pGCS1 1-314, pGCS1 L246A, pGCS1 L246D, pGCS1 F296D, and pGCS1 VI268/9AA) expressing the indicated C-terminal truncations and point mutations of Gcs1 were grown in selective medium to stationary phase by incubation at 30°C for 5 days; ten-fold serial dilutions of each were then spotted onto solid enriched medium and incubated at 14°C for 5 days or 23°C for 2 days. (B) Temperature-sensitive *gcs1-4 age2*Δ cells (strain JBY70; W303 genetic background) harbouring the same plasmids as in panel A were grown in selective medium at 23°C for 2 days; five-fold serial dilutions were then spotted onto solid enriched medium and incubated at 37°C or 23°C for 2 days. (C) Temperature-sensitive *gcs1-28 glo3*Δ cells (strain PPY147.28.2a; W303 genetic background) harbouring the same plasmids as in panel A were grown on solid selective medium at 23°C for 2 days and then replica-plated to solid enriched medium for further incubation at 37°C or 23°C for 2 days. Four individual transformants were assessed for each plasmid in panels A, B, and C and in each case showed consistent behaviour; in panels A and B one representative transformant is shown for each, in panel C two transformants are shown for each.

in the cold. Strikingly, even the most severe of the Gcs1 truncations (Gcs1 1-162) that is missing over half of the Gcs1 protein was still able to alleviate *gcs1*Δ cold sensitivity. The ALPS motif, however, did contribute to alleviation of the two temperature-sensitive situations tested. There was a marked difference in the ability of the mutant forms of Gcs1 with the ALPS motif (1-314 and 1-292) to alleviate *gcs1-4 age2*Δ and *gcs1-28 glo3*Δ temperature sensitivity compared to the mutant forms of Gcs1 lacking the ALPS motif (Figure 4.17B and C). This difference was most severe in the *gcs1-28 glo3*Δ situation, in which the mutant forms of Gcs1 without the ALPS motif were completely defective at 37°C (Figure 4.17C), indicating that the ALPS motif (or some other feature within the 211-292 region of Gcs1) is required for essential Gcs1 function in the absence of Glo3. Results with the truncated forms of Gcs1 were similar in the *gcs1-4 age2*Δ situation: cells expressing the Gcs1 truncations with the ALPS motif grew significantly better than cells expressing Gcs1 truncations lacking the ALPS motif. However, the ALPS motif was not required for essential Gcs1 function in the absence of Age2, as cells expressing the Gcs1 truncations lacking the ALPS motif, although impaired for growth, still grew better than the vector containing control cells (Figure 4.17B). These results highlight the importance of the ALPS motif for the essential Gcs1 function that is required for retrograde transport from the Golgi to the ER in the absence of Glo3, and for the essential Gcs1 function that is required for post-Golgi transport in the absence of Age2. The fact that deletion of the ALPS motif had a greater effect on Gcs1 ability to alleviate the growth defect of cells lacking Glo3 compared to cells lacking Age2 may indicate that the ALPS motif is more important for Gcs1 function for retrograde transport compared to post-Golgi transport; however, I cannot rule out that the different temperature sensitive forms of Gcs1 used in these two situations have an impact on growth. In sharp contrast, the ALPS motif is completely dispensable for the GAP-independent function of Gcs1 that is required for reentry in the cold. These results suggest that the ability of Gcs1 to sense membrane curvature is important for the Gcs1 function that overlaps with Glo3 and Age2 functions, but not for Gcs1 reentry function.

For the most part, the hydrophobic residues that were assessed were not required for Gcs1 function. The majority of these substitutions had no effect on Gcs1 function under any of the situations tested. However, the L246D substitution had a profound effect

on alleviation of *gcs1-28 glo3*Δ temperature sensitivity. Leucine 246 is one of several highly conserved hydrophobic residues contained in the ALPS motif of Gcs1. The ALPS motif is thought to function by adopting an amphipathic helical structure and inserting these hydrophobic residues between the loosely packed lipid head groups of curved membranes (Bigay *et al.*, 2005). Indeed, substitution of the analogous leucine in ArfGAP1 to an alanine (ArfGAP1-L207A) decreases the ability of the ArfGAP1 ALPS motif to bind highly curved membranes (Bigay *et al.*, 2005). Interestingly, substituting leucine 246 for alanine (a non-polar amino acid) in Gcs1 did not compromise alleviation of *gcs1-28 glo3*Δ temperature sensitivity, whereas substituting leucine 246 for aspartic acid (a polar and negatively charged amino acid) abolished alleviation. The stronger effect of the L246D substitution (hydrophobic to hydrophilic) compared to the L246A substitution (hydrophobic to hydrophobic) is consistent with the proposed mechanism of the ALPS motif; inserting L246 (and other conserved hydrophobic residues) into the membrane between loosely packed lipids to promote membrane adsorption of the ALPS motif. This result strongly indicates that the ALPS motif is required for the essential Gcs1 function in the absence of Glo3.

4.16 Increased Abundance of Imh1 Alleviates *gcs1*Δ Cold Sensitivity

A former PhD student in the lab, Xiangmin Wang, undertook an approach complementary to the screen described above that identified alleviating gene deletions. This alternative approach identified genes whose overexpression alleviates *gcs1*Δ cold sensitivity. To do so, *gcs1*Δ cells were transformed with a high-copy yeast genomic library and screened for transformants that were able to grow from stationary phase at 14°C. Wang found several library plasmids that alleviate cold sensitivity. DNA Sequence analysis of the genomic inserts on these plasmids identified genes that, in increased copy number, alleviate *gcs1*Δ cold sensitivity (Wang, 1996; Wang *et al.*, 1996). One of the alleviating library plasmids contained a 4.1-kb yeast genomic DNA insert containing the entire 2.7-kb *IMH1* open reading frame; upon direct testing, Wang determined that *gcs1*Δ cells carrying a plasmid providing increased expression of Imh1 were no longer cold sensitive (Wang, 1996). This overexpression screen (Wang, 1996) was carried out many years prior to the gene deletion screen (Drysdale, 2006). At the time of Wang's analysis

there was little known about Imh1, and nothing more was done with this result. We now appreciate that Imh1 is an effector of the Arl1 pathway (Panic *et al.*, 2003b; Setty *et al.*, 2003), and that deletions impairing Arl1 activation also alleviate *gcs1*Δ cold sensitivity (Drysdale, 2006). Increased insight into the regulation of Imh1 now leads to additional lines of investigation.

4.17 Increased Abundance of Imh1 Restores Effective Endocytic Transport in *gcs1*Δ Cells

To begin an evaluation of the alleviation provided by overexpression of *IMH1*, I assessed the endocytic-transport defect caused by the absence of Gcs1. For this approach, I used the lipophilic dye FM 4-64 to monitor endocytic transport in *gcs1*Δ cells carrying a high-copy plasmid expressing *IMH1*. As controls, *gcs1*Δ cells carrying vector or a plasmid expressing *GCS1* were also assessed. Fluorescence microscopy revealed that the *gcs1*Δ cells carrying the high-copy plasmid expressing *IMH1* efficiently transported the lipophilic dye FM 4-64 to the vacuole, whereas the dye remained trapped in endocytic compartments in *gcs1*Δ mutant cells (Figure 4.13). Like *gcs1*Δ-mediated cold sensitivity, defective endocytic transport in *gcs1*Δ mutant cells is alleviated by increased abundance of the Arl1 effector Imh1.

4.18 Arl1 Binding by the GRIP Domain of Imh1 is Necessary and Sufficient for Imh1 Effects

The Arl1 effector Imh1 is a long coiled-coil protein with a conserved GRIP domain. This GRIP domain, comprising the C-terminal 50 residues of the 911-residue Imh1 protein, mediates the interaction between Imh1 and activated Arl1 (Barr, 1999; Kjer-Nielsen *et al.*, 1999; Munro and Nichols, 1999; Panic *et al.*, 2003b; Setty *et al.*, 2003). As described above, Imh1 is recruited to the Golgi membrane by binding activated Arl1, and is cytoplasmically localized when the Arl1 or Ypt6 pathway is defective. Cytoplasmic Imh1 (a possible consequence of increased Imh1 abundance) does not contribute to the alleviation of *gcs1*Δ cold sensitivity in the *arl1*Δ situation (Figure 4.9). Therefore, I considered the possibility that increased abundance of Imh1 alleviates *gcs1*Δ cold sensitivity through Arl1 binding. To assess involvement of Arl1 binding by Imh1, I used

the Imh1-Y870A mutant form of Imh1 in which tyrosine 870 in the GRIP domain is substituted with alanine, a change that abolishes Imh1 binding to Arl1 (Panic *et al.*, 2003b). Fluorescence microscopy confirmed that GFP-Imh1-Y870A had the same diffuse cytoplasmic localization in *gcs1*Δ cells as reported in cells with wild-type Gcs1 (Panic *et al.*, 2003b), a finding that is consistent with the failure of Imh1-Y870A to bind activated Arl1 and become localized to the *trans*-Golgi membrane (Figure 4.18A). Although the abundance of the Imh1 and Imh1-Y870A GFP-fusion proteins are similar (Panic *et al.*, 2003b), I found that increased expression of the wild-type GFP-Imh1 fusion protein alleviated *gcs1*Δ cold sensitivity, whereas increased expression of the mutant GFP-Imh1-Y870A fusion protein failed to do so (Figure 4.18B). These results indicate that fusing GFP to the N terminus of Imh1 does not interfere with the ability of Imh1 to alleviate *gcs1*Δ cold sensitivity, and that a point mutation that disrupts Arl1 binding by Imh1 also abolishes alleviation. Thus, Arl1 binding by Imh1 is necessary for the alleviation of *gcs1*Δ cold sensitivity by increased abundance of Imh1.

The GRIP domain of Imh1 is sufficient to bind Arl1 and target a GFP-tagged GRIP domain to the Golgi, resulting in punctate staining (Kjer-Nielsen *et al.*, 1999; Munro and Nichols, 1999; Setty *et al.*, 2003). I therefore constructed a plasmid expressing GFP fused to the C-terminal 177 residues of Imh1 containing the GRIP domain (Setty *et al.*, 2003), and tested the ability of increased abundance of this protein to alleviate *gcs1*Δ cold sensitivity. Fluorescence microscopy confirmed that, like full-length GFP-Imh1, this GFP-GRIP fusion protein is targeted to the Golgi in wild-type and *gcs1*Δ cells, as revealed by punctate staining in cells of both genotypes (Figure 4.18A). As expected, the punctate distribution of the GFP-GRIP fusion protein was absent in cells lacking Arl1 (Panic *et al.*, 2003b; Setty *et al.*, 2003; Figure 4.18A), consistent with the Golgi targeting of the GFP-GRIP fusion protein being mediated by Arl1 binding. As seen for the wild-type GFP-Imh1 fusion protein, increased expression of the GFP-GRIP fusion protein alleviated *gcs1*Δ cold sensitivity (Figure 4.18B). Thus, the GRIP domain of Imh1, which is sufficient for Arl1 binding and Golgi localization, is also sufficient for alleviation of *gcs1*Δ cold sensitivity. The long coiled-coil N-terminal domain of Imh1, comprising 80% of the protein and involved in normal Imh1 function, is thus dispensable for Imh1-mediated alleviation of *gcs1*Δ cold sensitivity. This finding strongly suggests

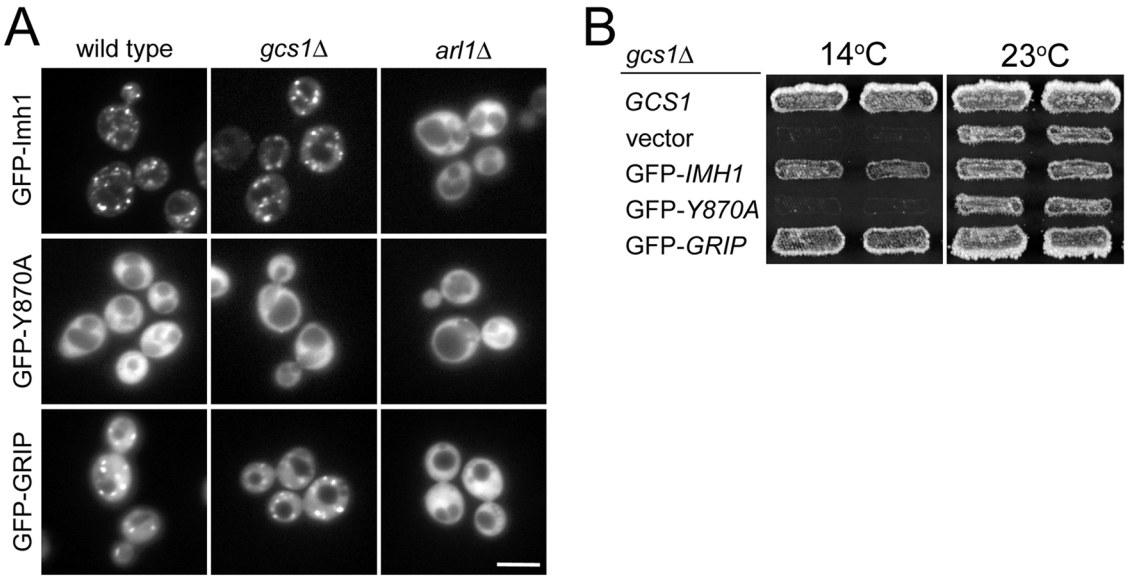

Figure 4.18 Binding of Arl1 by the GRIP domain of Imh1 is necessary and sufficient for Imh1-mediated alleviation of *gcs1*Δ cold sensitivity. (A) Fluorescence micrographs of live yeast cells with the indicated gene deletions (wild type, JBY72-21B; *gcs1*Δ, JBY72-12B; *arl1*Δ, JBY72-13C; W303 genetic background), each harbouring low-copy plasmids expressing N-terminally GFP-tagged Imh1 (pLK), Imh1-Y870A (pLL), or Imh1 GRIP domain (C-terminal 177 residues of Imh1; pGRIP-177) from the *TPI1* promoter. Cells growing logarithmically in selective medium at 30°C were concentrated in growth medium by centrifugation immediately prior to analysis by fluorescence microscopy. Scale bar, 5 µm. (B) Growth of the same *gcs1*Δ cells as in panel A, plus *gcs1*Δ cells harbouring vector (pRS314) or a *GCS1* plasmid (pGCS1-314) as controls for cold sensitivity. Cells were patched on solid selective medium and grown to stationary phase by incubation at 30°C for 5 days before being replica-plated to the same medium for incubation at 14°C for 6 days or 23°C for 4 days. Four individual transformants were assessed for each plasmid and in each case showed consistent behaviour; two transformants are shown for each. (Originally published in Benjamin *et al.*, 2011a.)

that the effect of increased Imh1 abundance is brought about by perturbing interactions involving Arl1, rather than by increased availability of the Imh1 protein itself.

4.19 A Working Model of Arl1 Involvement in *gcs1*Δ Cold Sensitivity

The results presented above lead to a working model for the involvement of Arl1 in *gcs1*Δ-mediated cold sensitivity. The model proposes that in the absence of a GAP-independent function of Gcs1, active Arl1 is dysregulated, resulting in either the formation of interactions with activated Arl1 that would not normally exist, or the stabilization of interactions with activated Arl1 that would not normally persist. These aberrant Arl1 interactions impose the growth and endocytic transport defects of *gcs1*Δ cells that become apparent in the cold. Disrupting these aberrant Arl1 interactions alleviates the *gcs1*Δ defects, and this alleviation can be achieved in two ways, either by blocking the activation of Arl1 to prevent the formation of such interactions, or by disrupting the interactions through competition for activated Arl1-binding sites. The alleviating deletions affecting components of the Arl1 and Ypt6 pathways prevent the activation of Arl1, whereas the increased abundance of the Arl1-binding GRIP domain of Imh1 has the potential to disrupt Arl1 interactions through competition.

The proposed aberrant interaction of some factor with activated Arl1 could be the underlying cause of *gcs1*Δ-mediated defects in two subtly different ways. The interaction with activated Arl1 could be toxic to processes required for growth and endocytic transport in the cold. In this case, the factor bound by dysregulated Arl1 *is not* required for growth and endocytic transport to take place in the cold, but the (presumably) persistent interaction with Arl1 is inhibitory. Alternatively, the factor bound by dysregulated Arl1 *is* independently required for growth and endocytic transport in the cold, in which case the interaction with Arl1 is inhibitory because dysregulated Arl1 (in the absence of Gcs1) sequesters this factor, thereby preventing the factor from carrying out processes required for growth and endocytic transport in the cold. These two models have different predictions as to the nature of the factor that is bound by Arl1.

The ‘toxic complex’ model predicts that deletion of the factor will alleviate *gcs1*Δ-mediated defects (just as elimination of Arl1 does). If a non-essential gene encodes such a toxic factor, then it would be expected to appear in the list of deletion

mutations that alleviate the *gcs1*Δ defect. None of the alleviating gene deletions that we have identified here (Table 4.3) encodes a protein reported to physically interact with Arl1. The potential that any of the alleviating gene deletions does encode a protein that physically interacts with Arl1 requires a protein-by-protein assessment for Arl1 complex formation and has not been pursued.

The alternative model postulates that a factor required for growth and transport in the cold becomes sequestered by dysregulated Arl1, restricting the factor from carrying out these required functions. For this 'restricted function' model, increased abundance of the factor would alleviate *gcs1*Δ defects by providing excess factor to carry out necessary processes in the cold. A second prediction of this model is that deletion of such a factor would recapitulate the *gcs1*Δ defects. Our previous high-copy suppressor analysis did not reveal an obvious candidate; none of the genes identified encode Arl1-binding proteins. Identification of candidate proteins would require a more extensive collection of proteins that alleviate the *gcs1*Δ defect when overexpressed. Indeed, our screen likely did not assess the increased expression of all possible yeast genes. Thus, there is possibly other yeast genes that are capable of alleviating *gcs1*Δ cold sensitivity when overexpressed that remain to be identified. In the following section a protein of interest that is known to bind Arl1 is directly assessed for the ability to alleviate *gcs1*Δ cold sensitivity.

4.20 Increased Abundance of Vps53 Does Not Alleviate *gcs1*Δ Cold Sensitivity

In addition to Imh1, another yeast protein, Vps53, is known to bind Arl1 in a GTP-dependent manner (Panic *et al.*, 2003b). Vps53 is a subunit of the GARP (Golgi-associated retrograde protein) tethering complex consisting of the four subunits Vps51, Vps52, Vps53, and Vps54 (Conibear *et al.*, 2003). As proposed in the restricted-function model above, dysregulated Arl1 may sequester a factor required for growth from stationary phase in the cold, and the Arl1-GRIP interaction may disrupt this sequestration and release the factor. The factor proposed in the model is a binding partner of activated Arl1 and, based on this criterion, Vps53 is a candidate for the factor sequestered by Arl1. One prediction of this model is that overexpression of the sequestered factor could saturate the available Arl1-binding sites and provide excess factor to carry out the functions required for reentry in the cold, thus alleviating *gcs1*Δ cold sensitivity. Another

possibility is that Vps53 could alleviate *gcs1*Δ cold sensitivity in the same manner as does Arl1 binding by the GRIP domain of Imh1 (the proposed release of the sequestered factor). To determine if increased abundance of Vps53 alleviates *gcs1*Δ cold sensitivity, I overexpressed the *VPS53* gene in *gcs1*Δ cells and assessed growth from stationary phase at 14°C. Increased expression of *VPS53* from a high-copy plasmid in *gcs1*Δ cells did not allow growth under these conditions (Figure 4.19). Overexpression of *VPS54*, which encodes a subunit of the GARP complex that does not directly bind Arl1 (Panic *et al.*, 2003b), was also tested for its ability to alleviate. (This was intended as a negative control in the event that increased abundance of Vps53 had allowed growth.) Increased expression of *VPS54* from a high-copy plasmid in *gcs1*Δ cells also failed to alleviate cold sensitivity (Figure 4.19). Thus unlike what is seen for the Arl1-binding protein Imh1, overexpression of the Vps53 subunit of GARP, that directly binds Arl1 in a GTP-dependent manner, does not alleviate *gcs1*Δ cold sensitivity. This result suggests that Vps53 is not the factor sequestered by dysregulated Arl1, at least in regard to the restricted-function model. This result also may indicate that alleviation by the Arl1-GRIP interaction is specific; increased expression of *any* protein that binds activated Arl1 does not necessarily alleviate. However, a consideration here is that the overexpression of *VPS53* was not confirmed by Western blot to increase the abundance of Vps53 protein. Indeed, the stoichiometry of GARP subunits is important, and imbalances between the abundance of the subunits results in the degradation of individual subunits that are not incorporated into complexes (Conibear and Stevens, 2000; Conibear *et al.*, 2003). Thus, the overexpression of the *VPS53* gene may not significantly increase Vps53 protein abundance, and co-overexpression of the four subunit genes may be required. Thus it may indeed be found to be the case that GARP (the 1:1:1:1 complex of all four subunits) is the sequestered factor.

4.21 The Vps53 Subunit of GARP is Not Required for *arl1*Δ Alleviation of *gcs1*Δ Cold Sensitivity

To further investigate any role that Vps53, as an Arl1-binding protein, may play in *gcs1*Δ cold sensitivity, I set out to assess the effect of deleting the *VPS53* gene on *gcs1*Δ cold sensitivity and on alleviating situations. In addition to Vps53, the GARP complex has

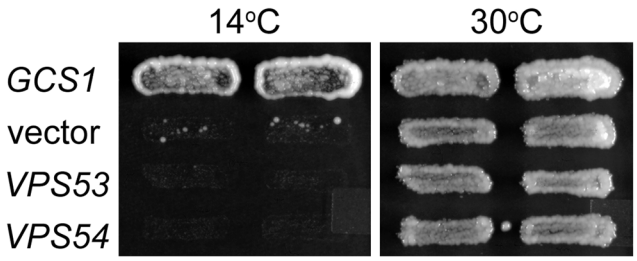

Figure 4.19 Increased abundance of Vps53 or Vps54 does not alleviate *gcs1*Δ cold sensitivity. Cold-sensitive *gcs1*Δ cells (strain JBY72-12B; W303 genetic background) harbouring plasmids (pSH4, pRS315, pVPS53-425, and pLC998) expressing the indicated genes were grown to stationary phase on solid selective medium by incubation at 30°C for 5 days before being replica-plated to solid enriched medium and incubated at 14°C for 11 days or 30°C for 1 day. Four individual transformants were assessed for each plasmid and in each case showed consistent behaviour; two transformants are shown for each. To construct pJBVPS53-425 the *VPS53* gene was PCR amplified from a wild-type S288C chromosomal DNA template using a proof-reading DNA polymerase (Platinum® *Taq* High Fidelity from invitrogen), and then cloned into the high-copy vector pRS425. The insert was not sequenced but three independent clones were assessed in the same way as shown here, with the same result.

three other subunits: Vps51, Vps52, and Vps54 (Conibear *et al.*, 2003); I therefore also assessed the involvement of these proteins. None of the genes encoding these proteins is essential, but *vps52*Δ and *vps54*Δ deletion mutations are reported to be cold sensitive (Kolling *et al.*, 1994; Abe and Minegishi, 2008). It is therefore possible that deletion of GARP subunits could recapitulate the *gcs1*Δ reentry defect. To assess this possibility I tested *vps51*Δ, *vps52*Δ, *vps53*Δ, and *vps54*Δ deletion mutations (S288C genetic background) for cold sensitivity from log phase and from stationary phase. The four deletion strains are in the deletion collection, but the *vps53*Δ deletion strain was shown by others to be faulty (Reggiori *et al.*, 2003). I therefore obtained an S288C strain with the proper *vps53*Δ mutation (FRY107; Reggiori *et al.*, 2003) from Amy Curwin in Dr. Chris McMaster's Laboratory at Dalhousie University.

All four strains deleted for individual subunits of GARP grew at 14°C from log phase and from stationary phase (Figure 4.20). Wild-type, *gcs1*Δ, and *glo3*Δ strains were used as controls; *glo3*Δ cells display cold sensitivity independent of developmental stage (Poon *et al.*, 1999), whereas *gcs1*Δ cells display reentry-specific cold sensitivity (Drebot *et al.*, 1987; Ireland *et al.*, 1994). These results were also confirmed using the W303 genetic background (data not shown). To create the deletion mutations in W303, deletion cassettes amplified from the S288C mutants were used to individually delete the four GARP-subunit genes in the W303 genetic background. The *vps51*Δ, *vps52*Δ, *vps53*Δ and *vps54*Δ deletion mutations in the W303 genetic background were confirmed by PCR. This result suggests that neither Vps53 nor any individual GARP subunit is required for reentry, suggesting that sequestration of Vps53 (or GARP) by dysregulated Arl1 is not likely the cause of the reentry defect, at least in regard to sequestration restricting the functions of a factor that is required for reentry in the cold.

Another possibility proposed in the model above is that dysregulated Arl1 aberrantly binds Vps53, forming a complex that is toxic to reentry. If this were the case, then deletion of *VPS53* should alleviate *gcs1*Δ cold sensitivity by preventing the formation of such a complex, just as the deletion of *ARL1* does. One way to directly assess this possibility is to generate *gcs1*Δ *vps53*Δ double-mutant cells and test them for growth from stationary phase at 14°C. However, a lethal genetic interaction was reported

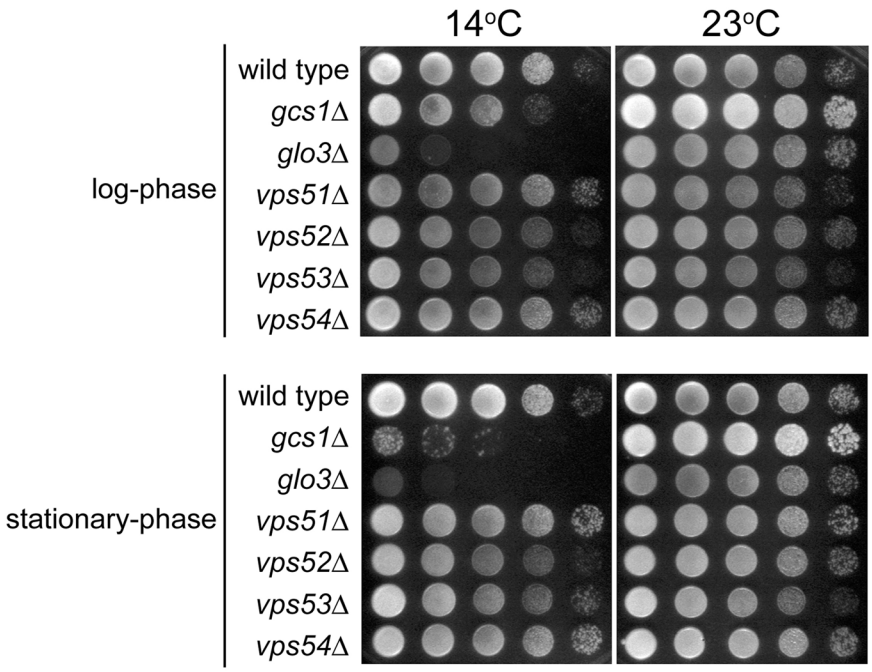

Figure 4.20 Cells individually deleted for the genes encoding the four subunits of GARP are not cold sensitive. Cells deleted for the indicated genes were harvested from logarithmically growing (top) or stationary-phase (bottom) cultures; ten-fold serial dilutions were then spotted onto solid enriched medium and incubated at 14°C for 8 days or 23°C for 2 days. The strains used were: wild type, JBY72-21B; *gcs1*Δ, JBY72-12B; *glo3*Δ, JBY18; *vps53*Δ, FRY107; and the *vps51*Δ, *vps52*Δ, and *vps54*Δ strains from the deletion collection.

between *gcs1*Δ and *vps51*Δ (Robinson *et al.*, 2006), raising the possibility that deletion of *GCS1* may also be lethal in combination with the deletion of the other GARP-subunit genes, and thus preventing such analysis. To test this possibility, I first constructed four diploid strains (W303 genetic background) each heterozygous for the *gcs1*Δ deletion mutation and either the *vps51*Δ, *vps52*Δ, *vps53*Δ, or *vps54*Δ deletion mutation. These strains were then sporulated and the resulting tetrads were dissected to obtain haploid meiotic segregants. In all four cases the double-mutant spores failed to form colonies at 30°C (Figure 4.21). Therefore, *gcs1*Δ is lethal in combination with the deletion of any of the four genes encoding a subunit of GARP. This lethality does not rule out the possibility that Vps53 binds dysregulated Arl1 forming a complex toxic to reentry, but it does prevent assessing *gcs1*Δ *vps53*Δ double-mutant cells for resumption of cell proliferation.

A lethal genetic interaction has also been reported for the deletions of *ARL1* and *VPS51* (Tong *et al.*, 2004). I assessed this genetic interaction in the W303 genetic background and also determined whether there is a similar genetic interaction between *arl1*Δ and deletion of the other genes encoding subunits of GARP. To do so I first constructed four diploid strains (W303 genetic background), each heterozygous for the *arl1*Δ deletion mutation and either the *vps51*Δ, *vps52*Δ, *vps53*Δ, or *vps54*Δ deletion mutation. These strains were then sporulated and the resulting tetrads were dissected to obtain haploid meiotic segregants. In all four cases the double-mutant segregants formed colonies that were smaller than those formed by the respective single-mutant segregants (Figure 4.22; black circles indicate *arl1*Δ *vps5X*Δ double-mutants, while white arrows indicate *vps5X*Δ single-mutants; and data not shown). Therefore in the W303 genetic background there is a deleterious genetic interaction between the deletion of *ARL1* and deletion of the genes encoding any one of the four subunits of GARP. In each case this genetic interaction results in impaired growth rather than lethality.

A surprising observation was that the lethality resulting from the combination of the deletion of *GCS1* and deletion of a gene encoding any of the four subunits of GARP was alleviated in each case by the additional deletion of *ARL1*. These observations were generated through the construction of four diploid strains (W303 genetic background), each heterozygous for the *gcs1*Δ and *arl1*Δ deletion mutations plus the *vps51*Δ, *vps52*Δ,

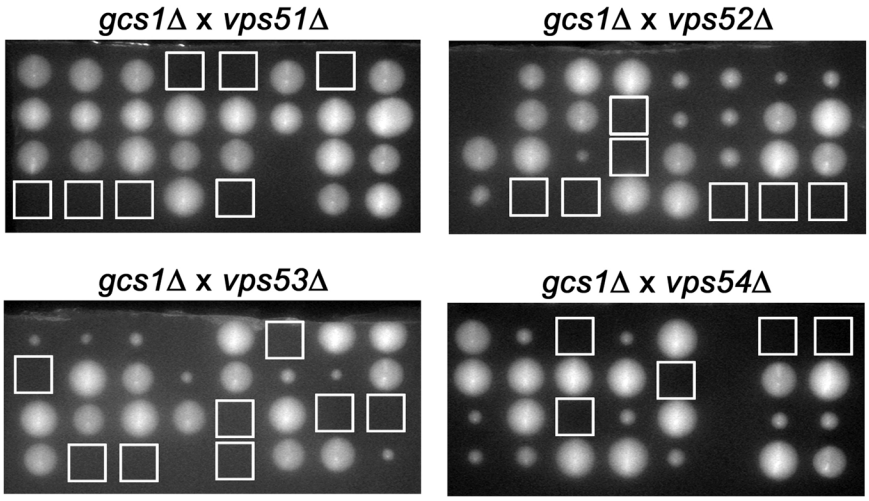

Figure 4.21 Deletion of *GCS1* is lethal in combination with the deletion of each of the four genes encoding a subunit of GARP. Meiotic tetrads from diploid strains (W303 genetic background) heterozygous for *gcs1*Δ::*nat* and either the *vps51*Δ::*kan* (JBY103), *vps52*Δ::*kan* (JBY104), *vps53*Δ::*kan* (JBY105), or *vps54*Δ::*kan* (JBY106) deletions as indicated, were dissected on enriched medium and the resulting meiotic segregants were incubated at 30°C. In each column of colonies the four meiotic segregants from a single sporulated diploid cell (tetrad) are displayed. The genotypes of viable segregants were determined by assessing nourseothricin (for *nat*) and G418 (for *kan*) drug resistance. All spores predicted to be double mutants (based on the genotypes of the living spores) failed to form colonies (boxes). There was variability in colony size; *vps52*Δ, *vps53*Δ, and *vps54*Δ single mutants produced small colonies. This size difference was less prominent when the meiotic segregants were dissected on synthetic complete medium, on which the double mutants were still dead (Figure 4.22). The diploid strains are also heterozygous for the *ade2-1* mutation, causing 2:2 segregation of red vs. white colony colour. (Originally published in Benjamin *et al.*, 2011a and cited as 'our unpublished results'.)

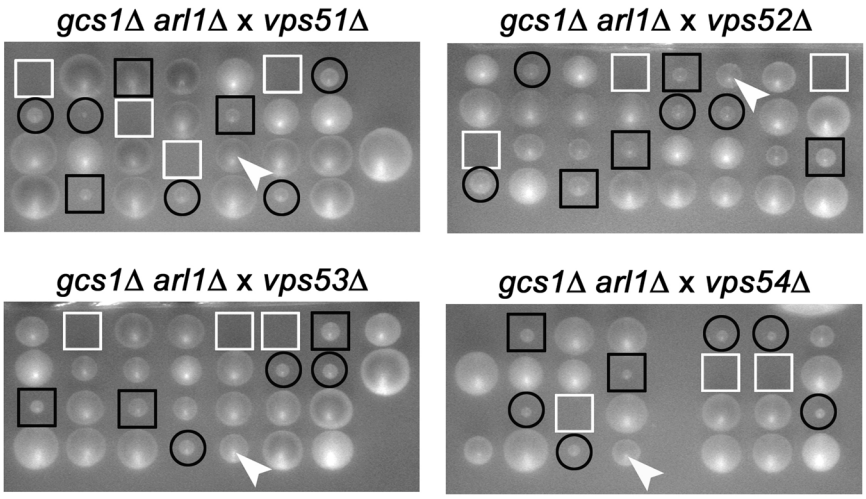

Figure 4.22 Deletion of *ARL1* alleviates the lethality of cells deleted for *GCS1* and each of the four genes encoding a subunit of GARP. Meiotic tetrads from diploid strains (W303 genetic background) heterozygous for *gcs1*Δ::*nat, arl1*Δ::*URA3* and either *vps51*Δ::*kan* (JBY85), *vps52*Δ::*kan* (JBY86), *vps53*Δ::*kan* (JBY87), or *vps54*Δ::*kan* (JBY88) deletions as indicated were dissected on synthetic complete medium and the resulting meiotic segregants were incubated at 30°C. In each column of colonies the four meiotic segregants from a single sporulated diploid cell (tetrad) are displayed. The genotypes of viable segregants were determined by assessing uracil prototrophy (for *URA3*), and nourseothricin (for *nat*) and G418 (for *kan*) drug resistance. As is seen on enriched medium (Figure 4.21), all spores predicted to be *gcs1*Δ *vps5X*Δ double mutants (based on the genotypes of the living spores) failed to form colonies (white boxes). All spores determined to be *arl1*Δ *vps5X*Δ double mutants formed colonies that were significantly smaller than the colonies formed by spores with either single mutation alone (black circles), indicating deleterious genetic interactions between these mutations. All spores determined to be triple mutants were viable and formed colonies (black boxes) comparable in size to the colonies formed by the corresponding *arl1*Δ *vps5X*Δ double-mutant spores. On enriched medium *vps52*Δ, *vps53*Δ, and *vps54*Δ single-mutant spores formed colonies that were significantly smaller than those formed by wild-type spores (Figure 4.21); this size difference was less pronounced on synthetic complete medium (representative *vps5X*Δ single mutants indicated by white arrowheads).

*vps53*Δ, or *vps54*Δ deletion mutation. These strains were sporulated and the resulting tetrads were dissected to obtain haploid meiotic segregants (Figure 4.22). As described above, the double-mutant spores deleted for *GCS1* and each of the genes encoding a subunit of GARP were dead; however, the triple-mutant spores (additionally deleted for *ARL1*) were able to form colonies that were comparable in size to the colonies formed by the corresponding *arl1*Δ *vps5X*Δ double mutants. Therefore, elimination of Arl1 relieves the lethality caused by the absence of Gcs1 in combination with the absence of any subunit of GARP, suggesting the lethality is caused by dysregulated Arl1 (resulting from the absence of Gcs1). This finding highlights a strong parallel between the *gcs1*Δ cold sensitivity, which is caused by dysregulated Arl1, and the lethality seen in the absence of GARP, which is also caused by dysregulated Arl1. Another way to view this situation is that dysregulated Arl1 causes GARP function to be essential. Dysregulated Arl1 may therefore inhibit the function of a cellular factor that shares an overlapping function with GARP. When GARP is intact, inhibition of this factor by dysregulated Arl1 results in reentry-specific cold sensitivity, but the elimination of GARP (by the elimination of any one subunit) now causes cell growth to be completely inhibited, resulting in the lethality of *gcs1*Δ *vps5X*Δ cells. Eliminating the dysregulated Arl1 (by deletion of *ARL1*) releases the inhibition of the factor and alleviates the lethality. It is likely that the factor proposed here to share an overlapping function with GARP and to be inhibited by dysregulated Arl1 is the same factor proposed above to be bound by dysregulated Arl1, thus causing the *gcs1*Δ defects.

This finding allowed me to determine if Vps53 is required for *arl1*Δ alleviation of *gcs1*Δ cold sensitivity by assessing the growth of *gcs1*Δ *arl1*Δ *vps53*Δ triple mutants at 14°C from stationary phase (Figure 4.23). The *gcs1*Δ *arl1*Δ *vps53*Δ segregant tested grew as well under these conditions as did the *arl1*Δ *vps53*Δ and *gcs1*Δ *arl1*Δ segregants. The same result was observed for the *vps51*Δ strains (data not shown). Thus, neither Vps53 nor Vps51 is required for *arl1*Δ alleviation of *gcs1*Δ cold sensitivity. This result suggests that sequestration of Vps53 (or GARP) by dysregulated Arl1 is not the cause of the *gcs1*Δ reentry defect, but does not eliminate the possibility that Vps53 (or GARP) forms a toxic complex with dysregulated Arl1.

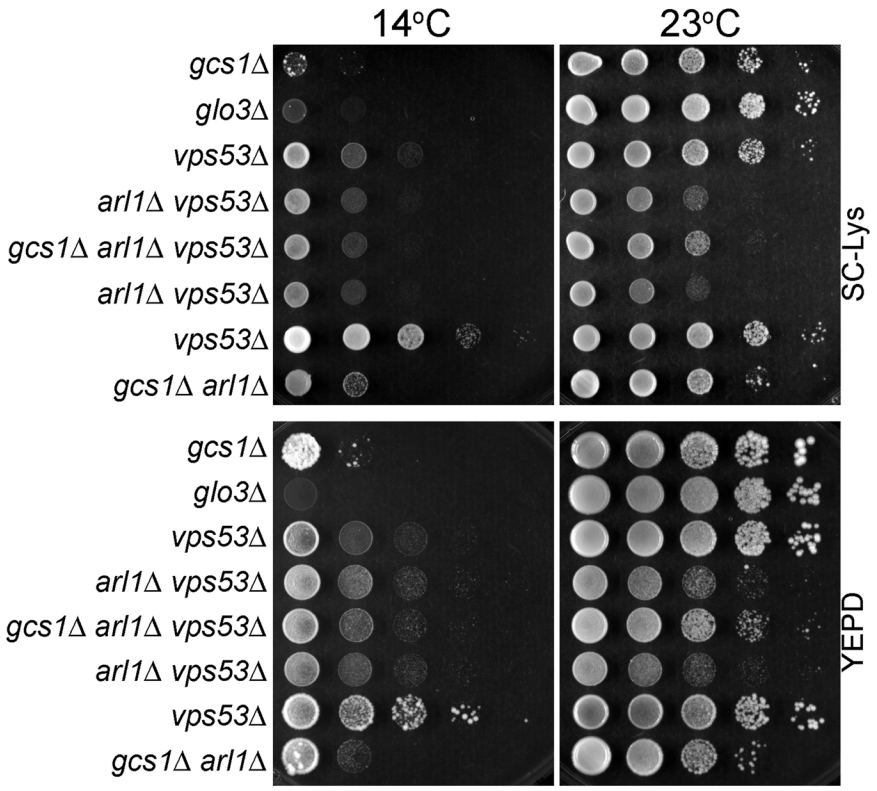

Figure 4.23 Vps53 is not required for *arl1*Δ alleviation of *gcs1*Δ cold sensitivity. The meiotic tetrads from a diploid strain (JBY87; W303 genetic background) heterozygous for *gcs1*Δ::*nat, arl1*Δ::*URA3* and *vps53*Δ::*kan* deletions were dissected on synthetic complete medium and the resulting meiotic segregants were incubated for 7 days at 30°C to allow colony formation and entry into stationary phase. Ten-fold serial dilutions of cells from these stationary-phase colonies were then spotted onto solid enriched and synthetic complete medium and incubated at 14°C for 15 days or 23°C for 4 days. *glo3*Δ cells (strain JBY18; W303 genetic background) were used as a cold-sensitive control. (Originally published in Benjamin *et al.*, 2011a and cited as 'our unpublished results'.)

A note of caution concerning the results presented above is warranted. The experiment assessing *arl1*Δ *vps53*Δ double-mutant segregants and *gcs1*Δ *arl1*Δ *vps53*Δ triple-mutant segregants described above and displayed in Figure 4.23 was technically difficult. Although alive, these mutant cells are severely impaired, resulting in a strong selective advantage for any suppressor mutations that arise. To avoid prolonged or repeated growth of these mutant cells that would allow accumulation of such suppressor mutations, the segregants in this serial-dilution assay were not grown to stationary phase in liquid cultures before spotting, as would normally be done. Instead, the cells for this assay were taken directly from colonies arising from tetrad dissection that were incubated for 7 days at 30°C to allow their constituent cells to enter stationary phase. The *gcs1*Δ control cells that were obtained in the same manner did exhibit cold sensitivity, indicating that these cells had entered stationary phase. Unfortunately, there is no way to ensure that the slower growing mutant segregants, from significantly smaller colonies, had actually entered stationary phase, and this is prerequisite to manifesting the cold-sensitive phenotype. Therefore, these results should be considered in light of these caveats.

4.22 Arl1-Q72L Does Not Recapitulate *gcs1*Δ Cold Sensitivity

Defective Gcs1 function (caused by either deletion or mutation of the *GCS1* gene) undoubtedly leads to dysregulation of Arl1 activity. Dysregulated mutant forms of Arl1 have been reported, including a constitutively active mutant form. To assess the potential that a dysregulated form of Arl1 that is thought to be constitutively active might recapitulate the effect of the absence of Gcs1, I expressed such a mutant form of Arl1, Arl1-Q72L, as the only version of Arl1 in the cell. This mutation in Arl1 is analogous to a dominant active mutation in Ras (Ras-Q61L) that keeps Ras in the GTP-bound form (Bourne *et al.*, 1991), and is predicted to be defective in GTP hydrolysis causing Arl1 to be constitutively active (Rosenwald *et al.*, 2002). Stationary-phase *arl1*Δ cells harbouring low-copy or high-copy plasmids expressing Arl1-Q72L grew as well in a serial-dilution assay at 14°C as did *arl1*Δ vector-control cells (Figure 4.24). The wild-type and *gcs1*Δ controls for this experiment were spotted on separate plates due to limited space, but were treated analogously to the *arl1*Δ transformants, and all serial-dilution assays were performed at the same time. Thus, the constitutively active Arl1-Q72L mutant form of

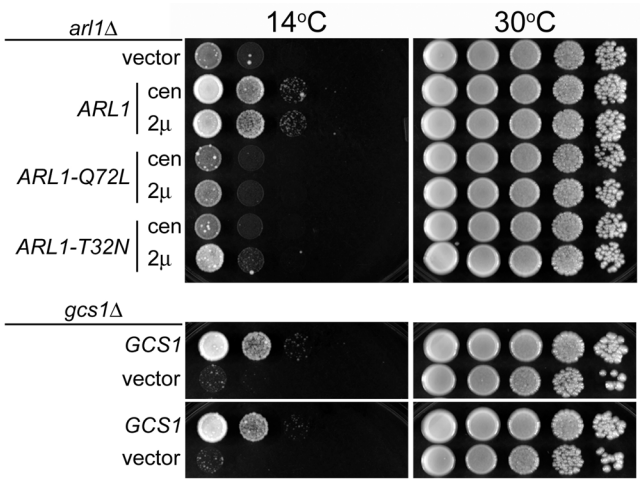

Figure 4.24 Expression of Arl1-Q72L as the only Arl1 in the cell does not recapitulate the *gcs1*Δ cold-sensitivity phenotype. An *arl1*Δ strain (JBY72-13C; W303 genetic background) carrying vector (pRS316), or low-copy (cen) or high-copy (2μ) plasmids expressing wild-type *ARL1* (pJBARL1-316, pARY1-3), *ARL1-Q72L* (pSR39, pJBARL1Q-426), or *ARL1-T32N* (pSR44, pJBARL1T-426), and an isogenic *gcs1*Δ strain carrying vector (pRS316) or a low-copy plasmid expressing *GCS1* (pGCS1-316), were grown in selective medium to stationary phase by incubation at 30°C for 7 days; ten-fold serial dilutions were then spotted onto solid enriched medium and incubated at 14°C for 10 days or 30°C for 3 days.

Arl1 does not create *gcs1*Δ-type cold sensitivity, even when overexpressed from a high-copy plasmid. I also expressed another dysregulated form of Arl1, the Arl1-T32N mutant protein, as the only version of Arl1 in the cell. The Arl1-T32N mutant is predicted to be defective in GTP binding and to preferentially bind GDP, causing Arl1 to be 'stuck' in the inactive GDP-bound state (Rosenwald *et al.*, 2002). Expression of this constitutively inactive mutant form of Arl1 from low-copy or high-copy plasmids in *arl1*Δ cells also had no effect on growth (Figure 4.24). Deletion of *ARL1* did cause a slight inhibition in growth: compare the growth of *arl1*Δ vector-control cells to that of wild-type cells. Expression of wild-type Arl1 from low- and high-copy plasmids complemented this growth impairment, whereas expression of the mutant forms of Arl1 did not (Figure 4.24). Thus, the dysregulated Arl1 that results when Gcs1 is absent and that inhibits cell-cycle reentry and endosomal transport in the cold is different from these dysregulated mutant versions of Arl1 that cause Arl1 to be constitutively active (Arl1-Q72L), or constitutively inactive (Arl1-T32N). Endogenous Gcs1 is intact in the cells tested here; their ability to reenter in the cold indicates that either Gcs1 is capable of regulating these mutant forms of Arl1 in the GAP-independent manner that is required to alleviate the *gcs1*Δ-type cold-sensitivity, or that these mutant versions of Arl1 are incapable of participating in the inhibitory interactions that cause the *gcs1*Δ reentry defect. An additional observation is that the elimination of Arl1 causes a slight growth impairment (this *arl1*Δ growth impairment is less pronounced on selective medium – data not shown) that the mutant forms of Arl1 (Q72L and T32N) fail to complement. This result suggests that, as intended, these mutant forms of Arl1 do not function as wild-type Arl1 does *in vivo*.

The mutant Arl1-Q72L protein binds the GRIP domain of Imh1 in an *in vitro* binding assay (Setty *et al.*, 2003), but GFP-Imh1 is diffusely distributed throughout the cytoplasm when Arl1-Q72L or Arl1-T32N is the only version of Arl1 in the cell (Liu *et al.*, 2005). However, this finding for Arl1-Q72L is at odds with my observation of GFP-Imh1 punctate localization in cells with persistently active Arl1 due to the absence of Gcs1, and suggests that Arl1-Q72L may not function as a persistently active Arl1 *in vivo*. To assess the ability of Arl1-Q72L (and Arl1-T32N) to bind and properly localize Imh1 *in vivo,* I analyzed the localization of GFP-Imh1 in *arl1*Δ cells harbouring plasmids

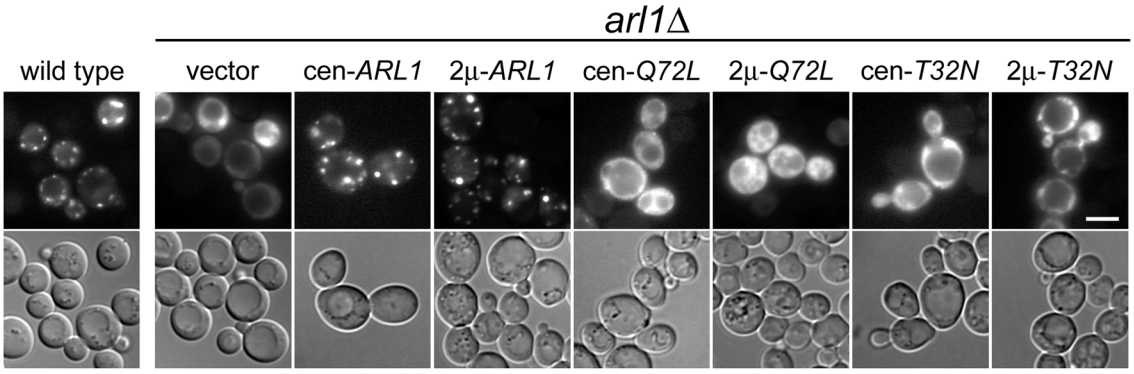

Figure 4.25 Arl1-Q72L and Arl1-T32N do not complement the loss of Arl1 for normal localization of GFP-Imh1. The localization of GFP-Imh1 was visualized by fluorescence microscopy (top panels) in live yeast cells expressing *GFP-IMH1* from a high-copy plasmid (pJB1598-9), and the same cells were visualized by differential interference contrast microscopy (bottom panels). Localization of GFP-Imh1 was assessed in wild-type cells (strain JBY72-21B; W303 genetic background) and in isogenic *arl1*Δ cells (strain JBY72-13C) carrying vector (pRS316) or low-copy (cen) or high-copy (2μ) plasmids expressing wild-type *ARL1* (pJBARL1-316, pARY1-3), *ARL1-Q72L* (pSR39, pJBARL1Q-426), or *ARL1-T32N* (pSR44, pJBARL1T-426). Cells growing logarithmically in selective medium at 30°C were concentrated in growth medium by centrifugation immediately prior to analysis by fluorescence microscopy. Scale bar, 5 μm.

expressing various forms of Arl1 (Figure 4.25). The mislocalization of GFP-Imh1 that is caused by the absence of Arl1 was corrected by wild-type Arl1 but not by the Arl1-Q72L or Arl1-T32N mutant forms of Arl1, consistent with published findings (Liu *et al.*, 2005). Thus, Arl1-Q72L does not mimic the persistently active Arl1 situation that presumably results when Gcs1 is absent.

The lack of a defect in *arl1*Δ cells expressing Arl1-Q72L (and purportedly mimicking a cell with persistently active Arl1) suggests that the underlying defect in cells lacking Gcs1 is not due to persistently active Arl1. However, Arl1-Q72L does not accurately mimic constitutively active Arl1 *in vivo* (in regards to GFP-Imh1 localization), making it difficult to interpret results with Arl1-Q72L *in vivo.*

4.23 Increased Abundance of Wild-Type or Mutant Forms of Arl1 Alleviates *gcs1*Δ Cold Sensitivity

I also assessed the effect on *gcs1*Δ cold sensitivity of expressing extra gene copies of wild-type and mutant forms of Arl1 from low-copy and high-copy plasmids. Stationary-phase *gcs1*Δ cells transformed with plasmids expressing wild-type and mutant forms of Arl1 were assessed for growth at 14°C (Figure 4.26). Expression of *ARL1* at one or two extra copies per cell had no effect on *gcs1*Δ cold sensitivity: *gcs1*Δ cells carrying *ARL1* on a low-copy plasmid remained cold sensitive. However, overexpression of *ARL1* from a high-copy plasmid alleviated *gcs1*Δ cold sensitivity. Increased expression of the Q72L and T32N mutant forms of Arl1 also alleviated *gcs1*Δ cold sensitivity. Unlike wild-type Arl1, the Q72L and T32N mutant forms of Arl1 relieved the cold sensitivity of *gcs1*Δ cells even when expressed from low-copy plasmids.

To follow up on the alleviation of *gcs1*Δ cold sensitivity caused by the overexpression of wild-type *ARL1*, I assessed the localization of GFP-Imh1 in *gcs1*Δ cells overexpressing *ARL1* from a high-copy plasmid (Figure 4.27). In sharp contrast to the normal punctate localization of GFP-Imh1 in *gcs1*Δ cells carrying vector or wild-type *GCS1*, the localization of GFP-Imh1 was clearly abnormal in the *gcs1*Δ cells overexpressing *ARL1*. In these cells, GFP-Imh1 was localized to one large 'structure' (Figure 4.27). I also assessed GFP-Imh1 localization in *gcs1*Δ cells expressing *ARL1*

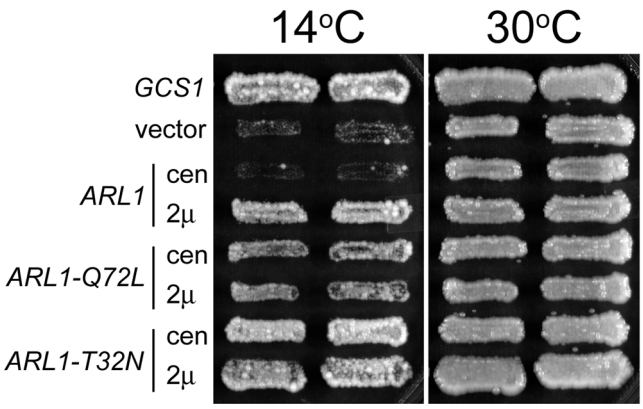

Figure 4.26 Increased abundance of wild-type or mutant forms of Arl1 alleviates *gcs1*Δ cold sensitivity. Cold-sensitive *gcs1*Δ cells (strain JBY72-12B; W303 genetic background) harbouring low-copy (cen) and high-copy (2μ) plasmids (pGCS1-316, pRS316, pJBARL1-316, pARY1-3, pSR39, pJBARL1Q-426, pSR44, and pJBARL1T-426) expressing the indicated genes were grown to stationary phase on solid selective medium by incubation at 30°C for 5 days before being replica-plated to solid enriched medium and incubated at 14°C for 11 days or 30°C for 2 days. Four individual transformants were assessed for each plasmid and in each case showed consistent behaviour; two transformants are shown for each.

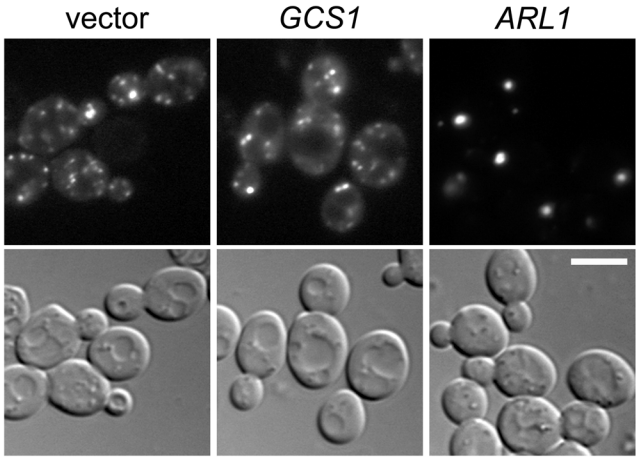

Figure 4.27 Increased abundance of Arl1 in the absence of Gcs1 causes aberrant localization of GFP-Imh1 to one large structure. The localization of GFP-Imh1 was visualized by fluorescence microscopy (top panels) in live *gcs1*Δ yeast cells (strain JBY72-12B; W303 genetic background) expressing *GFP-IMH1* from the *TPI1* promoter on a low-copy plasmid (pJB1711). The *gcs1*Δ cells additionally harboured vector (pRS316), a low-copy plasmid expressing *GCS1* (pGCS1-316) or a high-copy plasmid expressing *ARL1* (pARY1-3) as indicated. Cells growing logarithmically in selective medium at 30°C were concentrated in growth medium by centrifugation immediately prior to analysis by fluorescence microscopy. The same cells were visualized by differential interference contrast microscopy (bottom panels). Scale bar, 5 µm.

from a low-copy plasmid, a situation that does not alleviate *gcs1*Δ cold sensitivity. In these cells, GFP-Imh1 localization appeared normal and no large structures were present like those seen in cells with high-copy *ARL1* (data not shown). Although further work is required to develop these observations, it is clear that high-copy expression of *ARL1* not only alleviates *gcs1*Δ cold sensitivity but also appears to perturb Arl1 localization in a way that low-copy expression does not.

Alleviation of *gcs1*Δ cold sensitivity by high-copy expression of *ARL1* is difficult to reconcile with the model described above. If dysregulated Arl1 causes the defects at issue here then it is hard to imagine how increased Arl1 abundance can alleviate them, as it might be expected that increased Arl1 abundance would result in increased abundance of dysregulated Arl1 and only serve to exacerbate the defects. However, the aberrant localization of GFP-Imh1 seen in *gcs1*Δ cells overexpressing *ARL1* suggests that Arl1 localization is perturbed in these cells. Altering the localization of dysregulated Arl1 is the mechanism (suggested in the model) by which other alleviating conditions identified here (i.e. elimination of the Arl1 or Ypt6 pathway) are thought to alleviate *gcs1*Δ cold sensitivity.

Although I have not determined how the overexpression of *ARL1* in the absence of Gcs1 perturbs Arl1 localization, there appears to be a threshold level of excess Arl1 required to see this effect. Increased expression of *ARL1* from a high-copy plasmid is required to perturb Arl1 localization (assessed by aberrant localization of GFP-Imh1) and alleviate *gcs1*Δ cold sensitivity, whereas the lower level of *ARL1* expression from a low-copy plasmid does not elicit either of these effects. Therefore, increased expression of *ARL1* above a threshold results in the aberrant localization of GFP-Imh1 to one large structure per cell (which is indicative of perturbed Arl1 localization), and the alleviation of *gcs1*Δ cold sensitivity.

The large structure evident through GFP-Imh1 localization appears to contain virtually all of the GFP-Imh1 in the cell and therefore may contain much of the dysregulated Arl1. It is possible that increasing the amount of dysregulated Arl1 in the cell (above a threshold level) results in aggregation of the majority of the Arl1. This aggregation could occur through protein-protein interactions that are somehow forced or

stabilized in the presence of excess dysregulated Arl1. In this way, the dysregulated Arl1 could be prevented from exerting the inhibitory effects that cause cold sensitivity.

It is important to note that simply preventing the *majority* of the dysregulated Arl1 from having inhibitory effects may be sufficient to alleviate cold sensitivity. This insight is revealed by the viability of *ypt6*Δ cells, and requires some explanation. The deletion of *YPT6* is reported to be lethal in combination with the deletion of *ARL1* or *IMH1* (Setty *et al.*, 2003; Tong *et al.*, 2004), and I have confirmed these lethal interactions (Figure 4.10, and see Figure 4.28A below). Despite these lethal combinations, however, *ypt6*Δ cells themselves, which mislocalize Arl1 and Imh1 (Figure 4.8), are viable. Thus, the impairment of the Arl1 pathway due to the absence of Ypt6 must not completely eliminate Arl1-pathway function, and it is therefore likely that in the absence of Ypt6 at least some Arl1 and Imh1 are properly localized. Although any Arl1-GFP localized to the Golgi in the absence of Ypt6 was below my ability to visualize as punctate staining (Figure 4.8), I noted that cells lacking Ypt6 display some localization of Sys1-GFP and GFP-Imh1 to punctate structures that may correspond to proper Golgi localization (Figure 4.8). Another observation is that *gcs1*Δ *ypt6*Δ double-mutant cells are viable, indicating that the (presumably) small amount of Arl1 that is properly localized in *ypt6*Δ cells and able to keep them alive can do so even when it is dysregulated due to the absence of Gcs1 GAP and GAP-independent activities. An alternative interpretation is that in the absence of Gcs1, Arl1 and Ypt6 function are no longer essential. This is directly testable by assessing whether *gcs1*Δ *arl1*Δ *ypt6*Δ triple-mutant cells are viable. In any case, probably the most telling aspect of this is that the small amount of dysregulated Arl1 that is likely present at the *trans*-Golgi membrane in *gcs1*Δ *ypt6*Δ cells and able to provide Arl1 function to keep the cells alive is not sufficient to cause cold sensitivity and impaired endocytic transport. Thus, there appears to be a lower threshold amount of dysregulated Arl1 that is required to cause these inhibitory effects, in addition to the higher threshold amount of Arl1 that then alleviates the inhibitory effects. Alleviating situations such as deletion of *YPT6* or the overexpression of *ARL1*, which is at issue here, need only prevent the majority of the dysregulated Arl1 from participating in inhibitory interactions, and need not prevent all of the inhibitory interactions with dysregulated Arl1.

A second possibility is that, because Arl1 is involved in intracellular membrane transport, the increased abundance of dysregulated Arl1 may perturb transport within the endomembrane system, resulting in the formation of aberrant membrane-bound structures wherein the dysregulated Arl1 is accumulated. Under these conditions, Arl1 may be trapped in a compartment that no longer corresponds to the *trans*-Golgi, where dysregulated Arl1 is localized in *gcs1*Δ cells that are not overexpressing *ARL1*, thereby preventing the inhibitory effects that cause cold sensitivity.

A third possibility is that the alleviation of *gcs1*Δ cold sensitivity and aberrant localization of Arl1 are not directly caused by an increased abundance of Arl1 protein, but are rather caused by the increased abundance of the *ARL1* gene promoter that is also present on the low-copy and high-copy plasmids expressing *ARL1*. Increased copies of the *ARL1* promoter may well decrease the availability to other genes of transcription factors that recognize it. As such, the effects of *ARL1* overexpression could be caused by changes in the expression levels of other proteins that share transcription factors with *ARL1*. As an example, overexpression of the *ARL1* promoter could titrate a transcriptional activator and thus result in decreased transcription of genes that share that activator. The resulting decreased abundances of the proteins encoded by these genes could cause the mislocalization of Arl1 and the alleviation of *gcs1*Δ cold sensitivity. Indeed, we identified a number of genes whose deletion alleviate *gcs1*Δ cold sensitivity (Table 4.3). In these cells with alleviating deletions the localization of GFP-Imh1 was assessed (blinded analyses in section 4.7 above), and in no case did this localization resemble the localization seen when *ARL1* is overexpressed in *gcs1*Δ cells. However, an important difference is that Gcs1 was present in the cells observed in the blinded analysis; the significance of this difference is discussed below. In any case, this hypothesis of transcription factor titration is directly testable by the use of high-copy plasmids harbouring just the *ARL1* promoter in *gcs1*Δ cells and assessing alleviation of cold sensitivity and GFP-Imh1 localization.

Indeed, the absence of Gcs1 is an important contributing factor for the aberrant localization of GFP-Imh1 seen when *ARL1* is overexpressed. GFP-Imh1 is punctate in *arl1*Δ cells overexpressing *ARL1* in which the chromosomal *GCS1* locus is present (Figure 4.25). This result indicates that Gcs1 prevents the overexpression of *ARL1* from

causing the aberrant localization of GFP-Imh1. Furthermore, preliminary results showed that the GAP activity of Gcs1 is required for this effect (data not shown; these data are not shown here because the experiment was only done once, and although I recorded my observations, I did not capture images of the cells that I visualized by fluorescence microscopy). This experiment assessed the effect of expressing *GCS1* or *gcs1-R54K* on the aberrant localization of GFP-Imh1 in *gcs1*Δ cells overexpressing *ARL1*. Expression of *GCS1* in these cells from a low-copy plasmid resulted in normal punctate localization of GFP-Imh1 (high-copy expression had the same effect), whereas expression of vector or the GAP-deficient mutant, *gcs1-R54K*, from a low-copy or even a high-copy plasmid had no effect on the aberrant localization of GFP-Imh1, which remained localized to one large structure in these cells. Thus, the aberrant localization of GFP-Imh1 in these cells is likely caused by increased abundance of the activated GTP-bound form of Arl1, which would be decreased in the presence of Gcs1 but not Gcs1-R54K. It is not clear whether the activation of Arl1 is required for the alleviating effects of increased Arl1 abundance, because in the presence of Gcs1, which would reduce the levels of activated Arl1, there is no dysregulation of Arl1 to cause the defect.

The mutant forms of Arl1 (Q72L and T32N) both alleviate *gcs1*Δ cold sensitivity even when expressed from low-copy plasmids. These cells contain the chromosomally encoded wild-type Arl1 protein; thus, the alleviating effect of each of these mutant alleles is dominant. Based on the model that disruption of dysregulated Arl1 alleviates *gcs1*Δ cold sensitivity, it is possible that these mutant forms of Arl1 alter the localization or function of dysregulated Arl1. I have preliminary results that address this possibility by assessing GFP-Imh1 localization in *gcs1*Δ cells harbouring low-copy or high-copy plasmids expressing these mutant alleles of *ARL1* (only one transformant was assessed for each, and this experiment was not repeated). In *gcs1*Δ cells expressing the *ARL1-Q72L* allele from low-copy and high-copy plasmids, GFP-Imh1 was found to be localized normally with a punctate staining pattern (data not shown). These cells contained both wild-type Arl1, which binds GFP-Imh1, and Arl1-Q72L, which does not bind GFP-Imh1 (Figure 4.25). Thus, although the overexpression of *ARL1-Q72L* alleviates *gcs1*Δ cold sensitivity it did not interfere with GFP-Imh1 localization, indicating that wild-type Arl1 was functioning normally in these cells, at least with regard to GFP-Imh1 localization.

These observations therefore do not generate a simple hypothesis for how the expression of *ARL1-Q72L* alleviates *gcs1*Δ cold sensitivity.

The situation of overexpressed *ARL1-T32N* did provide insight into the alleviation of *gcs1*Δ cold sensitivity. There are no data for high-copy expression of *ARL1-T32N.* However, in the *gcs1*Δ cells expressing *ARL1-T32N* from a low-copy plasmid GFP-Imh1 was mislocalized and exhibited a diffuse cytoplasmic pattern despite the presence of wild-type Arl1 (data not shown). Thus, low-copy expression of *ARL1-T32N* alleviates *gcs1*Δ cold sensitivity and causes GFP-Imh1 to be mislocalized. This result is consistent with Arl1-T32N having a dominant effect that interferes with wild-type Arl1 function, and is consistent with alleviation by mislocalization of dysregulated Arl1. Arl1-T32N is predicted to bind GTP poorly, causing the mutant protein to preferentially bind GDP (Peyroche *et al.*, 1996). Similar GTPases with the analogous substitution have an increased affinity for their putative GEFs (Haney and Broach, 1994; Peyroche *et al.*, 1996). As such, Arl1-T32N could exert its effects by binding the Arl1 GEF(s) with high affinity, effectively blocking the activation of wild-type Arl1 by sequestering the GEF(s). Thus, the end result of this proposed mechanism for Arl1-T32N alleviation of *gcs1*Δ cold sensitivity is the same as the mechanism proposed for the alleviating mutations that eliminate components of the Arl1 and Ypt6 pathways: blocking the activation of dysregulated Arl1 and preventing its membrane localization.

4.24 Confirming Genetic Interactions Reported Between Genes Involved in this Study

Many genetic interactions have been reported between genes encoding components of the Arl1 and Ypt6 pathways, and also between genes within the Ypt6 pathway. Several of these reported genetic interactions were identified in large-scale genomic SGA screens (Tong *et al.*, 2004). Because these types of screens involve high-throughput analysis and rarely involve confirmation of all negative genetic interactions that are identified, the reported lists of deleterious genetic interactions often contain false positives and weak interactions (as shown above in the case of the *arl1*Δ *vps51*Δ interaction). I have also noticed that, for the genes encoding the subunits of GARP (*VPS51, VPS52, VPS53,* and *VPS54*), genetic interactions are often reported only for the deletion of *VPS51*, and not

for the other subunits. Upon further analysis, the deletions of the other three GARP genes reveal the same genetic interactions reported for deletion of *VPS51*. A possible explanation for this absence of published data is that the colonies formed by *vps52*Δ, *vps53*Δ, and *vps54*Δ cells on enriched medium are small compared to the relatively normal size of colonies formed by *vps51*Δ cells (Figure 4.21). In a high-throughput SGA screen the small colony sizes for the *vps52*Δ, *vps53*Δ, and *vps54*Δ single-mutant cells could appear as no growth on an arrayed plate, causing the results for these mutants to be ignored. For these reasons I assessed many of the reported genetic interactions for myself, using the W303 genetic background. Several of these genetic interactions were reported above; the remaining interactions that I assessed are presented here.

The deletion of *YPT6* was reported to be lethal in combination with the deletion of several genes in the Arl1 pathway including *ARL3, SYS1, MAK3, MAK10, ARL1* and *IMH1* (Setty *et al.*, 2003; Tong *et al.*, 2004). These genetic interactions highlight the perceived parallel nature of these two pathways to provide vesicle-tethering functions at the *trans*-Golgi. The *ypt6*Δ *imh1*Δ lethal interaction was confirmed as described (Figure 4.10). I also assessed the *ypt6*Δ *arl1*Δ lethal interaction. To assess the severity of this genetic interaction, I first constructed a diploid strain (JBY119; W303 genetic background) that is heterozygous for *YPT6* and *ARL1* gene deletions; each deletion was confirmed by PCR. This diploid was then sporulated and the resulting tetrads were dissected to assess the viability of the haploid meiotic segregants. In these tetrads the marker genes for each deletion segregated 2:2, confirming that the diploid strain was indeed heterozygous for each deletion, and that the deletion cassette did not additionally integrate at a second locus during strain construction. Although wild-type and single-mutant segregants were viable as indicated by colony formation, none of the double-mutant *ypt6*Δ *arl1*Δ segregants formed a colony (Figure 4.28A), indicating that *ypt6*Δ *arl1*Δ double-mutant cells are not viable and confirming the reported lethal interaction. Thus, it appears that the Arl1 and Ypt6 pathways provide an overlapping essential function, presumably for vesicle tethering at the *trans*-Golgi.

A surprising (and not fully understood) lethal interaction between *ypt6*Δ and *vps51*Δ was reportedly found in a high-throughput SGA screen (Tong *et al.*, 2004). This

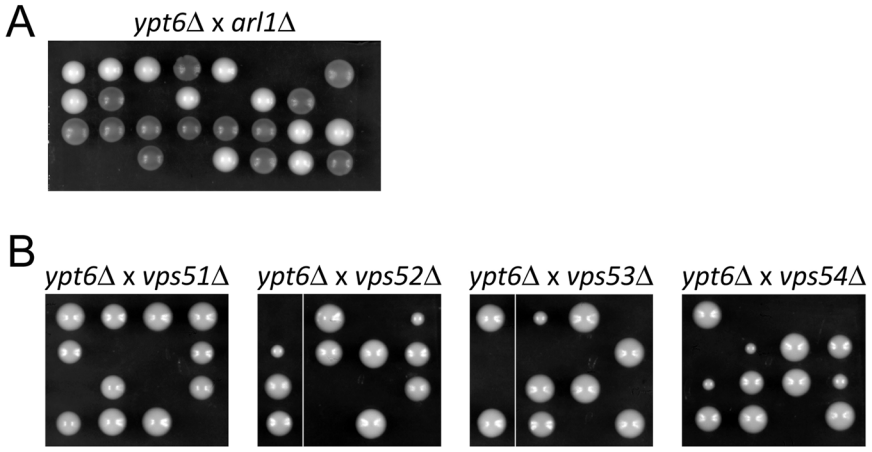

Figure 4.28 Confirmation of genetic interactions between genes involved in this study. (A) Deletion of *YPT6* is lethal in combination with the deletion of *ARL1*. (B) Deletion of *YPT6* is lethal in combination with the deletion of any of the four genes encoding a subunit of GARP. Meiotic tetrads of diploid strains (W303 genetic background) heterozygous for (A) *ypt6*Δ::*kan* and *arl1*Δ::*URA3* deletions (JBY114), or (B) *ypt6*Δ::*URA3* and either *vps51*Δ::*kan* (JBY1670:1), *vps52*Δ::*kan* (JBY1670:3), *vps53*Δ::*kan* (JBY1670:5), or *vps54*Δ::*kan* (JBY1670:8) deletions as indicated, were dissected on synthetic complete medium (panel A) or enriched medium (panel B) and the resulting meiotic segregants were incubated at 30°C. In each column of colonies the four meiotic segregants from a single sporulated diploid cell (tetrad) are displayed. The genotypes of viable segregants were determined by assessing uracil prototrophy (for *URA3*) and G418 drug resistance (for *kan*). All spores predicted to be double mutants (based on the genotypes of the living spores) failed to form colonies. In panel A the diploid strain is also heterozygous for the *ade2-1* mutation, causing 2:2 segregation of red vs. white colony colour. In panel B there was variability in colony size; small colonies are *vps52*Δ, *vps53*Δ, and *vps54*Δ single mutants. This size difference was less prominent when the meiotic segregants were dissected on synthetic complete medium. (Panel A was originally published in Benjamin *et al.*, 2011a and cited as 'our unpublished results'.)

interaction is surprising because Vps51, as a subunit of the GARP complex, is an effector of Ypt6. If Ypt6 and GARP function exclusively together in the Ypt6 pathway, there should be no lethal interaction between *ypt6*Δ and *vps51*Δ. The finding of an interaction suggests that Vps51 and/or Ypt6 have additional functions apart from those that they carry out together. In the case of Vps51, these functions could be independent of the GARP complex; no lethal interactions have been reported between the deletion of *YPT6* and the deletion of the other three genes that encode a subunit of GARP. However, if the deletion of *YPT6* were also lethal in combination with the deletion of the other three genes that encode a subunit of GARP, this would suggest that GARP itself has an additional function independent of the Ypt6 pathway, or conversely that Ypt6 has an additional function independent of GARP.

To assess genetic interactions between deletion of *YPT6* and deletion of the genes encoding subunits of GARP I first constructed four diploid strains (W303 genetic background), each heterozygous for the *ypt6*Δ deletion mutation and either the *vps51*Δ, *vps52*Δ, *vps53*Δ, or *vps54*Δ deletion mutation. These strains were then sporulated and the resulting tetrads were dissected to obtain haploid meiotic segregants. In each case the double-mutant spores did not form colonies (Figure 4.28B). These observations not only confirmed that deletion of *YPT6* and *VPS51* is indeed lethal, but also revealed that deletion of *YPT6* is lethal in combination with deletions of the other three genes encoding subunits of GARP. This result suggests that either GARP or Ypt6 (or both) provide a function independent of the function provided together within the Ypt6 pathway. An additional function of GARP could involve its interaction with Arl1 (Panic *et al.*, 2003b). Another point to consider is that Ypt6 is needed for effective Arl1 pathway function and Arl1 localization (see above). Therefore, Arl1 pathway function which is itself required in the absence of Ypt6 or GARP (see above) is severely diminished in cells lacking Ypt6 and GARP. This diminished Arl1 pathway function likely contributes to the lethality caused by deletion of *YPT6* in combination with deletion of genes encoding subunits of GARP.

CHAPTER 5. DISCUSSION

5.1 General Overview

The *GCS1* gene in yeast was initially identified, named, and cloned based on the unique cold-sensitive defect exhibited by cells bearing a *gcs1*Δ deletion mutation (Drebot *et al.*, 1987; Ireland *et al.*, 1994). These *gcs1*Δ cells are unable to resume mitotic cell proliferation from stationary phase at the restrictive temperature of 14°C, whereas mutant cells that are actively proliferating when shifted to 14°C continue to proliferate as long as nutrients are available (Drebot *et al.*, 1987). Thus, *gcs1*Δ mutant cells exhibit what we term a 'reentry phenotype', with cells unable to reenter the mitotic cell cycle from stationary phase. Over a decade later, sequence similarities between the *GCS1* gene product and a mammalian ArfGAP protein (Cukierman *et al.*, 1995) identified *GCS1* as the founding member of the ArfGAP family of genes in yeast (Poon *et al.*, 1996). This gene family now defines six proteins (Gcs1, Glo3, Age2, Age1, Sps18 and Gts1) based on the presence of the conserved ArfGAP domain, and four of these (Gcs1, Glo3, Age2, and Age1) have been shown to have ArfGAP activity *in vitro* (Poon *et al.*, 1996; Poon *et al.*, 1999; Poon *et al.*, 2001; Zhang *et al.*, 2003; Benjamin *et al.*, 2011b). Outside of the conserved ArfGAP domain, which promotes GTP hydrolysis by Arf (Goldberg, 1999; Robinson *et al.*, 2006), there is little sequence similarity among these proteins. These differences are thought to provide protein-specific functions that allow the various ArfGAP proteins to function at different stages of vesicular transport (Ireland *et al.*, 1994; Zhang *et al.*, 2003).

Although Arf itself is essential in yeast (Stearns *et al.*, 1990) none of the ArfGAPs that regulate Arf is individually essential, suggesting a level of functional redundancy among the ArfGAP proteins. Indeed, there are two essential pairs of ArfGAP proteins that function in distinct vesicular-transport pathways: one or the other of the Glo3 + Gcs1 pair is required for Golgi-to-ER retrograde transport (Poon *et al.*, 1999) and one or the other of the Age2 + Gcs1 pair is required for post-Golgi transport (Poon *et al.*, 2001). Our lab has created temperature-sensitive *GCS1* alleles encoding mutant forms of Gcs1 that display compromised function at 37°C, allowing us to study the Gcs1 transport pathways. When these mutant *GCS1* alleles are expressed in cells deleted for the Glo3 + Gcs1 or

Age2 + Gcs1 pair, the mutant versions of Gcs1 create cells that are conditionally impaired for growth at 37°C due to deficient ArfGAP function for Glo3-related retrograde transport or Age2-related post-Golgi transport, respectively.

My first objective was to further investigate genetic situations in which the overexpression of other yeast genes alleviate the temperature sensitivity of these ArfGAP-deficient cells. Overexpression of the *AGE1* gene, which encodes another ArfGAP protein, alleviates the deleterious effects of deficient Glo3 + Gcs1 and Age2 + Gcs1 ArfGAP activities (Auger, 2000; Lewis, 2004; Wong *et al.*, 2005; Benjamin *et al.*, 2011b). Furthermore, removal of the first 160 residues of Age1 improves the ability of Age1 (in this case, Age1ΔN) to alleviate the deficient Glo3 + Gcs1 situation (Lewis, 2004), suggesting that these N-terminal sequences inhibit Age1 activity for Golgi-to-ER retrograde transport. My findings show that removal of these N-terminal sequences also improves Age1 function for post-Golgi transport. An Age1 truncation analysis revealed that the first 80 amino acid residues of Age1 do not appreciably affect Age1 function in my assays, but that N-terminal sequences starting between residues 81-90 inhibit Age1 function at both the Golgi-to-ER retrograde transport and post-Golgi transport stages. I further showed that Age1 or Age1ΔN in increased abundance is able to functionally replace (bypass) Age2 + Gcs1, and that increased abundance of Age1ΔN can bypass Glo3 + Gcs1. I then looked at two other yeast genes, *GLO3* (encoding an ArfGAP) and *SFH2* (encoding a PITP) that, when overexpressed, alleviate the deleterious effects in cells deficient for Age2 + Gcs1 ArfGAP activity (Auger, 2000; Wong *et al.*, 2005), and found that in increased abundance Glo3 and Sfh2 could actually bypass the need for Age2 + Gcs1 completely.

Focusing my interest on the Sfh2 situation, I then found that Sfh2 requires Age1 for effective alleviation of the deleterious effects of defective Age2 + Gcs1 function. The ability of an increased abundance of Sfh2 to bypass the need for this essential ArfGAP pair may reflect Sfh2-mediated changes in lipid metabolism that allow endogenous Age1 to provide the ArfGAP activity required in the absence of Age2 and Gcs1. I propose that increased abundance of Sfh2 results in increased flux through an Sfh2-mediated phosphoinositide metabolic pathway that activates the phospholipase D activity of Spo14 and results in increased DAG and PA in the membrane, which in turn allows Age1 to

function in place of Age2 + Gcs1. Indeed, Spo14 is required for Age1 to effectively alleviate the deleterious effects of defective Age2 + Gcs1 function, and Dr. Pak Phi Poon used an *in vitro* assay to show that increased DAG concentrations and, to a lesser extent, increased PA concentrations, activate Age1 ArfGAP activity. Together, our results suggest that Age1 can provide ArfGAP function for post-Golgi and Golgi-to-ER transport, and that membrane lipid composition can regulate Age1 ArfGAP activity for post-Golgi transport.

My second objective was to further investigate the defects caused by absence of the founding member of the yeast ArfGAP family, Gcs1. A lack of Gcs1 function causes both cold sensitivity (the *gcs1*Δ reentry defect) and defective endocytic transport. Genetic screens for situations that alleviate the cold sensitivity of *gcs1*Δ cells showed that elimination of the Arl1 or the Ypt6 vesicle-tethering pathway at the *trans*-Golgi membrane (Drysdale, 2006), or increased expression of Imh1 (Wang *et al.*, 1996), an effector of the Arl1 pathway, alleviate *gcs1*Δ cold sensitivity. My findings show that these situations also alleviate the endocytic transport defect of *gcs1*Δ cells, and suggest that both of the impairments of *gcs1*Δ cells are caused by active but dysregulated Arl1. I found that elimination of the Arl1 pathway or the Ypt6 pathway impairs the activation and membrane localization of Arl1. In addition to functioning as an ArfGAP, Gcs1 also has Arl1GAP activity *in vitro* (Liu *et al.*, 2005); however, I found that a mutant version of Gcs1 that is deficient for both ArfGAP and Arl1GAP activity *in vitro* still allows reentry and endosomal transport, suggesting that the activity of Gcs1 that is required for these processes is independent of these GAP functions. I propose that, in the absence of this GAP-independent regulation by Gcs1, the resulting dysregulated Arl1 impairs reentry and endosomal transport. Elimination of the Arl1 or Ypt6 pathway alleviates these defects by blocking or minimizing the activation and recruitment of Arl1 to the membrane, thus preventing the accumulation of the problematic dysregulated Arl1.

Finally, I found that Imh1 is not required for the alleviation of *gcs1*Δ defects brought about by the absence of Arl1. However, increased expression of Imh1 does itself alleviate these defects, and does so through Arl1 binding. My results suggest that protein sequestration by active but dysregulated Arl1, which accumulates at the *trans*-Golgi

membrane in the absence of Gcs1, causes the *gcs1*Δ defects, and that Imh1 binding of Arl1 displaces the sequestered (yet-to-be-identified) protein, alleviating the defects.

5.2 N-Terminal Sequences in Age1 Inhibit Age1 Function

Increased abundance of Age1 alleviates the deleterious effects of deficient Glo3 + Gcs1 ArfGAP activity for Golgi-to-ER retrograde transport and deficient Age2 + Gcs1 ArfGAP activity for post-Golgi transport, restoring growth and effective transport to *glo3*Δ *gcs1-28* cells (Lewis, 2004), *age2*Δ *gcs1-3* cells (Auger, 2000), and *age2*Δ *gcs1-4* cells (Wong *et al.*, 2005; Benjamin *et al.*, 2011b). The ability of Age1 to function in these two transport pathways is consistent with previous observations involving Age1. Cells deleted for both *AGE1* and *GLO3* are temperature sensitive (Zhang *et al.*, 2003), while cells deleted for either gene alone are not (Zhang *et al.*, 2003), suggesting that Age1 and Glo3 share a functional overlap that most likely involves Golgi-to-ER retrograde transport where Glo3 is known to function (Poon *et al.*, 1999; Lewis *et al.*, 2004). Also, endocytic transport is delayed in cells deleted for *AGE1* in combination with the deletion of either *ARF1* or *AGE2* (Zhang *et al.*, 2003), suggesting that Age1 ArfGAP activity is also involved in post-Golgi transport, where Age2 is known to function (Poon *et al.*, 2001).

Unlike the other ArfGAP proteins in which the conserved ArfGAP domain is at the N terminus of the protein, Age1 has an N-terminal extension of approximately 185 residues that precedes the ArfGAP domain (Zhang *et al.*, 2003). Our lab has previously shown that an N-terminally truncated version of Age1 termed Age1ΔN (deleted for residues 3-166) provides more efficient alleviation of *glo3*Δ *gcs1-28* temperature sensitivity than does full-length Age1 (Lewis, 2004). I found that removal of these N-terminal residues of Age1 also improved the ability of Age1 to alleviate the temperature sensitivity of *age2*Δ *gcs1-4* cells. Thus, N-terminal sequences in Age1 inhibit the ability of Age1 to function in some aspects of vesicular transport. A similarly truncated Age1 protein retains ArfGAP activity *in vitro* (Zhang *et al.*, 2003) and, consistent with my findings, the N-terminal 160 residues of Age1 were suggested to negatively regulate or constrain Age1 ArfGAP activity and also to constrain Age1 function for suppression of Arf1-3 temperature sensitivity (Zhang *et al.*, 2003). My findings further refine our

understanding of this inhibitory segment of Age1, showing that the first 80 residues are not involved in the constraint of Age1 function, and that residues 81-90 are necessary to inhibit Age1 function in both transport pathways. Further experimentation is required to identify what segment of Age1 is sufficient for constraint of Age1 function, i.e. to define the C-terminal border of this inhibitory 'domain'.

The mechanism by which Age1 is constrained in its function is open to speculation. It has been suggested that the N-terminal segment may be involved in specific protein contacts (Zhang *et al.*, 2003). Protein interactions with the N-terminal segment of Age1 could restrict Age1 localization, or block other protein interactions that are required for optimal Age1 ArfGAP activity. It is also possible that this segment binds to Age1 itself (either in *cis* or in *trans*), inhibiting Age1 activity until some other interaction or signal releases the inhibition, thus spatially and/or temporally regulating Age1 activity. Indeed, domains within the functionally related Glo3 ArfGAP protein have intramolecular interactions that regulate Glo3 function (Schindler *et al.*, 2009). It is important to note that, although this N-terminal segment inhibits Age1 function in Glo3-related retrograde transport and in Age2-related post-Golgi transport, it may be important for the 'normal' function and regulation of endogenous Age1. In this regard, the N-terminal segment of Age1 may be more accurately thought of as a regulatory sequence that serves to spatially and/or temporally constrain Age1 activity rather than an inhibitory sequence that simply restricts Age1 activity with no regulatory function. Sequence analysis of the N-terminal region of Age1 (the first 180 residues) does not identify any similar segment in any other protein in *S. cerevisiae* or other closely related yeast species. Although closely related yeasts do have Age1-like ArfGAP proteins with extended N termini, there is very little conservation among the N-terminal segments of these proteins, while the ArfGAP domains and C-terminal sequences are highly conserved. The lack of conservation among the N-terminal extensions of these proteins suggests that the function of the N-terminal segments is not sequence specific, as it seems unlikely that the N terminus would be present in these proteins if it did not have an important function.

5.3 In Increased Abundance, ArfGAPs can Functionally Replace Essential ArfGAP Pairs

The ability of an ArfGAP in increased abundance to compensate for the absence of an essential ArfGAP pair (Age2 + Gcs1 or Glo3 + Gcs1) implies that the ArfGAP is able to provide all of the essential functions normally supplied by either member of the essential pair. I found that in increased abundance Age1 or Age1ΔN can functionally replace the Age2 + Gcs1 pair, and that Age1ΔN (but not Age1) can functionally replace the Glo3 + Gcs1 pair. The ability of Age1 to replace the Age2 + Gcs1 pair but not the Glo3 + Gcs1 pair suggests that Age1 is inherently more effective in functioning in the post-Golgi transport pathway compared to the Golgi-to-ER retrograde transport pathway. Perhaps the N-terminal sequences of Age1 that constrain function have a greater effect on Age1 function in Golgi-to-ER transport. Alternatively, the level of ArfGAP activity required for post-Golgi transport might be less than that required for Golgi-to-ER retrograde transport. Nonetheless, the absence of the N-terminal segment allows Age1ΔN to provide the essential functions normally supplied by each ArfGAP pair. Since Arf activity is essential in yeast (Stearns *et al.*, 1990), one function likely provided by Age1 and Age1ΔN is ArfGAP activity to regulate the GTPase cycle of Arf for Golgi-to-ER retrograde and post-Golgi transport. A function of Gcs1 and Glo3 that is independent of their GAP activity is the 'priming' of v-SNARE proteins to allow incorporation of the v-SNARE into a priming complex that initiates vesicle biogenesis, a process that ensures the incorporation of v-SNAREs into the nascent vesicles (Springer *et al.*, 1999; Rein *et al.*, 2002; Robinson *et al.*, 2006). In the absence of the proteins that normally carry out this v-SNARE priming activity, Age1 and Age1ΔN may be able to carry out this process, although whether this process is essential is not apparent. Thus, Age1 may support vesicular transport in the Golgi-to-ER retrograde and post-Golgi pathways by providing ArfGAP and ArfGAP-independent activities in the absence of the ArfGAP pairs that normally carry out these activities.

My results reveal that Age1 can provide ArfGAP-associated functions for vesicular transport at two distinct transport stages. I also confirmed that, in increased abundance, Glo3 can functionally replace the Age2 + Gcs1 ArfGAP pair for post-Golgi transport (Zhang *et al.*, 2003), indicating that, like Age1, Glo3 can carry out the essential

functions normally supplied by the Age2 + Gcs1 pair. Thus in increased abundance these ArfGAP proteins (Age1 and Glo3) can provide functions that they do not normally carry out at endogenous expression levels. Increased expression of Age1 and Glo3 may saturate the 'normal' binding sites for these proteins, allowing the excess protein to localize to compartments where Age1 and Glo3 do not normally localize and where ArfGAP activity is normally supplied by one or the other of the essential ArfGAP pairs they are functionally replacing. Increased expression may also provide the necessary levels of an interaction that is supplied less efficiently by the surrogate ArfGAP protein. The endogenous expression level of Age1 is the lowest of the four proteins with ArfGAP activity, 14-fold lower than Age2 and 24-fold lower than Gcs1 (Ghaemmaghami *et al.*, 2003), and deletion of *AGE1* on its own or in combination with deletion of the other ArfGAP genes has the least impact on the cell compared to single and double deletions of the other ArfGAP genes (Zhang *et al.*, 2003). With such a low level of expression and the lack of severe deletion phenotypes, it is hard to envision what the normal function of Age1 might be. My results with Age1 show that Age1 is capable of functioning in the post-Golgi and Golgi-to-ER retrograde transport pathways when overexpressed, but do not address the normal function or site of Age1 activity.

5.4 Sfh2 Bypass of the Essential Age2 + Gcs1 ArfGAP Pair Acts in Part Through Endogenously Expressed Levels of Age1

Our lab has previously shown that increased dosage of the *SFH2* gene, encoding a phosphatidylinositol transfer protein, alleviates the 37°C growth and transport defects caused by deficient ArfGAP activity in *age2*Δ *gcs1-4* cells (Wong *et al.*, 2005). A particularly informative finding in this thesis is that increased abundance of Sfh2 bypasses the requirement for the otherwise essential Age2 + Gcs1 pair. The previous interpretation regarding Sfh2 alleviation of *age2*Δ *gcs1-4* temperature sensitivity was that increased abundance of Sfh2 alleviates the *age2*Δ *gcs1-4* growth and transport defects by enhancing the activity of the enfeebled Gcs1-4 protein (Wong *et al.*, 2005). This conclusion arose from a plasmid-loss experiment in which *age2*Δ *gcs1*Δ double-mutant cells carrying *gcs1-4* on a low-copy plasmid and *SFH2* on a high-copy plasmid were grown under non-selective conditions and then assessed for maintenance of the plasmids.

Despite being grown in medium that did not select for the *gcs1*-4 plasmid, *age2*Δ *gcs1*Δ double-mutant cells that had spontaneously lost the *gcs1-4* plasmid and were now being kept alive by increased *SFH2* gene dosage were never recovered (Wong, 2005). I used a different approach (tetrad dissection) to obtain *age2*Δ *gcs1*Δ double-mutant cells being kept alive by increased *SFH2* gene dosage. The small sizes of the colonies formed by these *age2*Δ *gcs1*Δ [*SFH2*] cells suggest that, although the cells are alive, they are significantly impaired for growth and would likely be out-competed by *age2*Δ *gcs1*Δ [*gcs1-4*] [*SFH2*] cells if co-cultured, consistent with the failure to obtain *age2*Δ *gcs1*Δ [*SFH2*] cells through the plasmid-loss procedure. The viability of *age2*Δ *gcs1*Δ [*SFH2*] cells clearly demonstrates that the enfeebled Gcs1-4 protein is not required for Sfh2-mediated bypass of the essential Age2 + Gcs1 pair.

Age1 is required for Sfh2 to effectively alleviate the lethality of the *age2*Δ *gcs1*Δ combination, indicating that Sfh2 bypass functions, in part, through Age1. This requirement for Age1 suggests an *in vivo* function for endogenous levels of Age1, presumably to provide the ArfGAP activity required for post-Golgi transport in the absence of the essential Age2 + Gcs1 pair. It is important to note, however, that this finding still does not address the normal function or site of Age1 activity, but rather identifies a function that endogenous Age1 can provide when Sfh2 is overexpressed, and which is required in the absence of Age2 + Gcs1.

Although *age2*Δ *gcs1*Δ [*SFH2*] cells (with Age1) grow significantly better than *age2*Δ *gcs1*Δ *age1*Δ [*SFH2*] cells (without Age1), the elimination of Age1 does not completely abolish Sfh2-mediated alleviation of the lethality of *age2*Δ *gcs1*Δ double-mutant cells. The viability but impaired growth of *age2*Δ *gcs1*Δ *age1*Δ [*SFH2*] cells compared to *age2*Δ *gcs1*Δ [*SFH2*] cells suggests that the Sfh2-mediated bypass of *age2*Δ *gcs1*Δ lethality does not function exclusively through Age1. Thus, Sfh2 bypass may also function through Glo3, the last remaining protein in these cells known to have ArfGAP activity. Indeed, in increased abundance both Age1 and Glo3 are able to provide the essential ArfGAP activity that is required for post-Golgi transport in the absence of Age2 and Gcs1. The contribution of Glo3 to Sfh2-mediated bypass of the Age2 + Gcs1 pair is difficult to assess because the elimination of Glo3 from *age2*Δ *gcs1*Δ [*SFH2*] cells would

likely result in lethality due to the combined deletion of the *GCS1* and *GLO3* genes (Poon *et al.*, 1999), which is not alleviated by increased expression of *SFH2* (Wong *et al.*, 2005). For this reason Glo3 involvement was not tested. However, I suspect that, like Age1, Glo3 is also involved in Sfh2-mediated bypass of the Age2 + Gcs1 pair.

5.5 Increased Flux Through an Sfh2-Mediated Phosphoinositide Metabolic Pathway Activates Phospholipase D and Bypasses the Essential Age2 + Gcs1 ArfGAP Pair

Endogenous levels of Age1 and Glo3 can not maintain post-Golgi transport or cell viability in the absence of Age2 and Gcs1. How does an increased abundance of Sfh2 enable these ArfGAP proteins to functionally replace the essential Age2 + Gcs1 pair? Increased abundance of Sfh2 increases the levels of PI(4)P and $PI(4,5)P_2$, which activate the phospholipase D enzyme activity of Spo14 (Routt *et al.*, 2005), and our lab showed that Spo14 is required for Sfh2-mediated alleviation of the *age2*Δ *gcs1-4* temperature-sensitive growth defect (Wong *et al.*, 2005). Increased Spo14 activity results in increased levels of PA and DAG, and exogenous DAG, which increases the intracellular levels of DAG (Henneberry *et al.*, 2001), also alleviates *age2*Δ *gcs1-4* temperature sensitivity (Wong *et al.*, 2005). Furthermore, the *in vitro* ArfGAP activities of Age2, Gcs1, and the rat Gcs1 orthologue ArfGAP1 are stimulated by DAG and PA (Antonny *et al.*, 1997; Yanagisawa *et al.*, 2002). A model that arises from these results is that increased abundance of Sfh2 activates Spo14, resulting in membrane lipid modifications that activate the ArfGAP activity of Age1 (and perhaps also Glo3), allowing these proteins at endogenous levels to functionally replace the essential Age2 + Gcs1 pair. Indeed, our results show that increased levels of DAG and PA stimulate the *in vitro* ArfGAP activity of Age1 (as further discussed in the following section), and I have found that Spo14 is required for effective Age1-mediated alleviation of the *age2*Δ *gcs1-4* temperature sensitivity.

The Sfh2-mediated activation of Spo14 is known to function through increased delivery of substrates by Sfh2 activity to the PI kinases Stt4 and Mss4. Activity of these kinases results in augmented production of $PI(4,5)P_2$, which is required to activate Spo14 (Routt *et al.*, 2005). Increased dosage of the *MSS4* gene, encoding the only PI(4)P 5-kinase in yeast, results in increased levels of $PI(4,5)P_2$ (Desrivieres *et al.*, 1998), which

should translate into increased Spo14 activity. Despite our previous result that increased *SPO14* gene dosage alleviates *age2*Δ *gcs1-4* temperature sensitivity (Wong *et al.*, 2005), I found that increased PI-kinase and *SPO14* gene dosage actually fails to alleviate the *age2*Δ *gcs1-4* temperature sensitivity. I followed up on this contradictory finding and found that the high-copy *SPO14* plasmid that was previously used by our lab does not in fact contain *SPO14*. Growth of the *age2*Δ *gcs1-4* cells carrying this plasmid was therefore most likely due to a second-site suppressor mutation that arose in the transformed strain. In any case, my findings suggest that increased flux through the Sfh2-mediated phosphoinositide metabolic pathway alleviates the temperature sensitivity of *age2*Δ *gcs1-4* cells. In contrast, increased activity of downstream components of the Sfh2-mediated pathway does not cause such alleviation. A possible explanation for the lack of alleviation by increased kinase activity is that the rate-limiting step in the pathway leading to Spo14 activation is substrate delivery by Sfh2. As such, increasing the abundance of downstream components in the pathway may not be effective without an increased availability of substrate. Alternatively, localization of the activated Spo14 may be important. Perhaps Sfh2-mediated activation of Spo14 localizes activated Spo14 to membrane domains where the downstream activation of Age1 is required, allowing Age1 to replace Age2 + Gcs1 function for post-Golgi transport, whereas increasing the downstream components of the pathway may not provide this localization.

5.6 Phospholipase-D-Mediated Membrane Lipid Remodelling Activates Age1 ArfGAP Activity

As the sole phospholipase D enzyme in yeast, Spo14 catalyzes the hydrolysis of PC to produce PA, which is then further hydrolysed to produce DAG. The substrate of Spo14 and the most abundant phospholipid in yeast, PC, inhibits the ArfGAP activity of Gcs1, while PA and DAG, the products of Spo14, activate the ArfGAP activity of Gcs1 and Age2 (Antonny *et al.*, 1997; Yanagisawa *et al.*, 2002). We have previously shown that Spo14 is required for Sfh2 alleviation of *age2*Δ *gcs1-4* temperature sensitivity (Wong *et al.*, 2005), which I have shown functions in part through endogenous Age1. I have also found that Spo14 is required for Age1 to effectively alleviate the temperature sensitivity of *age2*Δ *gcs1-4* cells. These requirements for Spo14 are explained by the finding that the

products of Spo14 activity, DAG and PA, activate ArfGAP activity of Age1 (Benjamin *et al.*, 2011b). Thus, increased Spo14 activity produces increased levels of DAG and PA which activate the ArfGAP activity of the endogenous Age1 protein, allowing it to function in place of the Age2 + Gcs1 pair.

How do DAG and PA activate the ArfGAP activity of Age1? For Gcs1, increased DAG activates ArfGAP activity by spatially and temporally regulating Gcs1 (Antonny *et al.*, 2005). The ALPS motif in Gcs1 recruits Gcs1 to membranes with high curvature (Bigay *et al.*, 2005) and is the feature of Gcs1 that is responsible for this regulation through localization. Highly curved membranes are created in the process of vesicle budding, and ArfGAPs are a required component of the vesicle budding machinery (Springer *et al.*, 1999; Lewis *et al.*, 2004). Additionally, Arf, another key component of the vesicle budding machinery and the substrate of GAP activity, is itself an activator of Spo14 activity (Brown *et al.*, 1993; Cockcroft *et al.*, 1994), and the DAG and PA produced by Spo14 contribute to membrane curvature (Corda *et al.*, 2002). Thus, the ALPS motif in Gcs1 recruits Gcs1 to highly curved membranes where nascent transport vesicles are being formed and that are enriched in Arf and the products of Spo14 activity (DAG and PA). Activation of the ArfGAP activity of Gcs1 by DAG and PA may simply be a matter of regulating the localization of Gcs1 to membranes enriched in activated Arf, providing spatial and temporal regulation of Gcs1 ArfGAP activity. Although Age1 lacks an obvious ALPS motif (Drin *et al.*, 2007), the involvement of Spo14 and DAG in Age1 function suggests that Age1 may also be recruited to membranes with high curvature. Consistent with the ability of Age1 to functionally replace the Age2 + Gcs1 ArfGAP pair for post-Golgi transport, I found that Age1-GFP was localized to Golgi and endosomal compartments in wild-type and *age2*Δ *gcs1-4* cells. However, deletion of *SPO14* did not alter this localization; thus Spo14 may not be required for Age1-GFP localization to Golgi and endosomal compartments in general. It is therefore possible that Spo14 affects Age1 localization to microdomains within these compartments that are below the resolution of fluorescence microscopy. Alternatively, DAG and PA may activate the ArfGAP activity of Age1 in a manner that does not involve regulating Age1 localization.

5.7 Gcs1 is Required for Cell-Cycle Reentry and Endocytic Transport in the Cold

Our lab has previously shown that yeast cells lacking the Gcs1 protein are defective for cell-cycle reentry from stationary phase and display defective endocytic transport in the cold (Drebot *et al.*, 1987; Ireland *et al.*, 1994; Wang *et al.*, 1996). My results have advanced our understanding of the molecular conditions that impose these *gcs1*Δ defects. Although Gcs1 has GAP activity for the small G-proteins Arl1 and Arf1 *in vitro* (Poon *et al.*, 1996; Liu *et al.*, 2005), my results suggest that the Gcs1 activity required for cell-cycle reentry and endocytic transport in the cold is independent of these GAP activities. I therefore propose that in the absence of this GAP-independent regulation normally provided by Gcs1, active but dysregulated Arl1 accumulates at the *trans*-Golgi membrane, and that this dysregulated Arl1 is the cause of the characteristic defects of *gcs1*Δ cells. I imagine that the cold-induced nature of these defects is the combined result of dysregulated Arl1 and decreased membrane fluidity that results in the cold. In contrast, dysregulated Arl1 is tolerated at normal growth temperatures, where membrane fluidity does not impose additional stress. Furthermore, dysregulated Arl1 is specifically detrimental during the developmental transition from stationary phase to active mitotic growth (reentry). My results do not address the differences in the processes of reentry and continued cell proliferation that cause dysregulated Arl1 to only be detrimental during the reentry process. However, the transport pathways that are defective in the absence of Gcs1 and restored under all conditions that alleviate the reentry defect mediate the movement and localization of a wide variety of proteins (and lipids) within the cell and play important roles in signalling (Scita and Di Fiore, 2010). It is therefore possible that these transport and signalling pathways are required to remodel membranes and constituents of organelles as the cell completes the developmental transition between the non-proliferating stationary-phase state and active cell proliferation, but these remodelling events are no longer required once cell proliferation has been initiated.

5.8 A GAP-Independent Function of Gcs1 is Required for Cell-Cycle Reentry and Endocytic Transport in the Cold

Gcs1 is not the first example of an ArfGAP protein that provides a GAP-independent function that is only required under special circumstances. Our lab has shown that the

Glo3 ArfGAP protein regulates Golgi-to-ER retrograde transport and, like Gcs1, is essential for growth in the cold: *glo3*Δ cells are cold sensitive (Poon *et al.*, 1999). We have further shown that the GAP activity of Glo3 is dispensable for growth in the cold; a central 162-residue portion of Glo3 lacking the conserved GAP domain is sufficient to alleviate *glo3*Δ cold sensitivity (Schindler *et al.*, 2009). This segment of Glo3, which also lacks a conserved C-terminal regulatory domain, mediates several protein interactions (Schindler *et al.*, 2009). The function provided by the central region of Glo3 that is essential for growth in the cold appears to be as a scaffold for these protein interactions.

Like the Glo3 protein, it is possible that a central region of Gcs1 is sufficient to provide the essential GAP-independent function required for cell-cycle reentry and endocytic transport in the cold. Indeed, my data show that the C terminus of Gcs1 beyond residue 162 is dispensable for these processes. This severe truncation removes over half of the protein and yet the 162 residues of the Gcs1 N terminus that remain allow growth under restrictive conditions that is comparable to the growth provided by full-length Gcs1. Within the N-terminal 162 residues of Gcs1 that are sufficient to provide the essential GAP-independent Gcs1 function, the conserved ArfGAP domain makes up 120 residues (residues 8-129). I have no data that indicate whether the N-terminal GAP domain of Gcs1 is dispensable for the processes at issue here, but my data do indicate that the GAP activities provided by this domain are dispensable. It is therefore possible that the GAP domain of Gcs1 could be completely dispensable and that a central region of Gcs1 is sufficient to provide the essential GAP-independent function of Gcs1. Further truncations are needed to determine the minimal region of Gcs1 required to alleviate *gcs1*Δ cold sensitivity.

Also like the Glo3 situation, the GAP-independent function of Gcs1 may be a scaffolding function involved in protein-protein interactions. Another GAP-independent function provided by ArfGAP proteins in yeast that was already mentioned above is the v-SNARE priming function of Gcs1 and Glo3. This GAP-independent priming activity induces conformational changes in v-SNARE proteins that are required for the SNARE proteins to interact with Arf1 and coatomer facilitating their incorporation into nascent vesicles (Springer *et al.*, 1999; Rein *et al.*, 2002; Robinson *et al.*, 2006). Gcs1 (and GAPs like Gcs1) clearly can provide important GAP-independent functions. Further

experimentation is required to identify the non-GAP activity of Gcs1 that is required for cell-cycle reentry and endocytic transport in the cold.

The GAP-independent function of Gcs1 that is required for reentry may be Arl1 binding. Consistent with this hypothesis, Gcs1 binds Arl1 in a yeast two-hybrid assay, and the C-terminal 125 residues of Gcs1 containing most of the ALPS motif which is dispensable for alleviating *gcs1*Δ reentry are also dispensable for this interaction with Arl1 (Liu *et al.*, 2005). The N-terminal 71 residues of Gcs1 were also assessed for the ability to bind Arl1 in a yeast two-hybrid assay and failed to do so (Liu *et al.*, 2005). This truncation may also fail to provide reentry function, but no truncations of Gcs1 comparable to this truncation have yet been tested for reentry. In addition to interacting in a yeast two-hybrid assay, Gcs1 and Arl1 were shown to interact directly in an *in vitro* binding assay, and endogenous Gcs1 co-purified with GST-tagged Arl1 when GST-Arl1 was purified from yeast cells expressing this fusion protein (Liu *et al.*, 2005). Once the minimal region of Gcs1 that provides reentry function is identified through truncation analysis, determining the correlation between Gcs1 truncations that provide reentry function and are able to bind Arl1 may shed light on the role that Arl binding by Gcs1 may play to facilitate reentry in the cold.

Arl1 binding as the reentry function of Gcs1 also fits the model that dysregulated Arl1 causes the reentry defect by protein sequestration (this model is further discussed later). If Arl1 binding is the GAP-independent mechanism by which Gcs1 regulates Arl1, then Gcs1 binding of Arl1 could block the proposed sequestration interaction that causes the *gcs1*Δ reentry defect. In the absence of Gcs1 binding, Arl1 would be free to sequester the factor and impose the reentry defect.

5.9 The Other ArfGAP Proteins in Yeast Do Not Efficiently Provide the GAP-Independent Gcs1 Reentry Function

Whatever the GAP-independent function of Gcs1 is, it is not efficiently provided by the other ArfGAP proteins in yeast. Increased abundance of Glo3, Age1, or Age2 does not effectively alleviate *gcs1*Δ cold sensitivity, indicating that these ArfGAP proteins do not provide the GAP-independent activity required for reentry in the cold. Consistent with the hypothesis that the GAP-independent reentry function of Gcs1 is Arl1 binding, all six

yeast ArfGAP proteins were assessed for the ability to bind Arl1 in a yeast two-hybrid assay and only Gcs1 was able to do so (Liu *et al.*, 2005). I also tested an N-terminally truncated version of Age1, Age1ΔN, for alleviation of *gcs1*Δ cold sensitivity to assess whether the N terminus of Age1 inhibits its ability to supply the GAP-independent reentry function, because the Age1 N terminus does inhibit other Age1 functions (Zhang *et al.*, 2003; Benjamin *et al.*, 2011b; see above). However, even with the N terminus removed, Age1 still failed to alleviate *gcs1*Δ cold sensitivity, ruling out inhibition of the reentry function by the Age1 N terminus.

Overexpression of the Age2 ArfGAP did not effectively alleviate *gcs1*Δ cold sensitivity, but after prolonged incubation, cells overexpressing Age2 consistently exhibited a minimal level of growth that was not seen in the *gcs1*Δ control cells, or with the overexpression of the other ArfGAP proteins. Thus, Age2 may provide the GAP-independent function of Gcs1 required for reentry in the cold, albeit at a diminished level compared to Gcs1. Alternatively, the increased abundance of Age2 might alleviate *gcs1*Δ cold sensitivity in a manner that is different from, and less effective than, the GAP-independent function of Gcs1. Age2 and Gcs1 provide essential overlapping function required for transport from the *trans*-Golgi membrane (Poon *et al.*, 2001); thus Age2 is potentially localized to the same membranes as Arl1 and functions in transport pathways that are either the same as, or overlap with, the transport pathways in which Arl1 functions. One could imagine that the overexpression of Age2 could alleviate *gcs1*Δ cold sensitivity in a manner that is different from the GAP-independent activity provided by Gcs1, by somehow affecting these overlapping transport pathways. The lower level of growth provided by the overexpression of Age2 compared to other alleviating situations could be indicative of this alternate alleviation route being less efficient. Once more is known about the nature of the GAP-independent function provided by Gcs1, the ability of Age2 to provide this function can be assessed more directly.

5.10 Dysregulated Arl1 Imposes the *gcs1*Δ Reentry and Endocytic Transport Defects

A previous screen in our lab identified gene deletion mutations that alleviate the cold sensitivity of *gcs1*Δ cells (Drysdale, 2006; Table 4.1). Among these alleviating gene deletions are several that eliminate components of the Arl1 and Ypt6 pathways, which

function in vesicle tethering at the *trans*-Golgi membrane. Furthermore, the *arl1*Δ and *ypt6*Δ deletion mutations also alleviate the endocytic transport defect of *gcs1*Δ cells. Thus, the Arl1 and Ypt6 pathways are both implicated in the reentry and transport defects caused by the absence of Gcs1. Each component of the Arl1 pathway is required to recruit activated Arl1 to the *trans*-Golgi membrane (Panic *et al.*, 2003b; Setty *et al.*, 2003; Behnia *et al.*, 2004; Setty *et al.*, 2004), and I have shown that the Ypt6 pathway is also required to recruit activated Arl1 to the *trans*-Golgi membrane. These results suggest that the Arl1 and Ypt6 pathways impose the *gcs1*Δ reentry and transport defects through a common mechanism involving activated, membrane-bound Arl1.

Two vesicle-tethering factors, Imh1 and the multi-subunit GARP complex, are known effectors of the Arl1 and Ypt6 pathways, respectively (Panic *et al.*, 2003b; Setty *et al.*, 2003). The GARP complex also binds Arl1 through a direct interaction with the Vps53 GARP subunit (Panic *et al.*, 2003b), although GARP has not been further characterized as an effector of the Arl1 pathway. The ability of GARP to bind both Arl1 and Ypt6 at the *trans*-Golgi membrane introduces the potential for cross-talk between these two pathways. Cross-talk between these two pathways has been suggested in mammalian cells, where Arl1 and the Ypt6 homologue Rab6 were found to cooperate in binding and localizing the GRIP-domain golgin GCC185 to the *trans*-Golgi network (Burguete *et al.*, 2008), although whether Arl1 and Rab6 actually cooperate in the binding of GCC185 is controversial (Houghton *et al.*, 2009). Despite the potential for cross-talk, the Arl1 and Ypt6 pathways are considered to function in parallel at the *trans*-Golgi membrane in yeast. Therefore, my finding that the Ypt6 pathway affects the activation and Golgi localization of Arl1 was unexpected. My findings further explain this effect on Arl1 localization by showing that activated Ypt6 is required for the localization of Sys1 to the *trans*-Golgi membrane. Lack of activated Ypt6, due to elimination of the Ypt6 GEF Ric1–Rgp1 or elimination of Ypt6 itself, results in the mislocalization of Sys1 and this leads to the mislocalization of downstream components in the Arl1 pathway, namely Arl1 and Imh1.

In contrast, the Arl1 pathway does not affect the activation and Golgi localization of Ypt6 or recruitment of the GARP complex to the membrane through Ypt6 binding. Unlike the elimination of Ypt6, which results in the mislocalization of GARP subunit

Vps54-GFP, indicating the mislocalization of GARP, the elimination of Arl1 or Sys1 has no effect on the membrane localization of GARP, as indicated by the punctate localization of Vps54-GFP in *arl1*Δ and *sys1*Δ cells (Panic *et al.*, 2003b; data not shown). These results suggest that Ypt6 is sufficient for the localization of GARP to the *trans*-Golgi membrane, and that Arl1 is not needed.

Genetic interactions between gene deletions in the Arl1 and Ypt6 pathways suggest that vesicle tethering at the *trans*-Golgi membrane is essential and can be provided by either of these two pathways (Setty *et al.*, 2003; Tong *et al.*, 2004). Consistent with these published findings, I have shown that deletion of *YPT6* is lethal in combination with deletion of *ARL1* or *IMH1*; furthermore, deletion of *YPT6* is also lethal in combination with deletion of *ARL3* and *SYS1* (Setty *et al.*, 2003; Tong *et al.*, 2004). These results suggest that in the absence of Ypt6, activated Arl1 is required for cell viability. Therefore, even though I did not observe a punctate localization of Arl1-GFP in the absence of Ypt6, some Arl1 must be activated and properly localized in *ypt6*Δ cells; otherwise, they would be dead. Cells lacking Ypt6 did display some punctate localization of Sys1-GFP and GFP-Imh1, which may correspond to a small amount of these proteins that is properly localized in *ypt6*Δ cells. The fact that some Arl1 remains properly localized in the absence of Ypt6 raises the idea of a threshold amount of dysregulated Arl1 that is required to impose the *gcs1*Δ defects. Decreasing the amount of dysregulated Arl1 at the membrane below this threshold may alleviate the *gcs1*Δ defects, as seen in *ypt6*Δ cells. Likewise, the alleviation that I saw with elimination of Syt1, a GEF for Arl1, also speaks to a threshold amount of dysregulated Arl1 required to impose the *gcs1*Δ defects. In *syt1*Δ cells GFP-Imh1 is properly localized, suggesting that a certain amount of Arl1 remains properly localized in these cells, and yet the elimination of Syt1 alleviates *gcs1*Δ cold sensitivity. These results suggest that accumulation of dysregulated Arl1 above a threshold amount is required to cause the *gcs1*Δ defects, whereas a certain amount of dysregulated Arl1, below this threshold, is tolerated. This argument is also consistent with the reentry defect only being manifested in the cold, a condition that may impose additional stress on transport and reveal the *gcs1*Δ defect.

The mechanism by which Ypt6 contributes to Sys1 localization is open to speculation. To maintain residence at the *trans*-Golgi membrane Sys1 must either be

retained by mechanisms that exclude Sys1 incorporation into transport vesicles and/or Sys1 that is incorporated into transport vesicles is recycled back to the *trans*-Golgi membrane. The Ypt6 pathway is required for the localization of *trans*-Golgi membrane proteins through the latter mechanism, so that Golgi-resident proteins that have left the Golgi are retrieved from endosomal compartments through Ypt6-dependent retrograde transport (Tsukada and Gallwitz, 1996; Siniossoglou *et al.*, 2000; Bensen *et al.*, 2001). It is therefore likely that Sys1 is mislocalized in the absence of Ypt6 because it is not properly recycled back to the *trans*-Golgi membrane from endosomal compartments. The fact that *ypt6*Δ cells are viable suggests that, despite being mislocalized in the absence of Ypt6, there is sufficient Sys1 function to maintain viability (as discussed above). This Sys1 function may be provided by newly made Sys1 that is being delivered to the *trans*-Golgi membrane from the ER and *cis*-Golgi. Indeed, increased abundance of members of the Arl1 pathway, including Sys1, Arl1, and Imh1, alleviates the temperature sensitivity caused by the absence of Ypt6 (Tsukada and Gallwitz, 1996; Bensen *et al.*, 2001). This alleviation suggests that decreased Arl1 pathway function in the absence of Ypt6 is not sufficient to maintain viability at increased temperatures, but overexpression of proteins in the Arl1 pathway increases Arl1-pathway function to a level sufficient for viability at the higher temperature.

5.11 Sequestration of Some Factor by Dysregulated Arl1 Imposes the *gcs1*Δ Reentry and Endocytic Transport Defects

Our lab previously found that overexpression of Imh1, an effector of the Arl1 pathway, alleviates the cold-sensitive *gcs1*Δ reentry defect (Wang, 1996). This result is difficult to reconcile with my finding that diminution (or elimination) of activated Arl1 also alleviates *gcs1*Δ cold sensitivity, because the two results, at least initially, seem to be contradictory. Decreased Arl1 activation decreases Arl1 pathway activity, whereas one would expect that increased expression of Imh1, an effector of the Arl1 pathway, would have the opposite effect and result in increased Arl1 pathway activity. A simple resolution to this apparent contradiction is the model proposed above in which cytoplasmic Imh1 alleviates *gcs1*Δ cold sensitivity. This model fits all of the alleviating conditions at issue here, because elimination of the Arl1 and Ypt6 pathways results in the

cytoplasmic localization of Imh1 and increased expression of Imh1 should saturate any available Arl1 binding sites and also result in increased cytoplasmic Imh1. However, my findings, including the finding that Imh1 is actually not required for *arl1*Δ-mediated alleviation, led to the rejection of this model.

My finding that increased expression of only the GRIP domain of Imh1 alleviates *gcs1*Δ cold sensitivity suggests that Arl1 binding by Imh1 is sufficient for alleviation, and the normal functions of full-length Imh1 are dispensable. Moreover, the failure of a point-mutant form of Imh1 that is defective in Arl1 binding to alleviate *gcs1*Δ cold sensitivity suggests that Arl1 binding is necessary for Imh1-mediated alleviation of *gcs1*Δ cold sensitivity, and further demonstrates that the non-Arl1-binding functions of Imh1 are dispensable. These results led to the model that active but dysregulated Arl1 sequesters some cellular factor causing the gcs1Δ reentry and transport defects, and that increased abundance of Imh1 alleviates these defects by displacing the sequestered factor through competition for Arl1 binding sites. The GAP-independent function provided by Gcs1 would therefore minimize, either directly or indirectly, Arl1 binding by this factor. A model for how Gcs1 could directly regulate Arl1 binding by this factor was proposed above: the GAP-independent Gcs1 function may be Arl1 binding, which blocks Arl1 from interacting with the sequestered factor. In the absence of Gcs1 binding, Arl1 is available to sequester the factor, which then causes the *gcs1*Δ defects. Elimination of the Arl1 or Ypt6 pathway alleviates the *gcs1*Δ defects by decreasing Arl1 sequestration of this factor, either by eliminating Arl1 completely in the case of the *arl1*Δ deletion mutation, or by minimizing the amount of activated Arl1 available at the membrane in the case of the other Arl1 and Ypt6 pathway deletions. The sequestered factor may normally provide functions that are required for reentry and endocytic transport; in this case, sequestration by Arl1 restricts the factor from providing these functions (restricted-function model). Alternatively, the sequestered factor may be toxic to reentry and endocytic transport when complexed with Arl1 (toxic-complex model). Identification of the sequestered factor may be required to distinguish between these two alternatives.

From these two possibilities come predictions about the factor sequestered by Arl1. If the factor is a protein that provides a function required for reentry, then overexpression of the protein should alleviate the *gcs1*Δ reentry defect by saturating the

dysregulated-Arl1 binding sites, providing excess unsequestered protein to carry out the required functions. In this way a screen for genes that alleviate *gcs1*Δ cold sensitivity when overexpressed may identify the gene encoding such a protein. Indeed, our lab has already carried out such a screen (Wang, 1996), which in addition to identifying increased expression of *IMH1*, also identified increased expression of *YCK2, YCK3, YPT31,* and *YPT32* (Wang *et al.*, 1996; Zhang *et al.*, 2002). Thus, the proteins encoded by each of these genes are candidates for the factor sequestered by dysregulated Arl1. Also, this screen was most likely not comprehensive in identifying all genes that when overexpressed alleviate *gcs1*Δ cold sensitivity, so there are undoubtedly other proteins that remain to be identified. An additional prediction is that elimination of this protein required for reentry (provided that it is non-essential) should recapitulate the *gcs1*Δ reentry phenotype.

In the alternative scenario, if the factor sequestered by Arl1 is a protein that results in toxicity when complexed with dysregulated Arl1, then elimination of the protein should alleviate the *gcs1*Δ reentry defects by eliminating formation of the complex. Therefore, this factor may be encoded by one of the genes in the list of alleviating gene deletions (Table 4.3), providing many possible candidates. If, however, an essential gene encodes the sequestered factor, then its deletion would not likely alleviate the *gcs1*Δ defects, because cells deleted for any essential gene would not likely be viable.

5.12 Candidates for the Factor Sequestered by Dysregulated Arl1

Arl1-binding proteins are prime candidates for the factor sequestered by dysregulated Arl1. Several Arl1-binding proteins have been identified in both yeast and mammalian cells. In mammalian cells, four GRIP-domain proteins (golgin-245/p230, golgin-97, GCC88, GCC185) have been reported to bind Arl1 (Lu and Hong, 2003; Panic *et al.*, 2003a), although Arl1 binding by GCC88 and GCC185 is controversial (Derby *et al.*, 2004; Burguete *et al.*, 2008; Houghton *et al.*, 2009). The only known GRIP-domain protein in yeast is Imh1, which is an Arl1-binding protein but is not the sequestered factor. If Imh1 were the sequestered factor in the restricted-function model, then Imh1 would be expected to be required for *arl1*Δ alleviation of the *gcs1*Δ defects; however,

Imh1 is dispensable for *arl1*Δ-mediated alleviation (*gcs1*Δ *arl1*Δ *imh1*Δ triple-mutant cells reenter the cell cycle and form colonies in the cold). If Imh1 were the sequestered factor in the toxic-complex model, then deletion of *IMH1* would be expected to alleviate the *gcs1*Δ defects; however, deletion of *IMH1* does not affect the impairment of *gcs1*Δ cells (*gcs1*Δ *imh1*Δ double-mutant cells remain cold sensitive). Other Arl1-binding proteins that do not contain a GRIP domain have been identified in mammalian cells (Munro, 2005). However, only one of these proteins, termed SCOCO (short coiled-coil protein of unknown function), has a homologue in yeast, and the yeast homologue, termed Slo1 (SCOCO-like ORF), is not an Arl1-binding protein; Slo1 binds Arl3 but not Arl1 in an *in vitro* binding assay (Panic *et al.*, 2003b).

In addition to Imh1, I have investigated the possibility that the GARP tethering complex is the factor sequestered by dysregulated Arl1. GARP binds activated Arl1 *via* the Arl1-binding Vps53 subunit (Panic *et al.*, 2003b). Assessing GARP as the factor sequestered by dysregulated Arl1 is complicated by the fact that GARP has four protein subunits, Vps51, Vps52, Vps53, and Vps54 (Conibear *et al.*, 2003), which makes overexpressing the complex difficult. My analysis of GARP was limited to assessing the effects of deleting each of the four genes encoding GARP subunits individually in different genetic contexts and to the individual overexpression of the genes encoding the Vps53 and Vps54 subunits in *gcs1*Δ cells. My findings suggest that GARP is not required for reentry, which would eliminate GARP as the factor sequestered by dysregulated Arl1 in the restricted-function model. Each of the genes encoding subunits of GARP can be deleted without impairing cell-cycle reentry, and neither Vps53 nor Vps51 are required for *arl1*Δ alleviation of *gcs1*Δ cold sensitivity (*gcs1*Δ *arl1*Δ *vps53*Δ and *gcs1*Δ *arl1*Δ *vps51*Δ triple-mutant cells reenter the cell cycle and form colonies in the cold). Assessing GARP as the sequestered factor in the toxic-complex model proved to be no test. If GARP were the sequestered factor in the toxic-complex model, then elimination of GARP would be expected to alleviate the *gcs1*Δ defects; however, the deletion of *GCS1* is lethal in combination with deletion of each gene encoding a subunit of GARP, prohibiting the assessment of reentry in the double-mutant cells. Given the viability of *gcs1*Δ *arl1*Δ *vps53*Δ and *gcs1*Δ *arl1*Δ *vps51*Δ triple-mutant cells, the lethality of the double-mutant cells reveals complex interactions that remain to be fully characterized.

Deletion of any of the genes encoding GARP subunits is tolerated in *gcs1*Δ cells only if *ARL1* is deleted, suggesting that dysregulated Arl1 causes GARP function to be essential and arguing against the formation of a toxic GARP-Arl1 complex.

A few additional Arl1-binding proteins have been identified in yeast (Table 5.1). Three of these that are potentially interesting are Nse5, Pho85, and Tpk1, because these proteins function in cell-cycle arrest or cell-cycle progression in response to nutrients, and therefore it is easy to imagine how aberrant regulation of their function caused by abnormal binding by dysregulated Arl1 could cause the *gcs1*Δ reentry defect. Other than Imh1 and Vps53, none of the Arl1-binding proteins in Table 5.1 have been pursued in this context. I have, however, shown that deletion of *SYT1* alleviates *gcs1*Δ cold sensitivity, and based on this result it is possible that Arl1 binding by Syt1 forms a complex that is toxic to reentry; however, due to the finding that Syt1 has Arl1GEF activity (Chen *et al.*, 2010), it seems more likely that *syt1*Δ-mediated alleviation functions through decreased activation of Arl1. Further investigation is required to identify the proposed factor that inhibits growth and endocytic transport in the cold when sequestered by dysregulated Arl1.

5.13 Arginine 54 in Gcs1 is Required for Arf and Arl1GAP Activity

The ArfGAP Gcs1 is one of only a few proteins that display dual-specificity GAP activity, and the only yeast protein known to have Arl1GAP activity. Our findings indicate that these two G-proteins (Arf and Arl1) have similar requirements for GAP activity. The conserved ArfGAP domain of Gcs1 contains a cysteine-rich zinc-finger motif and a conserved arginine residue with characteristic spacing ($CxxCx_{16}CxxCx_4R$) that are required for ArfGAP activity (Kahn *et al.*, 2008). The conserved arginine (R54) is proposed to have a catalytic role, providing an arginine side-chain in the active site of Arf to stabilize the GTP-hydrolysis transition state (Kahn *et al.*, 2008). Indeed, substituting the conserved arginine (R54) in Gcs1 with lysine, glutamine, or alanine abolishes the ArfGAP activity of Gcs1 (Yanagisawa *et al.*, 2002), and *in vitro* GAP assays performed by Dr. Pak Phi Poon with the Gcs1-R54K mutant protein showed that this conserved arginine is also required for Gcs1 Arl1GAP activity *in vitro*. This finding suggests that the mechanisms involved in Gcs1 Arl1GAP and ArfGAP activities are

Table 5.1 Proteins that physically interact with Arl1

Name	Description/Function [a]	Experiment type	Reference
Dop1	Golgi-localized, leucine-zipper domain containing protein, involved in endosome to Golgi transport, organization of the ER, establishing cell polarity, and morphogenesis	protein-fragment complementation assay	(Tarassov et al., 2008)
Gcs1	ArfGAP/Arl1GAP	two-hybrid, affinity capture-Western, reconstituted complex	(Liu et al., 2005)
Imh1	GRIP-domain containing effector of Arl1, mediates transport between an endosomal compartment and the Golgi	affinity capture-Western	(Panic et al., 2003; Setty et al., 2003; Chen et al., 2010)
Mon2	GEF involved in endocytosis and vacuole integrity	affinity capture-Western, reconstituted complex	(Jochum et al., 2002; Efe et al., 2005)
Nse5	Essential subunit of the Mms21-Smc5-Smc6 complex, involved in DNA repair and maintaining cell cycle arrest following DNA damage	two-hybrid	(Hazbun et al., 2003)
Pho85	Cyclin-dependent kinase, regulates cellular response to: nutrient levels, environmental conditions, progression through the cell cycle	biochemical activity	(Ptacek et al., 2005)
Rpn11	Metalloprotease subunit of the 19S regulatory particle of the 26S proteasome lid,couples the deubiquitination and degradation of proteasome substrates	affinity capture-mass spec	(Kaake et al., 2010)
Syt1	Arl1GEF, predominantly binds GDP-bound Arl1, but binds GTP-bound Arl1 at a low level	two-hybrid, affinity capture-Western	(Chen et al., 2010)
Tpk1	cAMP-dependent protein kinase catalytic subunit; promotes vegetative growth in response to nutrients	biochemical activity	(Ptacek et al., 2005)
Vps53	Component of the GARP (Golgi-associated retrograde protein) complex, required for the recycling of proteins from endosomes to the late Golgi	affinity capture-Western	(Panic et al., 2003)

[a] SGD project. "Saccharomyces Genome Database" http://www.yeastgenome.org/ (Accessed June 18, 2011)

similar. There must, however, be aspects unique to Gcs1 that are required for Arl1GAP activity, because the related yeast ArfGAP protein Glo3 does not have Arl1GAP activity *in vitro* (Liu *et al.*, 2005). A mammalian protein called ELMOD2 has dual-specificity GAP activity for Arl and Arf proteins. However, ELMOD2 lacks the canonical ArfGAP domain and instead has an ELMO domain proposed to provide ArlGAP activity (Bowzard *et al.*, 2007). No yeast protein contains an ELMO domain (Brzostowski *et al.*, 2009); therefore it seems that the mechanisms used by ArlGAPs to simulate the GTPase activity of Arl proteins are varied.

5.14 Membrane Curvature Regulates Gcs1 ArfGAP-Related Functions for Vesicular Transport, but is Not Necessary for the GAP-Independent Reentry Function of Gcs1

The ALPS motif in Gcs1 is not strictly defined but is contained within a 75 residue segment (residues 205-280) of Gcs1 that is conserved in ArfGAP1, the human homologue of Gcs1 (Bigay *et al.*, 2005). The ALPS motif forms an amphipathic helix that imparts to Gcs1 the ability to bind regions of high membrane curvature (Bigay *et al.*, 2005). This binding is proposed to be an important feature that provides spatial and temporal regulation of Gcs1 ArfGAP activity. By regulating the localization of Gcs1, the ALPS motif restricts GTP hydrolysis on Arf to highly curved membranes, such as those membranes that arise during the late stages of transport-vesicle formation. Likewise, the ALPS motif biases against stimulation of GTP hydrolysis on Arf at the relatively flat membranes occupied by activated Arf during the early stages of vesicle biogenesis (Bigay *et al.*, 2005). In this way, GTP-bound Arf is stable on flat membranes, allowing the formation of transport vesicles to take place, and is unstable on the curved membranes of transport vesicles where Gcs1 GAP activity is required for coat destabilization to take place. My analysis of several mutant versions of Gcs1 (C-terminal truncations and point mutations) suggests that the ALPS motif contributes to Gcs1 function in Golgi-to-ER retrograde transport and post-Golgi transport but is dispensable for Gcs1 function in cell-cycle reentry.

For post-Golgi transport, Gcs1 provides overlapping essential function with another ArfGAP, Age2 (Poon *et al.*, 2001). Each protein can provide the ArfGAP activity

required for this transport. Indeed, the ArfGAP activity of Gcs1 is required for Gcs1 function in post-Golgi transport, because substitution of the conserved Arg-54 required for ArfGAP activity renders Gcs1 incapable of sustaining cell viability in the absence of Age2. The ALPS motif is also required for Gcs1 function in post-Golgi transport: removal of the C-terminal 60 residues of Gcs1 does not impair Gcs1 function, but additionally removing the preceding 80 residues containing the ALPS motif severely impairs Gcs1 function in the absence of Age2. As the ALPS motif is ideally suited to couple Gcs1 function with membrane curvature, my findings suggest that the coupling of Gcs1 ArfGAP activity with membrane curvature is important for Gcs1 function in post-Golgi transport. This is consistent with the overlapping function provided by Age2 and Gcs1 being ArfGAP activity, which is involved in vesicle formation and produces the types of highly curved membranes bound by the ALPS motif.

Although I do not have data showing that the GAP activity of Gcs1 is required in the absence of Glo3, it is likely the case that the ALPS motif also couples the ArfGAP activity of Gcs1 with membrane curvature in Golgi-to-ER retrograde transport. In fact, the ALPS motif appears to be more important for Gcs1 function in the Golgi-to-ER transport pathway than in the post-Golgi transport pathway, because its removal has a more severe phenotype in the absence of Glo3 than in the absence of Age2. The importance of the ALPS motif for Gcs1 function in Golgi-to-ER retrograde transport is further highlighted by a mutant Gcs1 protein in which a conserved hydrophobic residue in the ALPS motif is substituted with a hydrophilic residue (L246D); this L246D substitution abolishes Gcs1 function in Golgi-to-ER transport. The most conserved residues within the ALPS motif of Gcs1 and ArfGAP1 are several hydrophobic residues (including Leu-246) that form the hydrophobic face of the ALPS motif amphipathic helix and are thought to insert between the spaced lipid headgroups of highly curved membranes. Substituting the homologous residue to Leu-246 in the ALPS motif of ArfGAP1 (Leu-207) has drastic effects on the sensitivity of ArfGAP1 to membrane curvature (Bigay *et al.*, 2005), consistent with the loss of function caused by this substitution in Gcs1 being attributed to disruption of the ALPS motif.

In sharp contrast to the importance of the ALPS motif for Gcs1 function in these ArfGAP-dependent vesicular-transport pathways, the ALPS motif is completely

dispensable for a function of Gcs1 that is required during cell-cycle reentry in the cold. Even a severe C-terminal truncation of Gcs1 removing 190 residues, ~54% of the protein, had no effect of the ability of the truncated Gcs1 protein to provide reentry function. Thus, in contrast to the apparent importance of coupling Gcs1 ArfGAP activity with membrane-curvature sensing in the regulation of Arf for vesicular transport, neither ArfGAP activity nor sensing of membrane curvature is important individually for the Gcs1 activity required for reentry.

The ability of a Gcs1 protein bearing a C-terminal truncation at residue 162 to provide reentry function is inconsistent with previously published results from our lab in which the *GCS1* alleles *gcs1-2* and *gcs1-7*, encoding C-terminal truncations in Gcs1 at residues 227 and 200, respectively, were unable to provide reentry function (Ireland *et al.*, 1994). Contrary to those findings, my results strongly suggest that the C-terminal residues of Gcs1 are dispensable for Gcs1 function during the transition from stationary phase to active cell proliferation. The cause of this contradictory finding is not immediately apparent. The W303 strain of yeast was used in both cases, ruling out issues caused by different strain backgrounds. The *gcs1-2* allele encodes an additional 52 amino acids from out of frame *lacZ* sequences (Ireland *et al.*, 1994). It is possible that these additional residues appended onto the truncated Gcs1 C terminus prevent the Gcs1-2 mutant protein from providing reentry function. When my experiments were performed I was not aware of the previously published findings, and I therefore did not test the *gcs1-2* and *gcs1-7* alleles for reentry function in my own hands. Nevertheless, one of the Gcs1 truncations that I did test, and which did provide reentry function comparable to that of full length Gcs1, is truncated at the same residue as the Gcs1-7 mutant protein (residue 200). Unlike *gcs1-2*, the *gcs1-7* allele does not encode additional residues, and the *gcs1-7* sequence was confirmed by sequencing (Ireland *et al.*, 1994). Thus, I suspect that careful retesting of the Gcs1-7 mutant version of Gcs1 would show that this mutant protein allows reentry. Consistent with the ArfGAP activity of Gcs1 being dispensable for reentry, the Gcs1-7 protein is severely impaired for ArfGAP activity *in vitro* (Poon *et al.*, 1996). Therefore the C-terminal residues of Gcs1 are required for Gcs1 ArfGAP activity *in vitro*. Since the ALPS motif is absent from in the C-terminally truncated Gcs1-7 protein, but the ArfGAP domain remains intact, the loss of ArfGAP activity in this *in*

vitro ArfGAP assay most likely reflects the inability of the Gcs1-7 protein to bind to the lipid formed micelles or liposomes in which the GTP-loaded Arf is bound in the assay.

5.15 The Other Gene Deletions that Alleviate *gcs1*Δ Cold Sensitivity

I have characterized the effects of 11 of the 92 gene deletion mutations that were identified in our whole-genome screen for non-essential gene deletions that alleviate the cold-sensitive reentry defect of *gcs1*Δ cells. My findings show that dysregulated Arl1, resulting from the absence of a GAP-independent function of Gcs1, imposes the *gcs1*Δ reentry defect and the 11 deletions that I have characterized each alleviate the reentry defect by minimizing the accumulation of this dysregulated Arl1 at the *trans*-Golgi membrane. Five of these deletions eliminate members of the Arl1 pathway, 3 eliminate members of the Ypt6 pathway, and 3 eliminate dubious open reading frames that overlap genes in the Arl1 and Ypt6 pathways. In addition to the deletions that eliminate components of the Arl1 and Ypt6 pathways, I identified 3 other alleviating gene deletions that minimize the accumulation of dysregulated Arl1 at the *trans*-Golgi membrane (*mnn9*Δ, *rpe1*Δ, and *rpl43a*Δ). It is clear that these deletions alleviate *gcs1*Δ cold sensitivity by affecting the activation and membrane localization of Arl1; however, characterization of the mechanisms by which this is accomplished requires further research. Furthermore, I noted that 11 of the alleviating deletions are neighbouring genes on chromosome XIII. Although further analysis is required to fully understand the nature of these 11 neighbouring genes, they probably represent a linkage group around a mutation that alleviates *gcs1*Δ cold sensitivity, and are probably not themselves *bona fide* alleviators.

The remaining gene deletions that alleviate *gcs1*Δ cold sensitivity do not cause the mislocalization of Imh1, and therefore are not likely involved in the activation and membrane localization of Arl1. However, this suggestion needs to be viewed with caution, since I did find that deletion of *SYT1*, described to encode a GEF for Arl1 and therefore involved in the activation of Arl1 (Chen *et al.*, 2010), does indeed alleviate *gcs1*Δ cold sensitivity but does not cause Imh1 to be mislocalized, at least not to the same extent as other Arl1-pathway gene deletions. Therefore, it is possible that other alleviating deletions also have more subtle effects on Imh1 localization that may have

been missed in my analysis. It has been suggested that Syt1 is not the sole protein in yeast with Arl1GEF activity (Chen *et al.*, 2010), raising the possibility that other Arl1GEF protein(s) may be encoded by genes identified here. Nonetheless, most of the remaining gene deletions probably alleviate *gcs1*Δ cold sensitivity in a manner that does not involve minimizing the activation of Arl1. Further work is required to understand the mechanisms of these alleviating gene deletions. The deletions have not yet been confirmed by PCR, nor have the alleviating effects been further assessed by tetrad dissection or reconstruction of the gene deletion to confirm alleviation. For a small proportion of these deletions the protein encoded by the gene that is deleted has no known function; however, for the majority there is something known about the function of the protein. These functions are varied and include DNA repair, chromatin remodelling, gene transcription, mRNA translation, ER translocation, post-translational modifications, protein degradation, phospholipid synthesis, mitochondrial function, amino acid uptake, cell wall maintenance, polarized cell growth, cell-cycle progression, secretory transport, and post-Golgi transport.

The proteins eliminated by the gene deletions that I have characterized all function upstream of Arl1 and are required for the activation and membrane localization of Arl1. One possibility for the proteins encoded by the uncharacterized deleted genes is that these genes function downstream of Arl1. As discussed above, the toxic-complex model predicts that elimination of the factor proposed to be sequestered by Arl1 should result in alleviation of the *gcs1*Δ reentry defect; thus, provided that the factor is a non-essential protein, the gene that encodes it may be contained in the list of alleviating gene deletions. Likewise, the proteins eliminated by the alleviating gene deletions may affect the sequestered factor itself, or downstream functions influenced by the sequestered factor. Considering the list of functions provided by the proteins encoded by these genes, some have the potential to affect the sequestered protein upstream of its sequestration by Arl1, for example at the transcriptional, translational, or post-translational levels, while others have the potential to affect the sequestered protein downstream of its sequestration by Arl1, for example in post-Golgi transport, or cell growth process that may be required for reentry or may be inhibitory to reentry, depending on the nature of the mechanism of alleviation.

In the case of the *can1*Δ deletion mutation, the alleviation is likely an artefact of the genetics used to facilitate the screen. The *CAN1* gene encodes a plasma membrane-localized arginine permease (Ahmad and Bussey, 1986), the elimination of which confers resistance to the toxic arginine analog canavanine (Larimer *et al.*, 1978). In our screen the *gcs1*Δ query strain (PPY169-4) that was crossed to members of the deletion collection harbours a *can1*Δ mutation; thus the fact that this *gcs1*Δ *can1*Δ strain is cold sensitive proves that the *can1*Δ deletion mutation does not alleviate *gcs1*Δ cold sensitivity. The *can1*Δ mutation is used in the screen to aid in the selection of haploid segregants after the heterozygous diploid mutant cells are sporulated. Diploid cells that have failed to undergo sporulation are not desired, and because they are heterozygous for *CAN1*/*can1*Δ they are canavanine sensitive. The addition of canavanine to the haploid-selection medium selects against the growth of diploid cells while allowing the desired canavanine resistant *can1*Δ haploid cells to grow. The *can1*Δ deletion was likely identified in our screen as alleviating *gcs1*Δ cold sensitivity because in this case the diploid cells are homozygous *can1*Δ deletion mutants, and are therefore canavanine resistant. This likely allows cold resistant heterozygous *GCS1*/*gcs1*Δ diploid cells to escape the haploid selection process and give the appearance of an alleviating deletion mutation.

5.16 Concluding Remarks

In this study I have explored aspects of the regulatory repertoire for two members of the highly conserved family of proteins that provide ArfGAP function in yeast. Focusing on two members of this family, I found that increased abundance of the Age1 ArfGAP can functionally replace the essential ArfGAP pairs that normally provide ArfGAP function for post-Golgi and Golgi-to-ER transport. I have further defined an N-terminal segment of the Age1 protein that inhibits Age1 function in each of these transport pathways. The role this N-terminal segment plays in the regulation of normal Age1 function and, indeed, what normal Age1 function is remain unknown. My findings have explained the mechanism by which the increased abundance of the Sfh2 phosphatidylinositol transfer protein alleviates the effects of defective ArfGAP function in the post-Golgi transport pathway, and in doing so have demonstrated a requirement for endogenous Age1, providing evidence that endogenous Age1 can supply ArfGAP function required for post-

Golgi transport. Furthermore, I have also shown that the Age1 ArfGAP protein, like other yeast and mammalian ArfGAP proteins, can be regulated by membrane lipid composition *in vivo*, and Dr. Pak Phi Poon in our lab further confirmed that this is also the case *in vitro*. My work has also advanced our understanding of the roles for Gcs1, having demonstrated that a Gcs1 function required for reentry is independent of the ArfGAP and Arl1GAP functions of this protein, and that the active but dysregulated Arl1 that accumulates in the absence of this GAP-independent regulation imposes the *gcs1*Δ reentry and endocytic transport defects. The regulation of Gcs1 by membrane curvature is important for GAP-dependent Gcs1 function in the post-Golgi and Golgi-to-ER retrograde transport pathways, but dispensable for a Gcs1 function required for cell-cycle reentry in the cold. My investigations uncovered an unexpected functional relationship between the Ypt6 and Arl1 vesicle-tethering pathways. Finally, my studies have characterized the ability of increased Imh1 abundance to alleviate *gcs1*Δ cold sensitivity, showing that Arl1 binding by the GRIP domain of Imh1 is necessary and sufficient for these effects and suggesting a possible mechanism for how dysregulated Arl1 imposes the *gcs1*Δ defects, by protein sequestration. This model provides the basis for further experimentation aimed at identification of the sequestered protein, which could lead to a clearer picture of the *gcs1*Δ reentry defect and a better understanding of the poorly characterized processes that are involved in cell-cycle reentry.

REFERENCES

Abe, F. and Minegishi, H. (2008). Global screening of genes essential for growth in high-pressure and cold environments: searching for basic adaptive strategies using a yeast deletion library. Genetics *2*, 851-872.

Ahmad, M. and Bussey, H. (1986). Yeast arginine permease: nucleotide sequence of the CAN1 gene. Curr. Genet. *8*, 587-592.

Anand, V. C., Daboussi, L., Lorenz, T. C. and Payne, G. S. (2009). Genome-wide analysis of AP-3-dependent protein transport in yeast. Mol. Biol. Cell *5*, 1592-1604.

Antonny, B., Bigay, J., Casella, J. F., Drin, G., Mesmin, B. and Gounon, P. (2005). Membrane curvature and the control of GTP hydrolysis in Arf1 during COPI vesicle formation. Biochem. Soc. Trans. *Pt 4*, 619-622.

Antonny, B., Huber, I., Paris, S., Chabre, M. and Cassel, D. (1997). Activation of ADP-ribosylation factor 1 GTPase-activating protein by phosphatidylcholine-derived diacylglycerols. J. Biol. Chem. *49*, 30848-30851.

Archambault, J., Drebot, M. A., Stone, J. C. and Friesen, J. D. (1992). Isolation and phenotypic analysis of conditional-lethal, linker-insertion mutations in the gene encoding the largest subunit of RNA polymerase II in Saccharomyces cerevisiae. Mol. Gen. Genet. *3*, 408-414.

Audhya, A., Foti, M. and Emr, S. D. (2000). Distinct roles for the yeast phosphatidylinositol 4-kinases, Stt4p and Pik1p, in secretion, cell growth, and organelle membrane dynamics. Mol. Biol. Cell *8*, 2673-2689.

Auger, A. (2000). Identification of Yeast Proteins Compensating for the Loss of Arf GAP Function. MSc Thesis, Dalhousie University.

Barlowe, C. (1998). COPII and selective export from the endoplasmic reticulum. Biochim. Biophys. Acta *1-2*, 67-76.

Barr, F. A. (1999). A novel Rab6-interacting domain defines a family of Golgi-targeted coiled-coil proteins. Curr. Biol. *7*, 381-384.

Behnia, R., Panic, B., Whyte, J. R. and Munro, S. (2004). Targeting of the Arf-like GTPase Arl3p to the Golgi requires N-terminal acetylation and the membrane protein Sys1p. Nat. Cell Biol. *5*, 405-413.

Benjamin, J. J., Poon, P. P., Drysdale, J. D., Wang, X., Singer, R. A. and Johnston, G. C. (2011a). Dysregulated Arl1, a regulator of post-Golgi vesicle tethering, can inhibit endosomal transport and cell proliferation in yeast. Mol. Biol. Cell *13*, 2337-2347.

Benjamin, J. J., Poon, P. P., Lewis, S. M., Auger, A., Wong, T. A., Singer, R. A. and Johnston, G. C. (2011b). The yeast Arf GTPase-activating protein Age1 is regulated by phospholipase D for post-Golgi vesicular transport. J. Biol. Chem. *7*, 5187-5196.

Bensen, E. S., Yeung, B. G. and Payne, G. S. (2001). Ric1p and the Ypt6p GTPase function in a common pathway required for localization of trans-Golgi network membrane proteins. Mol. Biol. Cell *1*, 13-26.

Bigay, J., Casella, J. F., Drin, G., Mesmin, B. and Antonny, B. (2005). ArfGAP1 responds to membrane curvature through the folding of a lipid packing sensor motif. EMBO J. *13*, 2244-2253.

Birnboim, H. C. (1983). A rapid alkaline extraction method for the isolation of plasmid DNA. Methods Enzymol., 243-255.

Birnboim, H. C. and Doly, J. (1979). A rapid alkaline extraction procedure for screening recombinant plasmid DNA. Nucleic Acids Res. *6*, 1513-1523.

Bonangelino, C. J., Chavez, E. M. and Bonifacino, J. S. (2002). Genomic screen for vacuolar protein sorting genes in Saccharomyces cerevisiae. Mol. Biol. Cell *7*, 2486-2501.

Bonifacino, J. S. (2004). The GGA proteins: adaptors on the move. Nat. Rev. Mol. Cell Biol. *1*, 23-32.

Bonifacino, J. S. and Glick, B. S. (2004). The mechanisms of vesicle budding and fusion. Cell *2*, 153-166.

Bonifacino, J. S. and Hierro, A. (2011). Transport according to GARP: receiving retrograde cargo at the trans-Golgi network. Trends Cell Biol. *3*, 159-167.

Boronenkov, I. V. and Anderson, R. A. (1995). The sequence of phosphatidylinositol-4-phosphate 5-kinase defines a novel family of lipid kinases. J. Biol. Chem. *7*, 2881-2884.

Bourne, H. R., Sanders, D. A. and McCormick, F. (1991). The GTPase superfamily: conserved structure and molecular mechanism. Nature *6305*, 117-127.

Bowzard, J. B., Cheng, D., Peng, J. and Kahn, R. A. (2007). ELMOD2 is an Arl2 GTPase-activating protein that also acts on Arfs. J. Biol. Chem. *24*, 17568-17580.

Brachmann, C. B., Davies, A., Cost, G. J., Caputo, E., Li, J., Hieter, P. and Boeke, J. D. (1998). Designer deletion strains derived from Saccharomyces cerevisiae S288C: a useful set of strains and plasmids for PCR-mediated gene disruption and other applications. Yeast *2*, 115-132.

Brennwald, P., Kearns, B., Champion, K., Keranen, S., Bankaitis, V. and Novick, P. (1994). Sec9 is a SNAP-25-like component of a yeast SNARE complex that may be the effector of Sec4 function in exocytosis. Cell *2*, 245-258.

Broadie, K., Prokop, A., Bellen, H. J., O'Kane, C. J., Schulze, K. L. and Sweeney, S. T. (1995). Syntaxin and synaptobrevin function downstream of vesicle docking in Drosophila. Neuron *3*, 663-673.

Brown, H. A., Gutowski, S., Moomaw, C. R., Slaughter, C. and Sternweis, P. C. (1993). ADP-ribosylation factor, a small GTP-dependent regulatory protein, stimulates phospholipase D activity. Cell *6*, 1137-1144.

Brymora, A., Valova, V. A., Larsen, M. R., Roufogalis, B. D. and Robinson, P. J. (2001). The brain exocyst complex interacts with RalA in a GTP-dependent manner: identification of a novel mammalian Sec3 gene and a second Sec15 gene. J. Biol. Chem. *32*, 29792-29797.

Brzostowski, J. A., Fey, P., Yan, J., Isik, N. and Jin, T. (2009). The Elmo family forms an ancient group of actin-regulating proteins. Commun. Integr. Biol. *4*, 337-340.

Burd, C. G., Strochlic, T. I. and Gangi Setty, S. R. (2004). Arf-like GTPases: not so Arf-like after all. Trends Cell Biol. *12*, 687-694.

Burguete, A. S., Fenn, T. D., Brunger, A. T. and Pfeffer, S. R. (2008). Rab and Arl GTPase family members cooperate in the localization of the golgin GCC185. Cell *2*, 286-298.

Cai, H., Reinisch, K. and Ferro-Novick, S. (2007). Coats, tethers, Rabs, and SNAREs work together to mediate the intracellular destination of a transport vesicle. Dev. Cell. *5*, 671-682.

Chavrier, P. and Menetrey, J. (2010). Toward a structural understanding of arf family:effector specificity. Structure *12*, 1552-1558.

Chen, K. Y., Tsai, P. C., Hsu, J. W., Hsu, H. C., Fang, C. Y., Chang, L. C., Tsai, Y. T., Yu, C. J. and Lee, F. J. (2010). Syt1p promotes activation of Arl1p at the late Golgi to recruit Imh1p. J. Cell. Sci. *Pt 20*, 3478-3489.

Chen, S. H., Chen, S., Tokarev, A. A., Liu, F., Jedd, G. and Segev, N. (2005). Ypt31/32 GTPases and their novel F-box effector protein Rcy1 regulate protein recycling. Mol. Biol. Cell *1*, 178-192.

Christianson, T. W., Sikorski, R. S., Dante, M., Shero, J. H. and Hieter, P. (1992). Multifunctional yeast high-copy-number shuttle vectors. Gene *1*, 119-122.

Cockcroft, S., Thomas, G. M., Fensome, A., Geny, B., Cunningham, E., Gout, I., Hiles, I., Totty, N. F., Truong, O. and Hsuan, J. J. (1994). Phospholipase D: a downstream effector of ARF in granulocytes. Science *5146*, 523-526.

Coe, J. G., Murray, L. E. and Dawes, I. W. (1994). Identification of a sporulation-specific promoter regulating divergent transcription of two novel sporulation genes in Saccharomyces cerevisiae. Mol. Gen. Genet. *6*, 661-672.

Conboy, M. J. and Cyert, M. S. (2000). Luv1p/Rki1p/Tcs3p/Vps54p, a yeast protein that localizes to the late Golgi and early endosome, is required for normal vacuolar morphology. Mol. Biol. Cell *7*, 2429-2443.

Conibear, E. (2010). Converging views of endocytosis in yeast and mammals. Curr. Opin. Cell Biol. *4*, 513-518.

Conibear, E., Cleck, J. N. and Stevens, T. H. (2003). Vps51p mediates the association of the GARP (Vps52/53/54) complex with the late Golgi t-SNARE Tlg1p. Mol. Biol. Cell *4*, 1610-1623.

Conibear, E. and Stevens, T. H. (2000). Vps52p, Vps53p, and Vps54p form a novel multisubunit complex required for protein sorting at the yeast late Golgi. Mol. Biol. Cell *1*, 305-323.

Corda, D., Hidalgo Carcedo, C., Bonazzi, M., Luini, A. and Spano, S. (2002). Molecular aspects of membrane fission in the secretory pathway. Cell Mol. Life Sci. *11*, 1819-1832.

Cosson, P. and Letourneur, F. (1997). Coatomer (COPI)-coated vesicles: role in intracellular transport and protein sorting. Curr. Opin. Cell Biol. *4*, 484-487.

Cowles, C. R., Snyder, W. B., Burd, C. G. and Emr, S. D. (1997). Novel Golgi to vacuole delivery pathway in yeast: identification of a sorting determinant and required transport component. EMBO J. *10*, 2769-2782.

Cukierman, E., Huber, I., Rotman, M. and Cassel, D. (1995). The ARF1 GTPase-activating protein: zinc finger motif and Golgi complex localization. Science *5244*, 1999-2002.

Derby, M. C., van Vliet, C., Brown, D., Luke, M. R., Lu, L., Hong, W., Stow, J. L. and Gleeson, P. A. (2004). Mammalian GRIP domain proteins differ in their membrane binding properties and are recruited to distinct domains of the TGN. J. Cell. Sci. *Pt 24*, 5865-5874.

Desrivieres, S., Cooke, F. T., Parker, P. J. and Hall, M. N. (1998). MSS4, a phosphatidylinositol-4-phosphate 5-kinase required for organization of the actin cytoskeleton in Saccharomyces cerevisiae. J. Biol. Chem. *25*, 15787-15793.

Dilda, P. J., Don, A. S., Tanabe, K. M., Higgins, V. J., Allen, J. D., Dawes, I. W. and Hogg, P. J. (2005). Mechanism of selectivity of an angiogenesis inhibitor from screening a genome-wide set of Saccharomyces cerevisiae deletion strains. J. Natl. Cancer Inst. *20*, 1539-1547.

Drebot, M. A., Barnes, C. A., Singer, R. A. and Johnston, G. C. (1990). Genetic assessment of stationary phase for cells of the yeast Saccharomyces cerevisiae. J. Bacteriol. *7*, 3584-3589.

Drebot, M. A., Johnston, G. C. and Singer, R. A. (1987). A yeast mutant conditionally defective only for reentry into the mitotic cell cycle from stationary phase. Proc. Natl. Acad. Sci. U. S. A. *22*, 7948-7952.

Drin, G., Casella, J. F., Gautier, R., Boehmer, T., Schwartz, T. U. and Antonny, B. (2007). A general amphipathic alpha-helical motif for sensing membrane curvature. Nat. Struct. Mol. Biol. *2*, 138-146.

Drin, G., Morello, V., Casella, J. F., Gounon, P. and Antonny, B. (2008). Asymmetric tethering of flat and curved lipid membranes by a golgin. Science *5876*, 670-673.

Drysdale, J. D. (2006). Proteins that Negatively Regulate the Transition From Stationary Phase to the Cell Division Cycle in the Yeast *Saccharomyces cerevisiae*. MSc Thesis, Dalhousie University.

East, M. P. and Kahn, R. A. (2011). Models for the functions of Arf GAPs. Semin. Cell Dev. Biol. *1*, 3-9.

Efe, J. A., Plattner, F., Hulo, N., Kressler, D., Emr, S. D. and Deloche, O. (2005). Yeast Mon2p is a highly conserved protein that functions in the cytoplasm-to-vacuole transport pathway and is required for Golgi homeostasis. J. Cell. Sci. *Pt 20*, 4751-4764.

Fasshauer, D., Antonin, W., Subramaniam, V. and Jahn, R. (2002). SNARE assembly and disassembly exhibit a pronounced hysteresis. Nat. Struct. Biol. *2*, 144-151.

Flanagan, C. A., Schnieders, E. A., Emerick, A. W., Kunisawa, R., Admon, A. and Thorner, J. (1993). Phosphatidylinositol 4-kinase: gene structure and requirement for yeast cell viability. Science *5138*, 1444-1448.

Ghaemmaghami, S., Huh, W. K., Bower, K., Howson, R. W., Belle, A., Dephoure, N., O'Shea, E. K. and Weissman, J. S. (2003). Global analysis of protein expression in yeast. Nature *6959*, 737-741.

Giaever, G. *et al.* (2002). Functional profiling of the Saccharomyces cerevisiae genome. Nature *6896*, 387-391.

Gietz, R. D., Schiestl, R. H., Willems, A. R. and Woods, R. A. (1995). Studies on the transformation of intact yeast cells by the LiAc/SS-DNA/PEG procedure. Yeast *4*, 355-360.

Gillingham, A. K. and Munro, S. (2003). Long coiled-coil proteins and membrane traffic. Biochim. Biophys. Acta *2-3*, 71-85.

Gillingham, A. K., Tong, A. H., Boone, C. and Munro, S. (2004). The GTPase Arf1p and the ER to Golgi cargo receptor Erv14p cooperate to recruit the golgin Rud3p to the cis-Golgi. J. Cell Biol. *2*, 281-292.

Goldberg, J. (1999). Structural and functional analysis of the ARF1-ARFGAP complex reveals a role for coatomer in GTP hydrolysis. Cell *6*, 893-902.

Graham, T. R. (2004). Membrane targeting: getting Arl to the Golgi. Curr. Biol. *12*, R483-5.

Gray, J. V., Petsko, G. A., Johnston, G. C., Ringe, D., Singer, R. A. and Werner-Washburne, M. (2004). "Sleeping beauty": quiescence in Saccharomyces cerevisiae. Microbiol. Mol. Biol. Rev. *2*, 187-206.

Griac, P. (2007). Sec14 related proteins in yeast. Biochim. Biophys. Acta *6*, 737-745.

Guo, W., Roth, D., Walch-Solimena, C. and Novick, P. (1999). The exocyst is an effector for Sec4p, targeting secretory vesicles to sites of exocytosis. EMBO J. *4*, 1071-1080.

Gurr, E. (1965). Methylene blue (buffered) for differentiating between living and dead yeast cells. In: The Rational Use of Dyes in Biology and General Staining Methods, ed. Anonymous Leonard Hill: London, 213-214.

Haney, S. A. and Broach, J. R. (1994). Cdc25p, the guanine nucleotide exchange factor for the Ras proteins of Saccharomyces cerevisiae, promotes exchange by stabilizing Ras in a nucleotide-free state. J. Biol. Chem. *24*, 16541-16548.

Harsay, E. and Bretscher, A. (1995). Parallel secretory pathways to the cell surface in yeast. J. Cell Biol. *2*, 297-310.

Hartwell, L. H. (1967). Macromolecule synthesis in temperature-sensitive mutants of yeast. J. Bacteriol. *5*, 1662-1670.

Hayes, G. L., Brown, F. C., Haas, A. K., Nottingham, R. M., Barr, F. A. and Pfeffer, S. R. (2009). Multiple Rab GTPase binding sites in GCC185 suggest a model for vesicle tethering at the trans-Golgi. Mol. Biol. Cell *1*, 209-217.

Hazbun, T. R. *et al.* (2003). Assigning function to yeast proteins by integration of technologies. Mol. Cell *6*, 1353-1365.

Henneberry, A. L., Lagace, T. A., Ridgway, N. D. and McMaster, C. R. (2001). Phosphatidylcholine synthesis influences the diacylglycerol homeostasis required for SEC14p-dependent Golgi function and cell growth. Mol. Biol. Cell *3*, 511-520.

Hoffman, C. S. (1997). Preparation of yeast DNA, RNA, and proteins. In: Current Protocols in Molecular Biology, 13.11.1-13.11.4.

Houghton, F. J., Chew, P. L., Lodeho, S., Goud, B. and Gleeson, P. A. (2009). The localization of the Golgin GCC185 is independent of Rab6A/A' and Arl1. Cell *4*, 787-794.

Huh, W. K., Falvo, J. V., Gerke, L. C., Carroll, A. S., Howson, R. W., Weissman, J. S. and O'Shea, E. K. (2003). Global analysis of protein localization in budding yeast. Nature *6959*, 686-691.

Hunt, J. M., Bommert, K., Charlton, M. P., Kistner, A., Habermann, E., Augustine, G. J. and Betz, H. (1994). A post-docking role for synaptobrevin in synaptic vesicle fusion. Neuron *6*, 1269-1279.

Ireland, L. S., Johnston, G. C., Drebot, M. A., Dhillon, N., DeMaggio, A. J., Hoekstra, M. F. and Singer, R. A. (1994). A member of a novel family of yeast 'zn-finger' proteins mediates the transition from stationary phase to cell proliferation. EMBO J. *16*, 3812-3821.

Jackson, C. L. (2003). Membrane traffic: Arl GTPases get a GRIP on the Golgi. Curr. Biol. *5*, R174-6.

Jahn, R. and Scheller, R. H. (2006). SNAREs--engines for membrane fusion. Nat. Rev. Mol. Cell Biol. *9*, 631-643.

Jansen, G., Wu, C., Schade, B., Thomas, D. Y. and Whiteway, M. (2005). Drag&Drop cloning in yeast. Gene, 43-51.

Jedd, G., Mulholland, J. and Segev, N. (1997). Two new Ypt GTPases are required for exit from the yeast trans-Golgi compartment. J. Cell Biol. *3*, 563-580.

Jochum, A., Jackson, D., Schwarz, H., Pipkorn, R. and Singer-Kruger, B. (2002). Yeast Ysl2p, homologous to Sec7 domain guanine nucleotide exchange factors, functions in endocytosis and maintenance of vacuole integrity and interacts with the Arf-Like small GTPase Arl1p. Mol. Cell. Biol. *13*, 4914-4928.

Johnston, G. C., Pringle, J. R. and Hartwell, L. H. (1977). Coordination of growth with cell division in the yeast Saccharomyces cerevisiae. Exp. Cell Res. *1*, 79-98.

Jungmann, J. and Munro, S. (1998). Multi-protein complexes in the cis Golgi of Saccharomyces cerevisiae with alpha-1,6-mannosyltransferase activity. EMBO J. *2*, 423-434.

Kaake, R. M., Milenkovic, T., Przulj, N., Kaiser, P. and Huang, L. (2010). Characterization of cell cycle specific protein interaction networks of the yeast 26S proteasome complex by the QTAX strategy. J. Proteome Res. *4*, 2016-2029.

Kahn, R. A. *et al.* (2008). Consensus nomenclature for the human ArfGAP domain-containing proteins. J. Cell Biol. *6*, 1039-1044.

Kjer-Nielsen, L., Teasdale, R. D., van Vliet, C. and Gleeson, P. A. (1999). A novel Golgi-localisation domain shared by a class of coiled-coil peripheral membrane proteins. Curr. Biol. *7*, 385-388.

Kliouchnikov, L., Bigay, J., Mesmin, B., Parnis, A., Rawet, M., Goldfeder, N., Antonny, B. and Cassel, D. (2009). Discrete determinants in ArfGAP2/3 conferring Golgi localization and regulation by the COPI coat. Mol. Biol. Cell *3*, 859-869.

Kolling, R., Lee, A., Chen, E. Y. and Botstein, D. (1994). Nucleotide sequence of the SAC2 gene of Saccharomyces cerevisiae. Yeast *9*, 1211-1216.

Larimer, F. W., Ramey, D. W., Lijinsky, W. and Epler, J. L. (1978). Mutagenicity of methylated N-nitrosopiperidines in Saccharomyces cerevisiae. Mutat. Res. *2*, 155-161.

Letourneur, F., Gaynor, E. C., Hennecke, S., Demolliere, C., Duden, R., Emr, S. D., Riezman, H. and Cosson, P. (1994). Coatomer is essential for retrieval of dilysine-tagged proteins to the endoplasmic reticulum. Cell *7*, 1199-1207.

Lewis, S. M. (2004). Multiple ArfGAPs Regulate Vesicular Transport. PhD Thesis, Dalhousie University.

Lewis, S. M., Poon, P. P., Singer, R. A., Johnston, G. C. and Spang, A. (2004). The ArfGAP Glo3 is required for the generation of COPI vesicles. Mol. Biol. Cell *9*, 4064-4072.

Li, X., Routt, S. M., Xie, Z., Cui, X., Fang, M., Kearns, M. A., Bard, M., Kirsch, D. R. and Bankaitis, V. A. (2000). Identification of a novel family of nonclassic yeast phosphatidylinositol transfer proteins whose function modulates phospholipase D activity and Sec14p-independent cell growth. Mol. Biol. Cell *6*, 1989-2005.

Liu, Y. W., Huang, C. F., Huang, K. B. and Lee, F. J. (2005). Role for Gcs1p in regulation of Arl1p at trans-Golgi compartments. Mol. Biol. Cell *9*, 4024-4033.

Lu, L. and Hong, W. (2003). Interaction of Arl1-GTP with GRIP domains recruits autoantigens Golgin-97 and Golgin-245/p230 onto the Golgi. Mol. Biol. Cell *9*, 3767-3781.

Marcusson, E. G., Horazdovsky, B. F., Cereghino, J. L., Gharakhanian, E. and Emr, S. D. (1994). The sorting receptor for yeast vacuolar carboxypeptidase Y is encoded by the VPS10 gene. Cell *4*, 579-586.

Messing, J. (1983). New M13 vectors for cloning. Methods Enzymol., 20-78.

Miosga, T. and Zimmermann, F. K. (1996). Cloning and characterization of the first two genes of the non-oxidative part of the Saccharomyces cerevisiae pentose-phosphate pathway. Curr. Genet. *5*, 404-409.

Munro, S. (2005). The Arf-like GTPase Arl1 and its role in membrane traffic. Biochem. Soc. Trans. *Pt 4*, 601-605.

Munro, S. and Nichols, B. J. (1999). The GRIP domain - a novel Golgi-targeting domain found in several coiled-coil proteins. Curr. Biol. *7*, 377-380.

Novick, P., Field, C. and Schekman, R. (1980). Identification of 23 complementation groups required for post-translational events in the yeast secretory pathway. Cell *1*, 205-215.

Panic, B., Perisic, O., Veprintsev, D. B., Williams, R. L. and Munro, S. (2003a). Structural basis for Arl1-dependent targeting of homodimeric GRIP domains to the Golgi apparatus. Mol. Cell *4*, 863-874.

Panic, B., Whyte, J. R. and Munro, S. (2003b). The ARF-like GTPases Arl1p and Arl3p act in a pathway that interacts with vesicle-tethering factors at the Golgi apparatus. Curr. Biol. *5*, 405-410.

Pasqualato, S., Renault, L. and Cherfils, J. (2002). Arf, Arl, Arp and Sar proteins: a family of GTP-binding proteins with a structural device for 'front-back' communication. EMBO Rep. *11*, 1035-1041.

Peyroche, A., Paris, S. and Jackson, C. L. (1996). Nucleotide exchange on ARF mediated by yeast Gea1 protein. Nature *6608*, 479-481.

Piper, R. C., Bryant, N. J. and Stevens, T. H. (1997). The membrane protein alkaline phosphatase is delivered to the vacuole by a route that is distinct from the VPS-dependent pathway. J. Cell Biol. *3*, 531-545.

Planta, R. J. and Mager, W. H. (1998). The list of cytoplasmic ribosomal proteins of Saccharomyces cerevisiae. Yeast *5*, 471-477.

Polevoda, B. and Sherman, F. (2001). NatC Nalpha-terminal acetyltransferase of yeast contains three subunits, Mak3p, Mak10p, and Mak31p. J. Biol. Chem. *23*, 20154-20159.

Poon, P. P., Cassel, D., Spang, A., Rotman, M., Pick, E., Singer, R. A. and Johnston, G. C. (1999). Retrograde transport from the yeast Golgi is mediated by two ARF GAP proteins with overlapping function. EMBO J. *3*, 555-564.

Poon, P. P., Nothwehr, S. F., Singer, R. A. and Johnston, G. C. (2001). The Gcs1 and Age2 ArfGAP proteins provide overlapping essential function for transport from the yeast trans-Golgi network. J. Cell Biol. *7*, 1239-1250.

Poon, P. P., Wang, X., Rotman, M., Huber, I., Cukierman, E., Cassel, D., Singer, R. A. and Johnston, G. C. (1996). Saccharomyces cerevisiae Gcs1 is an ADP-ribosylation factor GTPase-activating protein. Proc. Natl. Acad. Sci. U. S. A. *19*, 10074-10077.

Ptacek, J. *et al.* (2005). Global analysis of protein phosphorylation in yeast. Nature *7068*, 679-684.

Quenneville, N. R., Chao, T. Y., McCaffery, J. M. and Conibear, E. (2006). Domains within the GARP subunit Vps54 confer separate functions in complex assembly and early endosome recognition. Mol. Biol. Cell *4*, 1859-1870.

Reggiori, F., Wang, C. W., Stromhaug, P. E., Shintani, T. and Klionsky, D. J. (2003). Vps51 is part of the yeast Vps fifty-three tethering complex essential for retrograde traffic from the early endosome and Cvt vesicle completion. J. Biol. Chem. *7*, 5009-5020.

Rein, U., Andag, U., Duden, R., Schmitt, H. D. and Spang, A. (2002). ARF-GAP-mediated interaction between the ER-Golgi v-SNAREs and the COPI coat. J. Cell Biol. *3*, 395-404.

Ren, Y., Yip, C. K., Tripathi, A., Huie, D., Jeffrey, P. D., Walz, T. and Hughson, F. M. (2009). A structure-based mechanism for vesicle capture by the multisubunit tethering complex Dsl1. Cell *6*, 1119-1129.

Rieder, S. E. and Emr, S. D. (1997). A novel RING finger protein complex essential for a late step in protein transport to the yeast vacuole. Mol. Biol. Cell *11*, 2307-2327.

Robinson, L. C., Bradley, C., Bryan, J. D., Jerome, A., Kweon, Y. and Panek, H. R. (1999). The Yck2 yeast casein kinase 1 isoform shows cell cycle-specific localization to sites of polarized growth and is required for proper septin organization. Mol. Biol. Cell *4*, 1077-1092.

Robinson, M., Poon, P. P., Schindler, C., Murray, L. E., Kama, R., Gabriely, G., Singer, R. A., Spang, A., Johnston, G. C. and Gerst, J. E. (2006). The Gcs1 Arf-GAP mediates Snc1,2 v-SNARE retrieval to the Golgi in yeast. Mol. Biol. Cell *4*, 1845-1858.

Rose, K., Rudge, S. A., Frohman, M. A., Morris, A. J. and Engebrecht, J. (1995). Phospholipase D signaling is essential for meiosis. Proc. Natl. Acad. Sci. U. S. A. *26*, 12151-12155.

Rosenwald, A. G., Rhodes, M. A., Van Valkenburgh, H., Palanivel, V., Chapman, G., Boman, A., Zhang, C. J. and Kahn, R. A. (2002). ARL1 and membrane traffic in Saccharomyces cerevisiae. Yeast *12*, 1039-1056.

Rothman, J. E. (1994). Mechanisms of intracellular protein transport. Nature *6501*, 55-63.

Routt, S. M., Ryan, M. M., Tyeryar, K., Rizzieri, K. E., Mousley, C., Roumanie, O., Brennwald, P. J. and Bankaitis, V. A. (2005). Nonclassical PITPs activate PLD via the Stt4p PtdIns-4-kinase and modulate function of late stages of exocytosis in vegetative yeast. Traffic *12*, 1157-1172.

Sacher, M., Barrowman, J., Wang, W., Horecka, J., Zhang, Y., Pypaert, M. and Ferro-Novick, S. (2001). TRAPP I implicated in the specificity of tethering in ER-to-Golgi transport. Mol. Cell *2*, 433-442.

Sagot, I., Pinson, B., Salin, B. and Daignan-Fornier, B. (2006). Actin bodies in yeast quiescent cells: an immediately available actin reserve?. Mol. Biol. Cell *11*, 4645-4655.

Schindler, C., Rodriguez, F., Poon, P. P., Singer, R. A., Johnston, G. C. and Spang, A. (2009). The GAP domain and the SNARE, coatomer and cargo interaction region of the ArfGAP2/3 Glo3 are sufficient for Glo3 function. Traffic *9*, 1362-1375.

Schmid, S. L. (1997). Clathrin-coated vesicle formation and protein sorting: an integrated process. Annu. Rev. Biochem., 511-548.

Schmitt, H. D. and Jahn, R. (2009). A tethering complex recruits SNAREs and grabs vesicles. Cell *6*, 1053-1055.

Schnabl, M., Oskolkova, O. V., Holic, R., Brezna, B., Pichler, H., Zagorsek, M., Kohlwein, S. D., Paltauf, F., Daum, G. and Griac, P. (2003). Subcellular localization of yeast Sec14 homologues and their involvement in regulation of phospholipid turnover. Eur. J. Biochem. *15*, 3133-3145.

Scita, G. and Di Fiore, P. P. (2010). The endocytic matrix. Nature *7280*, 464-473.

Seidman, C. E., Struhl, K., Sheen, J. and Jessen, T. (2001). Introduction of plasmid DNA into cells. Curr. Protoc. Mol. Biol., Unit1.8.

Serafini, T., Orci, L., Amherdt, M., Brunner, M., Kahn, R. A. and Rothman, J. E. (1991). ADP-ribosylation factor is a subunit of the coat of Golgi-derived COP-coated vesicles: a novel role for a GTP-binding protein. Cell *2*, 239-253.

Setty, S. R., Shin, M. E., Yoshino, A., Marks, M. S. and Burd, C. G. (2003). Golgi recruitment of GRIP domain proteins by Arf-like GTPase 1 is regulated by Arf-like GTPase 3. Curr. Biol. *5*, 401-404.

Setty, S. R., Strochlic, T. I., Tong, A. H., Boone, C. and Burd, C. G. (2004). Golgi targeting of ARF-like GTPase Arl3p requires its Nalpha-acetylation and the integral membrane protein Sys1p. Nat. Cell Biol. *5*, 414-419.

Sikorski, R. S. and Hieter, P. (1989). A system of shuttle vectors and yeast host strains designed for efficient manipulation of DNA in Saccharomyces cerevisiae. Genetics *1*, 19-27.

Siniossoglou, S., Peak-Chew, S. Y. and Pelham, H. R. (2000). Ric1p and Rgp1p form a complex that catalyses nucleotide exchange on Ypt6p. EMBO J. *18*, 4885-4894.

Siniossoglou, S. and Pelham, H. R. (2002). Vps51p links the VFT complex to the SNARE Tlg1p. J. Biol. Chem. *50*, 48318-48324.

Siniossoglou, S. and Pelham, H. R. (2001). An effector of Ypt6p binds the SNARE Tlg1p and mediates selective fusion of vesicles with late Golgi membranes. EMBO J. *21*, 5991-5998.

Sinka, R., Gillingham, A. K., Kondylis, V. and Munro, S. (2008). Golgi coiled-coil proteins contain multiple binding sites for Rab family G proteins. J. Cell Biol. *4*, 607-615.

Smaczynska-de, R.,II, Costa, R. and Ayscough, K. R. (2008). Yeast Arf3p modulates plasma membrane PtdIns(4,5)P2 levels to facilitate endocytosis. Traffic *4*, 559-573.

Sollner, T., Whiteheart, S. W., Brunner, M., Erdjument-Bromage, H., Geromanos, S., Tempst, P. and Rothman, J. E. (1993). SNAP receptors implicated in vesicle targeting and fusion. Nature *6418*, 318-324.

Spang, A., Shiba, Y. and Randazzo, P. A. (2010). Arf GAPs: gatekeepers of vesicle generation. FEBS Lett. *12*, 2646-2651.

Springer, S., Spang, A. and Schekman, R. (1999). A primer on vesicle budding. Cell *2*, 145-148.

Sreenivas, A., Patton-Vogt, J. L., Bruno, V., Griac, P. and Henry, S. A. (1998). A role for phospholipase D (Pld1p) in growth, secretion, and regulation of membrane lipid synthesis in yeast. J. Biol. Chem. *27*, 16635-16638.

Stearns, T., Kahn, R. A., Botstein, D. and Hoyt, M. A. (1990). ADP ribosylation factor is an essential protein in Saccharomyces cerevisiae and is encoded by two genes. Mol. Cell. Biol. *12*, 6690-6699.

Tanigawa, G., Orci, L., Amherdt, M., Ravazzola, M., Helms, J. B. and Rothman, J. E. (1993). Hydrolysis of bound GTP by ARF protein triggers uncoating of Golgi-derived COP-coated vesicles. J. Cell Biol. *6 Pt 1*, 1365-1371.

Tarassov, K., Messier, V., Landry, C. R., Radinovic, S., Serna Molina, M. M., Shames, I., Malitskaya, Y., Vogel, J., Bussey, H. and Michnick, S. W. (2008). An in vivo map of the yeast protein interactome. Science *5882*, 1465-1470.

Tong, A. H. *et al.* (2001). Systematic genetic analysis with ordered arrays of yeast deletion mutants. Science *5550*, 2364-2368.

Tong, A. H. *et al.* (2004). Global mapping of the yeast genetic interaction network. Science *5659*, 808-813.

Trahey, M. and Hay, J. C. (2010). Transport vesicle uncoating: it's later than you think. F1000 Biol. Rep., 47.

Tsui, M. M. and Banfield, D. K. (2000). Yeast Golgi SNARE interactions are promiscuous. J. Cell. Sci. *Pt 1*, 145-152.

Tsukada, M. and Gallwitz, D. (1996). Isolation and characterization of SYS genes from yeast, multicopy suppressors of the functional loss of the transport GTPase Ypt6p. J. Cell. Sci. *Pt 10*, 2471-2481.

Tsukada, M., Will, E. and Gallwitz, D. (1999). Structural and functional analysis of a novel coiled-coil protein involved in Ypt6 GTPase-regulated protein transport in yeast. Mol. Biol. Cell *1*, 63-75.

Vida, T. A. and Emr, S. D. (1995). A new vital stain for visualizing vacuolar membrane dynamics and endocytosis in yeast. J. Cell Biol. *5*, 779-792.

von Mollard, G. F., Nothwehr, S. F. and Stevens, T. H. (1997). The yeast v-SNARE Vti1p mediates two vesicle transport pathways through interactions with the t-SNAREs Sed5p and Pep12p. J. Cell Biol. *7*, 1511-1524.

Wang, X. (1996). Identification of Yeast Proteins That Can Compensate for Loss of the Gcs1 Arf GAP. PhD Thesis, Dalhousie University.

Wang, X., Hoekstra, M. F., DeMaggio, A. J., Dhillon, N., Vancura, A., Kuret, J., Johnston, G. C. and Singer, R. A. (1996). Prenylated isoforms of yeast casein kinase I, including the novel Yck3p, suppress the gcs1 blockage of cell proliferation from stationary phase. Mol. Cell. Biol. *10*, 5375-5385.

Wang, Y. and Burke, D. J. (1997). Cdc55p, the B-type regulatory subunit of protein phosphatase 2A, has multiple functions in mitosis and is required for the kinetochore/spindle checkpoint in Saccharomyces cerevisiae. Mol. Cell. Biol. *2*, 620-626.

Whyte, J. R. and Munro, S. (2002). Vesicle tethering complexes in membrane traffic. J. Cell. Sci. *Pt 13*, 2627-2637.

Whyte, J. R. and Munro, S. (2001). The Sec34/35 Golgi transport complex is related to the exocyst, defining a family of complexes involved in multiple steps of membrane traffic. Dev. Cell. *4*, 527-537.

Wong, T. A. (2005). Membrane Metabolism Mediated by Sec14 Family Members Influences ArfGAP Activity for Transport from the *trans*-Golgi. MSc Thesis, Dalhousie University.

Wong, T. A., Fairn, G. D., Poon, P. P., Shmulevitz, M., McMaster, C. R., Singer, R. A. and Johnston, G. C. (2005). Membrane metabolism mediated by Sec14 family members influences Arf GTPase activating protein activity for transport from the trans-Golgi. Proc. Natl. Acad. Sci. U. S. A. *36*, 12777-12782.

Yamakawa, H., Seog, D. H., Yoda, K., Yamasaki, M. and Wakabayashi, T. (1996). Uso1 protein is a dimer with two globular heads and a long coiled-coil tail. J. Struct. Biol. *3*, 356-365.

Yanagisawa, L. L., Marchena, J., Xie, Z., Li, X., Poon, P. P., Singer, R. A., Johnston, G. C., Randazzo, P. A. and Bankaitis, V. A. (2002). Activity of specific lipid-regulated ADP ribosylation factor-GTPase-activating proteins is required for Sec14p-dependent Golgi secretory function in yeast. Mol. Biol. Cell *7*, 2193-2206.

Yoshida, S., Ohya, Y., Goebl, M., Nakano, A. and Anraku, Y. (1994). A novel gene, STT4, encodes a phosphatidylinositol 4-kinase in the PKC1 protein kinase pathway of Saccharomyces cerevisiae. J. Biol. Chem. *2*, 1166-1172.

Zhang, C. J., Bowzard, J. B., Anido, A. and Kahn, R. A. (2003). Four ARF GAPs in Saccharomyces cerevisiae have both overlapping and distinct functions. Yeast *4*, 315-330.

Zhang, C. J., Bowzard, J. B., Greene, M., Anido, A., Stearns, K. and Kahn, R. A. (2002). Genetic interactions link ARF1, YPT31/32 and TRS130. Yeast *12*, 1075-1086.